# ARCHITECTURES FOR CONTROLLING SOLID STATE PROPERTIES OF CONJUGATED POLYMERS

A Dissertation
Presented to
The Academic Faculty

by

Rakesh R. Nambiar

In Partial Fulfillment
of the Requirements for the Degree
Doctor of Philosophy in the
School of Chemistry and Biochemistry

Georgia Institute of Technology
May 2010

# DESIGNING NEW ARCHITECTURES FOR CONTROLLING SOLID STATE PROPERTIES OF CONJUGATED POLYMERS

Approved by:


Dr. David M. Collard, Advisor
School of Chemistry and Biochemistry
*Georgia Institute of Technology*

Dr. Laren Tolbert
School of Chemistry and Biochemistry
*Georgia Institute of Technology*

Dr. Charles Liotta
School of Chemistry and Biochemistry
*Georgia Institute of Technology*

Dr. Haskell Beckham
School of Polymer, Textile and Fiber Engineering / School of Chemistry and Biochemistry
*Georgia Institute of Technology*

Dr. Anselm Griffin
School of Polymer, Textile and Fiber Engineering
*Georgia Institute of Technology*


Date Approved: December 10, 2009

*To my mom Sulochana, my dad Ramachandran and my sister Reshma*

# ACKNOWLEDGEMENTS

I would like to express my gratitude to my advisor, Dr. David M. Collard for his invaluable support, advice, and encouragement throughout my graduate studies at Georgia Institute of Technology. I want to specially thank him for cultivating in me a sense of independent thinking towards research. I find myself fortunate to work with a caring personality like Dr. Collard. His mentoring will be missed and his influence will certainly be apparent in any future endeavor I pursue. Special thanks to Dr. Charles Liotta, Dr. Laren Tolbert, Dr. Haskell Beckham and Dr. Anselm Griffin for their participation in my committee and their insight into my research. My sincere thanks to the National Science Foundation, Georgia Tech School of Chemistry and Biochemistry and Centre of Photonics and Electronics (COPE) for financial support.

I would like to thank Dr. Leslie Gelbaum for variable temperature NMR, Dr. Angus Wilkinson and Dr. Mehmet Cetinkol for X-ray diffraction and glove box, David Bostwick for mass spectrophotometer analysis and Dr. Ray Gunawidjaja for Langmuir measurements. I wish to express my special thanks to Avishek Iyer and Pei Koh for their collaboration in the ultrasonication and $scCO_2$ projects.

I would like to acknowledge members of the Collard group, past and present, for their assistance and support, including Dr. Knoblock, Dr. Watt, Dr. Raynor, Kathy Woody, Brad Carson, Whitney Komorner, Anjli Kumar, Samina Karim and Josh Ochocki. Special thanks to Dr. Glen Brizius and Dr. Bing Wang for all the helpful discussions and help with synthetic chemistry. Special thanks to Dr. David Noga and Subodh Jagtap for their friendship and keeping me sane in the lab.

I would like to thank all the School of Chemistry and Biochemistry faculty and staff who provided me encouragement and support during my time at Georgia Tech. Special thanks to Dr. Cam Tyson.

I would also like to thank all my friends at Tech especially Amal Jayapalan, Vishal Patil, Dadasaheb Patil and Sudhir Mulik for their continued friendship, support and laughter and help me remember that life exists outside of lab.

Finally, words alone cannot express the thanks I owe to my mother Sulochana Nambiar, my father Ramachandran Nambiar and sister Reshma Nambiar for their encouragement and love bestowed upon me throughout my life. It is to them, I dedicate my thesis.

# TABLE OF CONTENTS

# LIST OF TABLES

# LIST OF FIGURES

# LIST OF SYMBOLS AND ABBREVIATIONS

| | |
|---|---|
| oLEDs | organic light emitting diodes |
| oFETs | organic field effect transistors |
| oPVCs | organic photovoltaic cells |
| NLO | nonlinear optical |
| PPE | Poly(phenylene ethynylyne) |
| PPV | Poly(phenylene vinylene) |
| P3HT | Poly(3-hexyl thiophene) |
| PAT | Poly(3-alkyl thiophene) |
| $E_g$ | bandgap |
| HOMO | highest occupied molecular orbital |
| LUMO | lowest unoccupied molecular orbital |
| ht | head-to-tail |
| hh | head-to-head |
| NMR | Nuclear Magnetic Resonance Spectroscopy |
| THF | tetrahydrofuran |
| $Et_2O$ | diethylether |
| IR | infrared |
| ATR-IR | Attenuated Total Reflection Infrared Spectroscopy |
| CuI | copper (1) iodide |
| $CH_2Cl_2$ | dichloromethane |
| $H_2O$ | water |
| $MgSO_4$ | Magnesium sulfate |
| $I_2$ | iodine |

| | |
|---|---|
| $KIO_3$ | potassium iodate |
| $CCl_4$ | carbon tetrachloride |
| NaH | sodium hydride |
| $PPh_3$ | triphenyl phosphine |
| HRMS | high resolution mass spectroscopy |
| Rg | regioregular |
| Rn | regiorandom |
| $CH_3COOH$ | acetic acid |
| TMS | trimethyl silyl |
| DMF | dimethyl formamide |
| LDA | Lithium diisopropylamide |
| $TiCl_4$ | Titanium tetrachloride |
| $EG_3$ | triethylene glycol |
| $\lambda_{max}$ | wavelength at maximum intensity |
| NaOH | sodium hydroxide |
| EtoAC | ethyl acetate |
| OEG | oligo ethylene glycol |
| TIPSE | Triisopropyl silyl ethynylyne |
| Rn | regiorandom |
| Rn | regiorandom |
| Rn | regiorandom |
| $\delta$ | chemical shift |
| kg | kilograms |
| UV | Ultraviolet |
| UV-vis | Ultraviolet-visible |

| | |
|---|---|
| DIA | N,N-Diisopropyl amine |
| g | grams |
| mm | millimeters |
| μm | microns |
| FT-IR | Fourier-Transform Infrared Spectroscopy |
| GPC | Gel Permeation Chromatography |
| DSC | Differential Scanning Calorimetry |
| mg | milligrams |
| min | minutes |
| MHz | megahertz |
| ppm | parts per million |
| m | multiplet |
| s | singlet |
| t | triplet |
| nm | nanometers |
| *J* | coupling constant |
| MS | Mass Spectrometry |
| HRMS | High Resolution Mass Spectrometry |
| M | molar |
| mL | milliliters |
| dd | doublet of doublets |
| TLC | thin-layer chromatography |
| M.P. | Melting Point |
| PDI | polydispersity index |
| $M_w$ | weight-average molecular weight |

| | |
|---|---|
| $M_n$ | number-average molecular weight |
| P | Polymer |
| $T_g$ | glass transition temperature |
| MeOH | methanol |
| NBS | *N*-bromosuccinimide |
| SEM | Scanning Electron Microscopy |
| SEC | size-exclusion chromatography |
| SAXS | small-angle x-ray scattering |
| WAXD | wide-angle x-ray diffraction |
| DP | Degree of Polymerization |
| d-spacing | domain spacing |
| q | scattering vector |

# SUMMARY

Conjugated polymers and oligomers are great materials for use in the next generation devices namely organic field effect transistors, light emitting diodes and polymeric solar cells. Apart from having the potential for developing power-efficient, flexible, robust and inexpensive devices, conjugated polymers can also be tuned by molecular design to optimize device characteristics. One key problem for the full commercial exploitation of conjugated polymers is that the charge carrier mobility of the state-of-the-art polymer semiconductors is much lower than required for many applications. The performance of the devices is strongly dependent on the molecular structure and supermolecular assembly of the conjugated polymer chains. This thesis covers our attempts to design molecular structure to control and improve the solid state properties of conjugated polymers.

The relative placement of side chains along the backbone has a great influence on the solid state ordering of conjugated polymers. Poly(2,5-disubstituted-1,4-phenylene ethynylene)s (PPE)s, an important class of conjugated polymers, are generally synthesized by Pd-catalyzed coupling polymerizations of appropriately substituted diiodo and diethynyl benzenes (i.e., A-A and B-B type monomers). In asymmetrically substituted PPEs, this results in an irregular substitution pattern of the side chains along the polymer backbone. We report a new synthetic approach to prepare regioregular unsymmetrically substituted PPEs by polymerization of 4-iodophenylacetylenes (i.e., A-B type monomer). We provide a detailed discussion of various approaches to the

synthesis of PPEs with different regioregularities and provide a description of the differences between regioregular and regiorandom analogs.

The effect of regioregularity becomes even more important when the two side chains are very dissimilar or amphiphilic. We explore the effect of relative placement hydrophobic (dodecyloxy) / hydrophilic (tri(ethylene glycol) and hydrophobic (dodecyloxy)/fluorophilic (fluoroalkyl) side chains along the poly(1,4-phenylene ethynylene) backbone. We found that the regioregular substitution of the polymer backbone provides a structure in which the side chains segregate to afford a Janus-type structure. The regioregular polymer chains pack more densely in a monolayer at the air-water interface, and pack into a bilayer in the solid state to form a highly crystalline material.

Pentacenes are very important organic molecules for use as semiconductor in oFETs due to their low band gap and high field effect mobility. One approach to reduce the bandgap of a polymeric system and improve performance is to include low bandgap small molecules into the conjugated backbone. A new copolymer system consisting of pentacene and terthiophene was developed and its optical and electronic properties along with its stability were evaluated.

We report the use of ultrasonication of P3HT as a novel operationally-simple process to significantly improve the field effect mobility of P3HT-based FETs, thereby potentially eliminating the need for dielectric surface modifications or further processing of the device. Investigation of the sonicated polymer samples by number of characterization techniques indicates that ultrasonication leads to aggregation and ordering of the P3HT chains resulting in increase in the mobility.

# CHAPTER 1

# INTRODUCTION

## 1.1. CONJUGATED POLYMERS

Polymers were traditionally considered as insulating materials before the serendipitous discovery of highly conducting polyacetylene in 1977 which marked the birth of a new field of conjugated polymers.[1,2] Conjugated polymers are important materials for next generation technological advances. This was recognized by the award of the Nobel Prize in Chemistry in 2000 to Alan J. Heeger, Alan G. Macdiarmid and Hideki Shirakawa for the discovery and development of conjugated polymers. Conjugated polymeric materials have been studied in detail for incorporation into optical-electronic devices such as organic light emitting diodes (oLEDs)[3-5] and organic field effect transistors (oFETs),[6-8] organic photovoltaic cells (oPVCs)[9] for light harvesting, photorefractive devices,[10] organic sensors for biological and chemical sensing[11], nanoelectronics and nonlinear optical (NLO) devices.[12] Compared to traditional inorganic semiconductors, conjugated polymers have a number of advantages such as their low cost, easy processability, and lightweight nature. Moreover, there are numerous possibilities to modify the chemical structure of the conjugated polymers to tune the physical properties.[13] Important classes of conjugated polymers include polyacetylene, poly(3-alkylthiophene) (PAT), poly(phenylene-vinylene) (PPV), poly(phenylene ethynylyne) (PPE), polyaniline and polypyrrole.

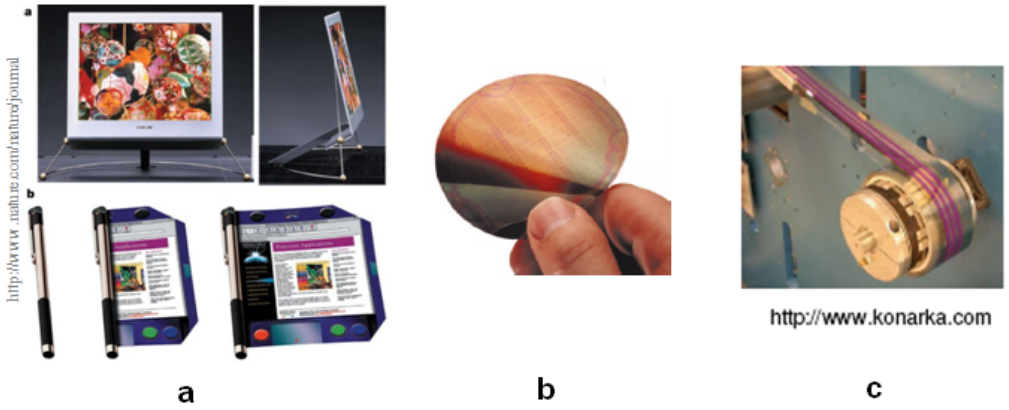


**Figure 1.1.** Applications of conjugated polymers in (a) light emitting diodes –displays (from www.universaldisplay.com), (b) field effect transistors (from www.phys.unsw.edu.au/.../Organics.html) and (c) photovoltaic cells (from www.konarka.com).

## 1.2. CHARGE TRANSPORT IN CONJUGATED POLYMERS

Conjugated polymers are characterized by a molecular structure that contains alternating single and multiple bonds. The electronic and physico-chemical characteristics of conjugated macromolecules are not only governed by the structure of the polymer backbone, but also by intermolecular interactions.[13] The continuous chain of $sp^2$ and/or sp hybridized carbon atoms leads to a situation where overlap of p-orbitals on successive atoms enables the delocalization of π-electrons along the polymer backbone. Electrical conductivity is a direct consequence of such delocalization. The large number of atomic orbitals in the macromolecules translates into a large number of molecular orbitals, which form a continuous band of energies.

In the case of a metal, this energy band exists as a continuum due to the high density of electronic states with electrons of relatively low binding energy ("free electrons") can easily redistribute, and under an applied electric field move easily therby rendering the material to be electrically conducting. In conjugated macromolecules π-electrons are delocalized over the entire chain and one would expect that the electronic properties of a polymeric material composed of sufficiently long conjugated chains are also described well by a continuous energy band. According to this model, an individual chain of the conjugated polymer would be a one-dimensional (1D) metallic conductor. However, as a result of the Peierls distortion,[14] the density of π-electrons in conjugated organic molecules is not the same between all atoms; there is a distinct alternation between single and multiple bond character. Thus, the electronic properties of conjugated polymers in their neutral oxidation state are usually better described by a filled valence band (π-band, bonding) and an empty conduction band (π*-band, antibonding). Because

the energy difference between the top of the occupied band and the bottom of the unoccupied band, referred to as band gap ($E_g$), is usually not zero, conjugated polymers are typically *semi*conductors in their neutral, *undoped* state.

Charge carriers which are responsible for the mobility and conductivity in conjugated polymers are generated by oxidation and reduction processes, either on application of an electrical potential or by reaction with chemical reagents. Oxidation leads to a material with positively charged charge carriers and is referred to as p-type doping. Reduction leads to negative charge carriers and is referred to as n-type doping. The charge transport characteristics of conjugated polymers are governed by both the nature of the polymer backbone and the intermolecular interactions which exert an important influence on the macroscopic materials properties. The charge carrier mobility of conjugated polymers is a function of *intra*chain charge diffusion and *inter*chain interactions, Figure 1.2.[13,15,16] Both factors depend on a number of variables; the former might be subject to changes based on the chemical structure of the polymer, the number and nature of defect sites, conformation of the polymer backbone, and the molecular weight, while the latter strongly depends on the supramolecular architecture, i.e., the degree of contact, order and orientation.[17-19]

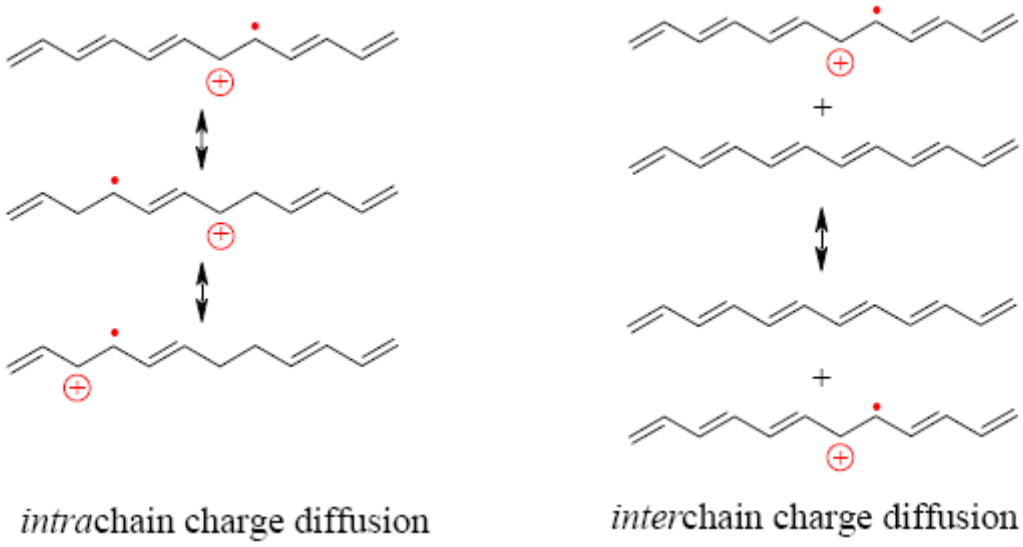


**Figure 1.2.** Schematic representation of *intra*chain charge diffusion (left) and *inter*chain charge diffusion "hopping" (right) in polyacetylene.

Breathtaking progress has been made in the last 25 years and the field has matured to the onset of commercial exploitation of conjugated polymers as conductors in corrosion control, in light-emitting diodes, sensors, and a number of other applications. One key problem for the full commercial exploitation of the field is that the charge carrier mobility of the state-of-the-art polymer semiconductors is much lower than required for many applications. Chemists may consider that there are mainly two ways of improving the performance of a semiconducting polymer:

1) Altering the conjugated polymer backbone; and

2) Improving the solid-state ordering and orientation of the polymer chains.

## 1.3. SOLID-STATE ORDERING AND ORIENTATION IN CONJUGATED POLYMERS

The orientation and packing of conjugated backbones affect the physical properties of conjugated polymers in a significant way and hence become important in the search for materials with better performance in electronic and photonic devices. Increasing the planarity of the backbone and the conjugation length would facilitate the delocalization of charge carriers along the polymer backbone and the potential for close packing of adjacent chains. Such a high degree of chain packing would increase the communication between the conjugated chains via π-π interactions, making the conduction two dimensional (intramolecular and intermolecular). Consequently, much work has been focused on maximizing the supramolecular order in conjugated polymers to optimize their charge transport properties such as field effect mobility. A good example is the effect of regioregularity in poly(3-alkylthiophene)s (PATs), Figure 1.3.

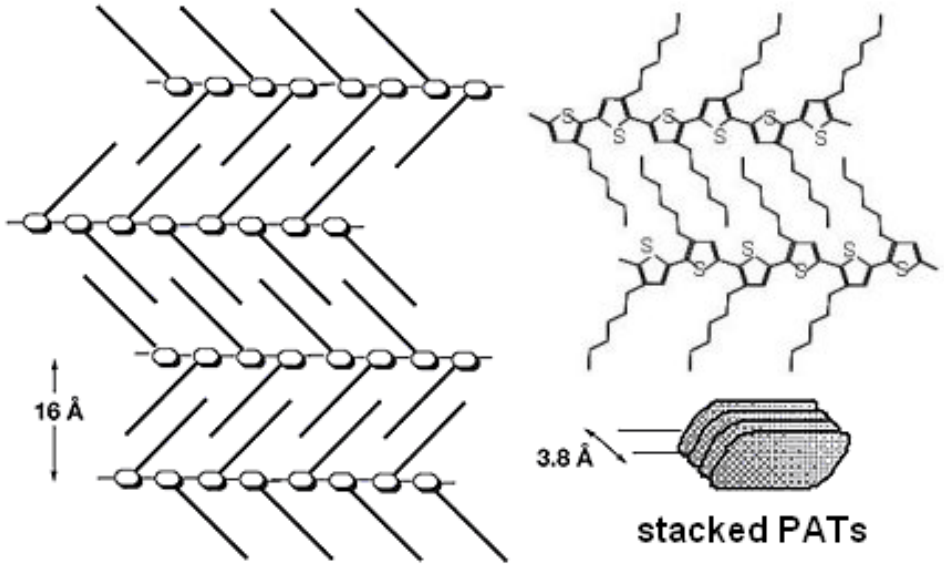


**Figure 1.3.** Ordered packing in regioregular poly(3-hexylthiopene)s. (from www.cmu.edu/news/040330-mccullough.html)

Regiorandom amorphous poly(3-hexylthiophene) (P3HT) exhibits a field effect mobility of the order of $10^{-5}$ $cm^2/Vs$ which is about five orders of magnitude lower than the mobility required for potential application of organic semiconductors in plastic thin film transistors. Regioregular P3HT, which forms highly ordered lamellar structure with an efficient π-π stacking between chains has charge carrier mobilities of the order of 0.1 $cm^2/Vs$ along with high on/off ratios, Figure 1.3.[18,20-22] Polymers with high regioregularities tend to orient perpendicular to a substrate with π-stacked conjugated polymer lamellae parallel to the substrate, leading to highly efficient in-plane charge transport, Figure 1.4.[18,20]

There are various other approaches to enhance chain orientation and packing of conjugated polymers. It was demonstrated for poly(3-alkylthiophene)s that the orientational order of drop-cast films is low when using low boiling solvents such as chloroform. However, the field effect mobility was observed to increase when films were developed from a high boiling solvent such as xylene or 1,2,4-trichlorobenzene[23,24] or a combination of low and high boiling solvents.[25] Use of high boiling solvents gives the polymer chains more time to orient, giving rise to better ordering. Thermal treatment e.g., annealing at high temperature in inert conditions, is also well understood to increase the field effect mobility of P3HT.[26] Poor solvent induced π-π stacking of P3HT chains forms ordered aggregates and raises the mobility by a order of magnitude without any post treatment.[27] Doping PATs with $HAuCl_4$ prior to film formation results in the formation of highly ordered molecular structure with high field effect mobility.[28]

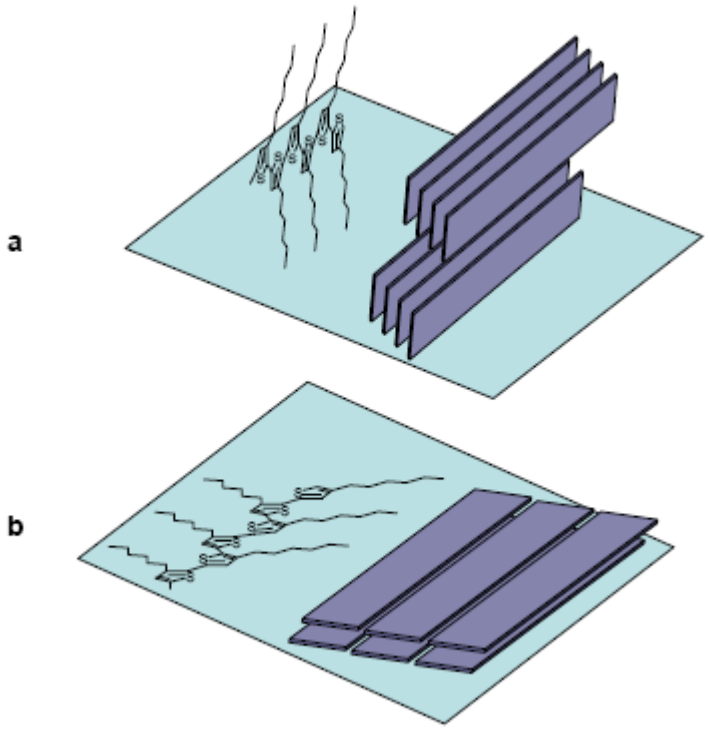


**Figure 1.4.** Two types of preferential orientation of the ordered P3HT domains with respect to the substrate: a) Edge-on orientation b) Face-on orientation.

Enhancement of field effect mobility can also be obtained in the case of transistors based on PATs if an ultrathin film of the semiconducting polymer was processed using a dip coating technique,[29] Langmuir-Blodgett deposition,[30,31] layer-by-layer assembly.[32] Aligned conjugated polymer chains have been made with templates such as nanoporous membranes[33] and nanochannels of mesoporous zeolites.[34,35] Nematic liquid crystalline media has also been used to increase the macroscopic alignment of poly-9,9'-dioctyl-fluorene-co-bithiophene,[36] poly(p-phenylene vinylene).[37]

## 1.4. ALTERING THE CONJUGATED BACKBONE IN SEMICONDUCTING POLYMERS.

The performance of conjugated polymers for use in transistors has achieved by altering the chemical structure of the conjugated backbone. The bandgap of conjugated organic molecules is the energy difference between the top of the valence band (HOMO) and bottom of the conduction band (LUMO). The band gap of well-studied conjugated polymers are typically $\geq$ 2 eV, e.g., 2.1 eV for polythiophene, 2.7 eV for poly(p-phenylene). For many years, chemists and physicists have tried to devise conjugated organic polymers where the bandgap is zero or extremely small, which would increase the field effect mobility of these materials. Lowering of the bandgap can be realized either by increasing the top of the valence band (HOMO) or by decrease in the conduction band (LUMO).

Over the years, several approaches have been developed to prepare low bandgap polymers. One of the approaches was to increase π-conjugation to the polymer. This can be accomplished by fusing arenes such as thieno- or benzo- rings to the conjugated

polymer backbone. Another way to insure greater conjugation is to rigidify the individual monomer units by employing additional rings that serve to enforce planarity. Ladder type conjugated polymers has also been used as a strategy for making one dimensional planar conjugated polymer with low band gap.[38] Finally, substituents on repeat units within the polymer backbone can serve to lower the bandgap by either electron-releasing[39] or electron-withdrawing[40] effects, that will respectively increase the HOMO level or lower the LUMO. This concept was later successfully extended to the synthesis of copolymers consisting of alternating electron donor and acceptor units forming low bandgap materials.[41-43]

## 1.5. SCOPE OF WORK

The concept of regioregularity in P3HT has had a tremendous impact on the application of these materials in the state-of-the-art devices. However, regioregularity as a tool to enhance structural as well as electronic properties has not been fully explored in other conjugated polymer systems, especially the phenylene type of polymers which is an important class of backbone for semiconducting polymers. Poly(1,4-phenylene ethynylyne) (PPE) is an interesting conjugated polymer with attractive electronic and optical properties.[44,45] They have been used as semiconductors and/or fluorescent materials in field effect transistors, light emitting diodes, solar cells, and sensors. PPEs inherently have very low field effect mobility and an effort to increase the mobility would be significant contribution. The linear structure of the PPE backbone facilitates the self assembly process. Chapter 2 in this thesis is focused on developing regioregular asymmetrically substituted PPEs and understanding the effect of regioregularity on the

electronic properties and molecular packing in the solid state. We believe that regioregularity would play an even more important role in amphiphilic systems where a polymer chain is substituted with two dissimilar side chains. Chapter 3 and 4 includes our efforts to study the effects of regioregularity in amphiphilic PPEs (hydrophilic/hydrophobic; fluorophilic/hydrophobic systems).

Acenes, and pentacene in particular, are very important organic molecules for use as semiconductors in oFETs due to their low band gap and high field effect mobility. One approach to reduce the bandgap of a polymeric system is to include low bandgap small molecules into the conjugated backbone. Chapter 5 includes studies to prepare a copolymer involving two low bandgap molecule namely pentacene and the terthiophene moiety.

Chapter 6 in this thesis reports the ultrasonication of P3HT as a novel operationally-simple process to significantly improve the field effect mobility of PAT-based FETs, thereby potentially eliminating the need for dielectric surface modifications or further processing of the device. Details of the process and the experiments to explore the reasons for this phenomenon form the basis of this chapter.

The conventional preparation of poly(arylene ethynylyne)s (PPEs) involves the Pd/Cu-catalyzed Sonagashira coupling of dihaloarenes and diethynylarenes in the presence of a large excess amine base. In Chapter 7 we report the polymerization of 1,4-diiodo-2,5-dialkoxybenzene and 1,4-diethynyl-2,5-dialkoxybenzene in supercritical carbon dioxide, a versatile environmentally-benign reaction medium.

## 1.6. REFERENCES


(1) Shirakawa, H.; Louis, E. J.; Macdiarmid, A. G.; Chiang, C. K.; Heeger, A. J. *J. Chem. Soc. Chem. Commun.* **1977**, 578.

(2) Chiang, C. K.; Fincher, C. R.; Park, Y. W.; Heeger, A. J.; Shirakawa, H.; Louis, E. J.; Gau, S. C.; Macdiarmid, A. G. *Phys. Rev. Lett.* **1977**, *39*, 1098.

(3) Burroughes, J. H.; Bradley, D. D. C.; Brown, A. R.; Marks, R. N.; Mackay, K.; Friend, R. H.; Burns, P. L.; Holmes, A. B. *Nature* **1990**, *347*, 539.

(4) Crawford, M. H. *IEEE J. Sel. Top. Quant.* **2009**, *15*, 1028.

(5) Kraft, A.; Grimsdale, A. C.; Holmes, A. B. *Angew. Chem., Int. Ed.* **1998**, *37*, 403.

(6) Garnier, F.; Horowitz, G.; Peng, X. H.; Fichou, D. *Adv. Mater.* **1990**, *2*, 592.

(7) Garnier, F.; Hajlaoui, R.; Yassar, A.; Srivastava, P. *Science* **1994**, *265*, 1684.

(8) Horowitz, G. *Adv. Mater.* **1998**, *10*, 365.

(9) Gunes, S.; Neugebauer, H.; Sariciftci, N. S. *Chem. Rev.* **2007**, *107*, 1324.

(10) Moerner, W. E.; Silence, S. M. *Chem. Rev.* **1994**, *94*, 127.

(11) Zheng, J.; Swager, T. M. *Poly(Arylene Etynylene)s: From Synthesis to Application*; Springer-Verlag Berlin: Berlin, 2005; Vol. 177, 151.

(12) Marder, S. R.; Perry, J. W. *Adv. Mater.* **1993**, *5*, 804.

(13) Skotheim, T. A.; Reynolds, J. R.; Editors *Handbook of Conducting Polymers, Third Edition: Conjugated Polymers, Theory, Synthesis, Properties, and Characterization*, Marcel Dekker: New York, 2007.

(14) Peierls, R. E. *Quantum Theory of Solids*, Oxford Univ Press, England, 1955.

(15) Brabec, C. J.; Sariciftci, N. S.; Hummelen, J. C. *Adv. Funct. Mater.* **2001**, *11*, 15.

(16) Nalwa, H. S.; Editor *Handbook of Organic Conductive Molecules and Polymers, Volume 3: Conductive Polymers: Spectroscopy and Physical Properties*, Wiley: Chicaster UK, 1997.

(17) Wang, Z. H.; Li, C.; Scherr, E. M.; MacDiarmid, A. G.; Epstein, A. J. *Phys. Rev. Lett.* **1991**, *66*, 1745.

(18) Bao, Z.; Dodabalapur, A.; Lovinger, A. J. *Appl. Phys. Lett.* **1996**, *69*, 4108.

(19) Aleshin, A.; Kiebooms, R.; Menon, R.; Wudl, F.; Heeger, A. J. *Phys. Rev. B: Condens. Matter* **1997**, *56*, 3659.

(20) Sirringhaus, H.; Brown, P. J.; Friend, R. H.; Nielsen, M. M.; Bechgaard, K.; Langeveld-Voss, B. M. W.; Spiering, A. J. H.; Janssen, R. A. J.; Meijer, E. W.; Herwig, P.; de Leeuw, D. M. *Nature* **1999**, *401*, 685.

(21) McCullough, R. D.; Lowe, R. D.; Jayaraman, M.; Ewbank, P. C.; Anderson, D. L.; Tristramnagle, S.; Elsevier Science Sa Lausanne: 1993, p 1198.

(22) McCullough, R. D.; Tristramnagle, S.; Williams, S. P.; Lowe, R. D.; Jayaraman, M. *J. Am. Chem. Soc.* **1993**, *115*, 4910.

(23) Kline, R. J.; McGehee, M. D.; Kadnikova, E. N.; Liu, J. S.; Frechet, J. M. J.; Toney, M. F. *Macromolecules* **2005**, *38*, 3312.

(24) Chang, J. F.; Sun, B. Q.; Breiby, D. W.; Nielsen, M. M.; Solling, T. I.; Giles, M.; McCulloch, I.; Sirringhaus, H. *Chem. Mat.* **2004**, *16*, 4772.

(25) Zhang, F. L.; Jespersen, K. G.; Bjorstrom, C.; Svensson, M.; Andersson, M. R.; Sundstrom, V.; Magnusson, K.; Moons, E.; Yartsev, A.; Inganas, O. *Adv. Funct. Mater.* **2006**, *16*, 667.

(26) Cho, S.; Lee, K.; Yuen, J.; Wang, G. M.; Moses, D.; Heeger, A. J.; Surin, M.; Lazzaroni, R. *J. Appl. Phys.* **2006**, *100*, 6.

(27) Park, Y. D.; Lee, H. S.; Choi, Y. J.; Kwak, D.; Cho, J. H.; Lee, S.; Cho, K. *Adv. Funct. Mater.* **2009**, *19*, 1200.

(28) Park, Y. D.; Kim, D. H.; Lim, J. A.; Cho, J. H.; Jang, Y.; Lee, W. R.; Park, J. H.; Cho, K. *J. Phys. Chem. C* **2008**, *112*, 1705.

(29) Wang, G. M.; Swensen, J.; Moses, D.; Heeger, A. J. *J. Appl. Phys.* **2003**, *93*, 6137.

(30) Xu, G. F.; Bao, Z. A.; Groves, J. T. *Langmuir* **2000**, *16*, 1834.

(31) Ando, M.; Watanabe, Y.; Iyoda, T.; Honda, K.; Shimidzu, T.; Elsevier Science SA Lausanne: 1989, p 225.

(32) Ferreira, M.; Rubner, M. F. *Macromolecules* **1995**, *28*, 7107.

(33) Martin, C. R. *Science* **1994**, *266*, 1961.

(34) Wu, C. G.; Bein, T. *Science* **1994**, *266*, 1013.

(35) Wu, C. G.; Bein, T. *Science* **1994**, *264*, 1757.

(36) Sirringhaus, H.; Wilson, R. J.; Friend, R. H.; Inbasekaran, M.; Wu, W.; Woo, E. P.; Grell, M.; Bradley, D. D. C. *Appl. Phys. Lett.* **2000**, *77*, 406.

(37) Smith, R. C.; Fischer, W. M.; Gin, D. L. *J. Am. Chem. Soc.* **1997**, *119*, 4092.

(38) Schluter, A. D.; Loffler, M.; Enkelmann, V. *Nature* **1994**, *368*, 831.

(39) Yu, Y.; Gunic, E.; Zinger, B.; Miller, L. L. *J. Am. Chem. Soc.* **1996**, *118*, 1013.

(40) Toussaint, J. M.; Bredas, J. L.; Elsevier Science Sa Lausanne: 1993, p 103.

(41) Huo, L. J.; He, C.; Han, M. F.; Zhou, E. J.; Li, Y. F. *J. Polym. Sci., Pol. Chem.* **2007**, *45*, 3861.

(42) Zhu, Y.; Champion, R. D.; Jenekhe, S. A. *Macromolecules* **2006**, *39*, 8712.

(43) Shi, C. J.; Yao, Y.; Yang, Y.; Pei, Q. B. *J. Am. Chem. Soc.* **2006**, *128*, 8980.

(44) Bunz, U. H. F. *Poly(Arylene Ethynylene)s: From Synthesis to Application*; Springer-Verlag Berlin: Berlin, 2005; Vol. 177, 1.

(45) Bunz, U. H. F. *Chem. Rev.* **2000**, *100*, 1605.

# CHAPTER 2

# SYNTHESIS AND CHARACTERIZATION OF REGIOREGULAR UNSYMMETRICAL DIALKOXY SUBSTITUTED POLY(1,4-PHENYLENE ETHYNYLENE)S

## 2.1. INTRODUCTION

Conjugated polymers exhibit interesting electronic and optical properties, and have great commercial potential as semiconductors for use in light emitting diodes, field effect transistors, solar cells and sensors.[1] While the charge carrier mobility of conjugated polymers is typically lower than that of doped silicon, the ease of processing (i.e., from solution or the melt) and the ability to tailor material properties through modification of the molecular structure provide opportunities for use of these materials in power efficient, flexible, robust and inexpensive consumer devices.

It is well established that the identity and relative position of side chains along the polymer backbone have a large impact on the properties of poly(alkylthiophene)s. Jen *et. al.* initially incorporated flexible alkyl side chains onto the backbone of polythiophene to develop soluble conjugated organic materials.[2] Defining the two 2- and 5-positions of a 3-alkylthiophen-2,5-diyl repeat unit of the polymer as the 'head' (*h*) and 'tail' (*t*), respectively, gives rise to three possible regiochemically distinct diads: *hh*, *ht* and *tt*. Oxidative polymerization of 3-alkylthiophenes affords materials with a mixture of these three diads along the backbone, Figure 2.1A. McCullough *et. al.* and Reike *et. al.* later independently realized the importance of controlling the relative position of the side

chains of poly(3-alkylthiophene) through development of new synthetic methods.[3,4] Polymerization of 5-metallo-2-bromo-3-alkylthiophenes by organometallic coupling affords a regioregular polymer primarily consisting of *ht* diads, Figure 2.1B. Regioregularity has a large impact on the properties of poly(3-alkylthiophene)s: The regioregular materials possess higher crystallinity, red shifted optical absorptions, greater conductivity and a smaller band gap than the regiorandom analogs.[5] However, the effect of the relative position of substituents on the properties of other classes of conjugated polymers has been restricted to poly(3-alkylthienylene vinylene),[6] poly[3-alkyl-2,5-thienylene-1,4-phenylene],[7] poly(1,4-phenylene vinylene)s[8] and poly(biphenylene vinylene).[9]

Poly(1,4-phenylene ethynylene)s, PPE, are a particularly interesting class of conjugated polymers due to their attractive electronic and optical properties.[10] They have been used as semiconductors and/or fluorescent materials in field effect transistors,[11] light emitting diodes,[12] solar cells,[13] and sensors.[14] Symmetrically 2,5-disubstituted PPEs (i.e., X = Y in Figure 2.1C) are inherently regioregular. While there are numerous examples of PPEs prepared from monomers bearing pairs of dissimilar side chains on the phenylene rings,[15-18] the polymerization of unsymmetrically substituted 1,4-diethynylbenzenes and 1,4-diiodobenzenes by alkyne-aryl iodide[10] coupling (i.e., by an A-A + B-B type condensation polymerization), or by alkyne metathesis of diethynes,[19] yields reg  The effect of regioregularity of PPEs has not been explored extensively.[20] We have recently developed synthetic routes to allow for the preparation of regular (*ht*) unsymmetrically-substituted PPEs by polymerization of 2,5-disubstituted-4-iodophenylacetylenes, i.e., difunctional A-B type monomers bearing dissimilar alkoxy side

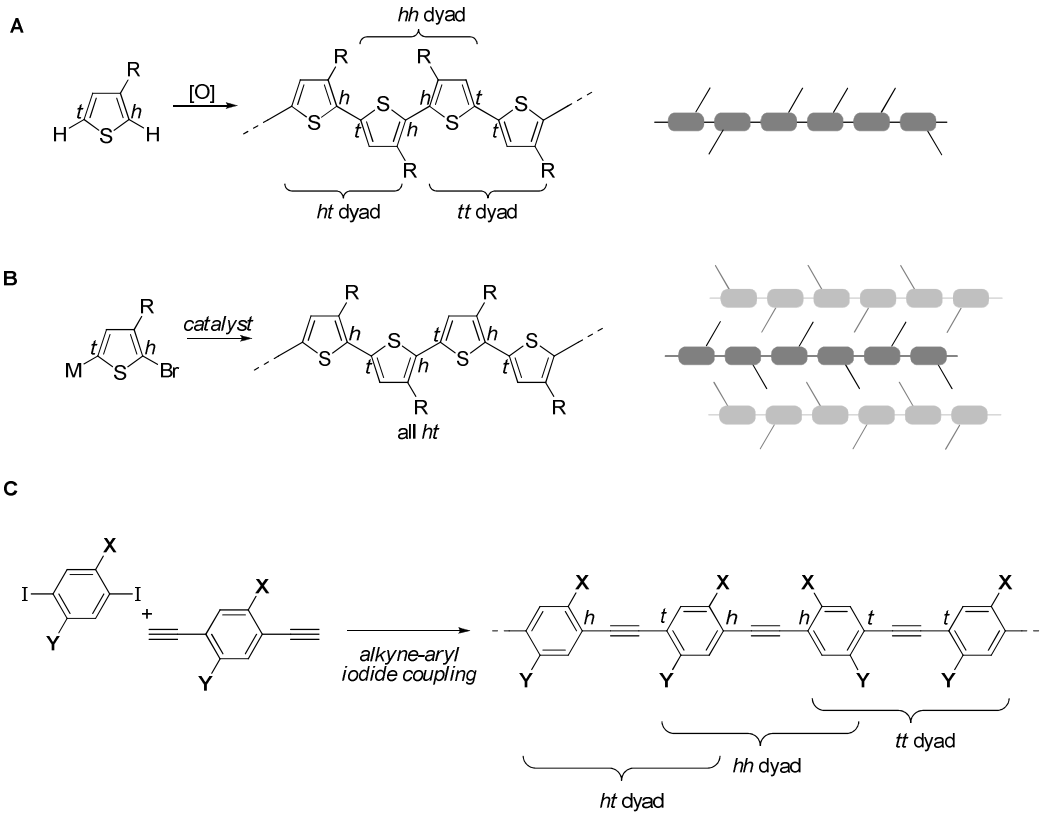


**Figure 2.1**. A, Oxidative polymerization of 3-alkylthiophenes affords regiorandom materials consisting of *ht*, *hh*, and *tt* diads. B, Regioselective polymerization affords regioregular *ht* polymers which crystallize as a result of side chain packing. C, Polymerization of unsymmetrically-substituted 1,4-diodobenzenes and 1,4-diethynylbenzenes affords a regiorandom PPE.

chains, Figure 2.2 (previous reports on preparation of PPEs by polymerization of A-B type monomers have been restricted to those with identical side chains to give symmetrical, inherently regioregular analogues[21-23]). iorandom PPEs containing a mixture of *hh*, *tt* and *ht* diads, Figure 2.1C. Following a preliminary report,[24] we now provide detailed optimized synthetic procedures for the preparation of this class of PPE, demonstrate control over regioregularity (using $^{1}H$ and $^{13}C$ NMR spectroscopy), and report on the effect of regioregularity on the supermolecular packing (X-ray diffraction) and electronic structure (UV-visible spectroscopy) of the materials. While this report is restricted to the development of methodology using combinations of dissimilar linear alkoxy side chains, we expect that these approaches will provide for greater control over the assembly and properties of amphiphilic analogs and those bearing functional side chains.

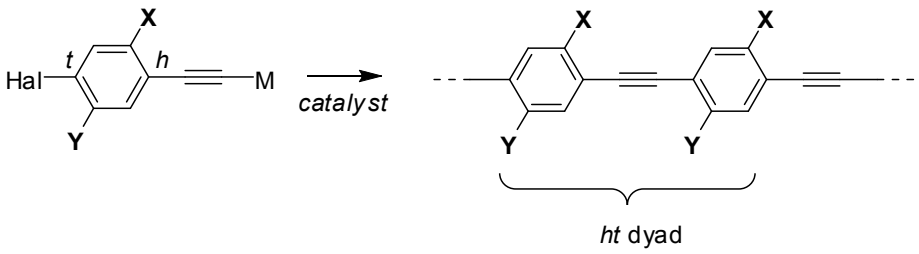


**Figure 2.2.** Preparation of regioregular unsymmetrically-substituted PPEs from an A-B type monomer.

## 2.2. EXPERIMENTAL

### 2.2.1. General Methods

All reagents were purchased from commercial sources and used without further purification unless stated. THF and $Et_2O$ were dried over sodium benzophenone ketyl prior to distillation under nitrogen. Column chromatography was performed on flash grade silica (32-60 Å, Sorbent Technologies, Atlanta, GA). Thin-layer chromatography was performed on 3 ×5 cm silica gel plates (0.2 mm thick, 60 F254) on an aluminum support (Sorbent Technologies). NMR analysis was performed on a Bruker DSX 400 or DSX 300 instruments. Chemical shifts are reported relative to internal tetramethylsilane. IR analyses were performed on a Nicolet 4700 FTIR with an ATR attachment from SmartOrbit Thermoelectronic Corporation. Elemental analyses were performed by Atlantic Microlab, Inc. (Norcross, GA). Ultraviolet-visible analysis was performed on a Shimadzu UV-2401PC spectrometer, and fluorescence spectroscopy was performed on a Shimadzu RF-5301PC spectrofluorophotometer. The X-ray diffraction data was obtained using a Scintag X1 diffractometer equipped with copper tube and a Peltier cooled solid state detector.

### 2.2.2. Synthesis of monomers 3 and 5 for preparation of regiorandom PPEs

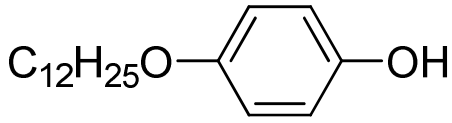


**4-Dodecyloxyphenol, II-1b.** NaH (12.96 g, 540 mmol), was added over 30 min to a stirred solution of 1,4-hydroquinone (60 g, 545.5 mmol) in anhydrous DMF (900 mL) under $N_2$ and the mixture was stirred for 20 min. 1-Bromododecane (134.46 g, 540 mmol) was added dropwise over 10 min and the mixture was stirred for 18 h. The resulting dark brown solution was acidified with 10% aqueous HCl and poured into $CH_2Cl_2$ (400 mL). The organic layer was extracted with 10% aqueous HCl (2 × 200 mL) and the solvent was removed under reduced pressure. The residue was recrystallized twice from EtOH, and once from hexane, to afford **II-1b** (40 g, 26 % yield) as a white solid, m.p. 79°C. $^1$H NMR (300 MHz, $CDCl_3$): δ 6.7-6.8 (m, 4H, Ar-H), 4.5-5.0 (bs, 1H, OH), 3.88 (t, $^3J_{HH}$ = 6.61 Hz, 2H, -$OCH_2$-), 1.7-1.8 (m, 2H, C-2 -$CH_2$-), 1.2-1.5 (m, 18H), 0.85 (t, $^3J_{HH}$ = 6.7 Hz, 3H, -$CH_3$). $^{13}$C NMR (75 MHz, $CDCl_3$): δ 153.49, 149.57 (Ar C-O), 116.26, 115.9 (Ar C-H), 69.06 (-$OCH_2$-), 32.17, 29.92, 29.89, 29.85, 29.66, 29.60, 26.29, 22.94, 14.38. IR ($\nu$, cm$^{-1}$): 3436, 3364 (O-H), 3034, 2953 (Ar C-H str), 2915, 2870, 2849, 1606, 1512, 1454, 1395, 1370, 1297, 1237 (C-O str.), 1169, 1104, 1037, 1007, 826, 768. HRMS: calc. for $C_{18}H_{30}O_2$ = 278.22458, obs. = 278.22513, Δ = 2.0 ppm.

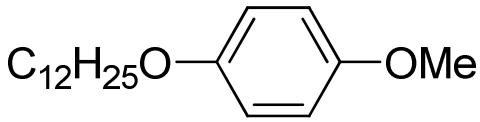


**4-Dodecyloxyanisole, II-2a.**[25] A suspension of 4-methoxyphenol (12.4 g, 100 mmol), $K_2CO_3$ (16.6 g, 120 mmol) and 1-bromododecane (29.8 g, 120 mmol) in degassed DMF (75 mL) was heated at 80°C for 18 h. The reaction mixture was cooled, diluted with chloroform (100 mL) and washed with 10% HCl (3 × 150 mL). The organic extracts were dried over $MgSO_4$ and the solvent was removed at under reduced pressure. The residue was recrystallized from methanol to afford **II-2a** (15.01, 51.4 % yield) as white flakes, m.p. = 216-217 °C. $^1$H NMR (300 MHz, $CDCl_3$): δ 6.85 (s, 4H, Ar-H), 3.90 (t, $^3J_{HH}$ = 6.7 Hz, 2H, -$OCH_2$-), 3.77 (s, 3H, -$OCH_3$), 1.70-1.82 (m, 2H), 1.20-1.51 (m, 18H), 0.89 (t, $^3J_{HH}$ = 6.6 Hz, 3H, -$CH_3$). $^{13}$C NMR (75 MHz, $CDCl_3$): δ 153.47, 153.14 (Ar C1,4), 115.24, 114.43 (Ar C2,3,5,6), 68.52 (-O-$CH_2$-), 55.57 (-O-$CH_3$), 31.77, 31.61, 29.52, 29.25, 29.21, 29.15, 25.91, 25.73, 22.68, 22.61, 14.11. IR ($\nu$, $cm^{-1}$): 2954, 2933 (Ar C-H str.), 2918, 2873, 2849, 1539, 1509, 1474, 1440, 1359, 1293, 1219 (C-O str.), 1036, 901, 826, 743, 529. HRMS: *calc*. for $C_{19}H_{32}O_2$ = 292.24023, *obs*. = 292.24237, Δ = 7.3 ppm.

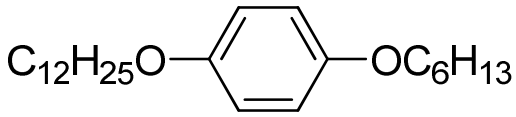

**1-Dodecyloxy-4-hexyloxybenzene, II-2b**. Phenol **II-1b** (4.51 g, 16.2 mmol) was added to a stirred solution of $PPh_3$ (5.12 g, 19.5 mmol) and hexanol (2.44 mL, 19.5 mmol) in $Et_2O$ (30 mL) in a dry flask under argon. Diethyl azodicarboxylate (DEAD) (3.54 mL, 19.5 mmol) was added dropwise by syringe and the resulting pale yellow solution was stirred at room temperature for 24 h. $Et_2O$ (45 mL) was added and the solution was washed with 10% aqueous NaOH (200 mL) followed by $H_2O$ (2 × 100 mL). The solution was dried over $MgSO_4$, the solvent was removed under reduced pressure and the residue was purified by flash column chromatography (5:95 v/v ethyl acetate:hexanes) to afford **II-2b** (4.42, 95% yield) as a pale orange solid, m.p. 52 °C. $^1$H NMR (300 MHz, $CDCl_3$): δ 6.82 (s, 4H, Ar-H), 3.93 (t, $^3J_{HH}$ = 6.5 Hz, 4H,-$OCH_2$-), 1.68-1.80 (m, 2H), 1.2-1.5 (m, 18H), 0.84-0.94 (m, 6H, 2 -$CH_3$). $^{13}$C NMR (75 MHz, $CDCl_3$): δ 153.16 (Ar C1,4), 115.34 (Ar C2,3,5,6), 68.62, 31.91, 31.61, 29.66, 29.63, 29.58, 29.41, 29.39, 29.35, 26.05, 25.73, 22.68, 22.61, 14.11, 14.03. IR ($\nu$, cm$^{-1}$): 2932 (Ar C-H str.), 2917, 2870, 2848, 1510, 1474, 1463, 1395, 1381, 1284, 1240 (C-O str.), 1113, 1031, 1008, 996, 826, 771. HRMS: calc. for $C_{24}H_{42}O_2$ = 362.31848, obs. = 362.32083, Δ = 6.5 ppm.

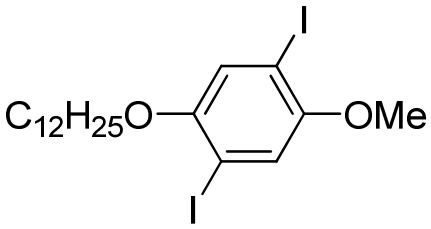


**4-Dodecyloxy-2,5-diiodoanisole, II-3a.** A solution of dialkoxybenzene **II-2a** (7.67 g, 26.3 mmol), $I_2$ (7.65 g, 29.9 mmol), $KIO_3$ (2.57 g, 12 mmol), $H_2O$ (14 mL) and $H_2SO_4$ (3.5 mL) in acetic acid (150 mL) was heated at 70 $^oC$ for 24 h. The reaction mixture was cooled, diluted with $CH_2Cl_2$ (200 mL) and washed with aqueous $Na_2SO_3$ solution. The combined extracts were washed with 10% aqueous NaOH (2 × 150 mL), dried over $MgSO_4$, and solvent was removed under reduced pressure. The residue was recrystallized twice from ethanol to afford diiodide **II-3a** (5.06 g, 35.2% yield) as white needles, m.p. = 62-64 $^oC$. $^1H$ NMR (300 MHz, $CDCl_3$): δ 7.18 (s, 1H, Ar-H), 7.17 (s, 1H, Ar-H), 3.92 (t, $^3J_{HH}$ = 6.4 Hz, 2H, -$OCH_2$-), 3.90 (s, 3H, -$OCH_3$), 1.72-1.87 (m, 2H), 1.22-1.56 (m, 18H), 0.89 (t, $^3J_{HH}$ = 6.6 Hz, 3H, -$CH_3$). $^{13}C$ NMR (75 MHz, $CDCl_3$): δ 153.88, 153.78 (Ar C1,4), 122.7, 121.80 (Ar C3,6), 86.14, 86.56 (Ar C2,5), 66.50 (-O-$CH_2$-), 53.57 (-O-$CH_3$), 29.78, 27.53, 27.50, 27.45, 27.83, 27.25, 27.21, 23.91, 20.55, 11.99. IR ($\nu$, $cm^{-1}$): 2913 (Ar C-H str.), 2848, 1483, 1469, 1462, 1434, 1381, 1349, 1266, 1212 (C-O str.), 1180, 1065, 1051, 1022, 994, 958, 921, 848, 813, 778, 757, 737, 716. HRMS: *calc*. for $C_{19}H_{30}O_2I_2$ = 544.03353, *obs*. = 544.03631, Δ = 5.1 ppm. Elemental Analysis: Theoretical = C 41.93%, H 5.56%, O 5.88%, I 46.63%; Found = C 41.99%, H 5.56%, O 5.97%, I 46.68%.

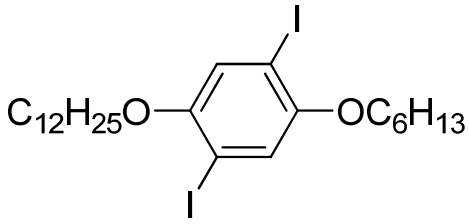


**1-Dodecyloxy-4-hexyloxy-2,5-diiodobenzene, II-3b.** (5.24 g, 80% yield) white solid, m.p. 42-44 °C. $^{1}$H NMR (300 MHz, $CDCl_3$): δ 7.18 (s, 2H, Ar-H), 3.92 (t, $^{3}J_{HH}$ = 6.4 Hz, 4H, -$OCH_2$-), 1.74-1.86 (m, 4H), 1.20-1.58 (m, 24H), 0.84-0.96 (m, 6H, 2 × -$CH_3$). $^{13}$C NMR (75 MHz, $CDCl_3$): δ 153.68 (Ar C1,4), 122.99 (Ar C3,6), 86.54 (Ar C2,5), 70.57 (-$OCH_2$-), 32.16, 31.7, 29.89, 29.83, 29.8, 29.6, 29.5, 29.38, 29.35, 26.26, 25.95, 22.94, 22.82, 14.38, 14.28. IR ($\nu$, $cm^{-1}$): 2943, 2924 (Ar C-H str.), 2847, 2359, 1485, 1456, 1387, 1348, 1264, 1209 (C-O str.), 1053, 1013, 1004, 993, 936, 850, 794. HRMS: calc. for $C_{24}H_{40}O_2I_2$ = 614.11178, obs. = 614.11330, Δ = 2.5 ppm. Elemental analysis: Theoretical = C 46.92 %, H 6.56 %, O 5.21 %, I 41.31 % Found = C 46.83 %, H 6.47 %, O 5.29 %, I 41.05 %.

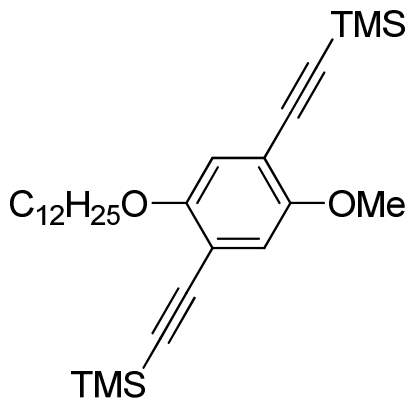


**[(2-Dodecyloxy-5-methoxy-1,4-phenylene)di-2,1-ethynediyl]bis[trimethylsilane], II-4a.** Diiodide **II-3a** (1.5 g, 2.76 mmol) was added to a stirred solution of $PdCl_2(PPh_3)_2$ (96 mg, 140 μmol) and CuI (26 mg, 136 μmol) in a mixture of piperidine (9 mL) and toluene (6 mL). The mixture was degassed by freeze-pump-thaw and back-filling with argon. Trimethylsilylacetylene (0.86 mL, 6.07 mmol) was added dropwise over 10 min and the mixture was stirred for 2 h. $CH_2Cl_2$ (100 mL) was added and the mixture was flushed through silica plug. The solvent was removed under reduced pressure to afford **II-4a** (0.97 g, 73% yield) as a pale brown solid, m.p. 71-73 °C. $^1$H NMR (300 MHz, $CDCl_3$): δ 6.90 (s, 1H, Ar-H), 6.88 (s, 1H, Ar-H), 3.95 (t, $^3J_{HH}$ = 6.1 Hz, 2H, -O-$CH_2$-), 3.90 (s, 3H, -$OCH_3$), 1.70-1.85 (m, 2H), 1.2-1.6 (m, 18H), 0.89 (t, $^3J_{HH}$ = 6.6 Hz, 3H, -$CH_3$), 0.25 (s, 18H, 2 × -$Si(CH_3)_3$). $^{13}$C NMR (75 MHz, $CDCl_3$): δ 154.05, 154 (Ar C2,5), 117.68, 115.49 (aromatic C3,6), 113.95, 113.27 (Ar C1,4), 100.84, 100.18 (-C≡C-), 69.40 (-O-$CH_2$-), 56.3(-O-$CH_3$), 31.87, 29.59, 29.39, 29.31, 25.98, 25.68, 22.65, 14.08. IR ($\nu$, $cm^{-1}$): 2955, 2922 (Ar C-H str.), 2852, 2372, 2347, 2151 (C≡C str.), 1540, 1495, 1467, 1398, 1386, 1271, 1247, 1222, 1200 (C-O str.), 1176, 1032, 939, 877, 838, 757. HRMS: calc. for $C_{29}H_{48}O_2Si_2$ = 484.31929, obs. = 484.32047, Δ = 2.4 ppm.

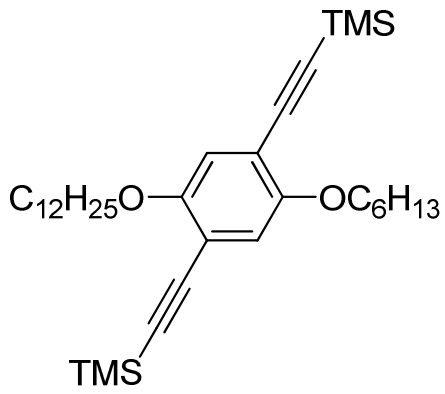


**[(2-Dodecyloxy-5-hexyloxy-1,4-phenylene)di-2,1-ethynediyl]bis[trimethylsilane], II-4b.** (79% yield) dark brown solid, m.p. 42-43°C. $^{1}$H NMR (300 MHz, $CDCl_3$): δ 6.89 (s, 2H, Ar-H), 3.95 (t, $^{3}J_{HH}$ = 6.3 Hz, 4H, -O-$CH_2$-), 1.70-1.85 (m, 4H), 1.2-1.6 (m, 24H), 0.84-0.94 (m, 6H, 2 × -$CH_3$), 0.25 (s, 18H, 2 × -Si ($CH_3$)$_3$). $^{13}$C NMR (75 MHz, $CDCl_3$): δ 153.98 (Ar C2,5), 117.15 (aromatic C3,6)), 113.89 (Ar C1,4), 101.04, 100.05 (-C≡C-), 69.40 (-O-$CH_2$-), 31.9, 31.59, 29.67, 29.63, 29.43, 29.34, 29.27, 26.01, 25.68, 22.68, 22.62, 14.11, 14.06. IR ($\nu$, cm$^{-1}$): 2954, 2922 (Ar C-H str.), 2852, 2153 (C≡C str.), 1495, 1467, 1406, 1379, 1271, 1247, 1222, 1200 (C-O str.), 1176, 1025, 939, 877, 838, 757. HRMS: calc. for $C_{34}H_{58}O_2Si_2$ = 554.39754, obs. = 554.39898, Δ = 2.6 ppm.

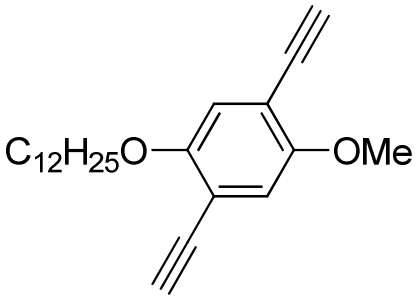


**4-Dodecyloxy-2,5-diethynylanisole, II-5a.** Tetra-*n*-butylammonium fluoride (1.15 g, 4.41 mmol) was added dropwise to a solution of bis(trimethylsilane) **II-4a** (970 mg, 2.41 mmol) in dry THF (15 mL) and the mixture was stirred overnight and poured into $H_2O$ (50 mL). The mixture was extracted with $CH_2Cl_2$ (100 mL), the combined extracts were dried over $MgSO_4$ and the solvent was removed under reduced pressure. The residue was recrystallized from ethanol to give diethyne **II-5a** (0.59 g, 85% yield) as a pale yellow solid, m.p. 71-73 °C. $^1$H NMR (300 MHz, $CDCl_3$): δ 6.97 (s, 1H, Ar-H), 6.96 (s, 1H, Ar-H), 3.97 (t, $^3J_{H1\text{-}H2}$ = 6.6 Hz, 2H, -$OCH_2$-), 3.85 (s, 3H, -$OCH_3$), 3.38 (s, 1H, -C≡H), 3.36 (s, 1H, -C≡H), 1.70-1.85 (m, 2H), 1.2-1.6 (m, 18H), 0.89 (t, $^3J_{HH}$ = 6.6 Hz, 3H, -$CH_3$). $^{13}$C NMR (75 MHz, $CDCl_3$): δ 154.52 (Ar C1,4), 118.09, 116.14 (Ar C3,6), 113.56, 112.73 (Ar C2,5), 82.81, 79.95 (-C≡C-), 69.85 (-$OCH_2$-), 56.6 (-O-$CH_3$), 32.15, 29.87, 29.81, 29.58, 29.55, 29.33, 29.29, 26.11, 22.92, 22.81, 14.36. IR ($\nu$, cm$^{-1}$): 3278 (≡C-H str.), 2943, 2918 (Ar C-H str.), 2846, 2105 (C≡C str.), 1497, 1459, 1383, 1273, 1214 (C-O str.), 1198, 1057, 1046, 1027, 1013, 985, 863. HRMS: calc. for $C_{23}H_{32}O_2$ = 340.24023, obs. = 340.24301, Δ = 8.2 ppm. Elemental Analysis: Theoretical = C 81.13%, H 9.47%, O 9.40%; Found = C 80.66 %, H 9.35 %, O 9.66 %.

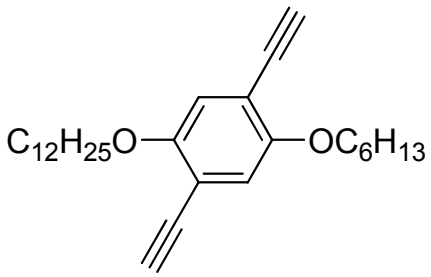


**1-Dodecyloxy-2,5-diethynyl-4-hexyloxybenzene, II-5b.** (69% yield) pale yellow solid, m.p. 62°C. $^{1}$H NMR (300 MHz, $CDCl_3$): δ 6.95 (s, 2H, Ar-H), 3.97 (t, $^{3}J_{H1\text{-}H2}$ = 6.6 Hz, 4H, -$OCH_2$-), 3.33 (s, 2H, -C≡H), 1.74-1.85 (m, 4H), 1.2-1.53 (m, 24H), 0.83-0.94 (m, 6H, 2 × -$CH_3$). $^{13}$C NMR (75 MHz, $CDCl_3$): δ 154.16 (Ar C1,4), 117.90, 117.86 (Ar C3,6), 113.41 (Ar C2,5), 82.65, 82.61 (-C≡C-), 69.85 (-O-$CH_2$-), 32.15, 31.73, 29.87, 29.81, 29.79, 29.58, 29.55, 29.33, 29.29, 26.11, 25.79, 22.92, 22.81, 14.36, 14.25. IR (*v*, $cm^{-1}$): 3283 (≡C-H str.), 2957, 2940, 2919 (Ar C-H str.), 2871, 2848, 2159 (C≡C str.), 1499, 1468, 1462, 1384, 1272, 1217 (C-O str.), 1198, 1057, 1046, 1028, 1000, 985, 863. HRMS: calc. for $C_{28}H_{42}O_2$ = 410.31848, obs. = 410.30775, Δ = 6.2 ppm. Elemental analysis: Theoretical = C 81.90 %, H 10.31 %, O 7.79 %, Found = C 81.89 %, H 10.42 %, O 7.87 %.

### 2.2.3. Synthesis of monomer 13 for preparation of regioregular PPEs

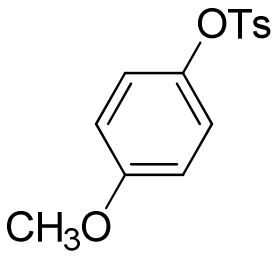


**4-Methoxyphenyl *p*-toluenesulfonate, II-6a.** Pyridine (15.80 g, 200 mmol) was added to a solution of 4-methoxyphenol (24.85 g, 200 mmol) and *p*-toluenesulfonyl chloride (38.15 g, 200 mmol) in dry THF (100 mL) and the mixture was stirred for 18 h at room temperature. The solution was washed with $H_2O$ (2 × 100 mL), dried over $MgSO_4$ and the solvent was removed under low pressure. The crude solid obtained was filtered and recrystallized from methanol to yield tosylate **II-6a** (45.3 g, 81.4 % yield) as a white solid, m.p. 71-72$^{o}$C. $^{1}$H NMR (300 MHz, $CDCl_3$): δ 7.7 (d, $^{3}J_{TosH2\text{-}TosH3}$ = 8.4 Hz, 2H, tosyl-H), 7.27 (d, $^{3}J_{TosH3\text{-}TosH2}$ = 8.4 Hz, 2H, tosyl-H), 6.87 (d, $^{3}J_{ArH2\text{-}ArH3}$ = 9.2 Hz, 2H, Ar C2,6-H), 6.75 (d, $^{3}J_{ArH2\text{-}ArH3}$ = 9.2 Hz, 2H, Ar C3,5-H), 3.75 (s, 3H, -$OCH_3$), 2.44 (s, 3H, tosyl -$CH_3$). $^{13}$C NMR (75 MHz, $CDCl_3$): δ 159.13 (Ar C4), 146.39 (Ar C1), 143.86 (tosylate C1), 133.06 (tosylate C4), 130.54, 129.23 (tosylate C2,3,5,6), 124.06, 115.21 (Ar C2,3,5,6), 56.32 (-O-$CH_3$), 22.19 (tosylate -$CH_3$). IR ($\nu$, cm$^{-1}$): 2971, 2931 (Ar C-H str.), 2903, 2840, 1591, 1498, 1456, 1442, 1383, 1345, 1309, 1293, 1248 (C-O str.), 1194, 1166, 1147, 1090, 1022, 1008, 849, 837, 815, 678, 544, 531. HRMS: *calc*. for $C_{14}H_{14}O_4S$ = 278.06128, obs. = 278.06143, Δ = 4.6 ppm.

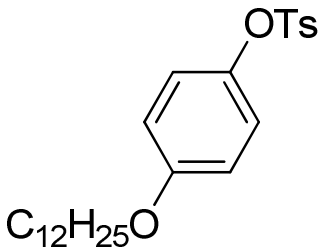


**4-Dodecyloxyphenyl *p*-toluenesulfonate, II-6b.** (89% yield) pale brown solid, m.p. 28-29°C. $^{1}$H NMR (300 MHz, $CDCl_3$): δ 7.67 (d, $^{3}J_{TosH2\text{-}TosH3}$ = 8.4 Hz, 2H, tosyl-H), 7.29 (d, $^{3}J_{TosH3\text{-}TosH2}$ = 8.6 Hz, 2H, tosyl-H), 6.85 (d, $^{3}J_{ArH2\text{-}ArH3}$ = 9.1 Hz, 2H, Ar C2,6-H), 6.7 (d, $^{3}J_{ArH2\text{-}ArH3}$ = 9.1 Hz, 2H, Ar C3,5-H), 3.87 (t, $^{3}J_{H}$ = 6.5 Hz, 2H, -$OCH_2$-), 2.43 (s, 3H, tosyl -$CH_3$), 1.70-1.85 (m, 2H), 1.65-1.80 (m, 18H), 0.87 (t, $^{3}J_{H11\text{-}H12}$ = 6.7 Hz, 3H, -$CH_3$). $^{13}$C NMR (75 MHz, $CDCl_3$): δ 157.71 (Ar C1), 145.78 (Ar C4), 145.13 (tosylate C1), 132.25 (tosylate C4), 129.61, 128.27 (tosylate C2,3,5,6), 123.19, 114.85 (Ar C2,3,5,6), 68.26 (-O-$CH_2$-), 31.84, 29.58, 29.56, 29.52, 29.49, 29.37, 29.30, 29.28, 29.10, 25.92, 22.61, 14.05. IR ($\nu$, $cm^{-1}$): 2921 (Ar C-H str.), 2851, 1596, 1500, 1467, 1373, 1295, 1248 (C-O str.), 1195, 1168, 1152, 1092, 1008, 865, 835, 811. HRMS: calc. for $C_{25}H_{36}O_4S$ = 432.23343, obs. = 432.23521, Δ = 2.0 ppm.

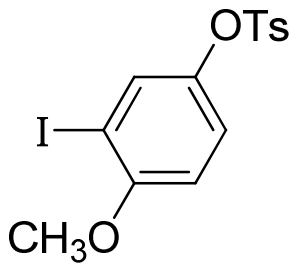


**3-Iodo-4-methoxyphenyl *p*-toluenesulfonate, II-7a.** Tosylate **II-6a** (38.05 g, 136.87 mmol) was added to a stirred mixture of $I_2$ (27.80 g, 109.45 mmol), sulfuric acid (5 mL), $CCl_4$ (27 mL), water (32 ml) and acetic acid (65 mL). $KIO_3$ (11.72 g, 54.77 mmol) was added and the mixture was heated at reflux for 48 hours. The reaction was cooled to room temperature and chloroform (70 mL) was added. The solution was washed with saturated aqueous $Na_2SO_3$ (200 mL). followed by 10% (w/w) aqueous NaOH (2 × 200 mL), and dried over $MgSO_4$. The solvent was removed under reduced pressure to give a brown solid. The residue was recrystallized from methanol to give iodide **II-7a** (50.02 g, 90.6% yield) as a white solid, m.p. 84-85$^{o}$C. $^{1}$H NMR: δ 7.68 (d, $^{3}J_{\text{TosH2-TosH3}}$ = 8.4 Hz, 2H, tosyl Ar-H), 7.34-7.37 (m, 3H, tosyl 2H and Ar C2-H), 6.93 (dd, $^{3}J_{\text{ArH6-ArH5}}$ = 8.9 Hz, $^{4}J_{\text{ArH6-ArH2}}$ = 2.8 Hz, 1H, Ar C6-H), 6.72 (d, $^{3}J_{\text{ArH5-ArH6}}$ = 9.0 Hz, 1H, Ar C5-H), 3.83 (s, 3H, -$OCH_3$), 2.45 (s, 3H, tosyl -$CH_3$). $^{13}$C NMR: δ 158.01 (Ar C4), 146.71 (Ar C1), 143.83 (tosylate C1), 133.92 (tosylate C4), 132.69, 130.64 (tosylate C2,3,5,6), 129.27, 124.01, 111.33 (Ar C2,6,5), 85.6 (Ar C3), 57.5 (-O-$CH_3$), 22.23 (tosylate -$CH_3$). IR ($\nu$, cm$^{-1}$): 3098, 2975, 2948 (Ar C-H str.), 2843, 2364, 2159, 2022, 1595, 1578, 1478, 1450, 1439, 1392, 1381, 1289, 1267 (C-O str.), 1179, 1156, 1120, 1088, 1040, 1016, 872. HRMS: *calc*. for $C_{14}H_{13}I_1O_4S$ = 403.95793, *obs*. = 403.95692. Δ = 2.7 ppm.

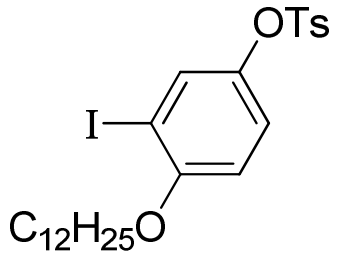


**4-Dodecyloxy-3-iodophenyl *p*-toluenesulfonate, II-7b.** (71% yield) viscous, brown oil. $^{1}$H NMR (300 MHz, $CDCl_3$): δ 7.68 (d, $^{3}J_{TosH2\text{-}TosH3}$ = 8.4 Hz, 2H, tosyl Ar-H), 7.29-7.34 (m, 3H, 2 tosyl H, 1 Ar C2-H), 6.92 (dd, $^{3}J_{ArH6\text{-}ArH5}$ = 8.9 Hz, $^{4}J_{ArH6\text{-}ArH2}$ = 2.8 Hz, 1H, Ar C6-H), 6.64 (d, $^{3}J_{ArH2\text{-}ArH3}$ = 8.9 Hz, 1H, Ar C5-H), 3.94 (t, $^{3}J_{H1\text{-}H2}$ = 6.37 Hz, 2H, -$OCH_2$-), 2.45 (s, 3H, tosyl -$CH_3$), 1.54-1.58 (m, 2H), 1.1-1.6 (m, 18H), 0.87 (t, $^{3}J_{H11\text{-}H12}$ = 6.7 Hz, 3H, -$CH_3$). $^{13}$C NMR (75 MHz, $CDCl_3$): δ 156.54 (Ar C4), 145.45 (Ar C1), 142.76 (tosyl C1), 133 (tosyl C4), 131.96 , 129.72 (tosyl C2,3,5,6), 128.51, 123.07, 111.25 (Ar C-H), 85.61 (Ar C-I), 69.61 (-O-$CH_2$-), 31.86, 29.59, 29.52, 29.49, 29.3, 29.22, 29.15, 28.94, 25.97, 22.64, 21.67, 14.08. IR ($\nu$, $cm^{-1}$): 2920 (Ar C-H str.), 2850, 1596, 1577, 1482, 1464, 1375, 1288, 1262 (C-O str.), 1193, 1179, 1160, 1092, 1035, 877, 810. HRMS: calc. for $C_{25}H_{35}O_4SI$ = 558.13008 obs. = 558.12539, Δ = 8.4 ppm.

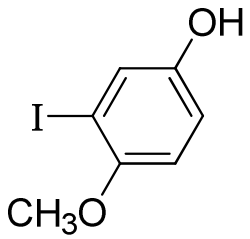


**3-Iodo-4-methoxyphenol**, **II-8a**. A solution of monoiodinated tosylate **II-7a** (15.00 g, 37.04 mmol) in *t*-butanol (20 mL) was bubbled with argon for 20 min. A degassed solution of 20% aqueous NaOH (20 ml) was added under argon and the mixture was heated at reflux for 24 h. The reaction mixture was cooled and washed with 10% HCl (50 mL) followed by $H_2O$ (2 × 100 mL) and dried over $MgSO_4$. The solvent was removed under reduced pressure and the residue was subjected to flash chromatography ($CH_2Cl_2$) to afford phenol **II-8a** (7.49g, 80.61% yield) as a white solid, m.p. 105-106 $^oC$. $^1H$ NMR (300 MHz, $CDCl_3$): δ 7.28 (d, $^4J_{ArH2\text{-}ArH6}$ = 2.9 Hz, 1H, aromatic C2-H), 6.81 (dd, $^3J_{ArH5\text{-}ArH6}$ = 8.8 Hz, $^4J_{ArH2\text{-}ArH6}$ = 2.9 Hz, 1H, Ar C6-H), 6.73 (d, $^3J_{ArH5\text{-}ArH6}$ = 8.8 Hz, 1H, Ar C5-H), 4.83 (bs, 1H, OH), 3.78 (s, 3H, -$OCH_3$). $^{13}C$ NMR (75 MHz, $CDCl_3$): δ 153.64, 150.95 (Ar C1,4), 126.95 (Ar C2), 116.78 (Ar C6), 112.67 (Ar C5), 86.50 (Ar C3), 57.72 (-O-$CH_3$). IR ($\nu$, $cm^{-1}$): 3174 (O-H), 3058, 3013, 2965, 2943, 2910 (Ar C-H str.), 2838, 2662, 1583, 1485, 1453, 1431, 1277, 1266, 1240, 1205 (C-O str.), 1184, 1150, 1140, 1129, 1043, 1012, 919, 877, 861, 598, 138, 698, 664, 570, 556. HRMS: *calc*. for $C_7H_7O_2I$ = 249.94908, *obs*. = 249.95123. Δ = 3.8 ppm.

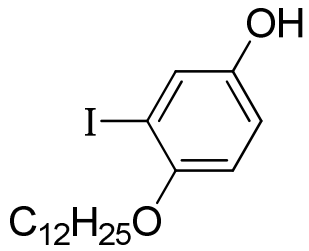


**4-Dodecyloxy-3-iodophenol, II-8b**. (88% yield) pale yellow oil. $^{1}$H NMR (300 MHz, $CDCl_3$): δ 7.29 (d, $^{4}J_{ArH2\text{-}ArH6}$ = 2.89 Hz, 1H, Ar C2-H), 6.78 (dd, $^{3}J_{ArH5\text{-}ArH6}$ = 8.8 Hz, $^{4}J_{ArH2\text{-}ArH6}$ = 2.9 Hz, 1H, Ar C6-H), 6.68 (d, $^{3}J_{ArH5\text{-}ArH6}$ = 8.8 Hz, 1H, Ar C5-H), 6.0-6.25 (bs, 1H, OH), 3.92 (t, $^{3}J_{H1\text{-}H2}$ = 6.4 Hz, 2H, -$OCH_2$-), 1.73-1.85 (m, 2H), 1.2-1.6 (m, 18H), 0.89 (t, $^{3}J_{H11\text{-}H12}$ = 6.6 Hz, 3H, -$CH_3$). $^{13}$C NMR (75 MHz, $CDCl_3$): δ 152.45, 150.38 (Ar C1,4), 126.4 (Ar C2), 116.33 (Ar C6), 113.8 (Ar C5), 87.3 (Ar C3), 70.68 (-O-$CH_2$-), 32.19, 29.94, 29.92, 29.87, 29.85, 29.63, 29.6, 29.51, 26.34, 22.97, 14.4. IR (*v*, $cm^{-1}$): 3348 (O-H), 2920 (Ar C-H str.), 2850, 1701, 1600, 1583, 1487, 1465, 1434, 1388, 1377, 1273, 1206 (C-O str.), 1145, 1033, 1008, 906, 861, 799, 779. HRMS: calc. for $C_{18}H_{29}O_2I$ = 404.12123, obs. = 404.12155, Δ = 0.8 ppm.

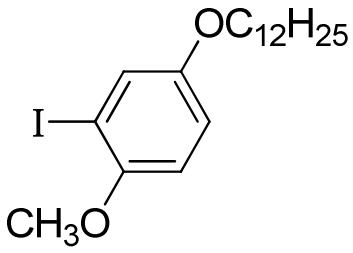


**4-Dodecyloxy-2-iodoanisole, II-9a.** NaH (60% dispersion in oil, 191 mg, 4.8 mmol) was added slowly to a solution of monoiodinated phenol **II-8a** (1.00 g, 3.98 mmol) in dry THF (50 mL) and the mixture was stirred for 15 minutes. 1-Bromododecane (1.19 g, 4.8 mmol) was added dropwise by syringe and the reaction mixture was heated at reflux for 12 h. The mixture was cooled and diluted with water (50 mL) and then extracted with $CHCl_3$ (2 × 100 mL). The solution was dried over $MgSO_4$ and the solvent was removed under low pressure to give a pale yellow oil. The residue was subjected to flash chromatography (25:75 v/v $CH_2Cl_2$/hexane) to afford **II-9a** (360 mg, 21.6 % yield) as a clear oil. $^1$H NMR (300 MHz, $CDCl_3$): δ 7.32 (d, $^4J_{ArH3\text{-}ArH5}$ = 2.8 Hz, 1H, Ar C3-H), 6.85 (dd, $^3J_{ArH5\text{-}ArH6}$ = 8.9 Hz, $^4J_{ArH3\text{-}ArH5}$ = 2.8 Hz, 1H, Ar C5-H), 6.74 (d, $^3J_{ArH5\text{-}ArH6}$ = 8.9 Hz, 1H, Ar C6-H), 3.88 (t, $^3J_{H1\text{-}H2}$ = 5.4 Hz, 2H, -$OCH_2$-), 3.82 (s, 3H, -$OCH_3$), 1.68-1.80 (m, 2H), 1.40-1.52 (m, 18H), 0.86 (t, $^3J_{H11\text{-}H12}$ = 6.1 Hz, 3H, -$CH_3$). $^{13}$C NMR (75 MHz, $CDCl_3$): δ 153.78, 152.50 (Ar C1,4), 125.50, 115.30, 111.51 (Ar C3,5,6), 85.94 (Ar C2), 68.82 (-O-$CH_2$-), 56.93 (-O-$CH_3$), 31.89, 29.54, 29.31, 29.22, 25.97, 22.65, 14.11. IR (*v*, $cm^{-1}$): 2920 (Ar C-H str.), 2851, 2372, 2348, 2326, 1622, 1616, 1600, 1569, 1575, 1549, 1542, 1467, 1437, 1419, 1393, 1269, 1210 (C-O str.), 1180, 1151, 1047, 1013, 921, 864, 843, 800, 748, 721, 664, 551. HRMS: *calc*. for $C_{19}H_{31}O_2I$ = 418.13688, *obs*. = 418.14106. Δ = 3.6 ppm.

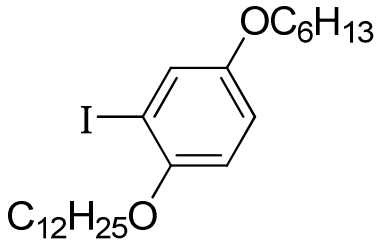


**1-Dodecyloxy-4-hexyloxy-2-iodobenzene, II-9b.** Monoiodinated phenol, **II-8b** (2.55 g, 6.30 mmol) was added to a stirred solution of $PPh_3$ (1.65 g, 7.55 mmol) and 1-hexanol (0.80 ml, 7.6 mmol) in $Et_2O$ (40 mL) under Ar. Diethyl azodicarboxylate (DEAD) (1.15 mL, 7.55 mmol) was added dropwise by syringe and the resulting pale yellow solution was stirred at room temperature for 24 h. $Et_2O$ (60 mL) was added and the solution was washed with 10% aqueous NaOH (200 mL) followed by $H_2O$ (100 mL). The solution was dried over $MgSO_4$, the solvent was removed under reduced pressure, and the residue was subjected to flash column chromatography (20:80 v/v ethyl acetate:hexanes) to afford **II-9b** (2.80 g, 91% yield) pale yellow oil. $^1$H NMR (300 MHz, $CDCl_3$): δ 7.33 (d, $^4J_{HH}$ = 2.90 Hz, 1H, Ar C3-H), 6.83 (dd, $^3J_{HH}$ = 8.9 Hz, $^4J_{HH}$ = 2.9 Hz, 1H, Ar C5-H), 6.71 (d, $^3J_{HH}$ = 8.9 Hz, 1H, Ar C6-H), 3.93 (t, $^3J_{HH}$ = 6.4 Hz, 2H, -$OCH_2$-), 3.87 (t, $^3J_{HH}$ = 5.4 Hz, 2H, -$CH_2$-), 1.65-1.85 (m, 4H), 1.20-1.58 (m, 24H), 0.84-0.94 (m, 6H, 2 × -$CH_3$). $^{13}$C NMR (75 MHz, $CDCl_3$): 153.97 (Ar C-O), 125.55, 115.62, 113.30 (Ar C-H), 87.22 (Ar C-I), 70.39, 69.05 (-O-$CH_2$-), 31.91, 31.59, 29.66, 29.62, 29.42, 29.34, 29.26, 26.01, 25.67, 22.68, 22.62, 14.11, 14.06. IR ($\nu$, $cm^{-1}$): 2920 (Ar C-H str.), 2851, 2030, 1733, 1597, 1568, 1486, 1466, 1387, 1350, 1271, 1209 (C-O str.), 1106, 1062, 935, 850, 801, 770, 721. HRMS: calc. for $C_{24}H_{41}O_2I$ = 488.21513, obs. = 488.21704, Δ = 3.9 ppm.

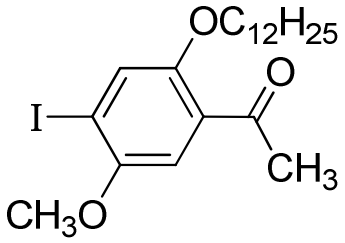


**2-Dodecyloxy-4-iodo-5-methoxyacetophenone II-10.** Monoiodinated diether **II-9a** (720 mg, 1.72 mmol) was dissolved in dry $CH_2Cl_2$ followed by the addition of acetyl chloride (148.52 mg, 1.89 mmol) and the solution was cooled to $0^oC$. $AlCl_3$ (251.63 mg, 1.89 mmol) was added in two parts to the above solution under nitrogen and the mixture was then allowed to warm to room temperature and stir for 2 h. The reaction was quenched by pouring it into a 1:10 w/w mixture of ice / conc. HCl. The organics was extracted with dichloromethane (2 × 50 mL), dried over $MgSO_4$ and the solvent was removed under low pressure to yield a crude solid. The residue was purified by recrystallization from hexane to afford acetophenone **II-10** (450 mg, 89.5%) as a yellow solid. m.p. = 110-111 $^oC$. $^1H$ NMR (300 MHz, $CDCl_3$): δ 7.38 (s, 1H, Ar C3-H), 7.22 (s, 1H, Ar C6-H), 4.07 (t, $^3J_{HH}$ = 6.5 Hz, 2H, -$OCH_2$-), 3.85 (s, 3H, -$OCH_3$), 2.60 (s, 3H, -$COCH_3$), 1.75-1.88 (m, 2H), 1.18-1.56 (m, 18H), 0.80-0.92 (t, $^3J_{HH}$ = 6.2 Hz, 3H, -$CH_3$). $^{13}C$ NMR (75 MHz, $CDCl_3$): δ 203.5 (-C = O), 156.6 (Ar C2), 150.7 (Ar C5), 129.5, 119.0 (Ar C1,3), 109.9 (Ar C6), 97.8 (Ar C4), 57.1 (-O-$CH_2$-), 26.6. IR ($\nu$, $cm^{-1}$): 2946, 2915, 2868, 2846 (Ar C-H str.), 1659 (C = O str.), 1586, 1556, 1482, 1463, 1375, 1266, 1207 (C-O str), 1171, 1075, 1041, 1023, 1001, 986, 908, 867, 841, 795, 731, 721, 696, 599. HRMS: *calc*. for $C_9H_9O_3I$ = 460.14744, *obs*. = 460.14745. Δ = 2.6 ppm**.**

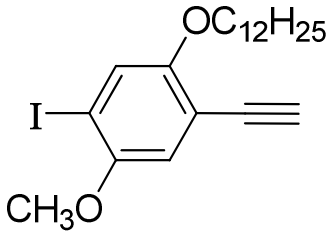


**Negishi-Tour procedure to prepare 4-Dodecyloxy-5-ethynyl-2-iodoanisole, II-13a.** A solution of LDA in THF (0.17 g, 1.55 mmol) was added dropwise to a solution of acetophenone **II-10** (0.68 g, 1.5 mmol) in dry THF (40 mL) at 0 $^{o}$C. The resulting yellow solution was stirred for 15 min and diethyl chlorophosphate (267 mg, 1.55 mmol) was added dropwise. The mixture was allowed to warm to room temperature and was stirred for 3 h. The solution was cooled to 0 $^{o}$C and a solution of LDA in THF (0.365g, 3.325 mmol) was added. The mixture was stirred for 3 h and $H_2O$ (5 mL) was added. The mixture was extracted with EtOAc and the combined extracts were dried over $MgSO_4$. The solvent was removed under reduced pressure to give yellow oil. The residue was subjected to column chromatography (10:90 v/v ethyl acetate/hexanes) to afford ethyne **II-13a** (200 mg, 30.5% yield) as a colorless oil. $^{1}$H NMR (300 MHz, $CDCl_3$): δ 7.30 (s, 1H, Ar C3-H), 6.88 (s, 1H, Ar C6-H), 3.97 (t, $^{3}J_{HH}$ = 6.6 Hz, 2H, -$OCH_2$-), 3.82 (s, 3H, -$OCH_3$), 3.31 (s, 1H, ≡C-H), 1.74-1.84 (m, 2H), 1.20-1.58 (m, 18H), 0.88 (t, $^{3}J_{HH}$ = 6.6 Hz, 3H, -$CH_3$). $^{13}$C NMR (75 MHz, $CDCl_3$): δ 155.21 (Ar C4), 152.50 (Ar C1), 124.62 (Ar C3), 115.82 (Ar C6), 112.90 (Ar C5), 87.46 (Ar C2), 81.77, 79.70 (-C≡C-), 70.27 (-O-$CH_2$-), 57.05 (-O-$CH_3$), 37.16, 31.87, 29.53, 29.29, 25.88, 22.59, 13.96. IR ($\nu$, cm$^{-1}$): 3289 (≡C-H str.), 2920 (Ar C-H str.), 2850, 2372, 2348, 2326, 1516, 1463, 1368, 1269, 1214 (C-O str.), 1140, 1045, 911, 857, 811, 733, 703, 672, 617, 604. HRMS: *calc*. for

$C_{21}H_{31}O_2I$ = 442.13688, *obs*. = 442.13023. Δ = 4.9 ppm. Elemental analysis: Theoretical = C 57.02 %, H 7.06 %, O 7.23 %, Found = C 57.37 %, H 7.18 %, O 7.58 %.

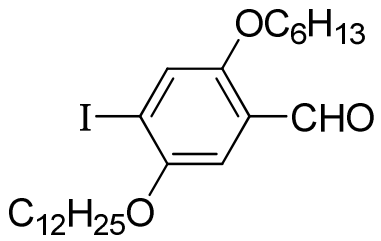


**5-Dodecyloxy-2-hexyloxy-4-iodobenzaldehyde, II-14.** $TiCl_4$ (11.7 g, 61.4 mmol) was added dropwise to a solution of monoiodinated diether **II-9b** (5.0 g, 10 mmol) in dry $CH_2Cl_2$ (50 mL) at -40 °C in a dry flask under Ar. The mixture was stirred for 15 min at -40 °C and dichloromethyl methyl ether (2.35 g, 20.5 mmol) was added dropwise and stirring was continued for another 2h. The reaction mixture was poured into mixture of conc. HCl and ice. The mixture was extracted with $CH_2Cl_2$ (100 mL) and the extract was washed with water (100 mL). The organic layer was dried over $MgSO_4$ and the solvent was removed under reduced pressure. Column chromatography (silica gel, 30% $CH_2Cl_2$/hexanes) afforded **II-14** as a white solid (2.91 g, 55 % yield), m.p. = 57°C. $^1$H NMR (300 MHz, $CDCl_3$): δ 10.40 (s, 1H, -CHO), 7.43 (s, 1H, Ar C3-H), 7.16 (s, 1H, Ar C6-H), 3.95-4.02 (m, 4H, -$OCH_2$-), 1.77-1.81 (m, 4H), 1.24-1.44 (m, 24H), 0.85-0.88 (m, 6H, 2 × -$CH_3$). $^{13}$C NMR (75 MHz, $CDCl_3$): δ 189.28 (-CHO), 155.77 (Ar C2), 152.12 (Ar C5), 125.11 (Ar C1), 124.51 (Ar C3), 108.81 (Ar C6), 96.78 (Ar C4), 69.90, 69.44 (-O-$CH_2$-), 31.90, 31.45, 29.63, 29.56, 29.54, 29.34, 29.26, 29.04, 29.00, 26.02, 25.66, 22.68, 22.54, 14.12, 14.00. IR ($\nu$, cm$^{-1}$): 2912 (Ar C-H str.), 2847, 1670 (C = O str.), 1587, 1458, 1383, 1213 (C-O str.), 1032, 867, 827, 748, 715, 611. HRMS: calc. for $C_{25}H_{41}O_3I$ = 516.20893, obs. = 516.20592, Δ = 5.8 ppm.

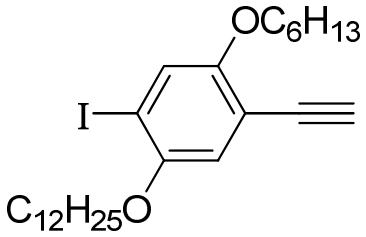


**Bestman homologation to prepare 1-Dodecyloxy-5-ethynyl-4-hexyloxy-2-iodobenzene, II-13b.** Bestman-Ohiro reagent, $)CH_3COC(=N_2)PO(CH_3O)_2$ (0.45 g, 2.3 mmol), was added dropwise to a mixture of aldehyde **II-14** (0.5 g, 0.9 mmol) and $K_2CO_3$ (0.19 g, 1.4 mmol) in 12 mL of a 1:5 v/v mixture of anhydrous $CH_2Cl_2$ and MeOH under argon and the mixture was stirred for 10 h. The solvent was removed under reduced pressure to obtain a pale yellow residue which was recrystallized from isopropanol to give ethyne **II-13b** (0.22 g, 49 % yield) as a white solid, m.p. = 39-41 °C. $^1$H NMR (300 MHz, $CDCl_3$): δ 7.28 (s, 1H, Ar C3-H), 6.86 (s, 1H, Ar C6-H), 3.92-3.95 (m, 4H, -$OCH_2$), 3.29 (s, 1H, -C≡C-H), 1.76-1.81 (m, 4H), 1.26-1.48 (m, 24H) 0.85-0.92 (m, 6H, 2 × -$CH_3$). $^{13}$C NMR (75 MHz, $CDCl_3$): δ 154.81 (Ar C4), 151.65 (Ar C1), 123.73 (Ar C3), 116.64 (Ar C6), 112.19 (Ar C5), 88.28 (Ar C2), 81.74, 79.64 (-C≡C-), 70.04, 69.83(-O-$CH_2$-), 31.90, 31.46, 29.62, 29.56, 29.33, 29.27, 29.10, 29.04, 26.02, 25.52, 22.68, 22.54, 14.11, 13.99. IR ($\nu$, cm$^{-1}$): 3269 (C-H str), 2953 (Ar-H str.), 2914, 2845, 2091 (C≡C str), 1473, 1465, 1371, 1209 (C-O str.), 1026, 856, 818, 725, 687, 642. HRMS: calc. for $C_{26}H_{41}O_2I$ = 512.21402, obs. = 512.2139, Δ = 1.0 ppm. Elemental analysis: Theoretical: C, 60.93%; H, 8.06%; I, 24.76; O, 6.24%; Found: C, 60.92%; H, 7.94%; I, 24.61%; O, 6.29%.

### 2.2.4. Synthesis of regiorandom and regioregular PPEs

**Regiorandom dodecyloxy/methoxy, RnPPE(12/1).** A solution of monomers **II-3a** (379 mg, 718 μmol) and **II-5a** (251 mg, 718 μmol), $Pd(PPh_3)_4$ (40.2 mg, 34.9 μmol) and CuI (8.0 mg, 40 μmol) in a mixture of morpholine (16 mL) and diisopropylamine (4 mL) was heated at 70 °C for 4 d. The mixture was poured into 50 mL of acetone and the precipitated solid was removed by filtration. The solid was then subjected to sequential extractions in a Soxhlet extractor with MeOH, acetone, and hexanes, followed by $CHCl_3$. The solvent was removed from the $CHCl_3$ fraction and the residue (380 mg, 79% yield) was characterized. GPC (THF, UV-vis detector): 18.1 kD, PDI = 3.7. NMR: see discussion. IR ($\nu$, $cm^{-1}$): 2918, 2849, 1511, 1494, 1413, 1387, 1274, 1212, 1030, 862, 720.

**Regiorandom dodecyloxy/hexyloxy, RnPPE(12/6).** A solution of monomers **II-3b** (500 mg, 814 μmol) and **II-5b** (345 mg, 838 μmol), $Pd(PPh_3)_4$ (47.2 mg, 34.9 μmol) and CuI (10 mg, 42 μmol) in a mixture of morpholine (16 mL) and diisopropylamine (4 mL) was heated at 70 °C for 4 days. Work up according to the procedure described above for **RnPPE(12/1)** gave **RnPPE(12/6)** as a yellow-orange solid (412 mg, 60 % yield) was obtained. GPC (THF, UV-vis detector): 37.8 kD, PDI = 3.7. NMR: see discussion. IR ($\nu$, $cm^{-1}$): 2918, 2849, 1511, 1494, 1413, 1387, 1274, 1212, 1030, 862, 720.

**Regioregular dodecyloxy/methoxy, RgPPE(12/1).** A-B type monomer **II-13a** (300 mg, 677 μmol) was treated with $Pd(PPh_3)_4$ (37.3 mg, 33.6 μmol) and CuI (7 mg, 36.8 μmol) in morpholine/diisopropylamine as described above. Precipitation and extraction as described above for **RnPPE(12/1)** gave a $CHCl_3$ soluble fraction (150 mg, 70% yield) that was characterized further. GPC (THF, UV-vis detector): 11.56 kD, PDI = 2.5. NMR: see discussion. IR (AT-IR, neat): 2918, 2849, 1511, 1494, 1413, 1386, 1275, 1211, 1030, 859, 720.

**Regioregular dodecyloxy/hexyloxy, RgPPE(12/6).** A solution of monomer **II-13b** (428 mg, 0.84 mmol), toluene (10 mL) and diisopropylamine (2 mL) were added to a 50 mL flask and degassed via freeze/pump/thaw. $Pd(PPh_3)_4$ (50.0 mg, 0.86 mmol) and CuI (8.0 mg, 0.84 mmol) were added to the solution. The mixture was stirred at 60 °C for 2 days. Precipitation from MeOH and sequential extractions in a Soxhlet extractor with acetone, hexanes and chloroform gave a chloroform fraction as an orange solid (261 mg, 81% yield). GPC (THF, UV-vis detector): 15.12 kD NMR: see discussion. IR (AT-IR, neat): 2920, 2852, 2370, 1514, 1428, 1388, 1277, 1213, 1045, 858, 725.

## 2.3. RESULTS AND DISCUSSION

To fully explore the synthesis of regioregular unsymmetrically substituted PPEs we prepared and characterized both regioregular (Rg) and regiorandom (Rn) analogs of poly(2,5-dialkoxy-1,4-phenylene ethynylene)s bearing dodecyloxy, hexyloxy and methoxy side chains, Figure 2.3. A symmetrically-substituted analog with two dodecyloxy side chains was prepared for comparison. Regiorandom polymers were prepared by polymerization of suitably substituted diiodoarenes and diethynylarenes (i.e., combination of two difunctional monomers A-A and B-B), Figure 2.1C. The regioregular analogs were synthesized by polymerization of a single 2,5-disubstituted 4-iodophenylene acetylene (i.e., a single A-B type monomer), Figure 2.2.

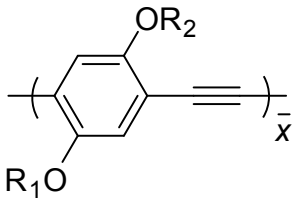


| | *regiorandom* | *regioregular* |
|---|---|---|
| $R_1$ = *n*-$C_{12}H_{25}$; $R_2$ = $CH_3$ | **RnPPE(12/1)** | **RgPPE(12/1)** |
| $R_1$ = *n*-$C_{12}H_{25}$; $R_2$ = *n*-$C_6H_{13}$ | **RnPPE(12/6)** | **RgPPE(12/6)** |
| $R_1$ = $R_2$ = *n*-$C_{12}H_{25}$ | | **PPE(12)** |

**Figure 2.3.** Regioregular (Rg) and regiorandom (Rn) poly(phenylene ethynylyne)s, **PPE(*m*/*n*)**, examined in this study.

### 2.3.1. Synthesis of the Monomers and Polymerization.

***Synthesis of regiorandom PPEs from A-A and B-B type monomers.*** Regiorandom PPEs were prepared by the palladium-catalyzed cross-coupling condensation of 2,5-dialkoxy-1,4-diiodobenzenes **II-3** and 2,5-dialkoxy-1,4-diethynylbenzenes **II-5**, Figure 2.4. The monomers were prepared using well-precedented procedures. 1,4-dialkoxybenzene **II-2** were synthesized from their respective phenols by either Williamson's synthesis or Mitsunobu coupling. The dialkoxybenzenes were then subjected to diiodination ($I_2$, $KIO_3$, $H_2SO_4$, AcOH) to afford **II-3**. The dioiodo compounds were then treated with TMS-acetylene in presence of $Pd(PPh_3)_4$ and CuI to form the bistrimethylsilyl dialkoxy benzenes **II-4**, The TMS groups were removed using *n*-$Bu_4NF$ to form the dialkyne monomer **II-5**.

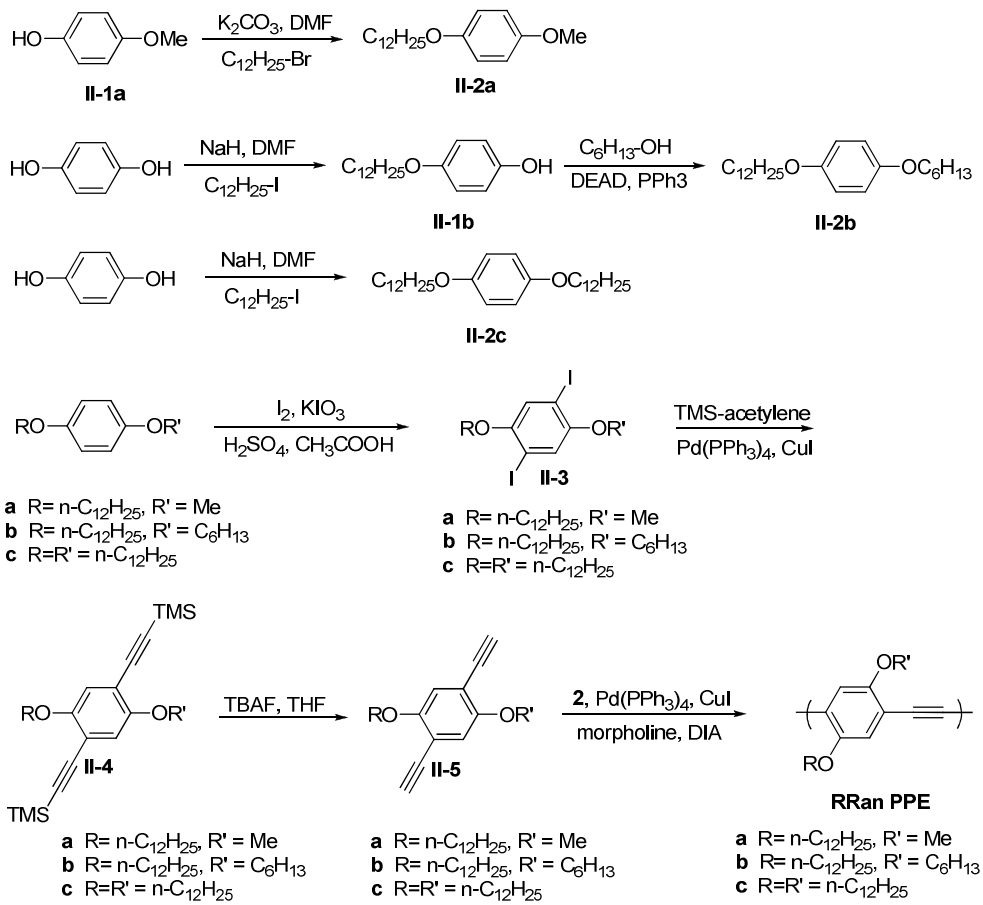


**Figure 2.4.** Preparation of regiorandom polymers **RnPPE(m/n)** by polymerization of diiodobenzene **II-3** and diethynylbenzene **II-5**.

***Synthesis of regioregular PPEs by polymerization of A-B type monomers.*** The preparation of the regioregular *ht* unsymmetrically substituted alkoxy PPEs relies on the synthesis of A-B type monomer **II-13** bearing both the iodo and ethynyl substituents, Figure 2.5. The substitution pattern of the A-B monomer sets the relative placement of the substituents in the resulting polymer. There is a challenge of installing the iodo and ethynyl substituents in specific positions adjacent to two dissimilar alkoxy substituents. This was achieved by tosylation of 4-alkoxyphenol **II-1** (TsCl, pyridine) to provide **II-6** in which the tosyl group lowers the electron donating ability of the oxygen. This assures that subsequent iodination takes place ortho to the alkoxy group, resulting in the monoiodinated tosylate **II-7**.[26] The tosylate group was then removed by base promoted hydrolysis to afford the monoiodinated phenol **II-8**. Alkylation of the 4-alkoxy-3-iodophenol using a Mitsunobu reaction (*n*-alcohol, DEAD, $Ph_3P$) or by Williamson ether synthesis (NaH, alkyl bromide) provided the 1,4-dialkoxy-2-iodobenzenes **II-9**, Figure 2.5.

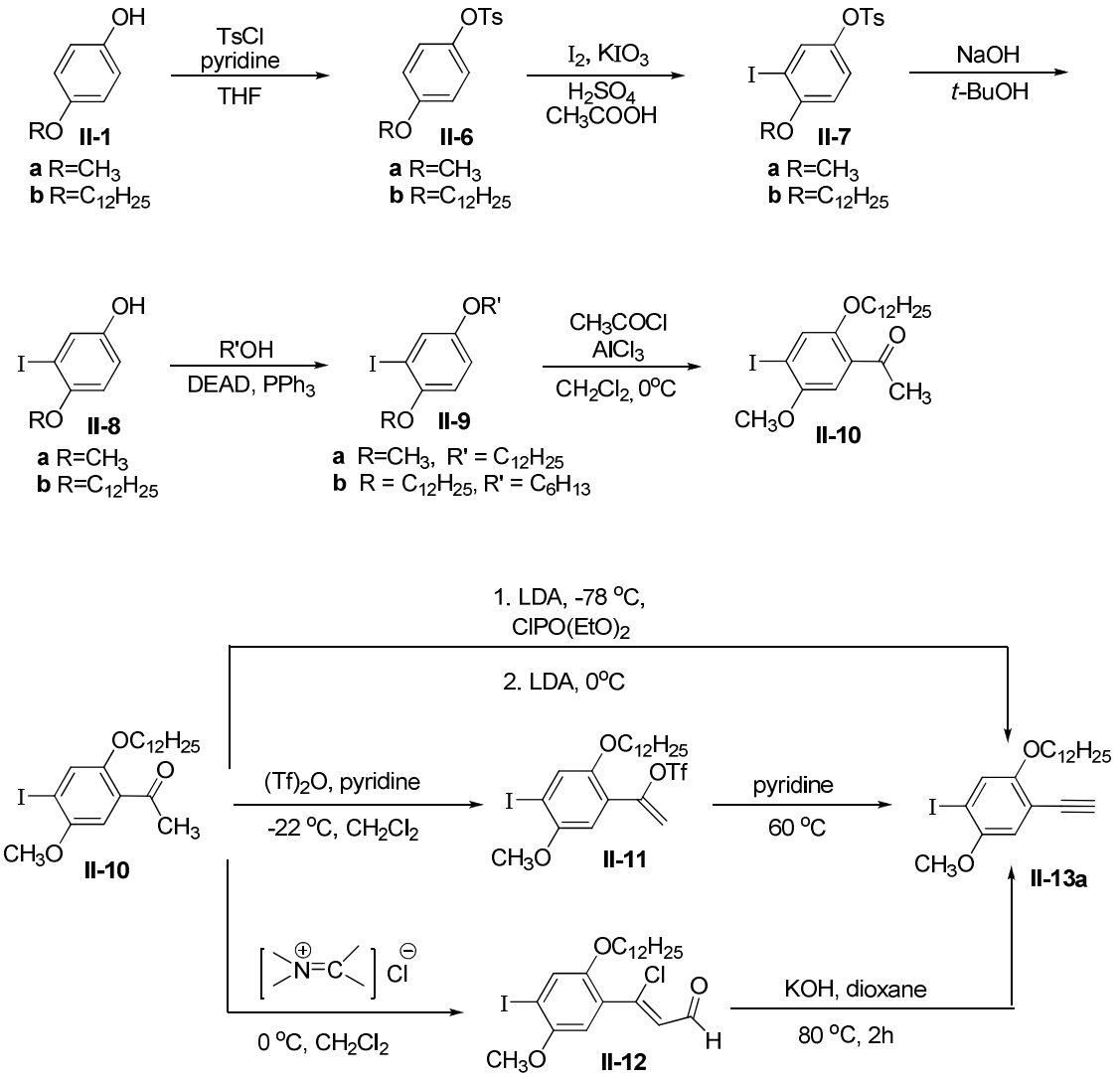


**Figure 2.5.** Synthesis of A-B monomer for the preparation of regioregular dodecyloxy/methoxy polymer, **RgPPE(12/1)**

Our initial synthesis of the 4-iodophenylacetylene monomer **II-13a** made use of Friedel-Crafts acetylation followed by dehydration of the resulting acetophenone. Friedel-Crafts acylation[27] (AcCl, $AlCl_3$) affords the acetophenone derivative **10** in good yield, with the desired substitution pattern arising from the ortho/para electronic directing effects and steric bulk of the iodine, Figure 2.5. We attempted several methods to efficiently convert the methyl ketone **10** into an ethynyl group. We initially used Stang's base-promoted elimination for an enol triflate[28] whereby the acetyl group is converted to an enol triflate and subsequent elimination is promoted by pyridine. Treatment of the acetophenone **II-10** with triflic anhydride in the presence of pyridine at -22 $^{o}$C gives triflate **II-11**, which on heating with excess pyridine at 60 $^{o}$C undergoes elimination to give the alkyne **II-13a**, Figure 2.5. However preparation of the vinyl triflate proceeded with low conversion (25 to 40 %). The in-situ conversion of the triflate to the alkyne resulted in the formation of number of side-products which were inseparable by column chromatography. Attempts to isolate the triflate were thwarted by rapid hydrolysis. In a related approach to prepare the alkyne we attempted the Vilsmeier haloformylation[29] of the acetyl group followed by a KOH-promoted Bodendorf reaction.[30] Reaction of benzophenone **II-10** with excess Vilsmeier complex at 0 $^{o}$C formed a mixture of E and Z β-chloroaldehydes **II-12** (Figure 2.5) with high conversion (90%). The mixture of β-chloroaldehydes was treated in-situ with KOH, resulting in complete conversion to the alkyne. However, analysis of the product (after separation by column chromatography) by $^{1}$H NMR spectroscopy and mass spectrometry revealed the presence of considerable amount (as much as 25 %) of the analogous 4-chlorophenylacetylene in which the iodo-substituent is replaced by chlorine. The two compounds appeared as a coincident spot by TLC and it was not possible to

separate the components by column chromatography. While we could lower the amount of the chlorine substituted impurity by using only a stoichiometric amount of Vilsmeier complex we were unable to completely suppress the formation of the chlorinated byproduct. Monomer **II-13a** was successfully prepared from acetophenone **II-10** by the Negishi-Tour phosphonation-elimination procedure. Treatment of **II-10** with LDA and $ClPO(OEt)_2$, followed by base promoted elimination with LDA[31] afforded the desired monomer **II-13a**, Figure 2.5.

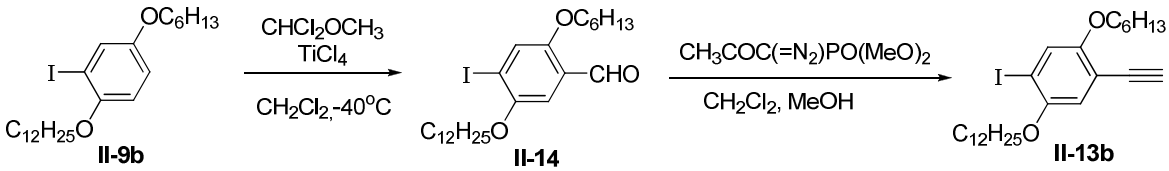


**Figure 2.6.** Synthetic scheme for preparing monomer **II-13b** using formylation-homologation.

While the Negishi-Tour phosphonation-elimination route worked well for analogs with hydrocarbon side chains, use of a strong base (LDA) represents a serious limitation to this method. This led us to also explore formylation of **II-9b** followed by homologation to synthesize the 2,5-dialkoxy-4-iodo-phenylacetylene monomer **II-13b**, Figure 2.6. Formylation of monoiodobenzene **II-9b** ($TiCl_4$, $CHCl_2OCH_3$) at low temperature (-15 to -40 $^oC$) provided benzaldehyde **II-14**. Analysis of the crude reaction mixture indicated the formation of a 2,5-dialkoxy-4-iodobenzaldehyde as the major product, but several byproducts are also formed, Figure 2.7. The crude reaction mixture

gave a $^{1}$H NMR spectrum that included the presence of three different aldehydes (Figure 2.8). Analysis of the aromatic region of the spectrum allowed for identification of these side products. The desired product gives singlets at 7.45 and 7.18 ppm. The remaining signals in the aromatic region of the spectrum indicate the presence of trisubstituted benzene: δ 7.30 (d, $^{4}J_{HH}$ = 3 Hz), δ 7.11 (dd, $^{4}J_{HH}$ = 3.3 Hz, $^{3}J_{HH}$ = 9 Hz), and 6.91 (d, $^{3}J_{HH}$ = 9 Hz). These protons are further downfield than the starting material, and are consistent with literature values for a 2,5-dialkoxy-benzaldehyde, which is formed by electrophilic aromatic substitution of the iodo substituent for a formyl group. The presence of a regioisomer of the desired product was shown by mass spectrometry, and can be identified from the appearance of a singlet at 6.93 ppm in the $^{1}$H NMR spectrum as a 2,5-dialkoxy-3-iodobenzaldehyde (i.e., from formylation meta to the iodo substituent). The 3,6-dialkoxy-2-iodobenzaldehyde regioisomer (formed by formylation ortho to the iodosubstituent) is not formed, likely due to steric interactions with the iodine. Two other byproducts formed during this reaction are 1,4-dialkoxybenzene and 1,4-dialkoxy-2,5-diiodobenzene. The signals for the aromatic protons of these compounds occur at 6.8 ppm and 7.18 ppm respectively. The former arises from protonation of the starting material followed by electrophilic loss of iodine to a second molecule of starting material to give the diiodinated material. Column chromatography allowed for separation of each of these byproducts and mass spectroscopy was used to verify the molecular weights of the side products. The overall conversion to the desired product is 61%, and the remaining 39% is accounted for in the byproducts: 1,4-dialkoxy-2,5-diiodobenzene (6%), 1,4-dialkoxybenzene (3%), 2,5-dialkoxy-benzaldehyde (18%) and 2,5-dialkoxy-3-iodobenzaldehyde (12%).

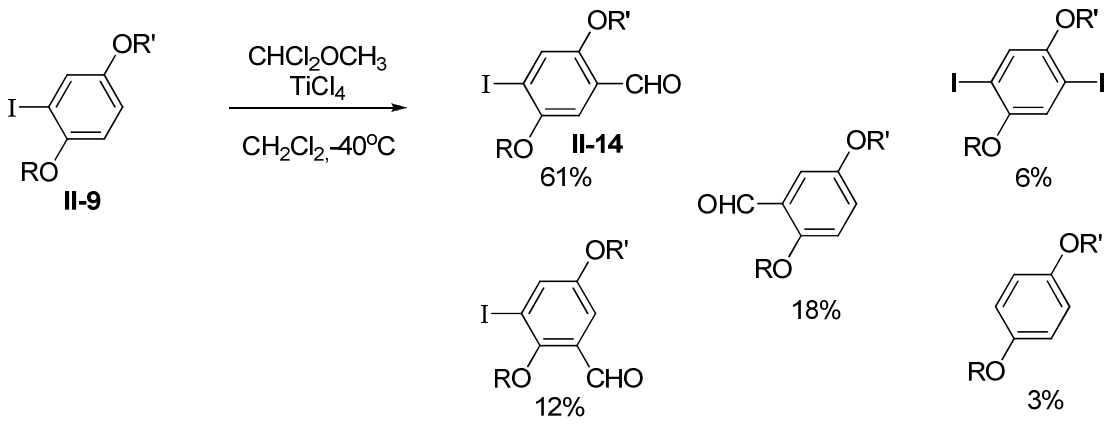


**Figure 2.7.** Sideproducts formed during the formylation of II-9b.

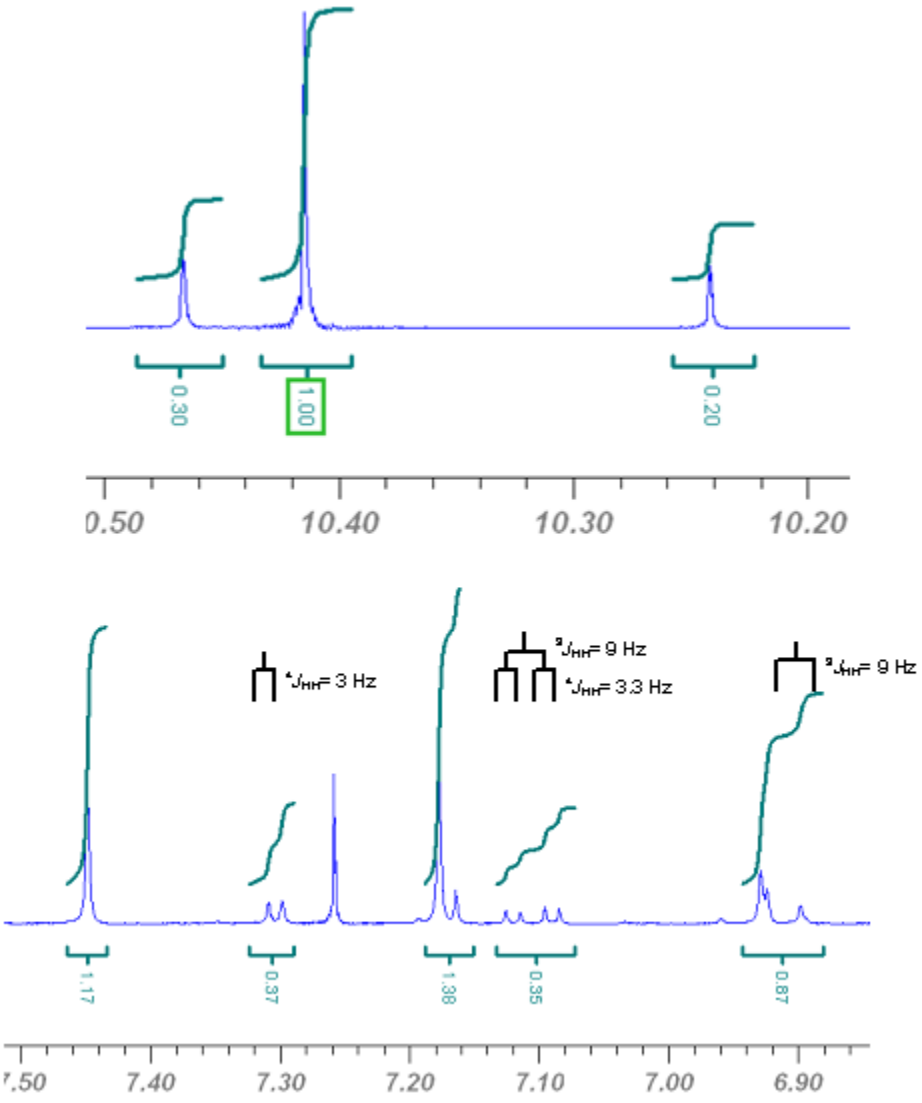


**Figure 2.8.** $^{1}$H NMR spectra of crude reaction mixture obtained upon formylation of 9b. Top, formyl (-CHO) region of the spectrum. Bottom, aromatic region.

.

The desired product was purified by column chromatography followed by recrystallization. The formyl group was converted to the ethynyl substituent using the Seyferth-Gilbert procedure.[32] Treatment of the benzaldehyde **II-14** with $CH(=N_2)PO(OCH_3)_2$ and potassium *tert*-butoxide resulted in the formation of phenylacetylene **II-13b**. The use of a strong base (*t*-BuOK) and relatively expensive Seyferth reagent led us to explore the use of milder and cheaper Bestman-Ohiro homologation procedure whereby aldehyde **II-14** was treated with $CH_3COC(=N_2)CPO(OCH_3)_2$ and $K_2CO_3$ in $MeOH/CH_2Cl_2$ to give alkyne **II-13b** in high yield, Figure 2.6.

The 4-iodophenylacetylene monomers (**II-13**) were polymerized using a Pd catalyzed condensation polymerization. Palladium tetrakis(triphenylphosphine) and CuI were used as the catalyst and cocatalyst, respectively. A combination of morpholine, diisopropylamine and toluene kept the polymer soluble throughout the course of the reaction. We observed fluorescence immediately upon heating the polymerization mixture to 70 $^{o}$C. The reaction was continued for 3-4 days to ensure complete conversion and the polymer was precipitated and then fractionated by extraction with different solvents.

***Alternate approach to prepare 4-iodophenylacetylene A-B type monomers***

In addition to the schemes described in Figures 2.5, 2.6 for the synthesis of 4-iodophenylacetylene (**II-13**), we also attempted to prepare these A-B type monomers by a shorter approach. This approach was designed to avoid the tosylation and detosylation step used in the previous scheme to regioselectively monoiodinate the benzene ring. This approach involved monoiodination of the symmetrical dialkoxybenzene **II-2** followed by Frieldel-Crafts acetylation followed by regioselective dealkylation of the alkoxyl group adjacent to the ketone substituent,[33] Figure 2.9.

Iodination of the symmetrical dialkoxy benzene **II-2** was achieved by lithiation followed by reaction with trimethylsilane chloride to afford the trimethylsilyl derivative **II-15**, followed by treatment with iodine monochloride. Treatment of the resulting iodobenzene **II-16** with excess $AlCl_3$ and acetyl chloride at reflux, led to the formation of a mixture of products, including the desired product **II-17** with the hydroxyl group adjacent to the acetyl group. However, the mixture also contained substantial amounts of the regioisomer in which dealkylation had taken place adjacent to the iodo subsubstituent and non-acetylated phenols. The separation of the mixture was tedious and provided product **17** in a low yield. The tetrasubstituted compound **II-18** could be obtained by attaching the desired second chain using Mitsunobu coupling. Negishi Tour phosphonation-elimination of **II-18** would provide the iodoalkyne monomer **13**. Overall, this approach was not efficient due to the tedious separation of the mono-iodinated product **II-16**, and the undesired cleavage of the alkyl side chains on the carbon at the 4 position. Apart from these reasons, the Neigishi-Tour reaction us not suitable for base sensitive side chains on the aromatic ring.

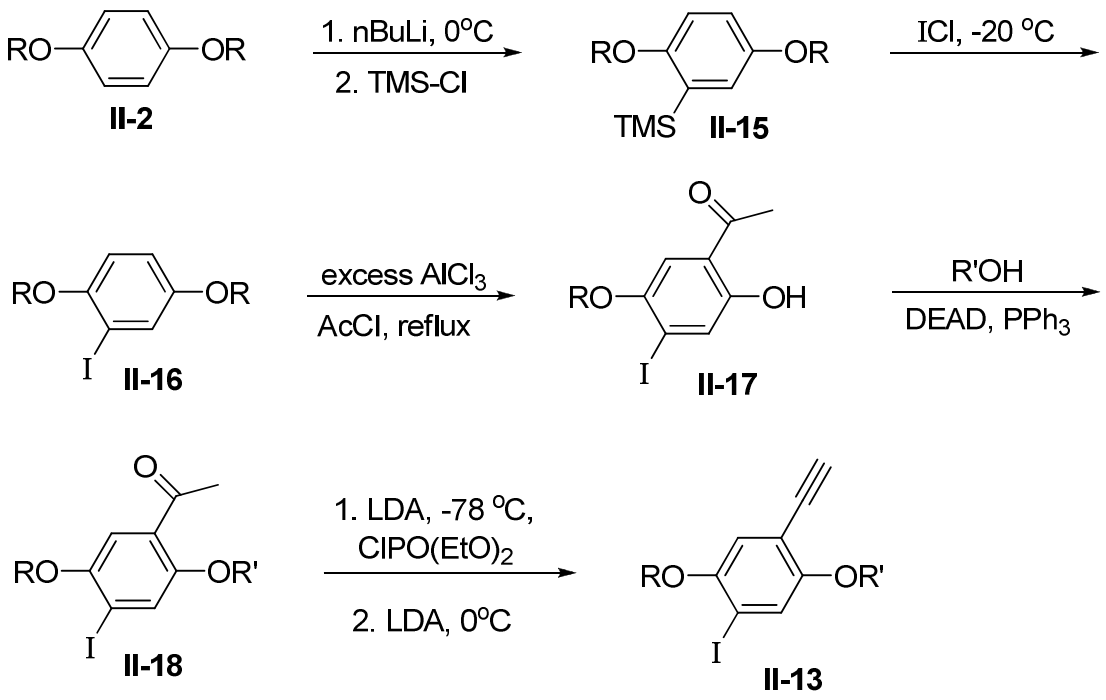


**Figure 2.9.** Synthesis of 4-iodophenylacetylene (**II-13**) monomer by Friedel-Crafts acylation and regioselective dealkylation.

### 2.3.2. Characterization of the Polymer Structure

The molecular structures of the polymers were characterized by $^{1}H$ and $^{13}C$ NMR spectroscopy, and gel permeation chromatography. Molecular weights of the polymers were determined by GPC and end group analysis by $^{1}H$ NMR spectroscopy. The PPE polymer chains have iodophenyl or phenylacetylene end groups. The chemical shift of the aromatic proton ortho to the iodide is further downfield (δ 7.3 ppm) than the protons on the polymer backbone (~δ 7.1). In contrast, the aromatic proton ortho to the alkyne end group is easily distinguished, occurring at around δ 6.9 ppm. The signals of the other proton associated with each of these end groups are coincident with signals for protons in the polymer backbone. In a traditional polymerization of diiodo and diethynyl monomers, a slight stoichiometric imbalance leads to different amounts of the iodo and ethynyl end groups. In this case the average amount of the two end groups was considered when calculating the number of repeat units present in the polymer. However, synthesis of regioregular polymers from A-B type 4-iodophenylacetylene monomers leads to chains bearing one end group of each type, as confirmed by the equal integrals for the peaks at δ 6.9 and δ 7.3 ppm for polymers prepared in this manner. The molecular weights of the polymers obtained by $^{1}H$ NMR and GPC are shown in Table 1. The molecular weights obtained by GPC are consistently higher than those determined by end group analysis, which can be explained by the relatively large hydrodynamic volume of the rigid-rod PPE compared to the coiled conformation of the polystyrenes used as a standard for GPC measurements.[10]

**Table 2.1.** Molecular Weights of PPEs.

| | $M_n/10^3$ g mol$^{-1}$ | |
|---|---|---|
| | $^1$H NMR end group analysis | GPC [a] |
| **RnPPE(12/1)** | 8.7 | 18 |
| **RgPPE(12/1)** | 8.2 | 12 |
| **RnPPE(12/6)** | 17 | 38 |
| **RgPPE(12/6)** | 6.2 | 15 |

[a] calibrated with polystyrene standards

The regioregularity of the polymers was determined by examining the regions of the $^1$H and $^{13}$C NMR spectra corresponding to the nuclei of the 1,4-phenylene units (as well as the methyl signals for analogs of **PPE(12/1)**). These nuclei give signals at different chemical shifts depending on the environment imposed by the relative placement of substituents along the polymer. The effect of regioregularity is most obvious in the difference between the spectra of regiorandom and regioregular **PPE(12/1)**. These differences can be understood in terms of the presence of the three diads expected in the polymer structures, Figure 2.10.

The **RgPPE(12/1)** polymer gives rise to a single sharp resonance in the aromatic region which can be assigned to the aromatic proton in the *ht* (*th*) linkage, Figure 2.11A (bottom). The proton in the 3-position (ortho to dodecyloxy substituent) and in the 6-position (ortho to the methoxy substituent) have a coincident chemical shift. This is in contrast to the regiorandom analog, **RnPPE(12/1)**, which displays three singlets in the

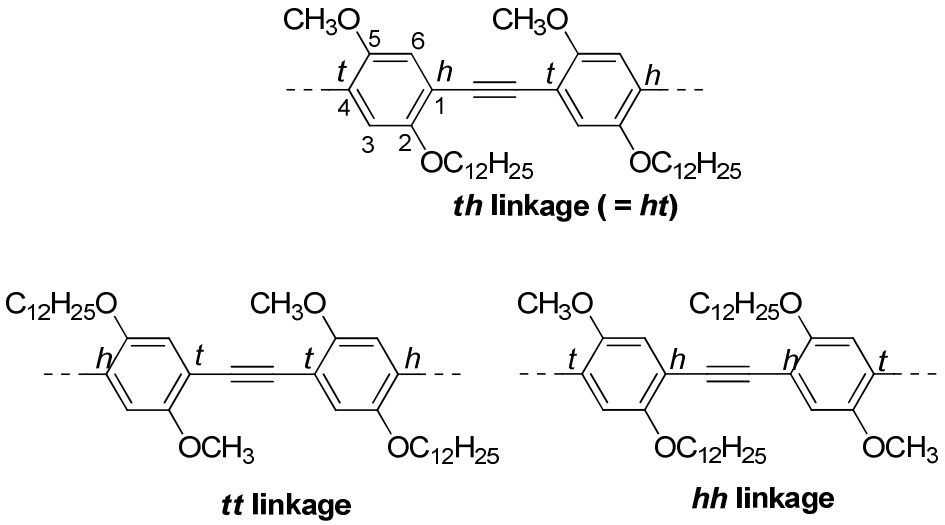


**Figure 2.10.** Three possible diads in the regiorandom **PPE(12/1)** polymer.

aromatic region of the $^1$H NMR spectrum, Figure 2.11A (top). These arise from the presence of three diads *hh*, *tt* and *ht* (*th*), Figure 2.10.

The differences in the chemical shifts of the protons in each diad can be understood in terms of the steric crowding experienced by the relevant hydrogen atom. Greater steric crowding around a hydrogen atom results in downfield shift arising from a perturbation of the electron distribution around the nucleus. The aromatic protons in the 3-position of the phenylene ring of the *tt* linkage, i.e., between the smaller methoxy side chains, experience the least steric hindrance and give rise to a singlet with a lower chemical shift (δ 7.0 ppm). Likewise, the proton in the 5-position in the *hh* linkage experiences the highest steric crowding due to the two dodecyloxy groups and is shifted further downfield (δ 7.04 ppm). The protons in 3- and 5-positions in the *ht* (*th*) diads (between the dodecyloxy and methoxy side chain) are represented by the central peak, which appears at the same chemical shift as the singlet for the aromatic protons of the regioregular (*ht*) regioregular analogue **RgPPE(12/1)**. The ratio of peak intensities (1:2:1) in this region of the spectrum of the regiorandom material reflects what would be expected based on a statistical distribution of diads.

The signals for the aromatic protons for both the **RnPPE(12,6)** (Figure 2.11B, top) and **RgPPE(12,6)** (Figure 2.11B, bottom) polymer appear as a sharp singlet at 7.01 ppm. This is in contrast to the $^1$H NMR spectra of **PPE(12/1)**, in which the complexity of the peaks in the regiorandom material can be ascribed to the different environments generated by relative placement of the dodecyl and methyl groups (see above). For the **PPE(12/6)** polymers, although the alkoxy side chains are different, they are both long

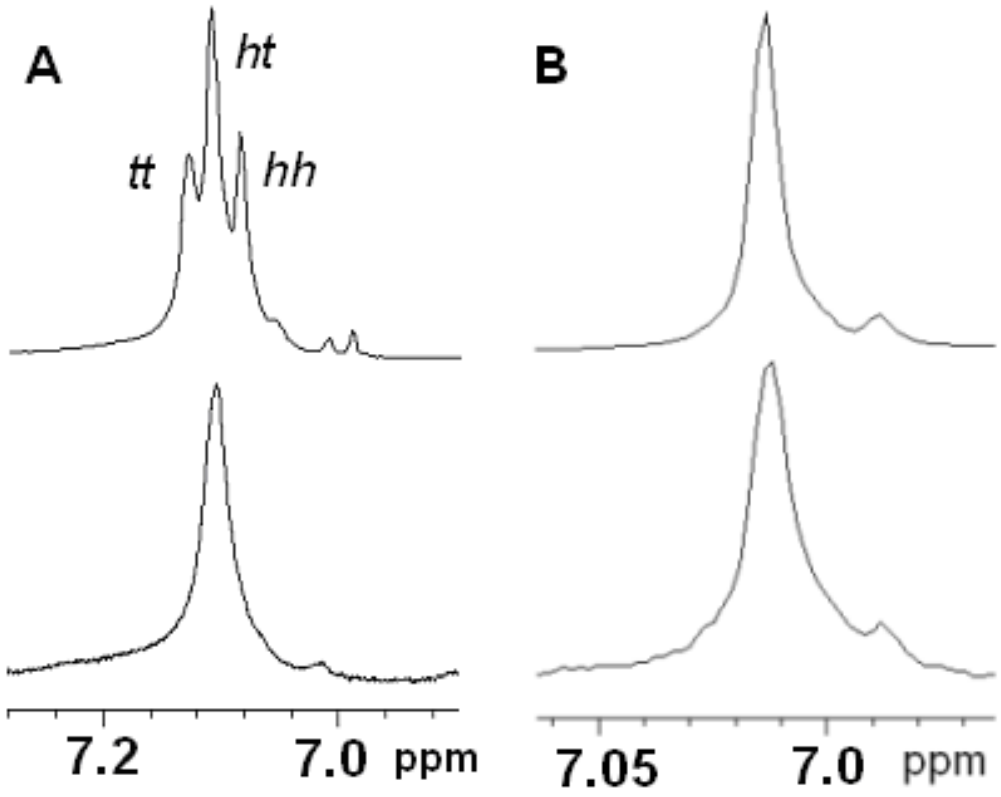


**Figure 2.11.** $^{1}H$ NMR (400 MHz, $C_2D_2Cl_4$) spectra of (A) **PPE(12/1),** Top, Regiorandom; Bottom, Regioregular (B) **PPE(12/6),** Top, Regiorandom; Bottom Regioregular.

enough to impart a similar steric environment around the respective nuclei of the backbone for all the three types of diads.

The $^{13}C$ NMR spectra of the polymers also provide evidence for the different relative placement of substituents in regioregular and regiorandom polymers. For the regiorandom polymer **RnPPE(12/1)**, the peaks for C2 and C5 (i.e., carbon atoms bearing the alkoxy groups) appear as four closely spaced peaks at around 154.0 ppm and two peaks at approximately 154.4 ppm, Figure 2.12A (top). This can be ascribed to the presence of the different linkages present in the regiorandom material, with separate signals for C2 in an *ht* and *hh* diad, and for C5 in *th* and *tt* diads (the chemical shift of C2 in the *tt* diad, and C5 of the *hh* diad, shown in Figure 2.7, is influenced primarily by the relative placement of substituents in the next repeat unit, i.e., the next diad). In contrast, the signals for these carbons in the **RgPPE(12/1)** regioregular polymer Figure 2.9A (bottom) containing only *ht* diads appear as single sharp peaks at 154.0 ppm for C2 and at 154.4 ppm for C5. The signals for C3 and C6 (the unsubstituted positions) appear as a single peak at 116.9 ppm in the regioregular sample, whereas in the spectrum for the regiorandom material these carbons appear as two closely spaced peaks (116.8 and 117.1 ppm). Likewise, the $^{13}C$ peak of the methoxy substituent of the regioregular **RgPPE(12/1)** gives a sharp signal at 70.4 ppm while there are two peaks (70.3 and 70.5 ppm) for the regiorandom sample. The C1 and C4 carbons of the phenylene appear as a single peak for both **RnPPE(12/1)** and **RgPPE(12/1)**. These carbons lie in the backbone of the polymer and the chemical shift is apparently not influenced by the differences in the steric environment arising from substituents on the neighbouring ring.

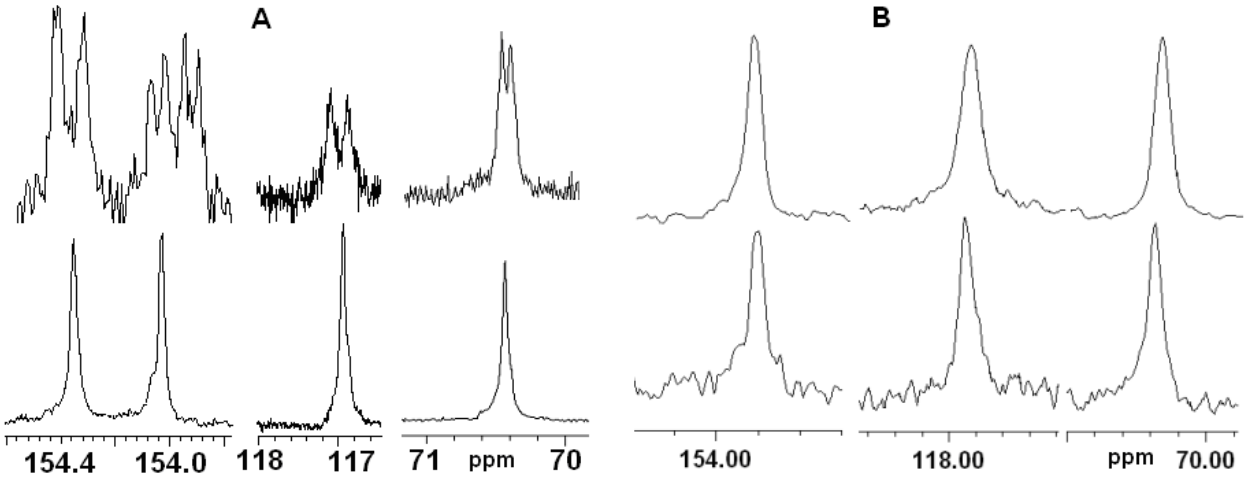


**Figure 2.12.** $^{13}C$ NMR (100 MHz, $C_2D_2Cl_4$) spectra of the aromatic regions of A,: **PPE(12/1)**, top, **RnPPE(12/1)** and bottom, **RgPPE(12/1)**. B,: **PPE(12/6),** top, **RnPPE(12/6)** and bottom, **RgPPE(12/6)**.

The C2 and C5 carbons (bearing the alkoxy groups), C3 and C6 carbons (bearing the aromatic protons) and carbons of the methylene units of the side chains attached to the oxygen for the **PPE(12/6)** polymers are shown in Figure 2.12B (left to right, respectively). All the peaks are sharp and the spectra of regioregular and regiorandom polymers are indistinguishable.

### 2.3.3. Electronic Properties of the PPEs.

The optical absorptions of conjugated polymers can be correlated to the degree of conjugation along the backbone, and can therefore be related to the molecular structure. The twisting around the backbone arising from the steric interactions between side chains on adjacent repeat units, and the supermolecular packing, may both have a strong influence on the electronic spectra. The spectra of the polymers were investigated in solution and the solid state. The absorption spectra obtained for the polymers in $CHCl_3$ solution are shown in Figure 2.13. Regiorandom and regioregular analogues of the **PPE(12/1)** and **PPE(12/6)** polymers have essentially identical spectra in solution. The absorption spectra exhibit a weak absorption band at around 320 nm and a broad main transition centered around 451 nm. These spectra are similar to symmetrically substituted PPEs in solution, and are consistent with the low rotational barrier of the PPE subunits (estimated to be <1 kcal $mol^{-1}$).[10]

The solid-state spectra of the PPEs were investigated using films prepared by drop-casting a solution of the polymer in $CHCl_3$ onto quartz slides followed by annealing at 120 $^{o}$C for 24 h. The absorptions of the solid state films are broader and red shifted

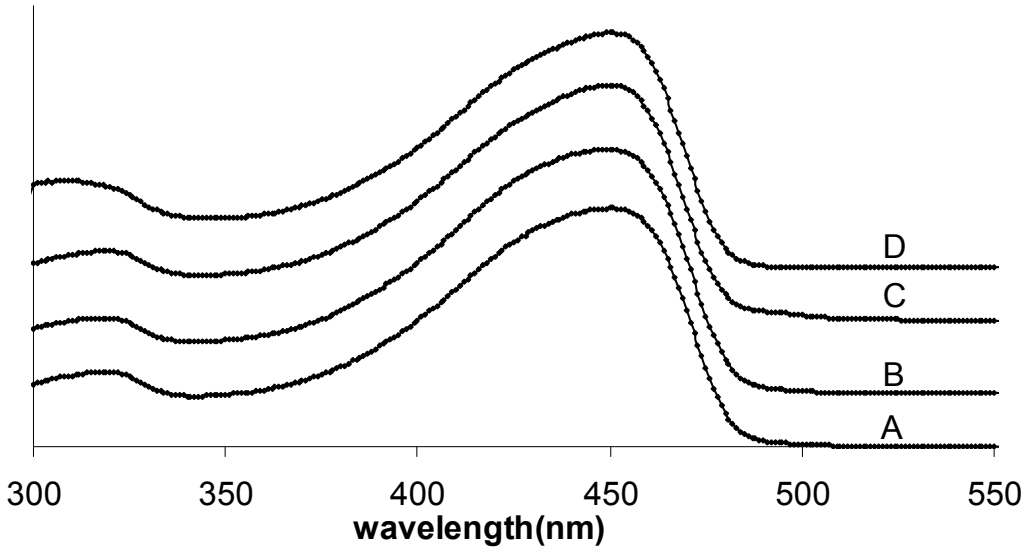


**Figure 2.13.** UV-vis spectra of polymer solutions ($CHCl_3$): A, **RnPPE(12/1)**; B, **RgPPE(12/1)**; C, **RnPPE(12/6)**; D, **RgPPE(12/6)**

relative to the solution spectra. This is expected based on the influence of interactions between the conjugated backbones in the solid state that are absent in solution. The effect of regioregularity on the appearance of the spectra is most pronounced in the analogs of **PPE(12/1**). The regioregular analog, Figure 2.14B, has a greater contribution at higher wavelength than the regiorandom analogue, Figure 2.14A.This may be ascribed to the ordered arrangement of the side chains in regioregular **RgPPE(12/1)** which leads to a more planar, more conjugated conformation that packs more closely in the solid state. The irregular placement of the substituents in the regiorandom analogue impedes the formation of an ordered assembly, thereby leading to conformational disorder, a decrease in conjugation length and weaker chain-chain interactions. This effect is not observed in the case of **PPE(12/6)** where the substituents are more similar: The regioregular (Rg),Figure 2.15B, and regiorandom (Rn) analogue, Figure 2.15A, have almost identical UV-vis absorption spectra. The spectra of these analogues are similar to that of the symmetrical, and thereby inherently "regioregular", **PPE(12)** analogue, Figure 2.15C. These results suggest that regioregularity has a stronger influence on the electronic properties of PPEs substituted with dissimilar side chains (C1 and C12) system than those bearing more similar side chains (C6 and C12) or an identical pair (C12).

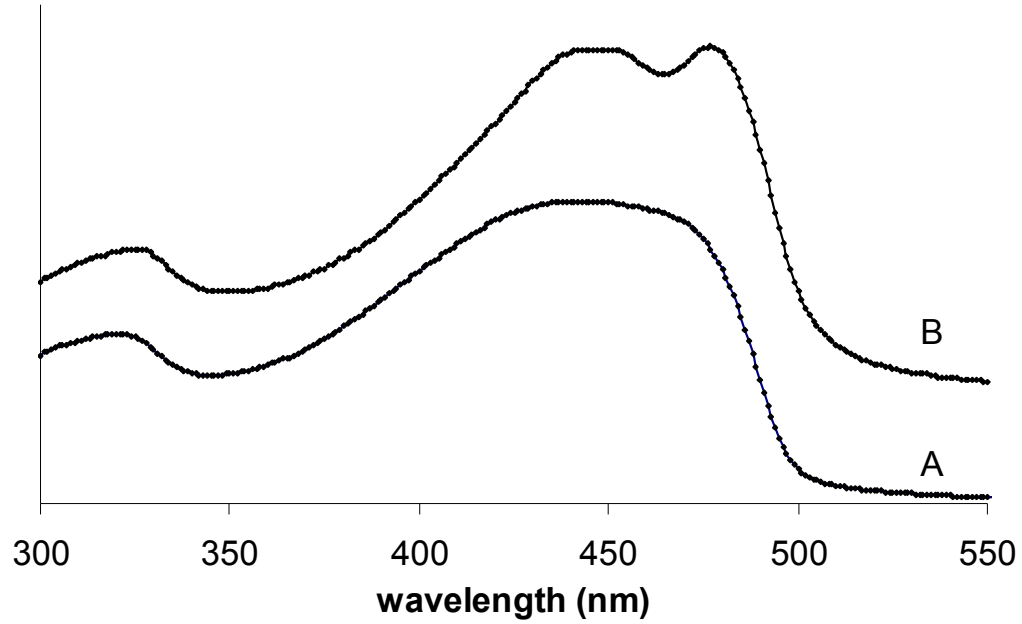


**Figure 2.14.** UV-vis spectra of polymer films. A, **Rn(12/1)**; B, **Rg(12/1)**.

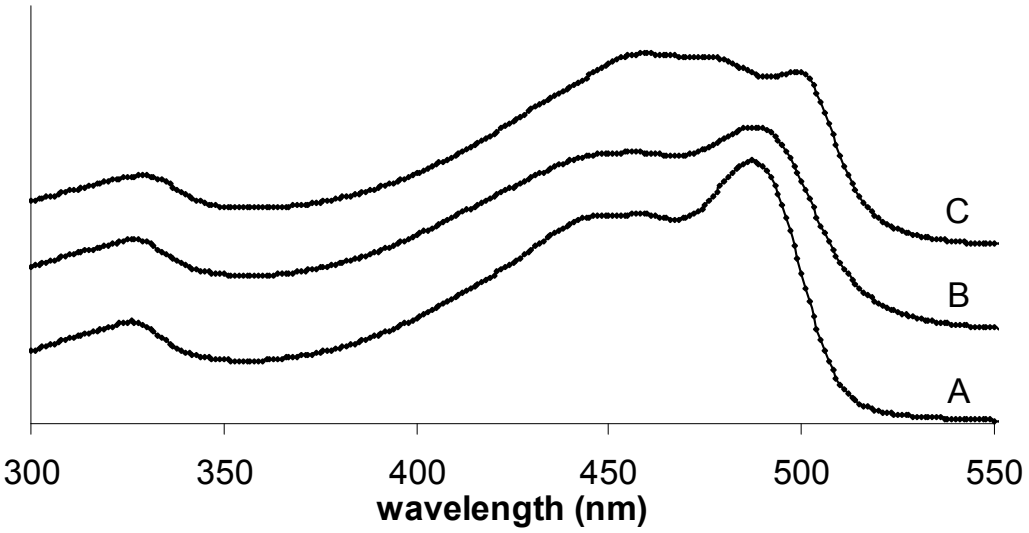


**Figure 2.15.** UV-vis spectra of polymer films A, **RnPPE(12/6)**; B, **RgPPE(12/6)**; C, **PPE(12)**.

### 2.3.4. Molecular Assembly of the Polymers.

X-ray diffraction studies were performed on the regiorandom and regioregular polymers to explore the effect of the relative placement of side chain on chain packing in the solid state. Experiments were conducted on thin films formed by drop casting xylene solutions of the polymer onto a silicon substrate. The X-ray experiments were run on both pristine and annealed samples (24 h at 120$^{o}$C, under $N_2$).

The X-ray diffractograms of **PPE(12/6)** regioisomers (regiorandom, Figure 2.16A; and regioregular, Figure 2.16B) both show a peak at $2\theta = 4.46^{o}$ (19.9 Å), and small peak at approximately 8.7$^{o}$ (10.2 Å). For comparison, the diffractogram for the symmetrical **PPE(12)** material shows four peaks, at $2\theta = 3.54^{o}$, 7.0$^{o}$, 10.45$^{o}$ and 17.45$^{o}$. These can be assigned as the (100), (200), (300) and (500) planes of a lamella crystal with an interlayer spacing of 24.9 Å.[34] The strong peaks for [*h*,0,0] relections when *h* is even, and weak peaks associated with the reflections when *h* is odd, can be interpreted as arising from an electron density within the unit cell consisting of planes with high electron density (i.e., the conjugated backbone) and low electron density (alkyl regions). Thus, by analogy, we assign the two diffraction peaks (one strong, one weak) in each of the **PPE(12/6)** materials to the (100) and (200) planes of a lamella structure with interlayer spacing of 19.9 Å, Figure 2.16 inset. The irregular placement of side chains would suggest that they are more likely interdigitated, and there is shorter-range order than in symmetrically substituted PPE(12). Thus, as expected, the combination of hexyl and dodecyl side chains results in a smaller interlayer spacing than is observed for

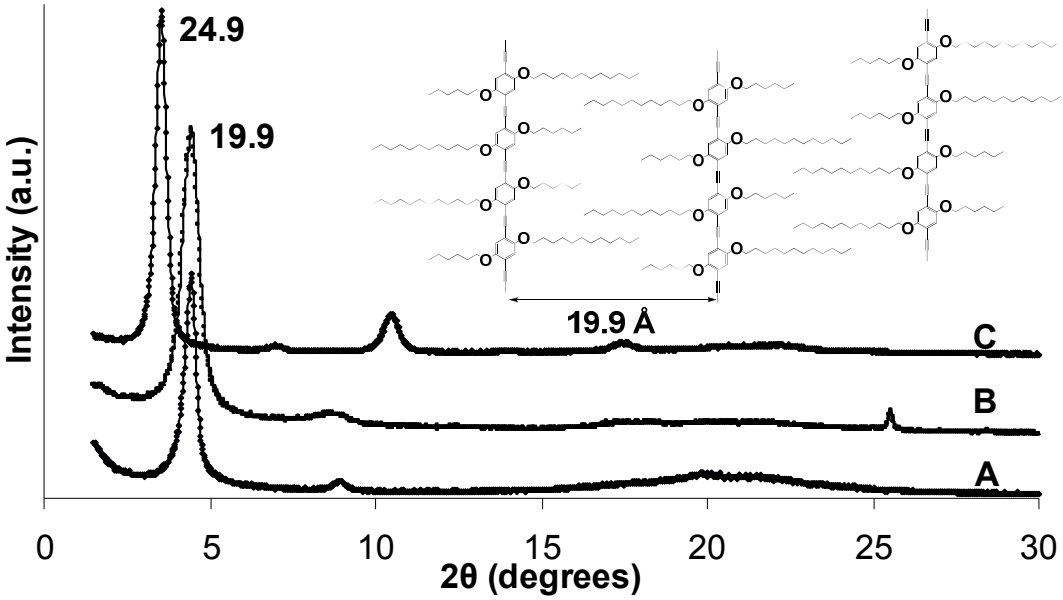


**Figure 2.16.** X-ray diffraction of annealed polymer films (annealed at 120 $^{o}$C for 24h): A, regiorandom **RnPPE(12/6)**; B, regioregular **RgPPE(12/6)**; C, **PPE(12)**.

**PPE(12)**. The broader diffraction peaks for the regiorandom **Rg(12/6)** analog might indicate the presence of less order than for the regioregular analogue (width at half height for the (100) peak: **Rg**, 0.45°; **Rn**, 0.64°).

The X-ray diffractograms of the regioregular and regiorandom **PPE(12/1)** analogues are shown in Figure 2.17. The regioregular analog, **RgPPE(12/1)**, Figure 2.17B, shows an intense and sharp first order reflection at a *d* spacing of 27.3 Å while the regiorandom analogue is featureless, Figure 2.17A. The absence of higher order reflections in the diffractogram of the regioregular polymer indicates that the although this material packs in an orderly fashion, this ordering is relatively short-range. The diffractogram of the regiorandom analogue remains largely unchanged even after extensive annealing. The *d* spacing value of 27.3 Å for the **RgPPE(12/1)** homolog is *larger* than observed for the analogs with longer side chains, **PPE(12)** and **RgPPE(12/6)**, and larger than the width of the polymer ribbon transverse to the polymer chain (i.e., with the side chains in an extended all-trans conformation, Figure 2.17 inset.) This suggests the formation of a bilayer type arrangement that would arise from segregation of the dodecyloxy side chains and methoxy substituents on different sides of the aromatic backbone.

The bilayer packing arises from segregation of the two types of side chain. This effect, which is not observed for the **PPE(12/6)** analogues, might arise from the optimization of intramolecular packing of dodecyloxy side chain on adjacent repeating units and intermolecular interaction of these side chain in packing together the molecular ribbons. A similar assembly has been reported by Suzuki and coworkers for a regioregularly-substituted poly(1,4-phenylene vinylene).[8]

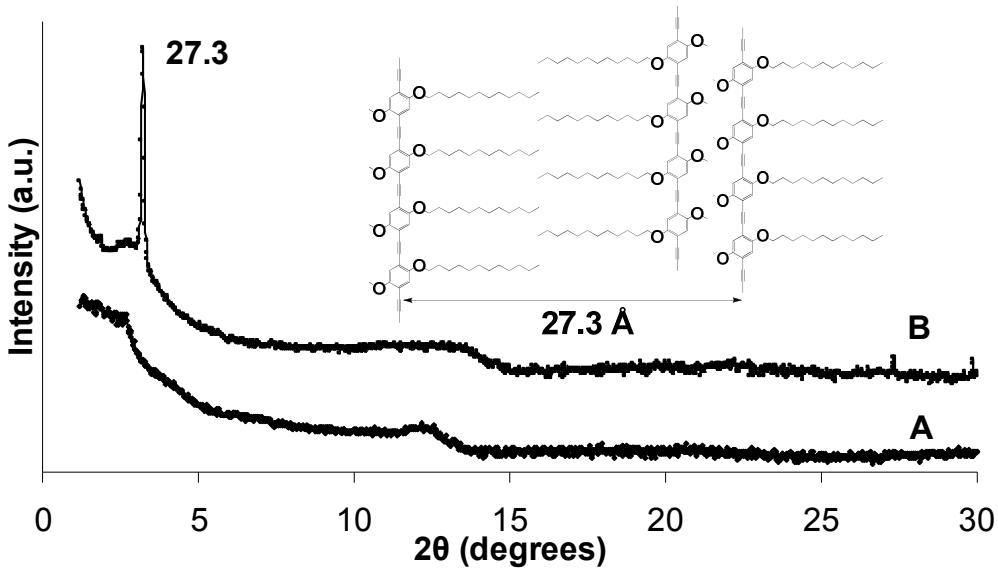


**Figure 2.17.** X-ray diffraction of annealed polymer films (annealed at 120 $^{o}$C for 24h): A, regiorandom **RnPPE(12/1)**; B, regioregular **RgPPE(12/1)**.

## 2.4. CONCLUSIONS

In conclusion, we have presented strategies for the synthesis of structurally homogenous regioregular unsymmetrically substituted poly(1,4-phenylene ethynylene)s, PPEs, by polymerization of unsymmetrically substituted 2,5-dialkoxy-4-iodophenylacetylenes. We have that control over the relative placement of substituents has an influence on molecular assembly and electronic structure of the PPE materials. The effect of regioregularity on the properties of unsymmetrically substituted PPEs is greatest when there is a large difference between the side chains. Expanding the choice of side chains should afford a further level of control over the molecular packing and orientation of conjugated polymer chains, which is paramount in the design of new materials for electronic and optical devices. Further work is underway to apply this approach to the development of polymers in which the choice and placement of distinctly different side chains provides a new solid-state and liquid-crystalline phases.

## 2.5. REFERENCES


(1) *Handbook of Conducting Polymers*; 2 ed.; T. Skotheim, J. R., R. Elsenbamer, Ed.; Marcel Dekker: New York, 1998, p 225.

(2) Jen, K. Y.; Miller, G. G.; Elsenbaumer, R. L. *J. Chem. Soc., Chem. Commun.* **1986**, 1346.

(3) McCullough, R. D.; Lowe, R. D. *J. Chem. Soc., Chem. Commun.* **1992**, 70.

(4) Chen, T. A.; Rieke, R. D. *Synth. Met.* **1993**, *60*, 175.

(5) McCullough, R. D. *Adv. Mater.* **1998**, *10*, 93.

(6) Loewe, R. S.; McCullough, R. D. *Chem. Mater.* **2000**, *12*, 3214.

(7) Ng, S. C.; Xu, J. M.; Chan, H. S. O.; Fujii, A.; Yoshino, K. *J. Mater. Chem.* **1999**, *9*, 381.

(8) Suzuki, Y.; Hashimoto, K.; Tajima, K. *Macromolecules* **2007**, *40*, 6521.

(9) Krebs, F. C.; Jorgensen, M. *Macromolecules* **2002**, *35*, 10233.

(10) Bunz, U. H. F. *Chem. Rev.* **2000**, *100*, 1605.

(11) Xiao, X. Y.; Nagahara, L. A.; Rawlett, A. M.; Tao, N. J. *J. Am. Chem. Soc.* **2005**, *127*, 9235.

(12) Pang, Y.; Li, J.; Hu, B.; Karasz, F. E. *Macromolecules* **1998**, *31*, 6730.

(13) Mwaura, J. K.; Pinto, M. R.; Witker, D.; Ananthakrishnan, N.; Schanze, K. S.; Reynolds, J. R. *Langmuir* **2005**, *21*, 10119.

(14) Weder, C.; Sarwa, C.; Bastiaansen, C.; Smith, P. *Adv. Mater.* **1997**, *9*, 1035.

(15) Arnt, L.; Tew, G. N. *Langmuir* **2003**, *19*, 2404.

(16) Arnt, L.; Tew, G. N. *Macromolecules* **2004**, *37*, 1283.

(17) Breitenkamp, R. B.; Tew, G. N. *Macromolecules* **2004**, *37*, 1163.

(18) Clark, A. P. Z.; Shen, K. F.; Rubin, Y. F.; Tolbert, S. H. *Nano Lett.* **2005**, *5*, 1647.

(19) Bunz, U. H. F. *Acc. Chem. Res.* **2001**, *34*, 998.

(20) Moroni, M. L. M., J.; Pham, T. A.; Bigot, J.-Y. *Macromolecules* **1997**, *30*, 1964.

(21) Francke, V. M., T.; Muellen, K. *Macromolecules* **1998**, *31*, 2447.

(22) Giardina, G. R., Patrizia; Ricci, Antonella; Lo Sterzo, Claudio *J. Poly. Sci., Part A: Polym. Chem.* **2000**, *38*, 2603.

(23) Kovalev, A. I. T., K.; Barzykin, A. V.; Asai, M.; Ueda, M.; Rusanov, A. L *Macromol. Chem. Physics* **2005**, *206*, 2112.

(24) Nambiar, R. R.; Brizius, G. L.; Collard, D. M. *Adv. Mater.* **2007**, *19*, 1234.

(25) Daoud, W. A.; Turner, M. L. *Bull. Chem. Soc. Jpn.* **2005**, *78*, 367.

(26) Hoger, S. *Liebigs Annalen-Recueil* **1997**, 273.

(27) Percec, V.; Bae, J. Y.; Zhao, M. Y.; Hill, D. H. *J. Org. Chem.* **1995**, *60*, 1066.

(28) Stang, P. J.; Hargrove, R. J. *J. Org. Chem.* **1975**, *40*, 657.

(29) Arnold, Z.; Zemlicka, J. *Proceedings of the Chemical Society of London* **1958**, 227.

(30) Malakhov, A. D.; Malakhova, E. V.; Kuznitsova, S. V.; Grechishnikova, I. V.; Prokhorenko, I. A.; Skorobogatyi, M. V.; Korshun, V. A.; Berlin, Y. A. *Bioorg. Khim.* **2000**, *26*, 39.

(31) Negishi, E.; King, A.; Tour, J. *Org. Synth.* **1985**, *64*, 44.

(32) Gilbert, J. C.; Weerasooriya, U. *J. Org. Chem.* **1982**, *47*, 1837.

(33) Park, K. K.; Lee, H. J.; Kim, E. H.; Kang, S. K. *J. Photochem. Photobiol., A* **2003**, *159*, 17.

(34) Bunz, U. H. F.; Enkelmann, V.; Kloppenburg, L.; Jones, D.; Shimizu, K. D.; Claridge, J. B.; zur Loye, H. C.; Lieser, G. *Chem. Mater.* **1999**, *11*, 1416.

# CHAPTER 3

# THE EFFECT OF REGIOREGULARITY ON THE SOLID-STATE AND INTERFACIAL ASSEMBLY OF AMPHIPHILIC POLY(1,4-PHENYLENE ETHYNYLENE)S

## 3.1. INTRODUCTION

The semiconducting properties of conjugated organic materials such as thiophene oligomers,[1] pentacene,[2] phthalocyanine,[3] polyphenylenes[4] and poly(3-alkylthiophenes),[5] combined with opportunity to process them by solution-based techniques, provide significant motivation to explore these materials as components of electronic and optical devices. The electronic structure of these materials, and the resulting semiconducting emissive properties, depend on both the π conjugated nature of the molecules and the supramolecular organization in the solid state.[6] Structural heterogeneity plays a significant role on the behavior of conjugated materials on a number of different scales. Molecular scale disorder (e.g., regioregularity of polymers consisting of unsymmetrical repeat units, molecular weight polydispersity, copolymer sequence), supermolecular organization arising from the semicrystalline nature of polymeric materials, and macroscopic-scale features such as grain boundaries between particles and interactions with substrates, present significant challenges in relating molecular structure to the properties of this class of material. Thus the possibility of generating polymers with improved electronic properties by controlling the solid state morphology and

supramolecular organization through optimization of molecular structure is of paramount importance.

The potential to improve the properties of poly(3-alkylthiophene)s by optimization of molecular packing in the solid state was demonstrated by Mcullough[7] and Rieke.[8] The regioregularity of materials prepared by controlled polymerization of 5-metallo-2-bromo-3-alkylthiophenes results in higher crystallinity, red shifted optical absorptions, greater conductivity and a smaller band gap compared to the regiorandom analogs.[9] Despite the large number of conjugated polymers prepared to date, investigation of such improvements in properties due to the relative placement of substituents on the backbone of the polymer has been restricted to poly(3-alkylthienylene vinylene)s[10], poly(3-alkyl-2,5-thienylene-1,4-phenylene)s[11], poly(1,4-phenylene vinylene)s[12], poly(1,4-phenylene ethynylynes)[13,14] and poly(biphenylene vinylene)s.[15] To achieve efficient packing of the PPE chains and to avoid steric hindrance in aggregates, the side chains or the substituents on the phenyl ring must be aligned.[16,17] Further improvements in controlling the supermolecular organization and orientation of conjugated polymers may also be realized by preparation of amphiphilic analogs consisting polymeric chains bearing a pair of dissimilar side chains that segregate to give rise to self assembled systems. Amphiphilic analogs of poly(3-alkylthiophene),[18-21] poly(phenylene)[22-24] and poly(1,4-phenylene ethynylene)[25-31] bearing alkyl/ionic and alkyl/oligoether combinations of side chains have been prepared to control the assembly of conjugated polymers. For example, regioregular amphiphilic poly(3-alkylthiophene)s containing hydrophilic oligoether and hydrophobic alkyl side chains on alternating thiophene units assemble at the air-water interface.[20,32,33] Similarly, combinations of

hydrophilic tri(ethylene oxide) and hydrocarbon side chains on the PPE backbone influence the orientation of the conjugated backbone in monolayer assemblies of the polymer at the air-water interface.[34]

Our previous work in the area of amphiphilic conjugated polymers has focused on the exploration of the segregation of alkyl and fluoroalkyl side chains on the solid-state molecular assembly of poly(3-semifluoroalkyl)thiophenes,[35-37] and the effect of regioregularity. We have recently extended this approach to prepare analogous regioregular amphiphilic semifluoroalkyl-substituted poly(1,4-phenylene ethynylene)s PPEs. [13,14,38] PPEs have received a great deal of attention for their potential in the development of new sensors, field effect transistors,[39,40] light emitting diodes[41] and solar cells. Dissimilar side chains of an amphiphilic PPE are optimally placed for the formation of a Janus-type structure, and thereby possess a propensity to self-organize, when they are substituted along the polymer backbone in a regioregular ("head-to-tail") manner, Figure 3.1B. Our development of the polymerization of appropriately substituted 4-iodophenylacetylenes (a bifunctional AB type monomer) provides us with accesss to PPEs with a regular placement of dissimilar side chains. Here we report the synthesis of regioregular and regiorandom analogs of amphiphilic PPEs with hydrophobic alkyl and hydrophilic tri(ethylene oxide) oligoether (-$(OCH_2CH_2)_3OCH_3$, EG3) side chains. We demonstrate for the first time that the relative placement of the side chains along the PPE backbone has a strong influence on the supermolecular packing in the solid state and at the air-water interface, and on the electronic structure of the materials.

## 3.2. EXPERIMENTAL

### 3.2.1. General Methods

All reagents were purchased from commercial sources and used without further purification unless stated. THF and $Et_2O$ were dried over sodium benzophenone ketyl prior to distillation under nitrogen. Column chromatography was performed on flash grade silica (32-60 Å, Sorbent Technologies, Atlanta, GA). Thin-layer chromatography was performed on 3 ×5 cm silica gel plates (0.2 mm thick, 60 F254) on an aluminum support (Sorbent Technologies). NMR analysis was performed on a Bruker DSX 400 or DSX 300 instruments. Chemical shifts are reported relative to internal tetramethylsilane. IR analyses were performed on a Nicolet 4700 FTIR with an ATR attachment from SmartOrbit Thermoelectronic Corporation. Elemental analyses were performed by Atlantic Microlab, Inc. (Norcross, GA). Ultraviolet-visible analysis was performed on a Shimadzu UV-2401PC spectrometer, and fluorescence spectroscopy was performed on a Shimadzu RF-5301PC spectrofluorophotometer. The X-ray diffraction data was obtained using a Scintag X1 diffractometer equipped with copper tube and a Peltier cooled solid state detector.

### 3.2.2. Synthesis of monomers III-2 and III-4 for preparation of $C_{12}/EG_3$ regiorandom PPEs

The procedure for synthesizing compounds **II-1b, II-6b, II-7b** and **II-8b** are described in Chapter 2.[14]

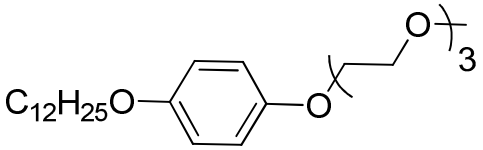

**1-Dodecyloxy-4-(2-(2-(2-methoxyethoxy)ethoxy)ethoxy)benzene, III-1.** 4-Dodecyloxyphenol, **II-1b** (4.31 g, 15.5 mmol), was added to a stirred solution of $PPh_3$ (4.87 g, 18.6 mmol) and triethylene glycol monomethyl ether (2.97 mL, 18.6 mmol) in $Et_2O$ (40 mL) under Ar. Diethyl azodicarboxylate (DEAD) (3.38 mL, 15.5 mmol) was added dropwise by syringe and the resulting pale yellow solution was stirred at room temperature for 24 h. $Et_2O$ (60 mL) was added and the solution was washed with 10% aqueous NaOH (200 mL) followed by $H_2O$ (100 mL). The solution was dried over $MgSO_4$, the solvent was removed under reduced pressure, and the residue was subjected to flash column chromatography (30:70 v/v ethyl acetate:hexanes) to afford **III-1** (6.58 g, 68 % yield) as a pale yellow solid, m.p. 36 °C. $^1$H NMR (300 MHz, $CDCl_3$): δ 6.76-6.86 (m, 4H, Ar-H), 4.08 (t, $^3J_{HH}$ = 5.1 Hz, 2H), 3.9 (t, $^3J_{HH}$ = 6.6 Hz, 2H), 3.82 (t, $^3J_{HH}$ = 5.1 Hz, 2H), 3.60-3.72 (m, 6H), 3.52 (t, $^3J_{HH}$ = 5.1 Hz, 2H), 3.37 (s, 3H, -$OCH_3$), 1.68-1.80 (m, 2H, -$CH_2$-, C-2), 1.20-1.50 (m, 18H), 0.88 (t, $^3J_{HH}$ = 6.6 Hz, 3H, -$CH_3$). $^{13}$C NMR (75 MHz, $CDCl_3$): δ 169.9 (Ar C1,4), 115.8 (Ar C3,5), 115.5 (Ar C2,6), 72.58, 71.7, 71.35, 71.2, 70.26, 70.21, 70.17, 59.69 (-$OCH_3$), 32.14, 31.72, 29.87, 29.80, 29.78, 29.58, 29.50, 29.34, 26.24, 22.92, 14.36 (-$CH_3$). IR ($\nu$, $cm^{-1}$): 2953, 2916 (Ar C-H str.), 2870, 2848, 1509, 1474, 1462, 1453, 1394, 1377, 1353, 1284, 1238 (C-O str.), 1201, 1112, 1061, 1024, 1007, 924, 824, 758. HRMS: *calc*. for $C_{25}H_{44}O_5$ = 424.31887, *obs*. = 424.31795, Δ = 0.9 ppm.

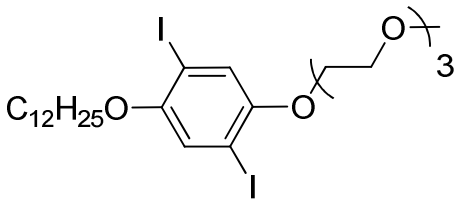

**1-Dodecyloxy-2,5-diiodo-4-(2-(2-(2-methoxyethoxy)ethoxy)ethoxy)benzene, III-2.** A solution of unsymmetrically substituted dialkoxybenzene **III-1** (4.02 g, 11.1 mmol), $I_2$ (3.23 g, 12.7 mmol), $KIO_3$ (1.45 g, 6.8 mmol), $H_2O$ (4 mL) and $H_2SO_4$ (0.5 mL) in acetic acid (40 mL) was heated at 70 $^oC$ for 36 h. The reaction mixture was cooled, diluted with $CH_2Cl_2$ (200 mL) and washed with aqueous $Na_2SO_3$ solution. The combined extracts were washed with 10% aqueous NaOH (2 × 150 mL), dried over $MgSO_4$, and solvent was removed under reduced pressure. The residue was recrystallized twice from methanol to afford diiodide **III-2** (2.75 g, 37% yield) as white needles, m.p. = 48-49 $^oC$. $^1H$ NMR (300 MHz, $CDCl_3$): δ 7.25 (s, 1H, Ar C3-H), 7.16 (s, 1H, Ar C6-H), 4.11 (t, $^3J_{HH}$ = 5.1 Hz, 2H), 3.92 (t, $^3J_{HH}$ = 6.6 Hz, 2H), 3.87 (t, $^3J_{HH}$ = 5.1 Hz, 2H), 3.78 (t, $^3J_{HH}$ = 5.1 Hz, 2H), 3.64-3.72 (m, 4H), 3.56 (t, $^3J_{HH}$ = 5.1 Hz, 2H), 3.38 (s, 3H, $-OCH_3$), 1.75-1.87 (m, 2H, $-CH_2-$, C-2), 1.2-1.58 (m, 18H), 0.89 (t, $^3J_{HH}$ = 6.6 Hz, 3H, $-CH_3$). $^{13}C$ NMR (75 MHz, $CDCl_3$): δ 169.88 (Ar C1,4), 123.88 (Ar C3), 122.79 (Ar C6), 86.72 (Ar C5), 86.45 (Ar C2), 72.18, 71.37, 70.99, 70.82, 70.56, 70.51, 69.86, 59.29 ($-OCH_3$), 32.14, 31.73, 29.87, 29.80, 29.78, 29.58, 29.50, 29.34, 26.24, 22.92, 14.36 ($-CH_3$). IR (AT-IR, neat): 2915 (Ar C-H str.), 2885, 2864, 2846, 1485, 1459, 1388, 1353, 1328, 1262, 1237, 1215 (C-O str.), 1120, 1094, 1068, 1057, 1030, 994, 956, 879, 854, 839, 814, 788, 761 $cm^{-1}$. HRMS: Calculated for $C_{19}H_{30}O_2I_2$, 676.11218; Observed, 676.11064; Δ = 2.3 ppm.

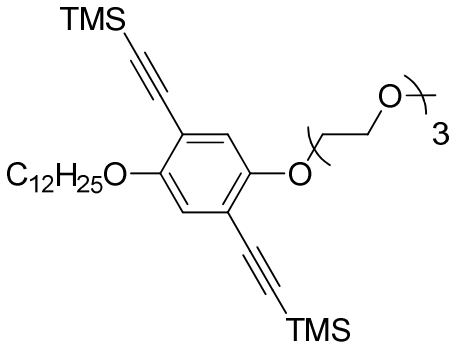


**(2-(Dodecyloxy)-5-(2-(2-(2-methoxyethoxy)ethoxy)ethoxy)-1,4-phenylene)bis(ethyne-2,1-diyl)bis(trimethylsilane), III-3.** Diiodide **III-2** (2.0 g, 3.1 mmol) was added to a stirred solution of $PdCl_2(PPh_3)_2$ (117 mg, 155 μmol) and CuI (29 mg, 155 μmol) in a mixture of piperidine (6 mL) and toluene (4 mL). The mixture was degassed by freeze-pump-thaw and back-filling with argon. Trimethylsilylacetylene (0.67 g, 6.8 mmol) was added dropwise over 10 min and the mixture was stirred for 2 h. $CH_2Cl_2$ (100 mL) was added and the mixture was flushed through silica plug. The solvent was removed under reduced pressure to afford **III-3** (1.62 g, 89% yield) as a yellow oil. $^1$H NMR (300 MHz, $CDCl_3$): δ 6.98 (s, 1H, Ar C6-H), 6.92 (s, 1H, Ar C3-H), 4.12 (t, $^3J_{HH}$ = 5.1 Hz, 2H), 3.92 (t, $^3J_{HH}$ = 6.6 Hz, 2H), 3.82 (t, $^3J_{HH}$ = 5.1 Hz, 2H), 3.76 (t, $^3J_{HH}$ = 5.1 Hz, 2H), 3.62-3.72 (m, 4H), 3.52 (t, $^3J_{HH}$ = 5.1 Hz, 2H), 3.35 (s, 3H, -$OCH_3$), 1.70-1.85 (m, 2H, -$CH_2$- C-2), 1.22-1.5 (m, 18H), 0.87 (t, $^3J_{HH}$ = 6.6 Hz, 3H, -$CH_3$), 0.25 (s, 18H, 2 × -$Si(CH_3)_3$). $^{13}$C NMR (75 MHz, $CDCl_3$): δ 154.83 (Ar C5), 154.22 (Ar C2), 118.95 (Ar C6), 118.06 (Ar C3), 114.06 (Ar C1,4), 100.85, 100.15 (-C≡C-), 72.58, 71.7, 71.35, 71.2, 70.26, 70.21, 70.17, 59.69 (-$OCH_3$), 32.14, 31.73, 29.88, 29.81, 29.78, 29.58, 29.50, 29.34, 26.25, 22.92, 14.37 (-$CH_3$). IR ($\nu$, $cm^{-1}$): 2922 (Ar C-H str.), 2852, 2372, 2347, 2157, 2151 (C≡C str.), 1966, 1496, 1467, 1401, 1390, 1273, 1221 (C-O str.), 1200, 1107, 1055, 864, 643. HRMS: *calc*. for $C_{25}H_{42}O_5I_2$ = 617.018900, *obs*. = 617.018904, Δ = 4.1 ppm.

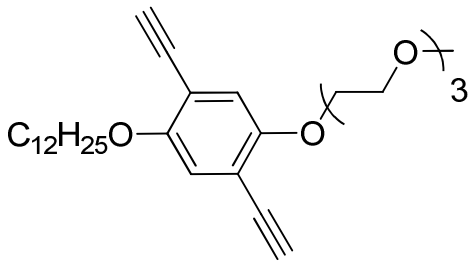


**1-(Dodecyloxy)-2,5-diethynyl-4-(2-(2-(2-methoxyethoxy)ethoxy)ethoxy)benzene, III-4.** Tetra-*n*-butylammonium fluoride (1.21 g, 4.64 mmol) was added dropwise to a solution of (2-bis(trimethylsilane) **III-3** (1.3 g, 2.11 mmol) in dry THF (15 mL) and the mixture was stirred overnight and poured into $H_2O$ (50 mL). The mixture was extracted with $CH_2Cl_2$ (100 mL), the combined extracts were dried over $MgSO_4$ and the solvent was removed under reduced pressure. The residue was recrystallized from ethanol to give diethyne **III-4** (0.91 g, 91% yield) as a pale yellow solid, m.p. = 71-74 °C. $^1$H NMR (300 MHz, $CDCl_3$): δ 6.98 (s, 1H, Ar C3-H), 6.92 (s, 1H, Ar C6-H), 4.12 (t, $^3J_{HH}$ = 5.1 Hz, 2H), 3.92 (t, $^3J_{HH}$ = 6.6 Hz, 2H), 3.82 (t, $^3J_{HH}$ = 5.1 Hz, 2H), 3.76 (t, $^3J_{HH}$ = 5.1 Hz, 2H), 3.62-3.72 (m, 4H), 3.52 (t, $^3J_{HH}$ = 5.1 Hz, 2H), 3.35 (s, 3H, -$OCH_3$), 3.32 (s, 1H, ≡C-H), 3.31 (s, 1H, ≡C-H), 1.72-1.85 (m, 2H, -$CH_2$- C-2), 1.22-1.5 (m, 18H), 0.87 (t, $^3J_{HH}$ = 6.6 Hz, 3H, -$CH_3$). $^{13}$C NMR (75 MHz, $CDCl_3$): δ 154.73 (Ar C4), 154.12 (Ar C1), 118.91 (Ar C5), 118.06 (Ar C2), 114.06 (Ar C3,6), 83.28, 83.20, 80.33, 80.23 (-C≡C-), 72.58, 71.7, 71.35, 71.2, 70.26, 70.21, 70.17, 59.69 (-$OCH_3$), 32.14, 31.72, 29.87, 29.80, 29.78, 29.58, 29.50, 29.34, 26.24, 22.92, 14.36 (-$CH_3$). IR (AT-IR, neat): 3280 (≡C-H str.), 2922 (Ar C-H str.), 2852, 2157 (C≡C str.), 1966, 1496, 1467, 1401, 1390, 1273, 1221 (C-O str.), 1200, 1107, 1055, 864, 643. HRMS: Calculated for $C_{19}H_{30}O_2I_2$, 472.31887; Observed, 472.31458; Δ = 9.1 ppm.

### 3.2.3. Synthesis of monomers III-7 for preparation of regioregular $C_{12}/EG_3$ PPE

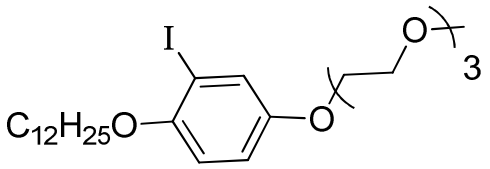


**1-(Dodecyloxy)-2-iodo-4-(2-(2-(2-methoxyethoxy)ethoxy)ethoxy)benzene, III-5.** Monoiodinated phenol, **II-8b** (8.47 g, 20.91 mmol) was added to a stirred solution of $PPh_3$ (6.56 g, 25.91 mmol) and 2-(2-(2-methoxyethoxy)ethoxy)ethanol (4.12 g, 25.91 mmol) in $Et_2O$ (60 mL) under Ar. Diethyl azodicarboxylate (DEAD) (4.37 g, 25.91 mmol) was added dropwise by syringe and the resulting pale yellow solution was stirred at room temperature for 24 h. $Et_2O$ (60 mL) was added and the solution was washed with 10% aqueous NaOH (200 mL) followed by $H_2O$ (100 mL). The solution was dried over $MgSO_4$, the solvent was removed under reduced pressure, and the residue was subjected to flash column chromatography (25:75 v/v ethyl acetate:hexanes) to afford **III-5** (10.7 g, 88.4 % yield) as a pale yellow oil. $^1$H NMR (300 MHz, $CDCl_3$): δ 7.34 (d, $^4J_{HH}$ = 2.9 Hz, 1H, Ar C3-H), 6.83 (dd, $^3J_{HH}$ = 8.9 Hz, $^4J_{HH}$ = 2.9 Hz, 1H, Ar C5-H), 6.71 (d, $^3J_{HH}$ = 8.9 Hz, 1H, Ar C6-H), 4.03 (t, $^3J_{HH}$ = 5.1 Hz, 2H, -$OCH_2$-, C-1), 3.91 (t, $^3J_{HH}$ = 6.6 Hz, 2H), 3.79 (t, $^3J_{HH}$ = 5.1 Hz, 2H), 3.72-3.60 (m, 6H), 3.52 (t, $^3J_{HH}$ = 5.1 Hz, 2H), 3.37 (s, 3H, -$OCH_3$), 1.65-1.85 (m, 2H, -$CH_2$- C-2), 1.2-1.58 (m, 18H), 0.89 (t, $^3J_{HH}$ = 6.6 Hz, 3H, -$CH_3$). $^{13}$C NMR: δ 153.54 (Ar C4), 152.60 (Ar C1), 125.83 (Ar C3), 115.79 (Ar C5), 113.08 (Ar C6), 87.05 (Ar C2), 72.15, 71.04, 70.87, 70.80, 70.28, 69.96, 68.52, 59.27 (-$OCH_3$), 32.15, 31.70, 29.88, 29.81, 29.59, 29.56, 29.47, 29.34, 26.31, 22.93, 14.34 (-$CH_3$). IR ($\nu$, $cm^{-1}$): 2920 (Ar C-H str.), 2851, 2030, 1733, 1597, 1568, 1486, 1466, 1387, 1350, 1271, 1209 (C-O str.), 1106, 1062, 935, 850, 801, 770, 721. HRMS: *calc*. for $C_{25}H_{43}O_5I$= 550.21553, *obs*. = 550.21641, Δ = 1.6 ppm.

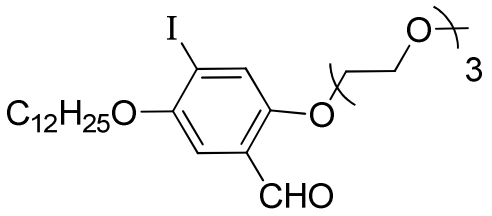


**5-(Dodecyloxy)-4-iodo-2-(2-(2-(2-methoxyethoxy)ethoxy)ethoxy)benzaldehyde, III-6.** $TiCl_4$ (8.65g, 45.5 mmol) was added dropwise to a solution of monoiodinated diether **III-5** (2.5 g, 4.55 mmol) in dry $CH_2Cl_2$ (50 mL) at -40 °C in a dry flask under Ar. The mixture was stirred for 15 min at -40 °C. dichloromethyl methyl ether (1.31 g, 11.38 mmol) was added dropwise and stirring was continued for another 2h. The reaction mixture was poured into mixture of conc. HCl and ice. The mixture was extracted with $CH_2Cl_2$ (100 mL) and the extract was washed with water (100 mL). The organic layer was dried over $MgSO_4$ and the solvent was removed under reduced pressure. The residue was recrystallized from hexanes to afford **III-6** as a white solid (1.7 g, 64 % yield), m.p. = 39-40 ºC. $^1$H NMR (300 MHz, $CDCl_3$): δ 10.41 (s, 1H, -CHO), 7.48 (s, 1H, Ar C3-H), 7.16 (s, 1H, Ar C6-H), 4.19 (t, $^3J_{HH}$ = 5.1 Hz, 2H), 3.97 (t, $^3J_{HH}$ = 6.6 Hz, 2H), 3.85 (t, $^3J_{HH}$ = 5.1 Hz, 2H), 3.74-3.60 (m, 6H), 3.52 (t, $^3J_{HH}$ = 5.1 Hz, 2H), 3.37 (s, 3H, -$OCH_3$), 1.65-1.85 (m, 2H, -$CH_2$- C-2), 1.2-1.58 (m, 18H), 0.89 (t, $^3J_{HH}$ = 6.6 Hz, 3H, -$CH_3$). $^{13}$C NMR (75 MHz, $CDCl_3$): δ 188.90 (-CHO), 155.20 (Ar C2), 152.33 (Ar C5), 125.41 (Ar C1), 125.12 (Ar C3), 108.63 (Ar C6), 96.42 (Ar C4), 71.91, 70.92, 70.67, 70.61, 69.88, 69.55, 69.31, 59.07 (-$OCH_3$), 32.00, 29.75, 29.73, 29.67, 29.64, 29.44, 29.37, 29.10, 26.13, 22.80, 14.26 (-$CH_3$). IR ($\nu$, $cm^{-1}$): 2920 (Ar C-H str.), 2850, 1680 (C = O str.), 1590, 1470, 1390, 1210 (C-O str.), 1130, 1032, 867, 827, 748, 715, 611. HRMS: calc. for $C_{25}H_{41}O_3I$ = 578.21044, obs. = 578.21385, Δ = 5.9 ppm.

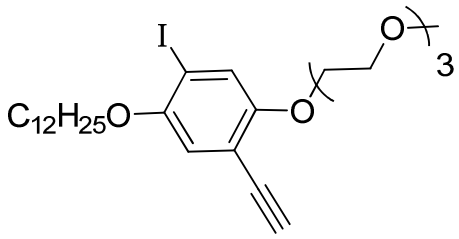


**1-(Dodecyloxy)-5-ethynyl-2-iodo-4-(2-(2-(2-methoxyethoxy)ethoxy)ethoxy)benzene, III-7.** Bestman-Ohiro reagent, $CH_3COC(=N_2)PO(CH_3O)_2$ (0.75 g, 3.9 mmol), was added dropwise to a mixture of aldehyde **III-6** (1.5 g, 2.6 mmol) and $K_2CO_3$ (0.894 g, 6.5 mmol) in 12 mL of a 1:1 v/v mixture of anhydrous $CH_2Cl_2$ and MeOH under argon, and the mixture was stirred for 10 h. The solvent was removed under reduced pressure and column chromatography (silica gel, 30% ethyl acetate/hexanes) afforded **III-7** (0.7 g, 47 % yield) as a yellow oily solid. $^1$H NMR (300 MHz, $CDCl_3$): δ 7.31 (s, 1H, Ar C3-H), 6.81 (s, 1H, Ar C6-H), 4.12 (t, $^3J_{HH}$ = 5.1 Hz, 2H), 3.92 (t, $^3J_{HH}$ = 6.6 Hz, 2H), 3.82 (t, $^3J_{HH}$ = 5.1 Hz, 2H), 3.72 (t, $^3J_{HH}$ = 5.1 Hz, 2H), 3.58-3.70 (m, 4H), 3.50 (t, $^3J_{HH}$ = 5.1 Hz, 2H), 3.37 (s, 3H, -$OCH_3$), 3.28 (s, 1H, -C≡C-H), 1.65-1.85 (m, 2H, -$CH_2$- C-2), 1.2-1.58 (m, 18H), 0.89 (t, $^3J_{HH}$ = 6.6 Hz, 3H, -$CH_3$). $^{13}$C NMR (75 MHz, $CDCl_3$): δ 154.75 (Ar C4), 152.26 (Ar C1), 124.77 (Ar C3), 116.66 (Ar C6), 112.8 (Ar C5), 88.36 (Ar C2), 82.32, 79.85 (-C≡C-), 72.15, 71.25, 70.91, 70.77, 70.19, 70.00, 69.84, 59.23 (-$OCH_3$), 32.14, 29.89, 29.87, 29.81, 29.79, 29.58, 29.51, 29.33, 26.26, 22.91, 14.38 (-$CH_3$). IR ($\nu$, $cm^{-1}$): 3300 (≡C-H str.), 2920 (Ar-H str.), 2850, 2159 (C≡C str.), 1480, 1465, 1371, 1220 (C-O str.), 1026, 856, 818, 725, 687, 642. HRMS: calc. for $C_{26}H_{41}O_2I$ = 574.21553, obs. = 574.21477, Δ = 1.3 ppm.

### 3.2.4. Synthesis of regiorandom and regioregular $C_{12}/EG_3$ PPEs

**Regiorandom $C_{12}/EG_3$, RnPPE.** A solution of monomers **III-2** (557 mg, 823 μmol) and **III-4** (400 mg, 848 μmol), $Pd(PPh_3)_4$ (47.5 mg, 41 μmol) and CuI (9.4 mg, 49 μmol) in a mixture of morpholine (16 mL) and diisopropylamine (4 mL) was heated at 70 °C for 4 d. The mixture was poured into 50 mL of hexane and the precipitated solid was removed by filtration. The solid was then subjected to sequential extractions in a Soxhlet extractor with MeOH, hexanes (for 48 h to ensure complete catalyst removal), followed by $CHCl_3$. The solvent was removed from the $CHCl_3$ fraction to afford **RnPPE**, (460 mg, 57% yield). $^1$H NMR (300 MHz, $CDCl_3$): δ 6.88-7.18 (b, 2H, Ar), 4.21 (b, 2H), 4.02 (b, 2H), 3.88 (b, 2H), 3.72 (b, 2H), 3.54-3.70 (b, 4H), 3.48 (b, 2H), 3.32 (s, 3H, $-OCH_3$), 1.83 (b, 2H), 1.06-1.60 (b, 18H), 0.85 (b, 3H, $-CH_3$). IR ($\nu$, $cm^{-1}$): 3458, 2920 (Ar C-H str.), 2851, 1273, 1212, 1104, 750.

**Regioregular dodecyloxy/$EG_3$, RgPPE.** A-B type monomer **III-7** (430 mg, 749 μmol) was treated with $Pd(PPh_3)_4$ (17.3 mg, 15 μmol) and CuI (7.1 mg, 37 μmol) in morpholine/diisopropylamine as described above. Precipitation and extraction as described above for **RnPPE** gave a $CHCl_3$ soluble fraction of **RgPPE** (150 mg, 70% yield) that was characterized further. $^1$H NMR (300 MHz, $CDCl_3$): δ 6.90-7.18 (b, 2H, Ar), 4.22 (b, 2H), 4.02 (b, 2H), 3.88 (b, 2H), 3.74 (b, 2H), 3.54-3.69 (b, 4H), 3.48 (b, 2H), 3.35 (s, 3H, $-OCH_3$), 1.82 (b, 2H), 1.12-1.58 (b, 18H), 0.85 (b, 3H, $-CH_3$). IR (AT-IR, neat): 3457, 2918 (Ar C-H str.), 2849, 1269, 1214, 1109, 755.

## 3.3. RESULTS AND DISCUSSION

### 3.3.1. Synthesis of the Monomers and Polymerization

To develop an understanding of the influence of regioregularity on the properties of amphiphilic PPEs we prepared both regioregular (**RgPPE**) and regiorandom (**RnPPE**) analogs bearing hydrophobic dodecyl and hydrophilic triethylene glycol ($EG_3$) side chains on each phenylene unit in the backbone. The polymerization of didiodide and bis(ethynylene) monomers which are each substituted with a pair of dissimilar side chains by alkyne-aryl iodide[42] coupling yields regiorandom PPEs containing *hh*, *tt* and *ht* dyads. We have recently developed synthetic routes to prepare regioregular (*ht*) asymmetrically-substituted PPEs by polymerization of 2,5-disubstituted-4-iodophenylacetylenes, Figure 3.1.[13,14]

***A-A and B-B type Monomers for Preparation of Regiorandom Amphiphilic PPEs.*** The regiorandom PPE was synthesized by the commonly used Sonagashira condensation polymerization of diiodo monomer **III-2** and the dialkyne monomer **III-4** as shown in Figure 3.2.[42] The monomers were synthesized by previously used methods whereby the unsymmetrically substituted 1,4-dialkoxybenzenes were subjected to diiodination to form the diiodo monomer **III-2**, followed by substitution of the iodines with protected alkyne (TMS-acetylene, $Pd(PPh_3)_4$, CuI) and deprotection ($n$-$Bu_4NF$) to give monomer **III-4**.

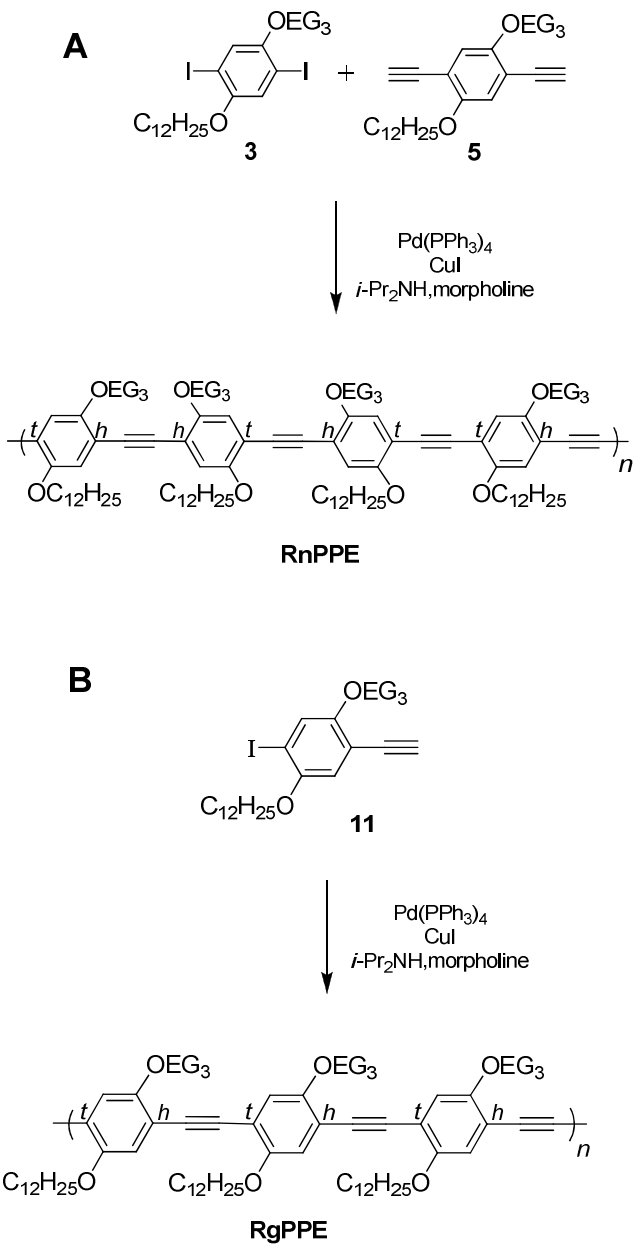


**Figure 3.1.** Preparation of the amphiphilic C12/$EG_3$-substituted PPEs. A, preparation of regiorandom analogs **RnPPE** by polymerization of diiodobenzene **III-2** and diethynylbenzene **III-4** (i.e., $A_2$ + $B_2$ polymerization); B, preparation of regioregular analogs **RgPPE** by polymerization of 4-iodophenyl acetylene (A-B type monomer) **III-7**.

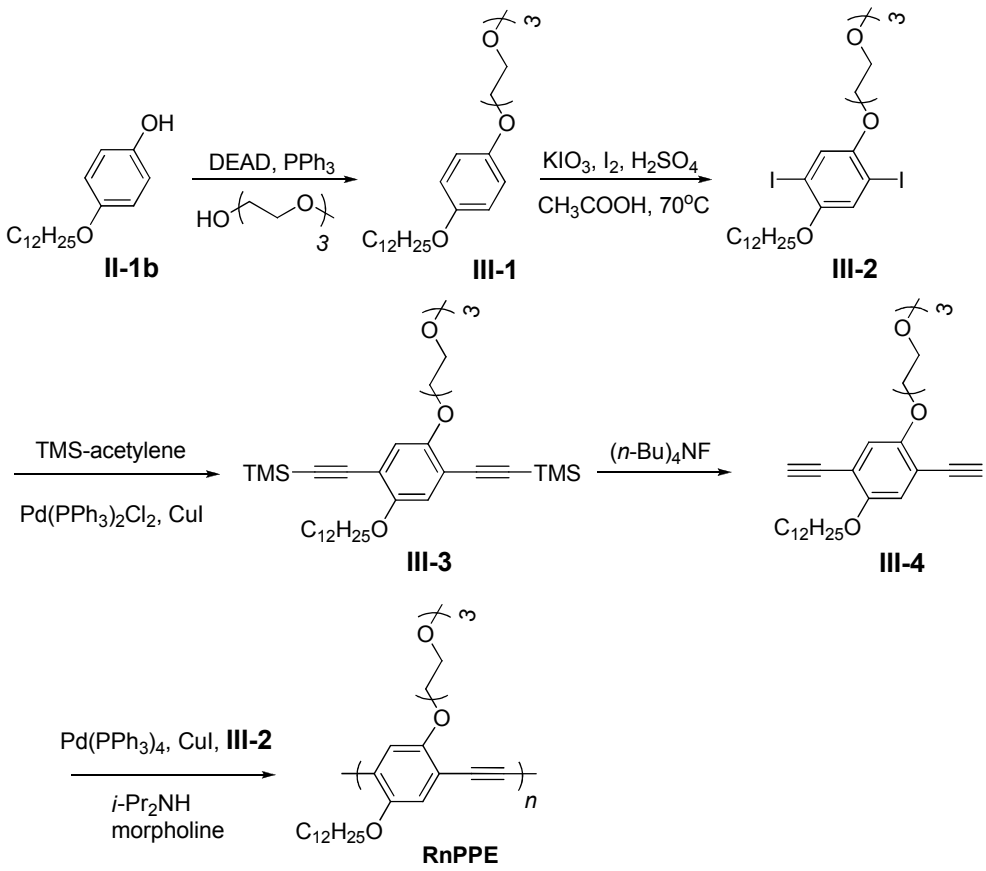


**Figure 3.2.** Scheme for the synthesis of the A-A and B-B type monomer **III-2** and **III-4** respectively for the preparation of **RnPPE.**

***A-B type Monomers for preparation of Regioregular Amphiphilic PPEs.*** The analogous regioregular polymer was prepared by polymerization of an A-B type monomer, **III-7**, having both the iodo and the alkyne in the same molecule. The synthesis of monomer **III-7** is shown in Figure 3.3. Selective monoiodination of the tosylate **II-6b**[14] followed by hydrolysis of the tosylate and installation of the triethylene glycol side chain by Mitsunobu coupling provides the 1,2,4-trisubstituted benzene **III-5**. Regioselective formylation of **III-5** using $TiCl_4$ and $CHCl_2OCH_3$ at low temperature lead to the formation of the benzaldehyde **III-6**. While simple dialkoxy-substituted arenes are subject to formylation with 4-6 equivalents of $TiCl_4$, in the case of the triethylene glycol analogs we had to use 10-12 equivalents, likely due to the coordination with the oxygens in the side chain. The homologation reaction of the benzaldehyde in presence of the Bestman reagent $CH_3COC(=N_2)CPO(OCH_3)_2$ and $K_2CO_3$ afforded the alkyne **III-7** in high yield. Polymerization of monomer **III-7** by Pd catalyzed Sonogashira condensation polymerization afforded the regioregular polymer **RgPPE**.

### 3.3.2. Characterization of the PPE Structure

The polymers were characterized by $^1H$ and $^{13}C$ NMR spectroscopy and gel permeation chromatography. Molecular weights of the regiorandom and regioregular analogs (chloroform fraction) determined by NMR spectroscopic analysis of end groups (by integration of peaks shown in Figure 3.4)[14] and by GPC were similar:

**RnPPE**,($M_n$(GPC) = 54.7 kD; $M_n$(NMR) = 47.9 kD; $M_w$(GPC) = 84.1 kD; PDI= 1.53);

**RgPPE** ($M_n$(GPC) = 59.2 kD; $M_n$(NMR) = 46.6 kD; $M_w$(GPC) = 92.1 kD; PDI= 1.56).

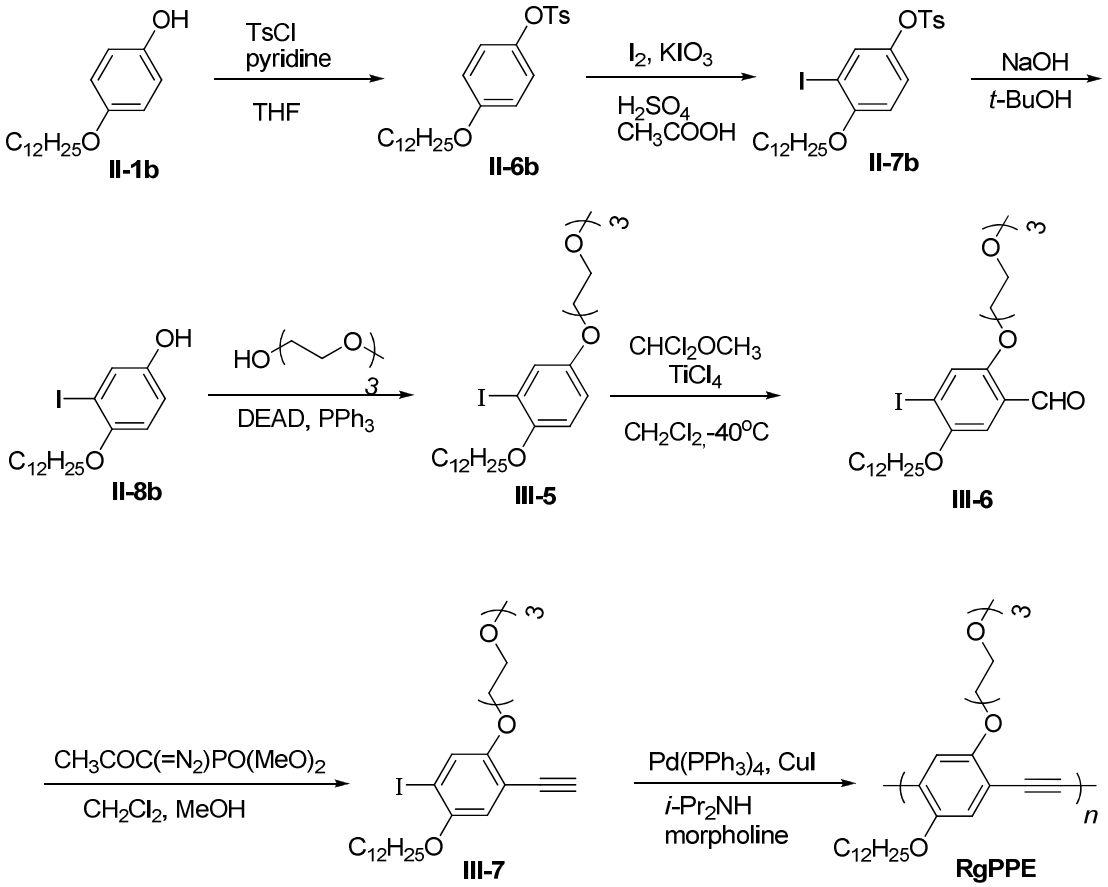


**Figure 3.3.** Scheme for the synthesis of the AB type monomer **III-7** for the preparation of **RgPPE**

The different relative placement of side chains along the polymer backbones was demonstrated using $^{1}H$ NMR spectroscopy by comparison of the peaks for the protons on the 1,4-phenylene units of the two analogs, Figure 3.4. The NMR spectra of the polymers were measured in $CDCl_3$ at 55 °C under identical conditions. The regioregular analogue,**RgPPE**,gives rise to two sharp peaks in the aromatic region corresponding to the protons in the 3 position (ortho to the dodecyloxy side chain) and the 6 position of the phenylene units (ortho to the $EG_3$ chains) at 7.05 and 6.95 ppm, respectively (Figure 3.4B). The regiorandom analogue, **RnPPE**, also shows two peaks with similar chemical shift but are much broader then the regioregular analogue (the width at half height being 0.02 and 0.01 ppm for **RnPPE** and **RgPPE**, respectively), Figure 3.4A. In our previous report on unsymmetrically dialkoxy (e.g. methoxy/dodecyloxy) substituted PPEs,[13] we observed similar broadening of peaks arising from the presence of different steric environments in the form of *hh*, *tt* and *ht* diads.[14] For the **RgPPE,** the spectral parts are sharp because all the protons are in a single type of dyad (*ht*).

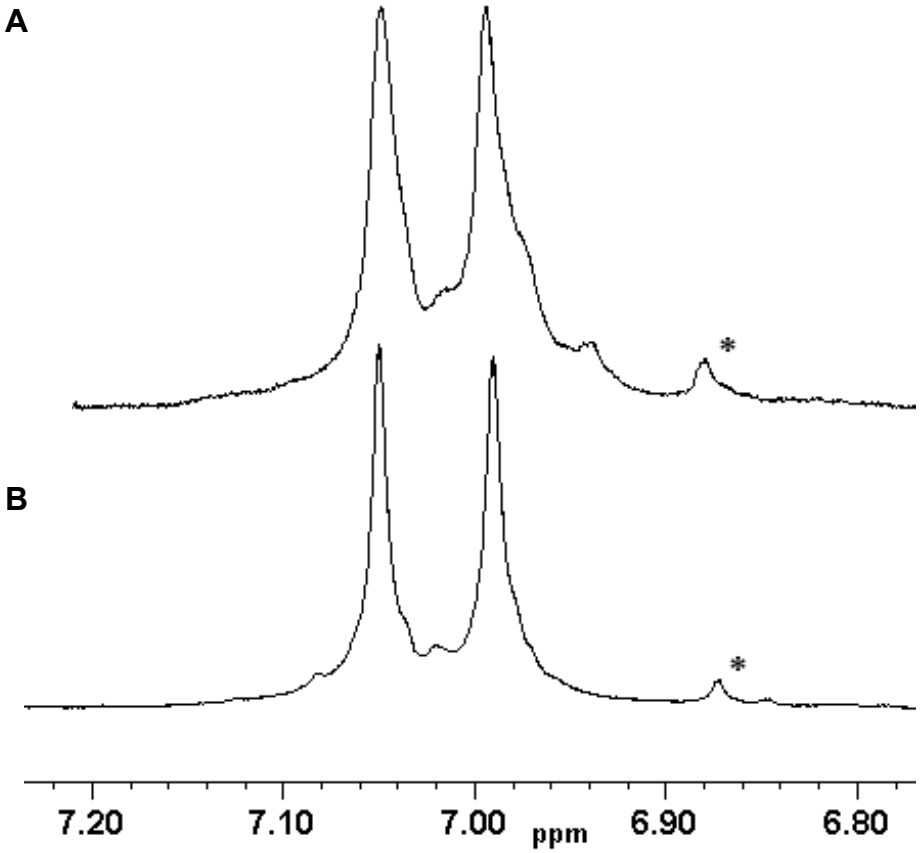


**Figure 3.4.** Aromatic region of $^{1}H$ NMR spectra (400 MHz, $CDCl_3$): A, regiorandom PPE **RnPPE** ; and B, regioregular PPE **RgPPE**. * Denotes end groups (used in the determination of molecular weight by $^{1}H$ NMR spectroscopy.

More significant differences arising from the relative placement of side chains are apparent in the $^{13}C$ NMR spectra of the polymers. In the regioregular polymer the carbons bearing the alkoxy groups appear as sharp peaks at 153.1 and 153.8 ppm (Figure 3.5B) whereas in the regiorandom analogue the signals of these carbons are broad and appear as two closely spaced peaks (Figure 3.5A). The peaks for the unsubstituted positions (C-3 and C-6) of **RnPPE** at 117.4 and 118.4 ppm are broader and complex compared to the sharp peaks in the spectrum of **RgPPE** The aromatic carbon atoms of the alkyne group appears in the form of two sharp peaks at 114.3 and 114.9 ppm in the regioregular polymer while the regiorandom sample has a broader peak with a maximum at 114.6 ppm (Figure 3.5). Thus the appearance of the peaks of the aromatic regions of the $^{1}H$ and $^{13}C$ NMR spectra confirm the presence of a single type of diad (*ht*) in the materials prepared by polymerization of AB monomer **III-7**, and the expected mixture of diads (*ht*, *hh*, and *tt*) in the material prepared by polymerization of $A_2$ and $B_2$ monomers **III-2** and **III-4**.

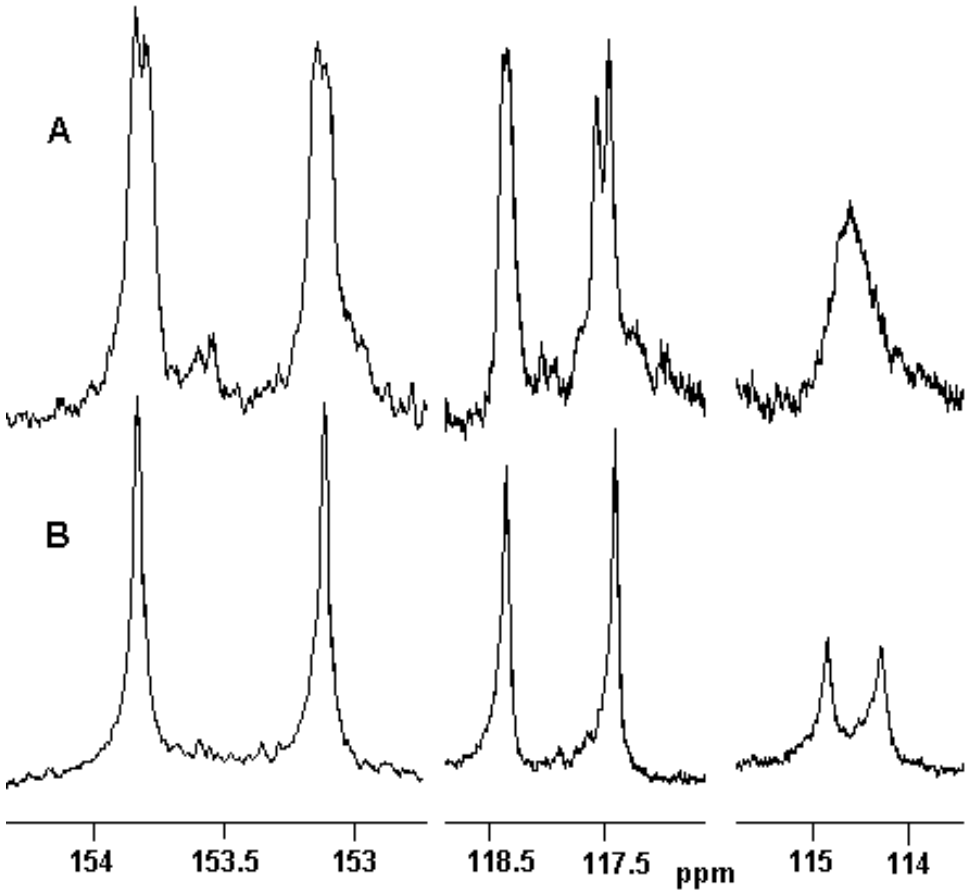


**Figure 3.5.** $^{13}C$ NMR spectra (400 MHz, $CDCl_3$), A. regiorandom PPE **RnPPE** and B. regioregular PPE **RgPPE** (bottom).

### 3.3.3. Electronic Properties of the PPEs

UV-vis spectroscopy allows for determination of bandgap and correlation of degree of conjugation with molecular structure. The UV-vis spectra of both the regiorandom and regioregular amphiphilic polymers were recorded in chloroform solution and as drop-casted thin films on a quartz substrate. In solution, the regioregular PPE exhibits an absorption maximum ($\lambda_{max}$) at 441 nm that is slightly red shifted compared to the regiorandom PPE analogue ($\lambda_{max}$ = 427 nm), Figure 3.6. In the case of unsymmetric dialkoxy-substituted PPEs (methoxy-dodecyloxy substituted PPEs),[13] the regioregular and regiorandom materials had identical UV-vis absorptions ($\lambda_{max}$ = 436 nm) due to the low energy barrier to conformational rotation around the polymer backbone (< 1 kcal $mol^{-1}$). In the case of the amphiphilic alkoxyl/$EG_3$ substituted polymer, the red shift of the regioregular analog relative to the regiorandom analog indicates a greater conjugation length arising from the regioregular placement of the dissimilar side chains. However the differences between the two analogues are remarkably high in the solid state.

In the solid state, Figure 3.6, the absorptions of both materials are broader and red shifted relative to the corresponding spectra in solution. The regioregular material has a greater contribution towards higher wavelength ($\lambda_{max}$ = 496 nm) and relatively lower contribution towards lower wavelength ($\lambda$ = 466 and 453 nm). On the other hand the regiorandom analogue has a significant contribution towards lower wavelength ($\lambda_{max}$ = 441 nm) and a very small one at 475 nm. This red-shift of $\lambda_{max}$ by 55 nm can be ascribed to a combination of a conjugated chain and highly overlapping intermolecular arrangement of $\pi$ systems in the solid state of the regioregular amphiphilic PPE.

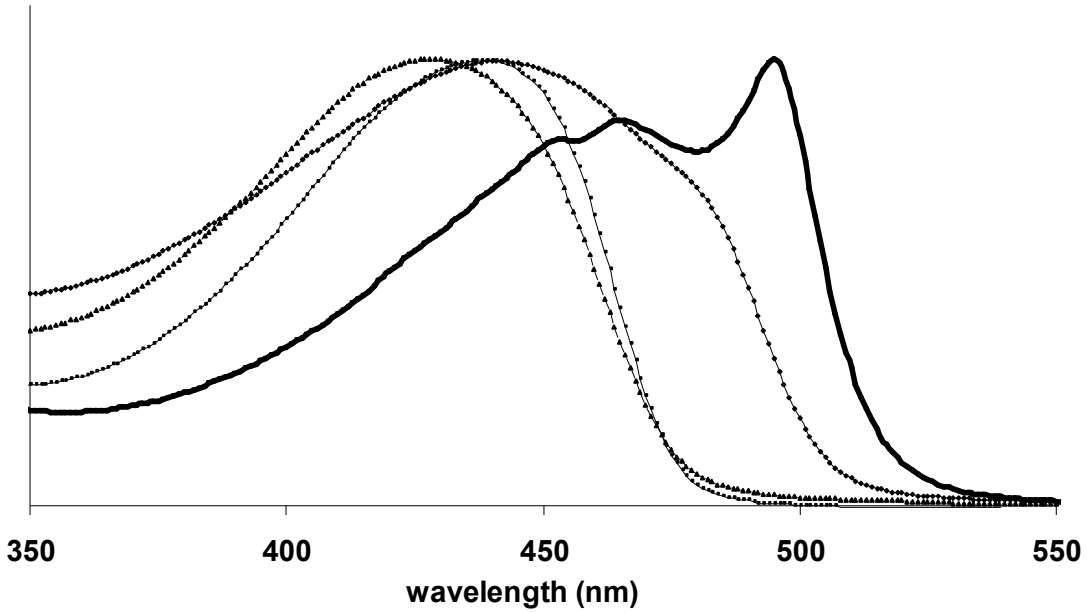


**Figure 3.6**. UV-vis spectra of RnPPE (···) and RgPPE (- - -) in $CHCl_3$ solution, RnPPE annealed film (—) and RgPPE annealed film (▬).

The steric hindrance (as shown in Figure 3.7a) associated with *hh* and *tt* linkages in the regiorandom analog, along with interaction of incompatible side chains (Figure 3.7b), results in twisting along the backbone disruption of planarity, and a decrease in conjugation length leading to a shift in the absorptions to higher energy. In the case of the regioregular PPE the *ht* arrangement of side chains allows for segregation of the two types of side chain on each side of the polymer backbone (Figure 3.7d) to form a highly ordered assembly of molecular with a planar, conjugated conformation in the solid state with close chain-chain interactions between the π systems. Thus the UV-vis spectra provide a strong evidence for the formation of a highly ordered phase due to the amphiphilic regioregular structure.

### 3.3.4. Molecular Assembly of the PPEs

A better understanding of the effect of the relative placement of side chain on chain packing in the solid state can be obtained from X-ray diffraction studies. The X-ray diffractogram for the regioregular and regiorandom PPE are shown in Figure 3.8. The diffractogram of a film prepared by drop casting a 20 mg/mL solution of **RgPPE** in xylene shows only two broad reflection, centered at 2.12° (41.6 Å) and 3.96° (22.3 Å), Figure 3.8B. Upon annealing (120 °C for 24 h under $N_2$), several sharp low-angle reflections appear, corresponding to a well ordered structure (Figure 3.8A). The regioregular material shows seven peaks at 2θ = 2.16° (40.9 Å), 4.22° (20.9 Å), 6.3° (14.1 Å), 8.36° (10.6 Å), 10.44° (8.5 Å), 12.5° (7.1 Å) and 14.54° (6.1 Å) which can be assigned as the (100), (200), (300), (400), (500), (600) and (700) planes of a bilayered crystal with an interlayer spacing of 40.9 Å (Figure 3.8 inset). This spacing is slightly

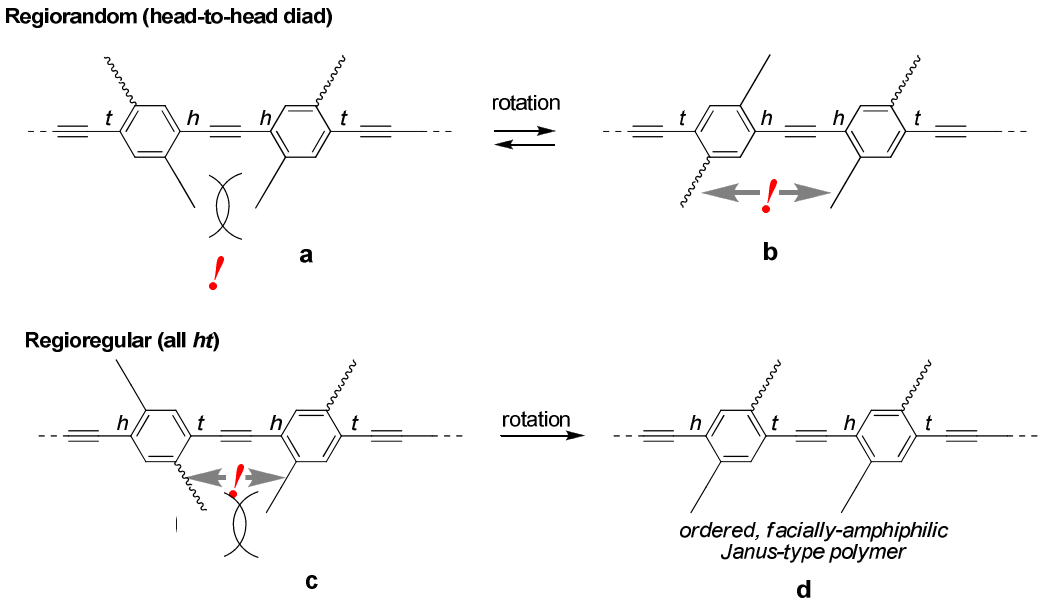


**Figure 3.7**. Conformation of amphiphilic regiorandom and regioregular PPEs.

smaller than the width of two Janus type polymer chains (~ 46 Å), which indicates a certain extent of interdigitation of the side chains. The lack of a peak corresponding to a π-π stacking distance between chains suggests that the material is highly oriented with the plane of the polymer backbone perpendicular to the substrate.

On the other hand, the X-ray diffractogram of the regiorandom PPE (Figure 3.8C) is devoid of the sharp peaks that are indicative of bilayer packing, suggesting the formation of a largely amorphous material, even after extended annealing. Thus, the unfavorable steric interactions and incompatibility of side chains disrupts the inter-chain interactions resulting in a disorder film.

### 3.3.5. Molecular Assembly of the PPEs at the Air-Water Interface

The Langmuir-Blodgett technique is useful for the study self organization and chain-chain interactions in polymers at the air-water interface.[43] A dilute solution of regiorandom and regioregular PPE in chloroform was transferred to the air-water interface of a Langmuir trough. Figure 3.9 shows the surface pressure - area isotherms of films of **RnPPE** and **RgPPE.** Both plots have the shape of conventional LB isotherms consisting of two-dimensional gas, liquid and solid phases. The onset of the liquid phase in the regiorandom PPE occurs at higher area per repeat unit compared to that of the regioregular PPE. The extrapolated area for the onset of the liquid phase, i.e., the measure of the packing density, is 0.20 $nm^2$/repeat unit for the regiorandom PPE and 0.17 $nm^2$/repeat unit for the regioregular analogue. This difference provides insight into the arrangement of the polymer chains: The lower extrapolated area per unit for **RgPPE**

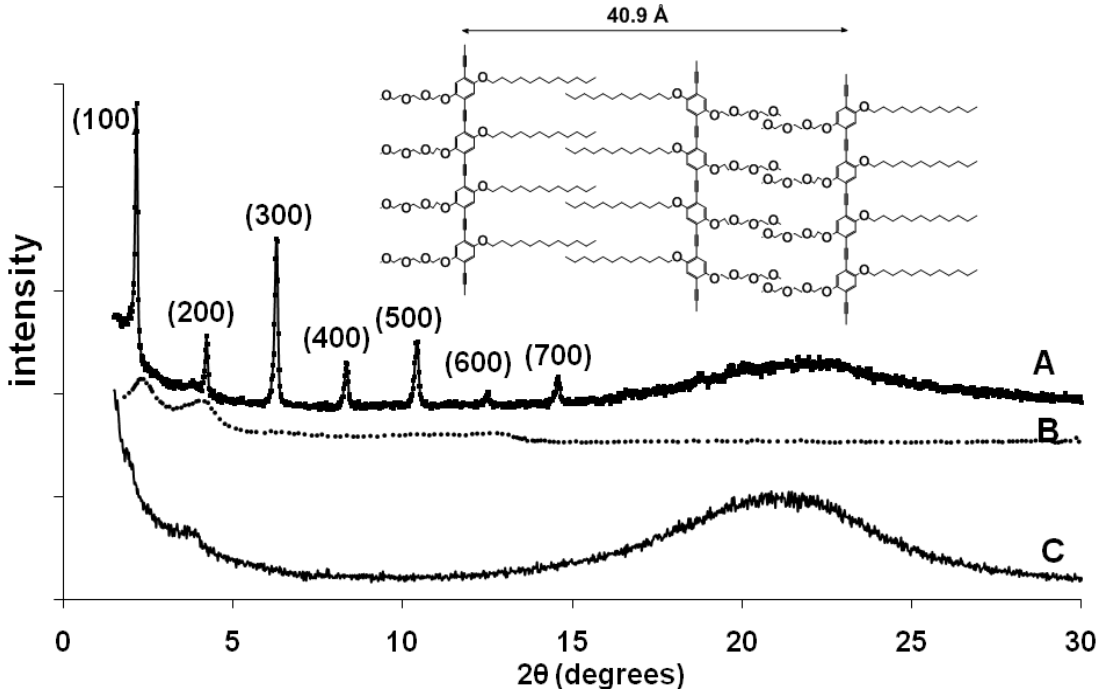


**Figure 3.8.** X-ray powder diffraction: A) annealed regioregular polymer film (RgPPE); B) unannealed regioregular polymer film; C) annealed regiorandom polymer film (RnPPE). Inset: Model of bilayer packing in the regioregular C12-$EG_3$ PPE.

indicates the ability of these chains to pack more closely due to its regular structure which can adopt a planar conformation, Figure 3.9A. In contrast, the irregular placement of incompatible side chains of the regiorandom PPE analog, and the resulting resistance to planarization, leads to interaction of molecules at the air-water interface (i.e., condensation of the two-dimensional gas to the liquid state) at a lower area density (larger areas per repeat unit), Figure 3.9B.

The slopes of the isotherms of the liquid phase of both the regioregular and regiorandom monolayers are similar. The maximum sustainable pressure of the solid state is attained at 0.09 $nm^2$ per repeat unit (44.5 mN/m) for the monolayer of regioregular polymer, and 0.11 $nm^2$ per repeat unit (43.7 mN/m) for the regiorandom analog. Accordingly, the more planarizable regioregular polymer chains pack more closely than the regiorandom polymers. As the 2D solid is compressed further the monolayer have high stability upto a pressure of about 54 mN/m. On the other hand, monolayer films of the regiorandom analog, **RnPPE**, collapse at 43 mN/m which can be explained by the combination of sterics and incompatible side chain interactions.

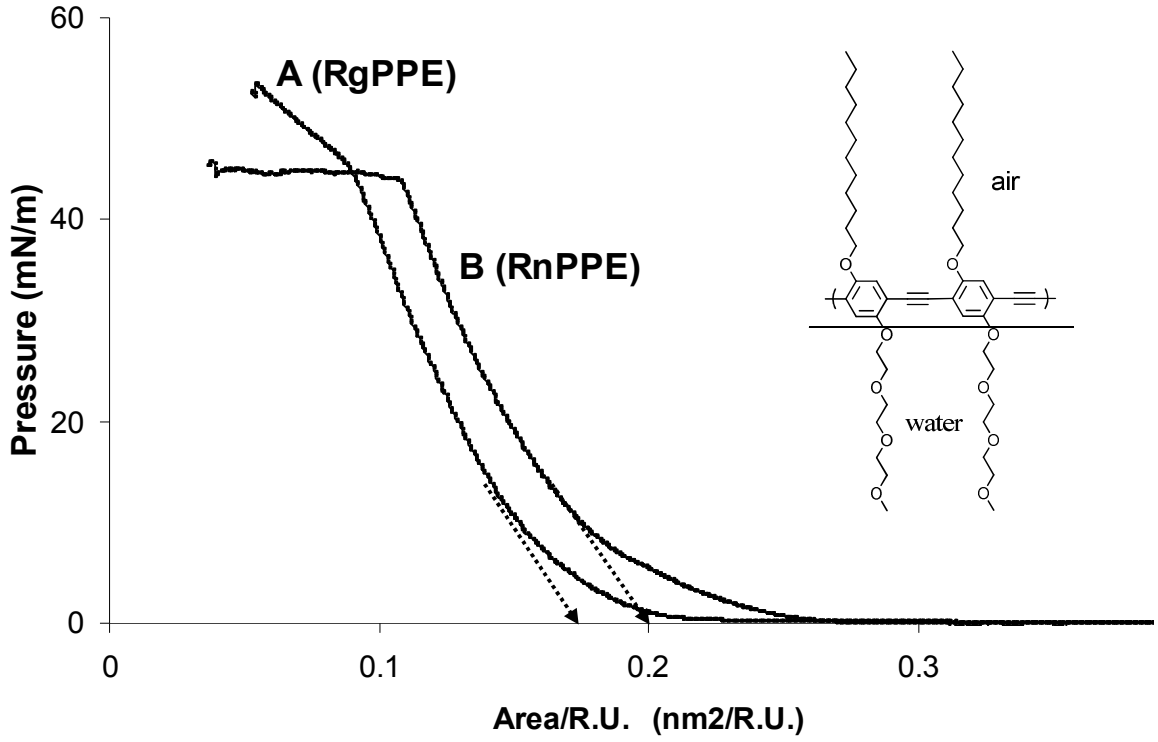


**Figure 3.9.** Surface pressure- Area isotherms: A) regioregular PPE; B) regiorandom PPE spread at a water subphase at 25 °C.

## 3.4. CONCLUSIONS

We have prepared novel amphiphilic regiorandom and regioregular PPEs and demonstrated that regioregularity has a strong influence on the molecular assembly and electronic structure to a great extent in the solid state and at the air-water interface. The regioregular PPE forms a particularly ordered bilayer lamellar structure in the solid state due to the segregation of hydrophilic and hydrophobic side chains on each side of the polymer backbone to form a Janus-like chain. Langmuir isotherm experiments indicate that the packing and stability of molecular monolayers of these amphiphilic polymers at the air-water interface depend on the relative placement (regioregularity) of the dissimilar side chains. Further work is currently underway to apply this approach to the development of similar materials for applications in thin film devices.

ACKNOWLEDGEMENTS

We gratefully acknowledge Dr. Vladimir Tsukruk and Ray Gunawidjaja for assistance in making Langmuir adsorption isotherm measurements.

## 3.5. REFERENCES


(1) Garnier, F.; Yassar, A.; Hajlaoui, R.; Horowitz, G.; Deloffre, F.; Servet, B.; Ries, S.; Alnot, P. *J. Am. Chem. Soc.* **1993**, *115*, 8716.

(2) Lin, Y. Y.; Gundlach, D. J.; Nelson, S. F.; Jackson, T. N. *IEEE Trans. Electron Devices* **1997**, *44*, 1325.

(3) Bao, Z.; Lovinger, A. J.; Dodabalapur, A. *Appl. Phys. Lett.* **1996**, *69*, 3066.

(4) Gundlach, D. J.; Lin, Y. Y.; Jackson, T. N.; Schlom, D. G. *Appl. Phys. Lett.* **1997**, *71*, 3853.

(5) Bao, Z.; Dodabalapur, A.; Lovinger, A. J. *Appl. Phys. Lett.* **1996**, *69*, 4108.

(6) Katz, H. E.; Bao, Z. *J. Phys. Chem. B* **2000**, *104*, 671.

(7) McCullough, R. D.; Lowe, R. D. *Journal of the Chemical Society-Chemical Communications* **1992**, 70.

(8) Chen, T. A.; Rieke, R. D. *Synth. Met.* **1993**, *60*, 175.

(9) McCullough, R. D. *Adv. Mater.* **1998**, *10*, 93.

(10) Loewe, R. S.; McCullough, R. D. *Chem. Mater.* **2000**, *12*, 3214.

(11) Ng, S. C.; Xu, J. M.; Chan, H. S. O.; Fujii, A.; Yoshino, K. *J. Mater. Chem.* **1999**, *9*, 381.

(12) Suzuki, Y.; Hashimoto, K.; Tajima, K. *Macromolecules* **2007**, *40*, 6521.

(13) Nambiar, R. R.; Brizius, G. L.; Collard, D. M. *Adv. Mater.* **2007**, *19*, 1234.

(14) Nambiar, R.; Woody, K. B.; Ochocki, J. D.; Brizius, G. L.; Collard, D. M. *Macromolecules* **2009**, *42*, 43.

(15) Krebs, F. C.; Jorgensen, M. *Macromolecules* **2002**, *35*, 10233.

(16) Dougherty, D. A. *Science* **1996**, *271*, 163.

(17) Ma, J. C.; Dougherty, D. A. *Chem. Rev.* **1997**, *97*, 1303.

(18) Bjornholm, T.; Greve, D. R.; Reitzel, N.; Hassenkam, T.; Kjaer, K.; Howes, P. B.; Larsen, N. B.; Bogelund, J.; Jayaraman, M.; Ewbank, P. C.; McCullough, R. D. *J. Am. Chem. Soc.* **1998**, *120*, 7643.

(19) Reitzel, N.; Greve, D. R.; Kjaer, K.; Hows, P. B.; Jayaraman, M.; Savoy, S.; McCullough, R. D.; McDevitt, J. T.; Bjornholm, T. *J. Am. Chem. Soc.* **2000**, *122*, 5788.

(20) de Boer, B.; van Hutten, P. F.; Ouali, L.; Grayer, V.; Hadziioannou, G. *Macromolecules* **2002**, *35*, 6883.

(21) Mattu, J.; Johansson, T.; Holdcroft, S.; Leach, G. W. *J. Phys. Chem. B* **2006**, *110*, 15328.

(22) Bo, Z. S.; Zhang, C. M.; Severin, N.; Rabe, J. P.; Schluter, A. D. *Macromolecules* **2000**, *33*, 2688.

(23) Futterer, T.; Hellweg, T.; Findenegg, G. H.; Frahn, J.; Schluter, A. D.; Bottcher, C. *Langmuir* **2003**, *19*, 6537.

(24) Nurmawati, M. H.; Renu, R.; Ajikumar, P. K.; Sindhu, S.; Cheong, F. C.; Sow, C. H.; Valiyaveettil, S. *Adv. Funct. Mater.* **2006**, *16*, 2340.

(25) Kim, J.; Levitsky, I. A.; McQuade, D. T.; Swager, T. M. *J. Am. Chem. Soc.* **2002**, *124*, 7710.

(26) Arnt, L.; Tew, G. N. *J. Am. Chem. Soc.* **2002**, *124*, 7664.

(27) Clark, A. P. Z.; Cadby, A. J.; Shen, C. K. F.; Rubin, Y.; Tolbert, S. H. *J. Phys. Chem. B* **2006**, *110*, 22088.

(28) Slutsky, M. M.; Phillip, J. S.; Tew, G. N. *New J. Chem.* **2008**, *32*, 670.

(29) Li, Y.; Li, G. T.; Wang, X. Y.; Lin, C. X.; Zhang, Y. H.; Ju, Y. *Chem.-Eur. J.* **2008**, *14*, 10331.

(30) Bouffard, J.; Swager, T. M. *Chem. Commun.* **2008**, 5387.

(31) Breitenkamp, R. B.; Tew, G. N. *Macromolecules* **2004**, *37*, 1163.

(32) Greve, D. R.; Reitzel, N.; Hassenkam, T.; Bogelund, J.; Kjaer, K.; Howes, P. B.; Larsen, N. B.; Jayaraman, M.; McCullough, R. D.; Bjornholm, T. *Synth. Met.* **1999**, *102*, 1502.

(33) Brustolin, F.; Goldoni, F.; Meijer, E. W.; Sommerdijk, N. A. J. M. *Macromolecules* **2002**, *35*, 1054.

(34) Kim, J.; Swager, T. M. *Nature (London, U. K.)* **2001**, *411*, 1030.

(35) Li, L.; Collard, D. M. *Macromolecules* **2005**, *38*, 372.

(36) Li, L.; Collard, D. M. *Macromolecules* **2006**, *39*, 6092.

(37) Wang, B.; Watt, S.; Hong, M.; Domercq, B.; Sun, R.; Kippelen, B.; Collard, D. M. *Macromolecules* **2008**, *41*, 5156.

(38) Woody, K. B.; Nambiar, R.; Brizius, G. L.; Collard, D. M. *Macromolecules* **2009**, 42, 8102.

(39) Xiao, X. Y.; Nagahara, L. A.; Rawlett, A. M.; Tao, N. J. *J. Am. Chem. Soc.* **2005**, *127*, 9235.

(40) Dong, H.; Li, H.; Wang, E.; Yan, S.; Zhang, J.; Yang, C.; Takahashi, I.; Nakashima, H.; Torimitsu, K.; Hu, W. *J. Phys. Chem. B* **2009**, *113*, 4176.

(41) Pang, Y.; Li, J.; Hu, B.; Karasz, F. E. *Macromolecules* **1998**, *31*, 6730.

(42) Bunz, U. H. F. *Chem. Rev.* **2000**, *100*, 1605.

(43) Wegner, G.; *Thin Solid Films* **1992**, 216, 105.

# CHAPTER 4

# SYNTHESIS AND PROPERTIES OF AMPHIPHILIC POLY(1,4-PHENYLENE ETHYNYLENE)S BEARING ALKYL AND SEMIFLUOROALKYL SUBSTITUENTS[#]

## 4.1. INTRODUCTION

In Chapters 2 and 3, we showed that control over the relative placement of side chains has an influence on the molecular assembly and electronic structure of the poly(1,4-phenyene ethynylene)s (PPEs). The effect of regioregularity was greatest when there is a large difference between the structures of the side chains. The regioregularity of amphipilic PPEs with hydrophilic (oligo ethylene glycol) and hydrophobic (dodecyl) side chains[1] has a particularily large effect on the organization of the polymer chains in solid state as well as in air-water interface. The regioregular amphiphilic PPE analog arranges in a bilayer type architecture in the solid state and forms materials with high crystallinity. However hydrophilic and hygroscopic side chains might present problems in semiconducting polymers in organic field effect transistors. Thus we were motivated to explore pairs of dissimilar side chains to provide an amphiphilic structures in which both types of chain are hydrophobic. This led us to prepare PPEs with a combination of alkyl and fluoroalkyl side chains.

[#] This chapter describes studies of PPE (m,n/p) prepared by Kathy Woody which were published in a co-authored paper: Woody, K. B.; Nambiar, R.; Brizius, G. L.; Collard, D. M. *Macromolecules* **2009**, *42*, 8102.

Semifluoroalkyl chains are interesting amphiphilic units in that the hydrocarbon and fluorocarbon sections phase separate on a molecular scale, despite both being hydrophobic and similar size. 1-Nonyloxy-4-(4,4,5,5,6,6,7,7,8,8,9,9,9-tridecafluorononyloxy)benzene serves as a small molecule model to illustrate the amphiphilic behavior and segregation of alkyloxy and semifluoroalkoxy side chains, Figure 4.1. Attachment of semifluoroalkyl groups onto polymers provides materials with increased hydrophobicity, thermal stability, chemical and oxidative resistance[2,3] and self organization of the fluorinated chains.[4-7] Previous work based on 3-semifluoroalkyl-substituted polythiophenes led to conjugated materials with solubility in sc-$CO_2$, liquid crystalline properties and highly ordered lamellar bilayer Janus-type structures.[8-10] With the polymer backbone in an anti-conformation, the structures had fluoroalkyl groups on one edge of the molecule and alkyl side chains on the other, Figure 4.2. The segregation of the two different side chains gives rise to a highly ordered crystalline material. Moreover, these polymeric molecules self-orient perpendicular to a substrate surface. It was suggested that this orientation arises so as to avoid interaction of both types of chain with the substrate. Such an orientation is ideal for charge transport in semiconducting polymers.[11,12]

Here we extend this approach to prepare amphipilic regiorandom and regioregular PPEs bearing both semifluoroalkoxy (-$O(CH_2)_m(CF_2)_nF$) and alkoxy sidechains (-$O(CH_2)_pH$), Figure 4.3, to impart amphiphilicity and thereby vary the molecular structure

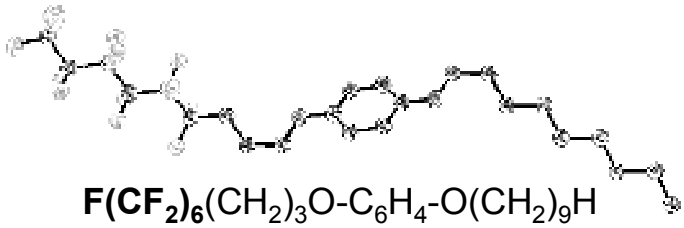


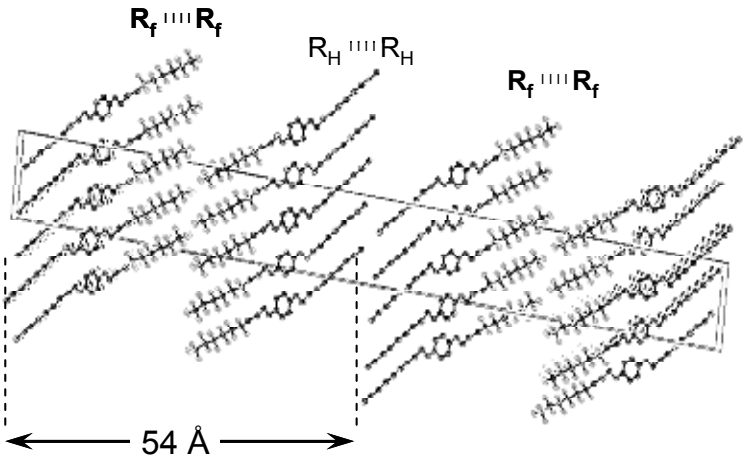


**Figure 4.1.** Amphiphilic 1-nonyloxy-4-(4,4,5,5,6,6,7,7,8,8,9,9,9-tridecafluorononyloxy)benzene: Top, Molecular structure; bottom, unit cell. Hydrogen atoms have been omitted for clarity.

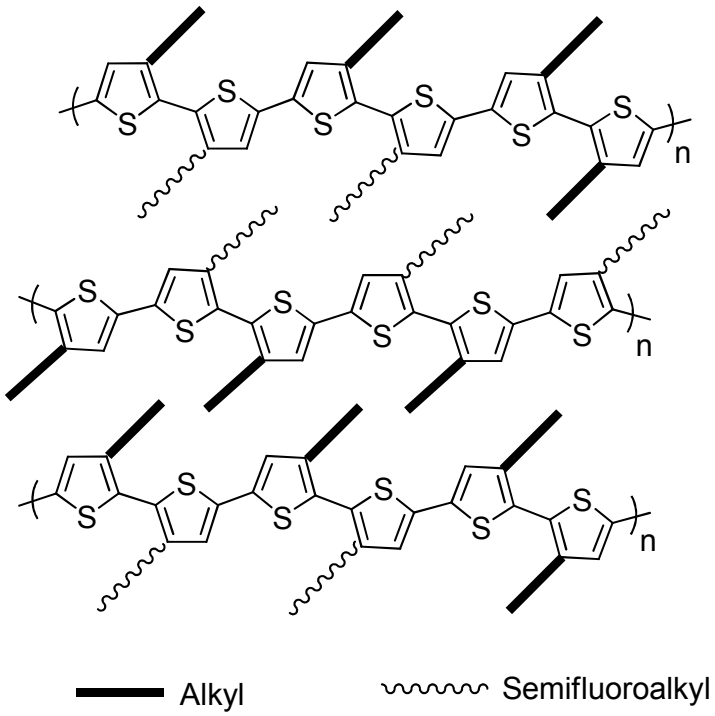


**Figure 4.2.** Highly ordered amphiphlic PATs with semifluoroalkyl and alkyl side chains on each repeat unit.

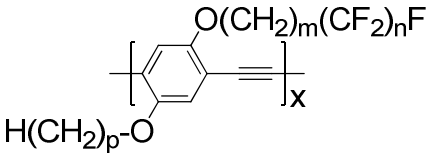


| | *regiorandom* | *regioregular* |
|---|---|---|
| m= 3, n=6, p = 9 | **RnPPE(3,6/9)** | **Rg(PPE(3,6/9)** |

**Figure 4.3.** Amphiphlic PPEs with semifluoroalkoxy and alkoxy side chains on each repeat unit.

to attain further control over interchain interaction and supramolecular assembly of PPEs. The hydrocarbon spacer ($(CH_2)_m$) in the semifluoroalkoxy chain insulates the conjugated backbone from the electron withdrawing effect of the fluorocarbon segment. Thus any change in the electronic properties of the polymers can be directly correlated to the molecular packing and not the electronic substituent effect.

## 4.2. EXPERIMENTAL

### 4.2.1. General Methods

All starting materials were purchased from commercial sources and used without further purification. THF and $Et_2O$ were dried over sodium benzophenone ketyl prior to distillation under argon. Column chromatography was performed on flash grade silica (32-60 Å, Sorbent Technologies, Atlanta, Georgia). Thin-layer chromatography was performed on 3×5 cm silica gel plates (0.2 mm thick, 60 F254) on an aluminum support (Sorbent Technologies). NMR analysis was performed on a Bruker DSX 400 or DSX 300 instruments using $CDCl_3$ as the solvent. Chemical shifts are reported relative to internal tetramethylsilane. IR analyses were performed on a Nicolet 4700 FTIR with an ATR attachment from SmartOrbit Thermoelectronic Corporation. Ultraviolet-visible analysis was performed on a Perkin-Elmer Lambda 19 spectrophotometer, and fluorescence spectroscopy was performed on a SPEX Fluorolog 1680/1681 0.22m spectrometer. Elemental analyses were performed by Atlantic Microlab, Inc. (Norcross, GA). The Bestman-Ohiro reagent was prepared using previously reported methods.[13]

### 4.2.2. Synthesis of the monomer for Regioregular PPEs

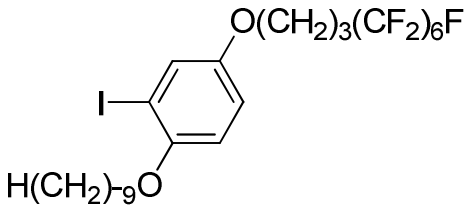


**2-Iodo-1-(nonyloxy)-4-(4,4,5,5,6,6,7,7,8,8,9,9,9-tridecafluorononyloxy)benzene, IV-1.** 4-(nonyloxy)-3-iodophenol[1] (13.78 g, 38.0 mmol) was added to a solution of 4,4,5,5,6,6,7,7,8,8,9,9,9-tridecafluorononan-1-ol (17.27 g, 45.7 mmol) and $PPh_3$ (11.97 g, 45.7 mmol) in $Et_2O$ (100 mL) in a dry flask under argon. DEAD (7.5 mL, 45.7 mmol) was added dropwise via syringe and the solution was stirred for 24 h. The mixture was poured into 10% aqueous NaOH (200 mL) and the resulting solution was extracted with $Et_2O$ (2 × 100 mL). The combined extracts were dried over $MgSO_4$ and the solvent was removed under reduced pressure. The residue was subjected to flash column chromatography (silica gel; 10:90 v/v EtOAc:hexanes) to afford **IV-1** as a colorless solid ( 13.9 g, 51 %): m.p.= 28-29 $^oC$. $^1H$ NMR (300 MHz, $CDCl_3$): δ 7.33 (d, $^4J_{ArH2\text{-}ArH6}$ = δ2.90 Hz, 1H, Ar C3-H), 6.83 (dd, $^3J_{ArH5\text{-}ArH6}$ = 8.9 Hz, $^4J_{ArH2\text{-}ArH6}$ = 2.9 Hz, 1H, Ar C5-H), 6.73 (d, $^3J_{ArH5\text{-}ArH6}$ = 8.9 Hz, 1H, Ar C6-H), 3.96 (t, $^3J$ = 5.9 Hz, 2H, -$OCH_2$-), 3.94 (t, $^3J$ = 6.5 Hz, 2H, -$OCH_2$-), 2.2-2.39 (m, 2H, -$CF_2CH_2$-), 2.01-2.15 (m, 2H), 1.72-1.84 (m, 2H), 1.16-1.6 (m, 12H), 0.89 (t, $^3J$ = 7 Hz, 3H, -$CH_3$). $^{13}C$ NMR (75 MHz, $CDCl_3$): δ 152.86, 152.34 (Ar C-O), 125.24, 115.22, 112.82 (Ar C-H), 86.92 (Ar C-I), 70.10, 67.13 (-O-$CH_2$-), 31.99, 29.65, 29.45, 29.38, 29.34, 28.00 (t, $^3J_{CF}$ = 22 Hz), 26.20, 22.82, 20.72, 20.63, 14.26. IR (ATIR): 2924 (Ar C-H str.), 2854, 1598, 1569, 1489, 1467, 1384, 1365,

1270, 1204 (C-O str.), 1143, 1026, 843, 730, 706 $cm^{-1}$. HRMS: calc. for $C_{24}H_{28}F_{13}O_2I$ = 722.09264, obs. = 722.09265, Δ = 2.9 ppm.

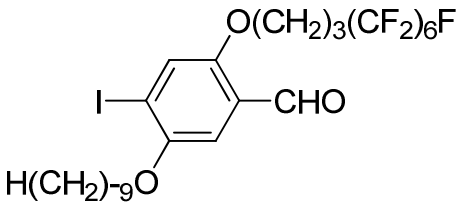


**2-(4,4,5,5,6,6,7,7,8,8,9,9,9-Tridecafluorononyloxy)-4-iodo-5-(nonyloxy)benzaldehyde, IV-2**. $TiCl_4$ (2.1 mL, 19 mmol) was added in three portions to monoiodinated diether **IV-1** (2.3 g, 3.2 mmol) in dry flask at -40 ºC under argon. The mixture was stirred for 15 min and dichloromethyl methyl ether (0.56 mL, 6.4 mmol) was added dropwise. The mixture was stirred for another 1.5 h at -40 ºC and then poured into a mixture of 1N HCl and ice. The mixture was extracted with $CH_2Cl_2$ (2 × 50 mL) and the combined organic extracts were washed with $H_2O$ (100 mL) and dried over $MgSO_4$. The solvent was removed under reduced pressure and the residue was subjected to column chromatography (silica gel, 40:60 $CH_2Cl_2$:hexanes) followed by recrystallization from isopropanol to afford **IV-2** as a colorless crystalline solid (1.05 g, 44 %). m.p. = 64-66 ºC. $^1$H NMR (300 MHz, $CDCl_3$): δ 10.35 (s, 1H, -CHO), 7.40 (s, 1H, Ar C3-H), 7.12 (s, 1H, Ar C6-H), 4.07 (t, 2H, -$OCH_2$Rf), 3.94 (t, 2H, -$OCH_2$), 2.2-2.39 (m, 2H), 2.08-2.19 (m, 2H), 1.72-1.84 (m, 2H), 1.16-1.53 (m, 12H), 0.85 (t, 3H, -$CH_3$). $^{13}$C NMR (75 MHz, $CDCl_3$): 187.90 (-CHO), 154.58 (Ar C2), 152.35 (Ar C5), 125.00 (Ar C1), 124.11 (Ar C3), 108.77 (Ar C6), 96.35 (Ar C4), 69.85, 67.73 (-O-$CH_2$-), 31.94, 29.60, 29.37, 29.33, 29.10, 27.87 (t, $^3J_{CF}$ =

22Hz), 26.12, 22.75, 20.66, 20.62, 14.08. IR (ATIR): 2918 (Ar C-H str.), 2847, 1670 (C = O str.), 1590, 1458, 1383, 1211 (C-O str.), 1039, 978, 863, 827, 749, 715, 611 $cm^{-1}$ . HRMS: calc. for $C_{25}H_{28}F_{13}O_3I$ = 750.08755, obs. = 750.08756, Δ = 2.9 ppm.

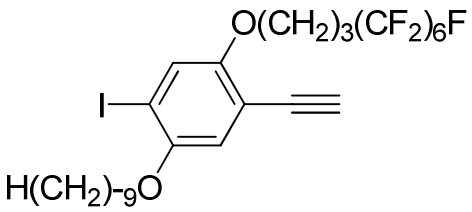


**1-Ethynyl-2-(4,4,5,5,6,6,7,7,8,8,9,9,9-tridecafluorononyloxy)-4-iodo-5-(nonyloxy)benzene, IV-3.** Bestman-Ohiro reagent, $(MeO)_2P(=O)C(=N_2)COCH_3$ (0.6 g, 3.0 mmol), was added dropwise to a mixture of aldehyde **IV-2** (1.00 g, 1.35 mmol) and $K_2CO_3$ (0.55 g, 4.0 mmol) in a 1:1 v/v mixture of anhydrous $CH_2Cl_2$ and MeOH (20 mL). The mixture was stirred for 48 h at room temperature, poured into 10% aqueous HCl (50 mL), and extracted with $CH_2Cl_2$ (2 × 50 mL). The combined organic extracts were dried over $MgSO_4$ and the solvent was removed under reduced pressure. The residue was recrystallized twice from isopropanol to afford **IV-3** as a colorless solid (0.55 g, 55 %): m.p. = 55-56 °C. $^1$H NMR (300 MHz, $CDCl_3$): δ 7.29 (s, 1H, Ar C3-H), 6.86 (s, 1H, Ar C6-H), 4.05 (t, 2H, -$OCH_2R_f$), 3.94 (t, 2H, -$OCH_2$), 3.28 (s, 1H, -C≡C-H), 2.31-2.48 (m, 2H), 2.06-2.17 (m, 2H), 1.74-1.86 (m, 2H), 1.19-1.58 (m, 12H), 0.88 (t, 3H, -$CH_3$). $^{13}$C NMR (75 MHz, $CDCl_3$): δ153.89 (Ar C4), 152.09 (Ar C1), 124.23 (Ar C3), 116.37 (Ar C6), 112.61 (Ar C5), 88.14 (Ar C2), 81.99, 79.23 (-C≡C-), 70.07, 68.44(-O-$CH_2$-), 31.99, 29.64, 29.40, 29.37, 29.22, 27.95 (t, $^3J_{CF}$ = 22 Hz), 26.16, 22.82, 20.77, 20.73, 14.27. IR

(ATIR): 3266 (C-H str), 2951 (Ar-H str.), 2919, 2865, 2085 (C≡C str), 1473, 1465, 1371, 1213 (C-O str.), 1028, 997, 856, 813, 725, 687, 637 $cm^{-1}$. HRMS: calc. for $C_{26}H_{28}F_{13}O_2I$ = 746.09264, obs. = 746.09265, Δ = 1.7 ppm. Elemental analysis: Theoretical: C, 41.84%; H, 3.78%; F, 33.09%; I, 17.00%; O, 4.29%; Found: C, 42.06%; H, 3.76%; F, 32.9%; I, 16.77%; O, 4.38%.

**Regioregular, RgPPE(3,6/9).** A solution of monomers **IV-3** (400 mg, 536 μmol), $Pd(PPh_3)_4$ (31.0 mg, 26.8 μmol) and CuI (6.0 mg, 30 μmol) in a mixture of piperidine (8 mL) and chloroform (3 mL) was heated at 70 °C for 4 d. The mixture was poured into 50 mL of methanol and the precipitated solid was removed by filtration.

## 4.3. RESULTS AND DISCUSSION

### 4.3.1. Monomer Synthesis and Polymerization

The regioregular PPEs with semifluoroalkoxy and alkoxy side chains were prepared by the synthetic route previously reported[14] in Chapters 2 and 3, Figure 4.4. A Mitsunobu reaction was used to install the semifluoroalkyl side chain onto 4-(nonyloxy)-3-iodophenol to form the monoiodinated dialkoxy benzene **IV-1**. A formylation reaction mediated by $TiCl_4$ gave the benzaldehyde **IV-2** which was then transformed to alkyne **IV-3** using a Bestman-Ohiro homologation reaction. The 4-iodophenylacetylene A-B type monomer was polymerized using Pd-catalyzed Sonogashira condensation reaction to produce regioregular PPEs.

The product formed during the polymerization reaction precipitated out of the reaction medium within 2-3 h. Analysis of the reaction product by $^{1}$H NMR and GPC indicated the formation on oligomers with DPs of 3-7. We concluded that the high fluorine-to-hydrogen ratio (*n*=6 and *m*=3) of the semifluoroalkyl side chain, along with a relatively short alkoxy side chain (*p*=9) resulted in lower solubility of the oligomers formed. In order to prepare soluble high molecular weight semifluorinated PPEs and to develop an understanding of the effect of variation of the fluoroalkyl chain length (*n*) on the self assembly properties, Kathy Woody from our group synthesized PPEs with different *m* and *n* values for the semifluoroalkyl side chain, Figure 4.5[15] The alkoxy side chain length was increased to *p*=12 and was kept the same for all the polymers.

The degrees of polymerization (*DP*) range for the more soluble polymers between 21 and 33 repeat units with the exception of **RgPPE(6,6/12)** which had a *DP* of only 12 as a result of poor solubility of the polymer in chloroform. The differences in the $^{1}$H and $^{13}$C NMR spectra for the regiorandom and regioregular polymers were as observed before (Chapters 2 and 3) for the $C_{12}$/OEG and $C_{12}$/$C_1$ PPEs. Thermal properties of the PPEs were characterized by differential scanning calorimetry (DSC). The thermal transition corresponding to melting is higher for PPEs with greater fluorine content. In general, the regioregular PPEs had higher melting transition temperatures than the regiorandom analogues, likely as a result of the higher crystallinity arising from their more regular structures.

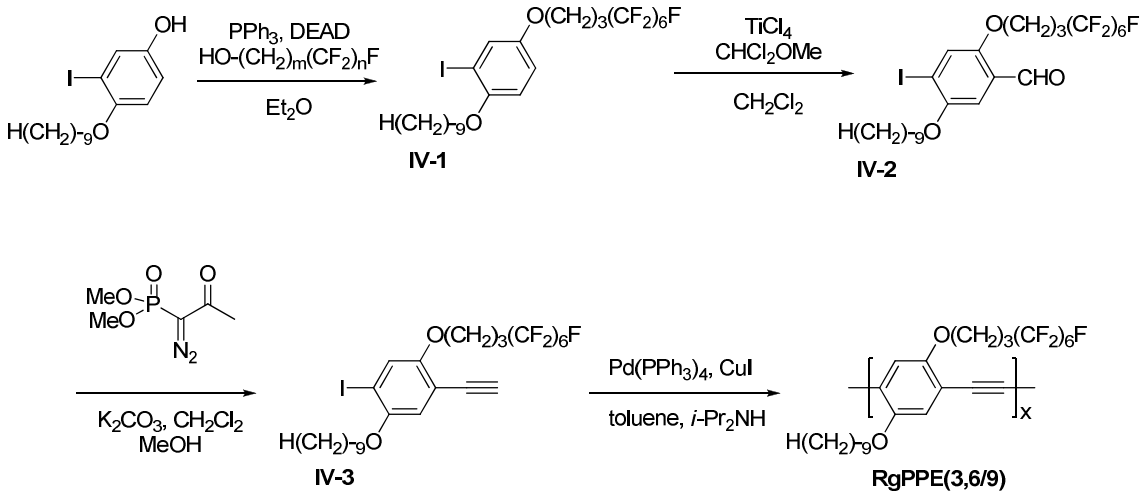


**Figure 4.4.** Synthesis of regioregular PPEs.

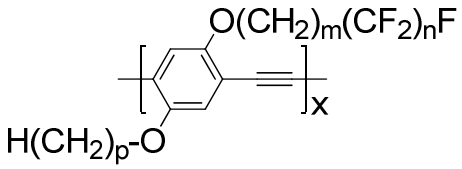


| | *regiorandom* | *regioregular* |
|---|---|---|
| m = 6, n = 6, p = 12 | **RnPPE(6,6/12)** | **RgPPE(6,6/12)** |
| m = 8, n = 4, p = 12 | **RnPPE(8,4/12)** | **RgPPE(8,4/12)** |
| m = 10, n = 2, p = 12 | **RnPPE(10,2/12)** | **RgPPE(10,2/12)** |
| m= 3, n=3, p = 12 | **RnPPE(3,3/12)** | **RgPPE(3,3/12)** |

**Figure 4.5.** Amphiphlic PPEs with semifluoroalkoxy and alkoxy side chains on each repeat unit prepared by Kathy Woody.[15]

### 4.3.2. Electronic Properties of the fluorinated PPEs

The electronic properties of the PPEs were studied using UV-vis absorption spectroscopy. The largest differences between regioregular and regiorandom materials were observed for thin films of PPEs formed by drop-casting followed by annealing at 110 $^{o}$C under vacuum for 24 h. The regioregular PPE (**RgPPE(6,6/12)**) shows a greater contribution in the higher wavelength region (510 nm) compared to the regiorandom analogue, **RnPPE(6,6/12)**, Figure 4.6. A similar shift in peak intensity towards higher wavelength (~ 500 nm) in regioregular analogues was observed for **RgPPE(8,4 /12)** and **RgPPE(10,2/12)**. This can be attributed to a portion of the materials that has a greater conjugation length arising from more ordered, planar structure. For the regiorandom analogues the absence of peaks at higher wavelength indicates that irregular placement of alkoxy and semifluoroalkoxy side chains hinder side chain crystallization and planarization and thus lead to a disordered structure.

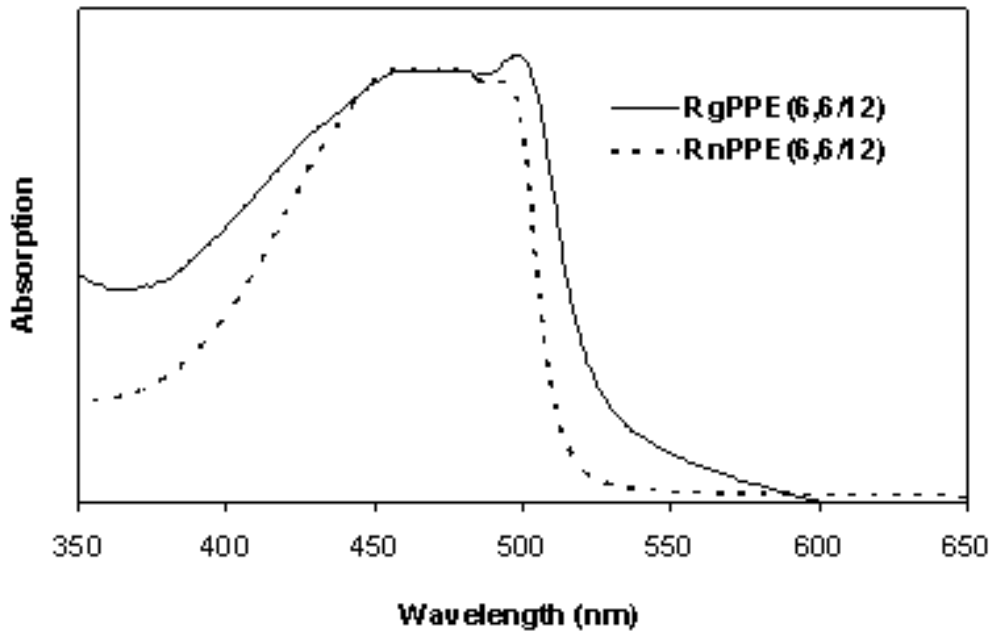


**Figure 4.6.** UV-vis spectra of annealed thin films of regioregular and regiorandom analogs of **PPE(6,6/12)**.

### 4.3.3. Molecular Packing in fluorinated PPEs

The supramolecular structures of PPEs were characterized by X-ray diffraction (WAXD), of drop-cast films on a silicon substrate. Problems with adhesion of the polymer films on silicon were overcome by pretreating the surface with fluorinated silanes. In contrast to our previous findings with OEG/$C_{12}$ amphiphilic PPEs and Janus type PATs, in which imparting amphiphilicity gave rise to highly ordered structures, the semifluoroalkyl side chains disrupts the lamellar packing of the PPE backbone. None of the fluoroalkyl substituted PPEs show all the reflections present in the symmetrical **PPE(12/12)**, Figure 4.7F. Surprisingly, the regiorandom materials (Figure 4.7B and 4.7D) gave stronger diffraction peaks than the corresponding regioregular materials (Figure 4.7A and 4.7C).

The disorder of the solid state structures of semifluoroalkyl PPEs compared to other amphiphilic PPEs and PATs can be explained by Figure 4.8. In symmetrically substituted alkoxy PPEs, the side chains interdigitate due to the longer spacing between the side chains than in substituted PATs, Figure 4.8A. Interpenetration of semifluoroalkyl chains would result in alkyl-fluoroalkyl contacts thus leading to incomplete interdigitation and disordered structure that can accomdate the segregation of the side chains (Figure 4.8B).

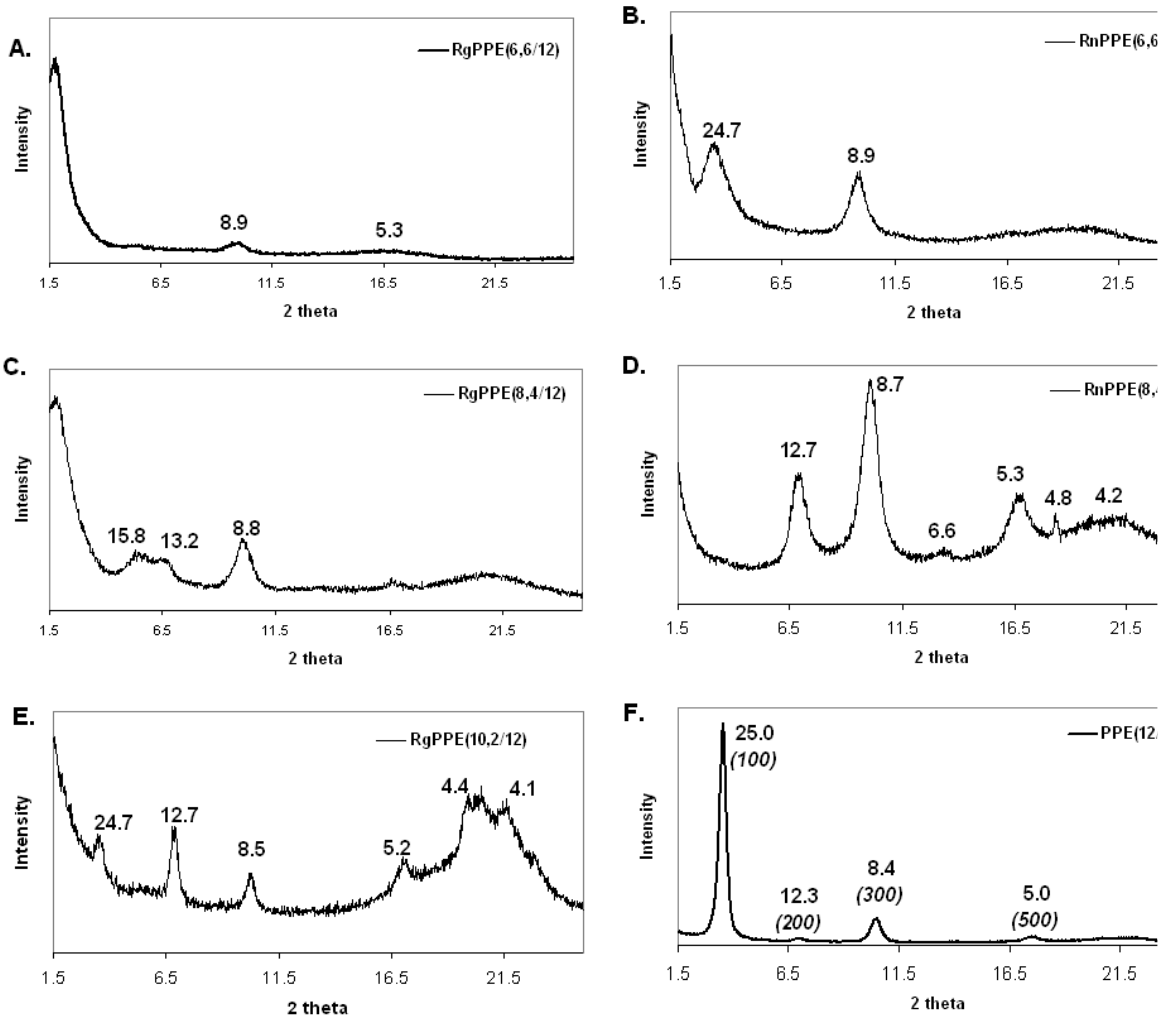


**Figure 4.7.** Wide angle X-ray diffraction patterns for annealed films: A, **RgPPE(6,6/12)**; B, **RnPPE(6,6/12)**; C, **RgPPE(8,4/12)**, D, **RnPPE(8,4/12)**; E, **RgPPE(10,2/12)**; and F, **PPE(12/12)**. Peaks are labeled with *d* spacings in Ångstroms.

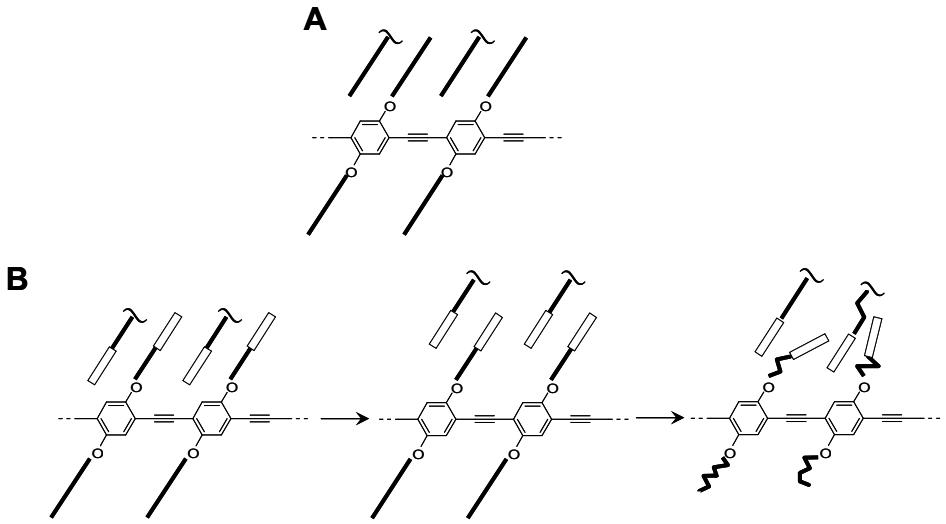


**Figure 4.8.** Incorporation of amphiphilic side chains imparts disorder to the structure of PPEs. A, The side chains of symmetrically-substituted dialkoxyl-PPEs, e.g., **PPE(12/12)** interdigitate to form a lamellar structure. B, Aggregation of fluoroalkyl segments limited extent of interpenetration of side chains, requiring that the alkylene spaces, $(CH_2)_m$, undergo conformational disordering to fill space efficiently, thereby introducing molecular disorder.

## 4.4. CONCLUSIONS

Amphiphilic regioregular and regiorandom PPEs bearing semifluoroalkoxy and alkoxy side chains was prepared based on our previously developed strategies. The fluorocarbon chain length affects the thermal transitions in these polymers. The amphiphilic PPEs show a red shift in optical absorptions compared to symmetrically substituted PPEs, but no longer display a lamellar morphology. Thus, in contrast to the highly ordered alkyl/semifluoroalkyl substituted poly(bithiophene)s, the segregation of the side chains in PPEs impedes interdigitation with the formation of disordered structures.

## 4.5. REFERENCES


(1) Nambiar, R.; Woody, K. B.; Ochocki, J. D.; Brizius, G. L.; Collard, D. M. *Macromolecules* **2009**, *42*, 43.

(2) Ren, Y.; Lodge, T. P.; Hillmyer, M. A. *Macromolecules* **2001**, *34*, 4780.

(3) Robitaille, L.; Leclerc, M. *Macromolecules* **1994**, *27*, 1847.

(4) Li, Y.; Li, G. T.; Wang, X. Y.; Lin, C. X.; Zhang, Y. H.; Ju, Y. *Chemistry-a European Journal* **2008**, *14*, 10331.

(5) Johansson, G.; Percec, V.; Ungar, G.; Zhou, J. P. *Macromolecules* **1996**, *29*, 646.

(6) Hayakawa, T.; Wang, J. G.; Xiang, M. L.; Li, X. F.; Ueda, M.; Ober, C. K.; Genzer, J.; Sivaniah, E.; Kramer, E. J.; Fischer, D. A. *Macromolecules* **2000**, *33*, 8012.

(7) Small, A. C.; Pugh, C. *Macromolecules* **2002**, *35*, 2105.

(8) Wang, B.; Watt, S.; Hong, M.; Domercq, B.; Sun, R.; Kippelen, B.; Collard, D. M. *Macromolecules* **2008**, *41*, 5156.

(9) Li, L.; Collard, D. M. *Macromolecules* **2005**, *38*, 372.

(10) Li, L.; Counts, K. E.; Kurosawa, S.; Teja, A. S.; Collard, D. M. *Adv. Mater.* **2004**, *16*, 477.

(11) Sirringhaus, H.; Brown, P. J.; Friend, R. H.; Nielsen, M. M.; Bechgaard, K.; Langeveld-Voss, B. M. W.; Spiering, A. J. H.; Janssen, R. A. J.; Meijer, E. W.; Herwig, P.; de Leeuw, D. M. *Nature* **1999**, *401*, 685.

(12) Mena-Osteritz, E.; Meyer, A.; Langeveld-Voss, B. M. W.; Janssen, R. A. J.; Meijer, E. W.; Bauerle, P. *Angew. Chem.-Int. Edit.* **2000**, *39*, 2680.

(13) Ohira, S. *Synth. Commun.* **1989**, *19*, 561.

(14) Nambiar, R. R.; Brizius, G. L.; Collard, D. M. *Adv. Mater.* **2007**, *19*, 1234.

(15) Woody, K. B.; Nambiar, R.; Brizius, G. L.; Collard, D. M. *Macromolecules* **2009**, *42*, 8102.

# CHAPTER 5

# LOW BANDGAP POLYMERS: A NEW PENTACENE-TERTHIOPHENE ALTERNATING COPOLYMER

## 5.1. INTRODUCTION

Conjugated organic molecules have emerged as an important class of materials with semiconducting properties which has potential application in organic field effect transistors (oFETs),[1-3] organic light-emitting diodes (oLEDs)[4] and organic polymeric solar cells (oPSCs).[5] The class includes polymers (e.g., polyarenes, poly(arylene vinylenes) and poly(arylene ethynylenes) and small molecules (e.g., fused arenes and oligoarenes.) Among the latter, pentacene and related linear fused arenes (acenes) are at the forefront for use as semiconductors in oFETs, as electron donors in organic polymeric solar cells.[6] and as the emissive layer in oLEDs,[7] due to their low band gap and high field effect mobility Pentacenes itself has the highest measured mobility (5 $cm^2V^{-1}s^{-1}$) of all conjugated organic materials. While pentacene and other small molecules are amenable to vacuum deposition, they lack the solubility common to substituted conjugated polymers and are therefore difficult to process from solution.The solubility of pentacene is improved significantly by attaching triisopropylsilylethynyl (TIPSE) substituents at the 6 and 13 positions.[8] The substituents impart pentacene with good solubility in organic solvents, and better air stability without compromising electronic performance.[9] Silyl ethynylene substituted pentacenes have also been incorporated into polymer structures.[10] Incorporating pentacene units into conjugated polymeric structures would provide

materials for which the electronic properties, solubility,stability, and film formation ability might also be varied by molecular design. However, there are few examples of polymers containing fused arenes such as pentacene, due in part to synthetic accessibility of suitable monomers.

Random copolymers consisting of 2,7-fluorene with 9,10-anthracene have been explored for potential applications in oLEDs.[11] In these copolymers, the acene cores were attached through the central ring, orthogonal to the conjugated backbone. Only recently have Bao and coworkers successfully developed polymers which incorporate pentacene units substituted along the long axis. For example, a poly(2,9/2,10-pentacene-*alt*-1,4-phenylene ethynylene) bearing TIPSE units on the 6 and 13 positions of each pentacene was prepared by a Sonogashira coupling reaction of mixture of 2,9- and 2,10-dibromopentacene and 1,4-phenylenediacetylene.[12] The copolymers formed had good solubility in common organic solvents, and possessed better air stability and a lower optical band gap (1.68 eV) than conventional semiconducting polymers, making it a good candidate as solution processable semiconductors and in polymer solar cells. Similarly, new copolymer systems containing 2,7-fluorene units alternating 2,9- and 2,10-pentacene and 2,8-anthradithiophene units had optical bandgaps of 1.78 and 1.98 eV, respectively.[13]

Thiophene-based conjugated copolymers and oligomers (e.g., α,ω-dihexylsexithiophene)[14,15] have been studied extensively as low bandgap materials for application in oFETs and oPSCs.[16-20] Thus, given the low bandgap of both pentacene and oligothiophenes, and ongoing interests in developing semiconducting conjugated polymers,we have embarked on a study of copolymers consisting of both pentacene and

oligothiophenes. In this paper, we report our effort on design, synthesis and characterization of a thiophene-pentacene based copolymer.

## 5.2. EXPERIMENTAL

### 5.2.1. General Methods

All starting materials were purchased from commercial sources and used without further purification. THF and $Et_2O$ were dried over sodium benzophenone ketyl prior to distillation under argon. Column chromatography was performed on flash grade silica (32-60 Å, Sorbent Technologies, Atlanta, Georgia). Thin-layer chromatography was performed on 3×5 cm silica gel plates (0.2 mm thick, 60 F254) on an aluminum support (Sorbent Technologies). NMR analysis was performed on a Bruker DSX 400 or DSX 300 instruments using $CDCl_3$ as the solvent. Chemical shifts are reported relative to internal tetramethylsilane. IR analyses were performed on a Nicolet 4700 FTIR with an ATR attachment from SmartOrbit Thermoelectronic Corporation. Ultraviolet-visible analysis was performed on a Perkin-Elmer Lambda 19 spectrophotometer, and fluorescence spectroscopy was performed on a SPEX Fluorolog 1680/1681 0.22m spectrometer. Elemental analyses were performed by Atlantic Microlab, Inc. (Norcross, GA).

### 5.2.2. Synthesis of Pentacene Monomer V-4 and V-5

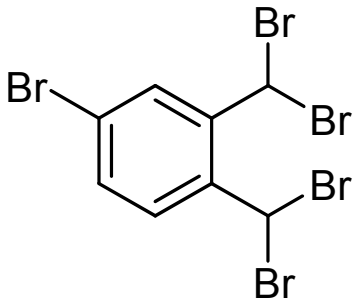


**4-Bromo-1,2-bis(dibromomethyl)benzene, V-1.** Benzoyl peroxide (1.06 g, 4.4 mmol), which was dried over phosphorus pentoxide under vacuum overnight, was added to a solution of *N*-bromosuccinimide (NBS) (48.75 g, 273.9 mmol) in carbon tetrachloride (150 mL). 4-Bromo-1,2-dimethylbenzene (25.15 g, 135.2 mmol) was added dropwise to the mixture under argon over an interval of 15 min. The resulting suspension was heated at reflux for 9 h. The mixture was cooled to room temperature, NBS (48.75 g, 273.9 mmol) and benzoyl peroxide (1.06 g, 4.4 mmol) were added, and the mixture was heated at reflux overnight. The reaction mixture was cooled, precipitated succinimide was removed by filtration and thoroughly washed with $CHCl_3$. The filtrate was washed with $H_2O$ (2 × 100 mL) followed by satd. sodium sulfite solution (2 × 50 mL), the solution was dried over $MgSO_4$ and the solvent was removed under reduced pressure. The resulting solid was recrystallized twice from hexanes, followed by isopropyl alcohol, to afford **V-1** as a colorless solid (37.6 g, 56% yield). m.p. = 106-108 °C (lit:[21] 110 °C. $^1$H NMR (300 MHz, $CDCl_3$): δ 7.81 (s, 1H, Ar C3-H), 7.66-7.41 (m, 2H, Ar C5,6-H), 7.05 (s, 1H), 7.02 (s, 1H). $^{13}$C NMR (75 MHz, $CDCl_3$): δ 139.4, 136.8, 133.7, 132.5, 131.3, 124.3, 35.5, 35.0. IR (AT-IR, neat): 3048, 1587, 1562, 1481, 1395, 1234, 1134, 890, 826, 664. HRMS: calc. for $C_8H_5Br_2$ = 495.6308, obs. = 495.6311, Δ = 0.6 ppm.

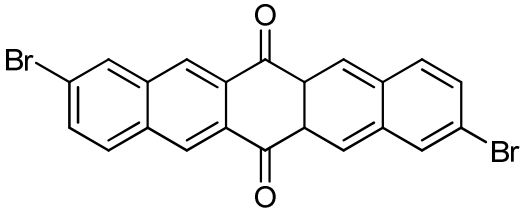

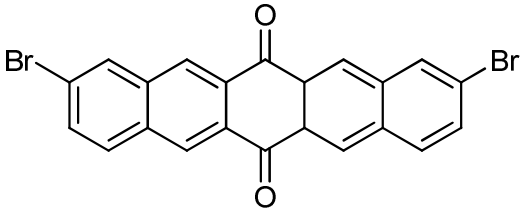


**2,9-Dibromopentacene-6,13-dione, V-2 and 2,10-dibromopentacene-6,13-dione, V-3.** Sodium iodide (61.0g, 407 mmol) was added to a solution of 4-bromo-1,2-bis(dibromomethyl)benzene, **V-1** (33.35g, 97.2 mmol), and 1,4-benzoquinone (3.27g, 30.3 mmol) in anhydrous DMF (300 mL). , and the mixture turned rusty red. The mixture was heated at 60 °C for 56 h under argon. After cooling the mixture to room temperature, $H_2O$ (100 mL) was added and the solid precipitate was collected by filtration The collected solid was washed with $H_2O$ and methanol multiple times, followed by hot MeOH and hot $CHCl_3$, and then dried under vacuum to afford **V-2** and **V-3** as a pale yellow solid (7.83 g, 35% yield). m.p. = dec. 170 °C. MS (EI): 465.9 ($M^+$), HRMS: Calculated for $C_{22}H_{12}O_2Br_2$, 463.90475; Observed, 463.90209; $\Delta$ = 5.7 ppm.

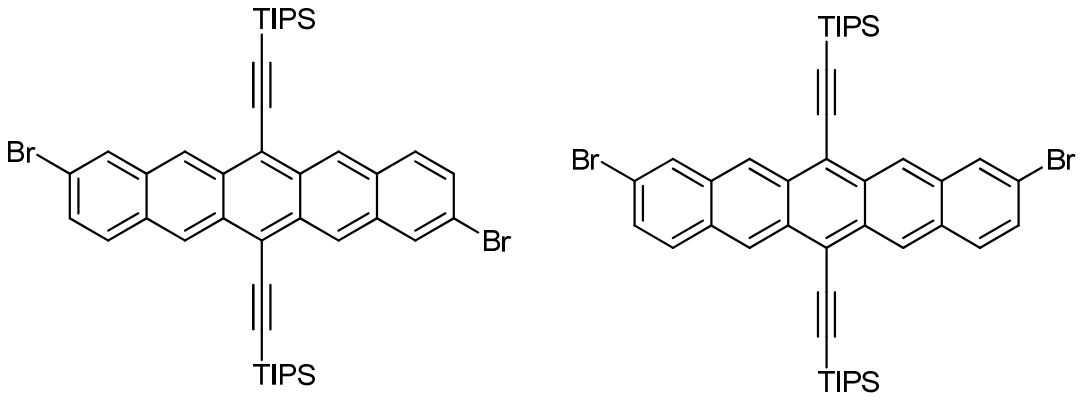


**6,13-Bis(triisopropylsilylethynyl)-2,9-dibromopentacene, V-4 and 6,13-Bis(triisopropylsilylethynyl)-2,10-dibromo-pentacene, V-5.** *n*-Butyllithium (0.78 mL of a 2.5 M solution in THF, 1.94 mmol) was added dropwise to a solution of triisopropylsilylacetylene (0.72 mL, 3.2 mmol) in anhydrous THF (5 mL). The resulting solution was heated to 60 °C for 1h. The solution was cooled to room temperature and the mixture of 2,9 and 2,10-dibromopentacene-6,13-diones **V-2** and **V-3** (0.30 g, 0.65 mmol) was introduced under a stream of nitrogen. The mixture was heated to 60 °C overnight, cooled to room temperature, and a solution of stannous chloride dihydrate (0.74 g, 3.3 mmol) in 10% aq. HCl (10 mL) was added to form a dark blue biphasic mixture. THF was removed under reduced pressure and the resulting aqueous mixture was extracted with $CHCl_3$ (2 × 50 mL). The combined extracted were washed with water (2 × 50 mL), the organic layer was dried with $MgSO_4$ and the solvent removed under reduced pressure. The crude product was then flushed over a silica plug with hexanes as the eluent to give the desired products **V-4 and V-5** (0.32 g, 63% yield). m.p.: dec. 170 °C. $^1$H NMR (300 MHz, $CDCl_3$): δ 9.25 (s, 2H), 9.23 (s, 2H), 9.17 (s, 2H), 9.16 (s, 2H), 8.12 (s, 4H), 7.82 (d, 4H, $J$ = 9.3 Hz), 7.44 (d, 4H, $J$ = 9.0 Hz), 1.53-1.28 (b, 84H). $^{13}$C NMR (75 MHz, $CDCl_3$): δ 132.75, 132.65, 131.75, 131.05, 130.85, 130.35, 130.25,

130.05, 129.95, 129.71, 129.67, 126.93, 126.88, 125.50, 125.45, 120.53, 120.47, 19.11, 19.01, 18.6, 11.61. IR: 2940, 2916, 2863, 2848, 1992, 1968, 1943, 1619, 1461, 1368, 1044, 936, 919. HRMS: Calculated for $C_{44}H_{52}Si_2Br_2$, 794.1974; Observed, 794.1943; $\Delta$ = -3.9 ppm.

### 5.2.3. Synthesis of Terthiophene Monomer V-9

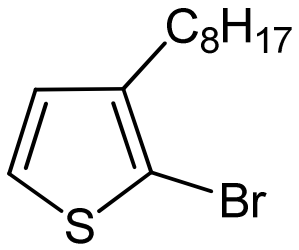


**2-Bromo-3-octylthiophene, V-6.** NBS (10.8 g, 60.6 mmol) was added to the stirred solution of 3-octylthiophene (11.32 g, 57.76 mmol) in anhydrous THF (100 mL) at 0 °C and the mixture was stirred at 0 °C for 1.5 h. Aqueous 5% sodium sulfite (100 mL) was added and the mixture was concentrated by removing THF under reduced pressure. The resulting mixture was extracted with hexane (2 × 100 mL) and the organic exctracts were washed with water (2 × 50 mL), and dried over MgSO4. The hexane solution was passed through a silica plug which was flushed with hexane. The solvent was removed to afford **V-6** (15.23 g, 96 % yield) as colorless oil. $^1$H NMR (300 MHz, $CDCl_3$): δ 7.18 (d, 1H, *J* = 5.7 Hz, Ar C5-H), 6.79 (d, 1H, *J* = 5.8 Hz, Ar C4-H), 2.56 (t, 2H, *J* = 7.7 Hz, Ar-$CH_2$), 1.66-1.17 (b, 12H, -$CH_2$), 0.89 (t, 3H, *J* = 6.9 Hz, -$CH_3$). $^{13}$C NMR (75 MHz, $CDCl_3$): δ 142.1, 128.2, 125.1, 108.8, 31.9, 29.7, 29.4, 29.2, 22.7, 14.1. IR ($\nu$, $cm^{-1}$): 2953, 2923,

2853, 1461, 1408, 1375, 991, 828, 713, 635. HRMS: Calculated for $C_{12}H_{19}SBr$, 274.0391; Observed, 274.0398; $\Delta$ = 2.6 ppm.

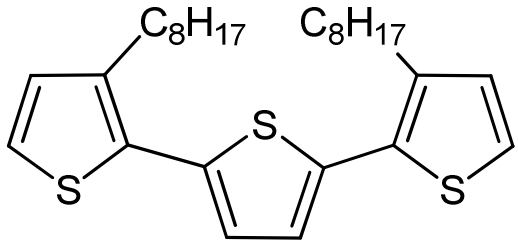


**3,3''-Dioctyl-2,2':5',2''-terthiophene, V-7.** Freshly ground Mg turnings (1.35 g, 56.3 mmol) were suspended in $Et_2O$ (100 mL). 1,2-Dibromoethane (1.4 g, 7.4 mmol) was added to initiate the reaction. A solution of **V-6** (7.66 g, 27.9 mmol) in $Et_2O$ (30 mL) was added slowly over the course of 30 min, and the resulting mixture was heated at reflux for 3 h. The solution was cannulated to an addition funnel connected to second flask containing a solution of 2,5-dibromothiophene (3.06 g, 12.7 mmol) and Ni(dppp)$Cl_2$ (0.12 g, 0.25 mmol) in $Et_2O$ (50 mL). The Grignard reagent was added slowly via the addition funnel, and the resulting solution was heated at reflux for 4 h. The solution was cooled to 0 °C and 1M HCl (50 mL) was added followed by $H_2O$ (30 mL). The two layers were separated and the $H_2O$ was washed with additional $Et_2O$. The organic extracts were washed with saturated aqueous $Na_2CO_3$ (100 mL) and dried over $MgSO_4$. The solvent was removed under reduced pressure and the resulting brown oil was subjected to column chromatography (silica gel; hexanes) to afford **V-7** (3.66 g, 61 % yield) as yellow oil. $^1$H NMR (300 MHz, $CDCl_3$): δ 7.18 (d, 2H, *J* = 5.5 Hz, Ar C5,5''-H), 7.06 (s, 2H, Ar C3',4'-H), 6.95 (d, 2H, *J* = 5.5 Hz, Ar C4,4''-H), 2.79 (t, 4H, *J* = 7.7 Hz, Ar-$CH_2$), 1.70-1.17 (b, 24H, -$CH_2$), 0.88 (t, 6H, *J* = 6.7 Hz, -$CH_3$). $^{13}$C NMR (75 MHz, $CDCl_3$): δ 139.7

(Ar C-2,2”), 136.0 (Ar C-3,3”), 130.4 (Ar C-2’,5’), 130.0 (Ar C-4,4”), 126.0 (Ar C-5,5”), 123.7 (Ar C-3’,4’), 31.9, 30.7, 29.6, 29.3, 22.7, 14.1. IR ($\nu$, $cm^{-1}$): 2952, 2919, 2850, 1462, 1419, 1394, 1376, 1243, 1085, 875, 833, 795, 720, 691. HRMS: Calculated for $C_{28}H_{40}S_3$, 472.22922; Observed, 472.22870; $\Delta$ = 1.1 ppm.

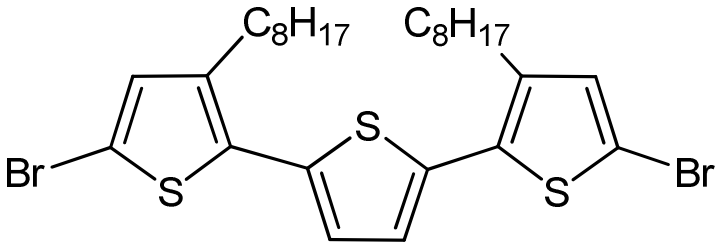


**3,3’’-Dioctyl-5,5”-dibromo-2,2’:5’,2’’-terthiophene, V-8.** NBS (1.02 g, 5.9 mmol) was added to a solution of **V-7** (1.3 g, 2.8 mmol) in anhydrous THF (50 mL) at 0 °C . The mixture was stirred under nitrogen for 3 h in the dark. The solvent was removed under reduced pressure and the resulting brown oil was eluted through a silica plug with hexanes as the eluent to provide **V-8** (1.64 g, 95 % yield) as yellow oil. This compound has to be stored in dark as it is highly light sensitive. $^1$H NMR (300 MHz, $CDCl_3$): δ 6.98 (s, 2H, Ar C3’,4’-H), 6.90 (s, 2H, Ar C4,4”-H), 2.71 (t, 4H, $J$ = 7.7 Hz, Ar-$CH_2$), 1.70-1.17 (b, 24H, -$CH_2$), 0.89 (t, 6H, $J$ = 6.7 Hz, -$CH_3$). $^{13}$C NMR (75 MHz, $CDCl_3$): δ 140.4 (Ar C-2,2”), 135.1 (Ar C-3,3”), 132.7 (Ar C-2’,5’), 131.6 (Ar C-4,4”), 126.4 (Ar C-3’,4’), 110.6 (Ar C-5,5”), 31.9, 30.6, 29.71, 29.4, 29.3, 22.7, 14.1. IR ($\nu$, $cm^{-1}$): 2952, 2922, 2852, 1461, 1427, 830, 794, 721. HRMS: Calculated for $C_{28}H_{38}S_3Br_2$, 628.05024; Observed, 628.04660; $\Delta$ = 5.8 ppm.

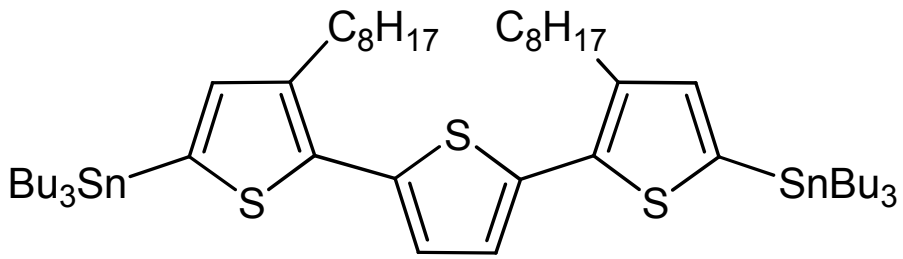


**5,5”-Bis(tributylstannyl)-3,3’’-Dioctyl-2,2’:5’,2’’-terthiophene, V-9.** *n*-Butyllithium (0.53 mL of a 2.5 M solution in hexane, 1.3 mmol) was added dropwise to a solution of **V-8** (0.40 g, 0.64 mmol) in anhydrous THF (20 mL) at -78 °C.. The solution was stirred at -78 °C for 30 min, warmed to 0 °C for 30 min and then recooled to -20 °C. Tri(*n*-butyl)tin chloride (0.38 g, 1.9 mmol) was added once and the mixture was stirred overnight at room temperature. The reaction solution was poured into $H_2O$ and the mixture was extracted with $CH_2Cl_2$ (100 mL). The organic extracts were dried over $MgSO_4$ and the solvent was removed under reduced pressure to afford **V-9** as yellow oil. The compound is highly unstable to light and silica and hence used without further purification.

**Poly(3,3’’-Dioctyl-2,2’:5’,2’’-terthiophene-*alt*-6,13-bis(triisopropylsilylethynyl)pentacene) .** A mixture of **V-4** and **V-5** (0.60 g, 0.75 mmol), **V-9** (0.79 g, 0.76 mmol), $Pd(PPh_3)_4$ (43.2 mg, 40.0 μmol) and $PPh_3$ (55.1 mg, 210 μmol) was degassed with Ar. Anhydrous toluene (20 mL) was added and the solution and heated to 80 °C for 48 h. The black solution was added to MeOH (30 mL) and the crude precipitated polymer was collected by filtration. The polymer was sequentially extracted in a Soxhlet extractor with acetone, hexanes and $CHCl_3$. The $CHCl_3$ exctract was poured into methanol to precipitate the fractionated polymer as a black solid (0.22 g, 52 % yield). $^1$H NMR (300 Hz, $CDCl_3$): δ 9.42-9.0 (br), 8.2-6.8 (br),

3.0-2.4 (br), 2.0-1.0 (br), 1.0-0.6 (br). GPC: $M_n$= 19,355 kD; PDI = 1.89. A black high molecular weight fraction left in the Soxhlet thimble was which dissolved in chlorobenzene on heating (0.15 g, 35 % yield).

## 5.3. RESULTS AND DISCUSSION

### 5.3.1. Synthesis of Pentacene Monomer

The preparation of the TIPSE substituted dibromopentacene monomer 3 is as shown in Figure 5.1. Treatment of 4-bromo-o-xylene with *N*-bromosuccinimide (NBS) in presence of benzoyl peroxide results in bromination of the benzylic positions and the formation of the desired bis(dibromomethyl) compound **V-1** along with the less brominated xylenes. Recrystallization from hexanes gives compound **V-1**. Compound **V-1** undergoes elimination of bromine in the presence of sodium iodide to afford *ortho*-xylene, which undergoes an *in situ* Diels-Alder reaction with 1,4-benzoquinone to yield a ca. 1:1 mixture of 2,9- and 2,10-dibromopentacene-diones, **V-2** and **V-3** respectively. The oligomers were inseparable and the mixture was used for the preparation of the monomer. The mixture of **V-2** and **V-3** was converted to a mixture of TIPSE substituted dibromopentacenes **V-4** and **V-5** by nucleophilic addition of lithiated (2-triisopropylsilyl)ethynylene to the carbonyl groups followed by $SnCl_2$ mediated reduction. The regioisomeric mixture of **V-4** and **V-5** was used in the polymerization without separation.

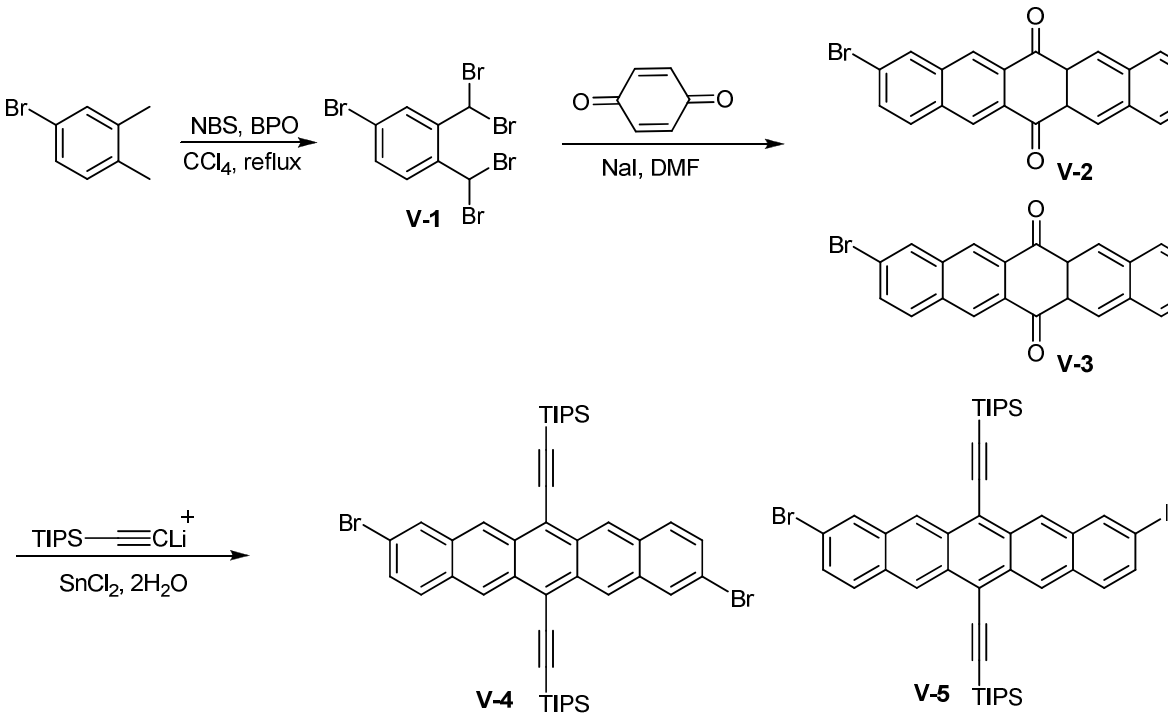


**Figure 5.1**. Synthesis of pentacene monomer **V-4 and V-5**.

### 5.3.2. Synthesis of Terthiophene Monomer

The synthesis of the terthiophene monomer **V-9**, according to a previously reported route,[22] is presented in Figure 5.2. Bromination of 3-octylthiophene with *N*-bromosuccinimide at 0 °C gave 2-bromo-3-octylthiophene, **V-6**, in quantitative yield. Treatment of the bromothiophene with magnesium gave the corresponding Grignard reagent which was coupled with 2,5-dibromothiophene in the presence of Ni(dppp)$Cl_2$ to form 3,3”-dioctyl-2,2’:5’,2” -terthiophene **V-7**. Upon exposure to NBS at low temperature, terthiophene **V-7** gave the dibromoterthiophene **V-8** in high yield. The dibromo monomer is highly unstable in light, and was therefore stored for only short times in the dark.

We were initially interested in performing the polymerization of the dibromopentacene **V-4** , **V-5** and the bis(boronate ester) of the terthiophene monomer by a Suzuki polymerization. Bromine-lithium exchange of dibromoterthiophene **V-8** with BuLi followed by addition of 2-isopropoxy-4,4,5,5-tetramethyl-1,3,2-dioxoborolane resulted in the terthiophene with boronate ester functionality on the 5 and 5” position (as shown by the singlet for the protons in the 4 and 4” position of the terthiophene in the $^1$H NMR spectra). However, the rapid decomposition of this terthiophene bis(boronate ester) on aqueous workup and upon passing it through both treated and untreated silica led us to explore the possibility of preparing the bis(stannane) terthiophene monomer which could be polymerized by a Stille reaction. Dibromoterthiophene **V-8** was lithiated and treated with tributylstannyl chloride to form the 5,5”-bis(tributylstannyl)terthiophene **V-9**. This compound is stable to aqueous work up, but starts to decompose upon passing through a

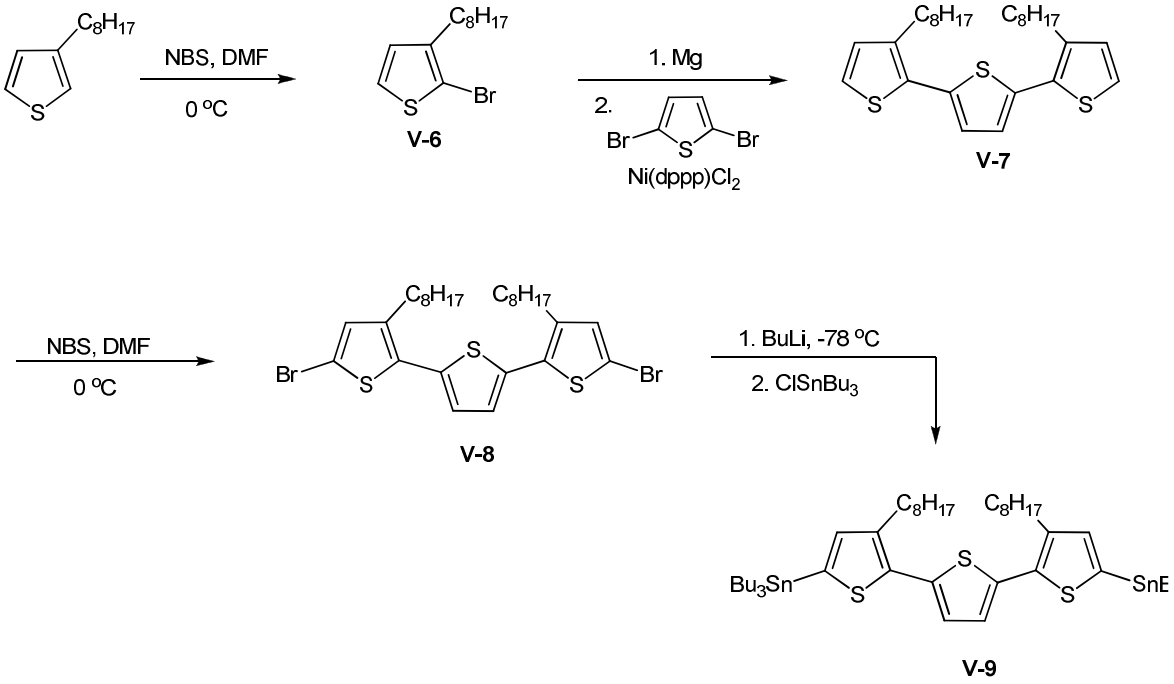


**Figure 5.2**. Synthesis of dibromoterthiophene monomer **V-9**.

silica column. Compound **V-9** was used in the polymerization without further purification.

### 5.3.3. Polymerization of dibromopentacene monomers V-4 and V-5 with terthiophene bis(stannane), V-9.

The copolymers involving pentacene were previously prepared by Sonagashira and Suzuki coupling reaction. We used the Stille coupling reaction between the dibromo TIPSE-substituted pentacene **V-4 and V-5** and bis(tributylstannyl) terthiophene **V-9** in presence of palladium tetrakis(triphenylphosphine) to prepare the copolymer (Figure 5.3). The reaction was run for 48 h to ensure high conversion and to prepare copolymers with high molecular weight. Precipitation of the copolymer using methanol and fractionation (Soxhlet extraction) using acetone, hexanes and chloroform solvents resulted in the copolymer in 52 % yield. The molecular weight of the copolymer was determined to be 19.5 kD by gel permeation chromatography (GPC) using THF as the eluent and polystyrene standards.

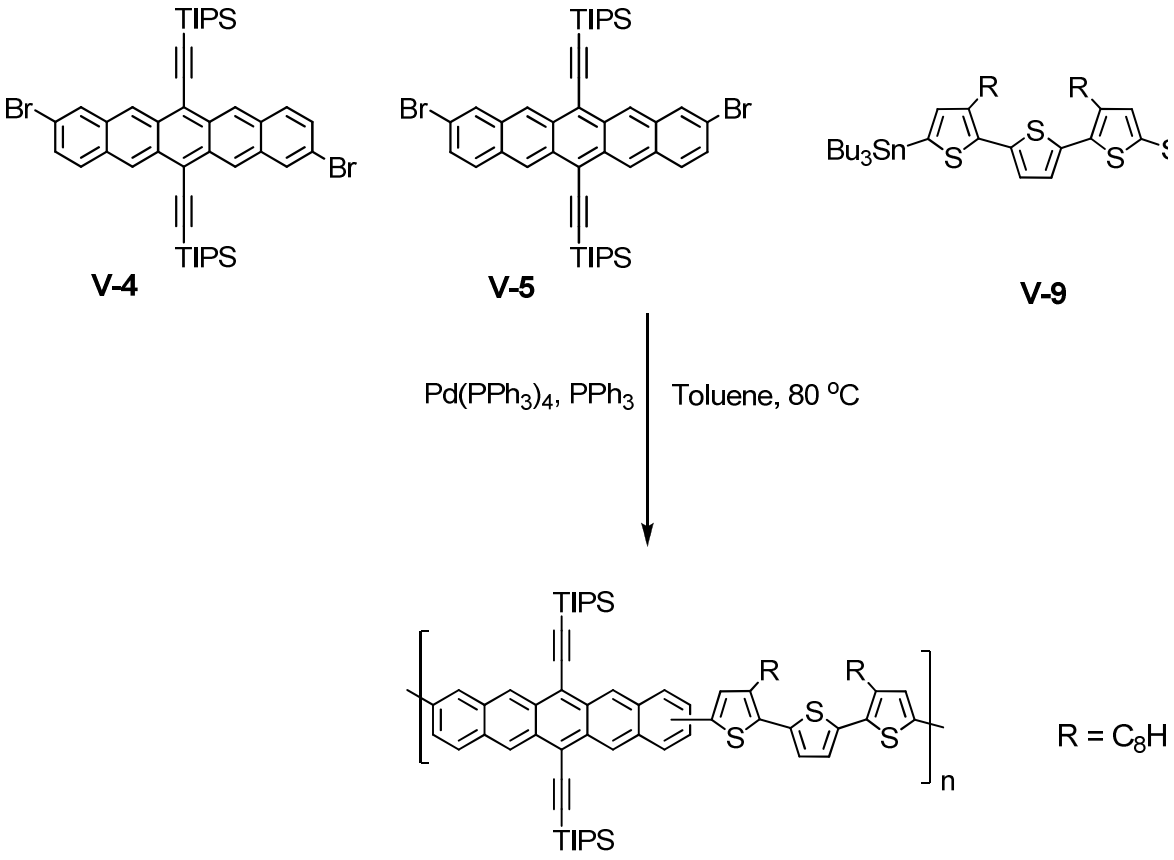


**Figure 5.3.** Polymerization of **V-4, V-5** and **V-9** to afford alternating pentacene-terthiophene copolymer.

### 5.3.4. Characterization of the copolymer

The UV-vis spectra of the TIPSE-pentacene and terthiophene monomers, and the copolymer were recorded in $CHCl_3$ solution, Figure 5.4. The spectrum of the TIPE-pentacene monomer shows a sharp absorption at 321 nm, and small peaks at 584 and 639 nm, and the terthiophene monomer has a single absorption at 346 nm. The spectrum of the copolymer in solution state is significantly red shifted relative to the spectra of the two monomers with a peak at, $\lambda_{max}$ = 436 nm corresponding to the extended conjugation of the polymeric structure. The spectrum of the copolymer retains the peaks from pentacene unit, which are red shifted to 624 and 681 nm, with the absorption onset shifted out to 710 nm.

As expected, the spectrum for the thin film of the copolymer is broader compared to the solution spectrum. The peak with $\lambda_{max}$ = 465 nm for the thin film spectrum is red shifted by 29 nm in comparison to the solution state spectrum for the copolymer. Moreover, the spectrum tails out to 821 nm in the solid state due to the increased π-π interactions in the solid state. The absorption edge of 821 nm corresponds to an optical bandgap of 1.51 eV- This optical band gap is significantly lower than that of reported pentacene- PPE (1.76 eV) and pentacene-fluorene copolymers (1.78 eV). Based on these values it can be inferred that the terthiophene unit was effective in lowering the optical bandgap of pentacene copolymers compared to phenylene ethnylyne (2.4 eV for PPE)[23] and fluorene (2.9 eV for polyfluorene).[24]

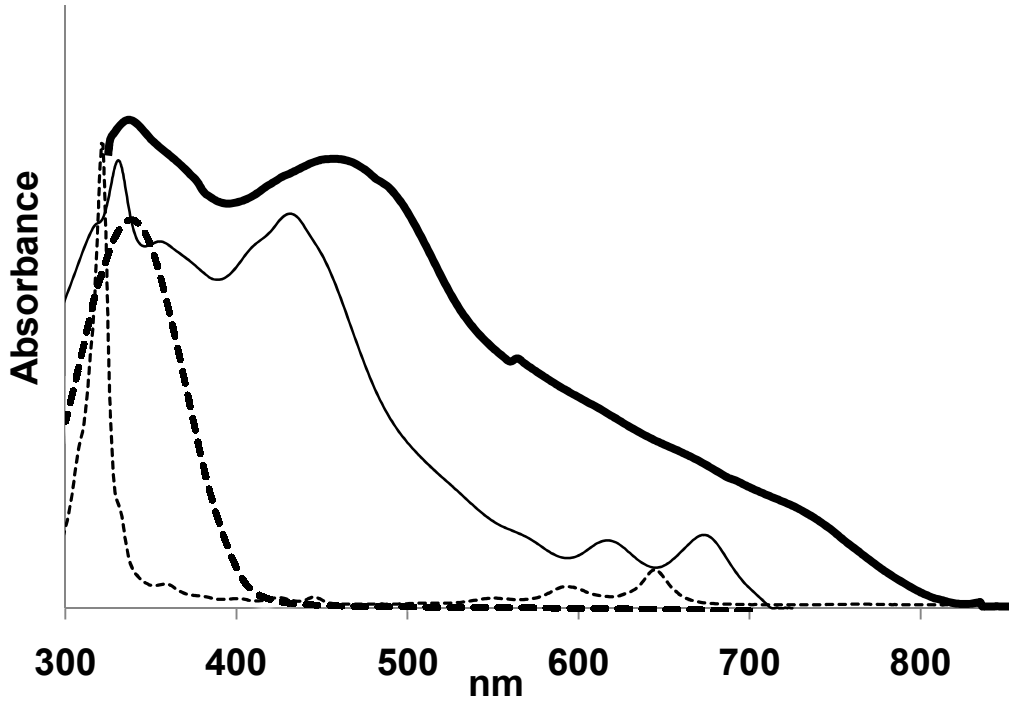


**Figure 5.4.** UV-vis spectra of the copolymer as thin film (——), copolymer in $CHCl_3$ (— —), terthiophene monomer in $CHCl_3$ (▪▪▪▪▪▪) and TIPSE pentacene monomer in CHCl3 (·····).

The redox properties of the copolymer were determined by recording the cyclic voltammogram of a thin film of the material on a platinum electrode. The electrode was coated with a thin film of the copolymer by dipping it into a dilution solution of copolymer inchloroform, withdrawing it and allowing the solvent to evaporate. Cyclic voltammograms were recorded by immersing the film-coated electrode in a 0.1 M solution of tetra-*n*-butylammonium hexafluorophosphate in acetonitrile (the copolymer is insoluble in acetonitrile) and scanning the potential at 100 mV/s. The copolymer exhibited one reversible oxidation and an irreversible reduction (Figure 5.5) suggesting that the reduced form is unstable. With the onset of the reduction at –0.77 V, and the onset for oxidation at +0.66 V, this behavior corresponds to a bandgap of 1.43 eV.

The thermal stability of the copolymer in the solid state was studied by thermal gravimetric analysis (TGA) and differential gravimetric analysis (DSC) under argon. The onset for degradation of the polymer is at approximately 400 °C similar to other pentacene copolymers, Figure 5.6. Previous studies have shown that triisopropylsilylethynyl substituents are removed around this temperature.[13] The DSC studies on the copolymer shows no thermal transitions in between 25 to 250 °C, indicating that pentacene-terthiophene copolymer has good thermal stability.

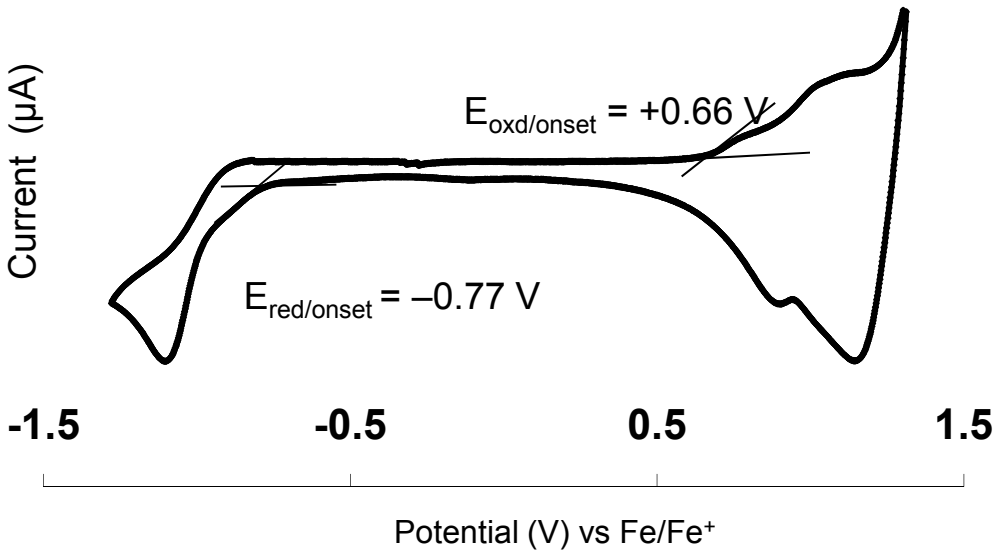


**Figure 5.5.** Cyclic voltammogram of a thin film of the pentacene-terthiophene copolymer (Ag quasi reference electrode, 100 mV/s.)

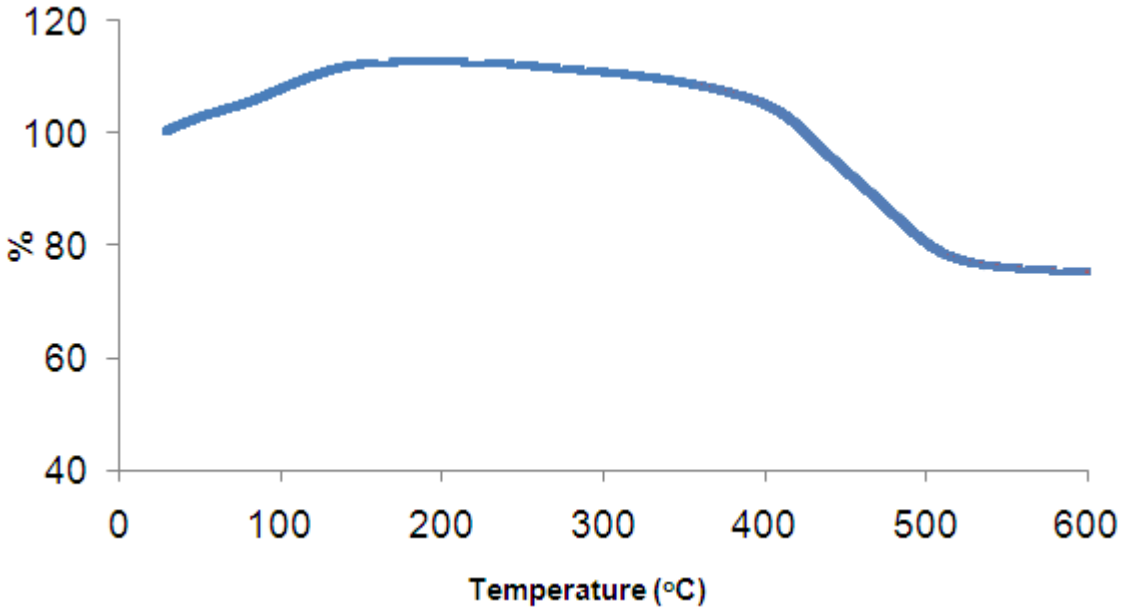


**Figure 5.6.** TGA data for the pentacene-terthiophene copolymer.

The electrical characteristics of the copolymer were studied by constructing bottom contact oFETs. The transistors were prepared by spin coating ~20 nm films of the copolymer onto silicon (oxide) substrates decordated with gold source and drain electrodes. Initial results, based on the plot of source-drain ($I_D$) current versus gate voltage ($V_G$), exhibited a mobility of $6 \times 10^{-5}$ $cm^2/Vs$ for the copolymer.

## 5.4. CONCLUSIONS

In summary, we have prepared a new type of copolymer containing alternating pentacene and terthiophene units by Stille coupling polymerization reactions. The resulting copolymer had a high molecular weight and good solubility in organic solvents. The optical absorption as well as the redox bevavior of the pentacene-terthiophene copolymer corresponds to a bandgap value of 1.51 and 1.43 eV, respectively. The band gap of the terthiophene containing materials is lower than other pentacene based copolymer and has potential as a solution processable material for device applications.

## 5.5. REFERENCES


(1) Babel, A.; Jenekhe, S. A. *J. Am. Chem. Soc.* **2003**, *125*, 13656.

(2) McCulloch, I.; Heeney, M.; Bailey, C.; Genevicius, K.; Macdonald, I.; Shkunov, M.; Sparrowe, D.; Tierney, S.; Wagner, R.; Zhang, W. M.; Chabinyc, M. L.; Kline, R. J.; McGehee, M. D.; Toney, M. F. *Nature Materials* **2006**, *5*, 328.

(3) Sirringhaus, H.; Tessler, N.; Friend, R. H. *Science* **1998**, *280*, 1741.

(4) Burroughes, J. H.; Bradley, D. D. C.; Brown, A. R.; Marks, R. N.; Mackay, K.; Friend, R. H.; Burns, P. L.; Holmes, A. B. *Nature* **1990**, *347*, 539.

(5) Guenes, S.; Neugebauer, H.; Sariciftci, N. S. *Chemical Reviews (Washington, DC, United States)* **2007**, *107*, 1324.

(6) Gorodetsky, A. A.; Cox, M.; Tremblay, N. J.; Kymissis, I.; Nuckolls, C. *Chemistry of Materials* **2009**, *21*, 4090.

(7) Tang, C. W.; Vanslyke, S. A. *Applied Physics Letters* **1987**, *51*, 913.

(8) Anthony, J. E.; Brooks, J. S.; Eaton, D. L.; Parkin, S. R. *J. Am. Chem. Soc.* **2001**, *123*, 9482.

(9) Anthony, J. E.; Eaton, D. L.; Parkin, S. R. *Organic Letters* **2002**, *4*, 15.

(10) Lehnherr, D.; McDonald, R.; Ferguson, M. J.; Tykwinski, R. R. *Tetrahedron* **2008**, *64*, 11449.

(11) Klarner, G.; Davey, M. H.; Chen, W. D.; Scott, J. C.; Miller, R. D. *Advanced Materials* **1998**, *10*, 993.

(12) Okamoto, T.; Bao, Z. A. *J. Am. Chem. Soc.* **2007**, *129*, 10308.

(13) Okamoto, T.; Jiang, Y.; Qu, F.; Mayer, A. C.; Parmer, J. E.; McGehee, M. D.; Bao, Z. N. *Macromolecules* **2008**, *41*, 6977.

(14) Fichou, D. *J. Mater. Chem.* **2000**, *10*, 571.

(15) Mishra, A.; Ma, C. Q.; Bauerle, P. *Chem. Rev.* **2009**, *109*, 1141.

(16) Chen, M. X.; Crispin, X.; Perzon, E.; Andersson, M. R.; Pullerits, T.; Andersson, M.; Inganas, O.; Berggren, M. *Applied Physics Letters* **2005**, *87*, 3.

(17) Yue, W.; Zhao, Y.; Tian, H. K.; Song, D.; Xie, Z. Y.; Yan, D. H.; Geng, Y. H.; Wang, F. S. *Macromolecules* **2009**, *42*, 6510.

(18) Yen, W. C.; Pal, B.; Yang, J. S.; Hung, Y. C.; Lin, S. T.; Chao, C. Y.; Su, W. F. *Journal of Polymer Science Part a-Polymer Chemistry* **2009**, *47*, 5044.

(19) Peng, Q.; Xu, J.; Zheng, W. X. *Journal of Polymer Science Part a-Polymer Chemistry* **2009**, *47*, 3399.

(20) Bundgaard, E.; Krebs, F. C. *Solar Energy Materials and Solar Cells* **2007**, *91*, 1019.

(21) Kerfanto, M.; Soyer, N. *Bull. Soc. Chim. Fr.* **1966**, 2966.

(22) Janzen, D. E.; Burand, M. W.; Ewbank, P. C.; Pappenfus, T. M.; Higuchi, H.; da Silva, D. A.; Young, V. G.; Bredas, J. L.; Mann, K. R. *J. Am. Chem. Soc.* **2004**, *126*, 15295.

(23) Bunz, U. H. F. *Chem. Rev.* **2000**, *100*, 1605.

(24) Bernius, M.; Inbasekaran, M.; Woo, E.; Wu, W. S.; Wujkowski, L. *J. Mater. Sci.-Mater. Electron.* **2000**, *11*, 111.

# CHAPTER 6

# ULTRASOUND INDUCED ENHANCEMENT OF THE FIELD MOBILITY OF POLY(3-HEXYLTHIOPHENE) [#]

## 6.1. INTRODUCTION

Significant improvements in the field effect mobility of conjugated polymers have been realized[1,2] since the first report of field effect transistors (FETs) fabricated from poly(3-alkylthophene)s (PATs).[2,3] The structure of the alkyl side chains and the regioregularity of the sample have a strong influence on the mobility, with values as high as 0.1 $cm^2V^{-1}s^{-1}$ for highly regioregular (ca. 96% head-to-tail) poly(3-hexylthiophene) (P3HT), although values of $10^{-3}$ $cm^2V^{-1}s^{-1}$ for commercially available materials are much more common. Side chain crystallization of regularly placed linear alkyl side chains leads to highly ordered solid state films in which planar polymer chains are closely packed, thereby leading to strong interchain interactions between π-conjugated systems. Preferential orientation of the planar conjugated backbone perpendicular to the semiconductor-dielectric interface of an FET provides an optimal pathway for charge transport between the source and drain electrodes.

Ultrasonic irradiation is commonly used to induce rapid mixing of solutions and for homogeneous dispersion of fillers in liquid media.[4] Application of ultrasound enhances the dissolution of P3HT in chloroform ($CHCl_3$),[5] and facilitates the dispersion

[#] This chapter describes studies of effect of ultrasonication on mobility of P3HT and will be submitted to JACS communication as a co-authored paper: Aiyar, A.; Nambiar, R; Collard, D. M.; Reichmanis; E.

of nanoparticles (e.g., carbon nanotubes, germanium nanowires, silicon nanocrystals) in solutions of P3HT and P3HT:PCBM for the preparation of composites.[6-8] In a study of the field effect mobility of conjugated polymers we have routinely sonicated $CHCl_3$ solutions of P3HT for ca. 5 min prior to fabrication of thin film devices. While a solution of P3HT (Sigma Aldrich, 94 % regioregularity, Mn= 18.1 kD, Mw= 42.6 kD, PDI = 2.35) in $CHCl_3$ (ca 3 mg/mL) is bright orange, the color changes to dark brown upon ultrasonication (Bransonic 2510, 40 kHz, 130W), Figure 6.1. Surprisingly, films prepared by spin coating the ultrasonicated polymer solution on bottom-contact FET devices in air, resulted in a increase of the field effect mobility by approximately two orders of magnitude (from ca. $10^{-4}$ $cm^2V^{-1}s^{-1}$ to ca. $10^{-2}$ $cm^2V^{-1}s^{-1}$) compared to the original orange solution, Figure 6.2. Herein, we investigate this ultrasound induced two order of magnitude increase in the mobility in regioregular P3HT FETs.

## 6.2. EXPERIMENTAL

### 6.2.1. General Methods

The P3HT used in this study was purchased from Sigma-Aldrich and was used as it is. The molecular weight of the P3HT was measured by GPC in THF based on polystyrene standards using Polymer Laboratories PLgel Mixed-C columns and a Waters 2690 differential refractive index detector. NMR analysis was performed on a Bruker DSX 400 or DSX 300 instruments using $CDCl_3$ as the solvent. Chemical shifts are reported relative to internal tetramethylsilane. Ultraviolet-visible analysis was performed on a Perkin-Elmer Lambda 19 spectrophotometer and fluorescence spectroscopy was performed using FluroMax Compact Spectrofluorometer from Horiba Scientific. The

AFM measurements were performed on with a multimode atomic force microscope (Digital Instruments, Innova) in tapping mode.

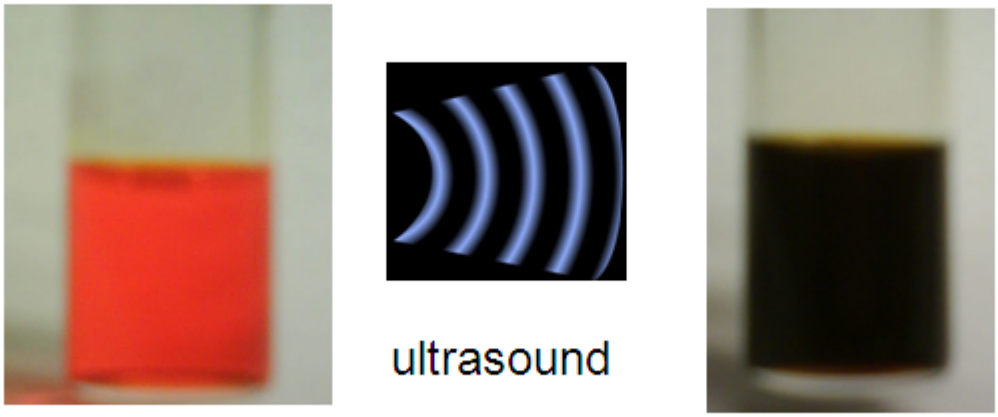


**Figure 6.1**. Color change in P3HT solution in chloroform on ultrasonication for 5 min.

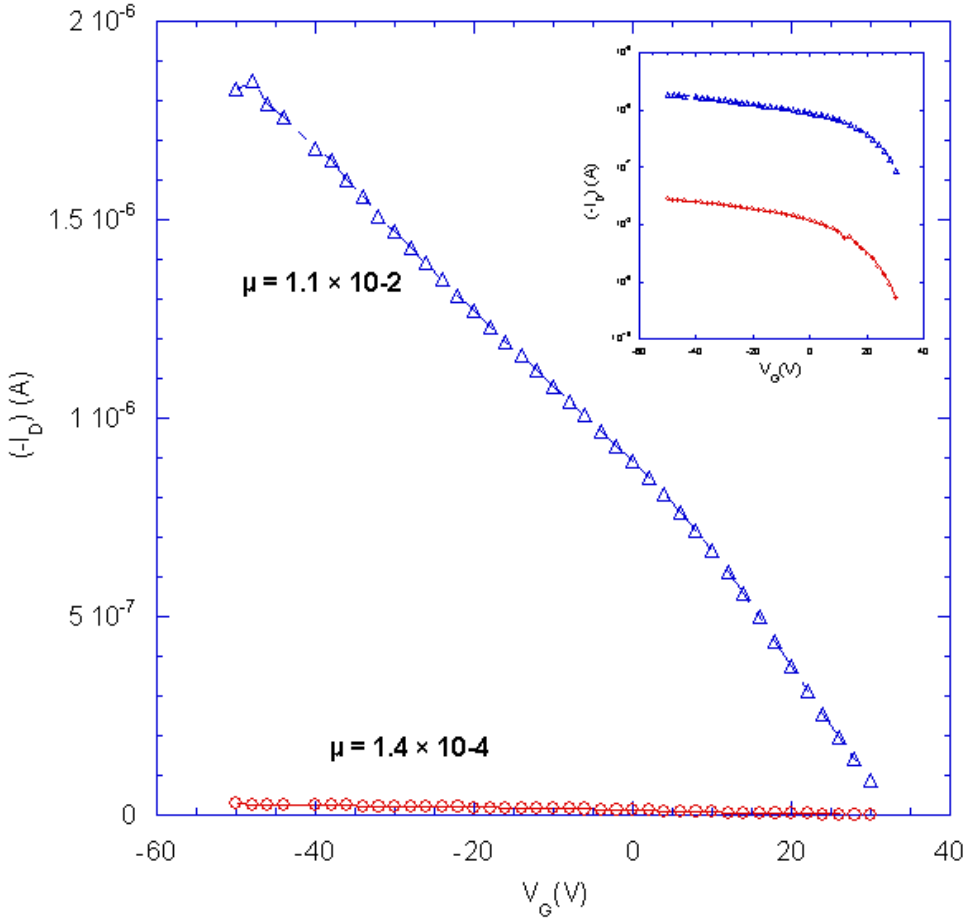


**Figure 6.2**. Plot of $-I_D$ versus $V_G$ at a fixed $V_D$ on both linear axis and log axis (inset) for unsonicated P3HT solution (oooo) and sonicated P3HT solution (ΔΔΔΔ).

## 6.3. RESULTS AND DISCUSSIONS

### 6.3.1. Solution state studies on sonicated P3HT

The ultrasound induced color change was investigated to determine the origin of this increase in mobility. There are marked differences in the absorption spectra of the pristine and ultrasonicated solutions, Figure 6.3. The spectrum of a pristine solution of P3HT in $CHCl_3$ consists of a single peak with an absorption maximum at ca. 450 nm which is associated with the π-π* transition of the solvated (i.e., isolated) conjugated polymer.[9-12] Although the spectrum of the sonicated solution displays a similar π-π* absorption band, additional peaks begin to appear at ca. 570 and 620 nm within a minute of irradiation, and the intensities of these absorption increase with ultrasonication time, Figure 6.3. These new bands are similar in appearance to those of aggregates of PATs that are formed upon the addition of a poor solvent (e.g., MeOH) to solutions of the polymers in good solvents (e.g., $CHCl_3$), Figure 6.4.[10,11,13,14,15] The photoluminescence (PL) spectra of ultrasonicated solutions are also similar to those of aggregates formed upon addition of a poor solvent, Figure 6.5. The emission spectra (excitation λ = 450 nm) of pristine solutions of P3HT in $CHCl_3$, 10% MeOH-aggregated P3HT, and ultrasonicated solutions were recorded. The spectra of the ultrasonicated and MeOH-aggregated solutions have a greater contribution at ca. 630 nm compared to the pristine solution, consistent with the formation of a π-stacked aggregate. Compared to the original pristine P3HT solution, the intensity of photoluminescence decreases by ca. 47% and 36% upon ultrasonic irradiation and upon addition of 10% methanol,[16-18] respectively. Also, the UV-vis spectra reverted back to the original pristine state upon heating the

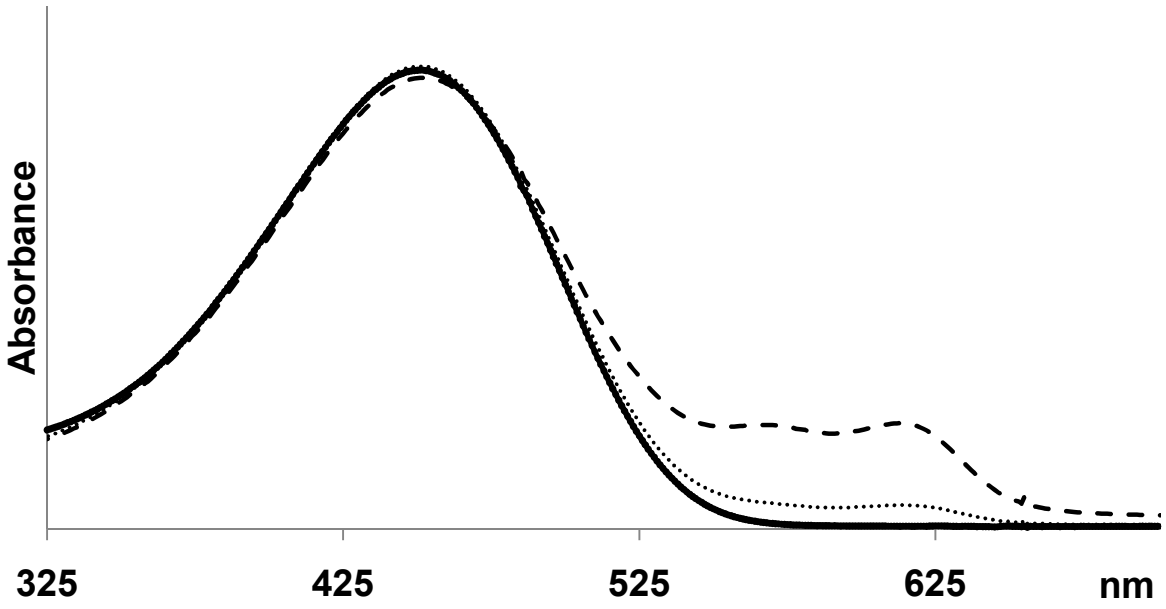


**Figure 6.3**. UV-vis absorption spectra of the diluted P3HT solutions in chloroform at different sonication times, t=0 (——), t=1 min (▪▪▪▪▪) and t = 6 min (- - - -).

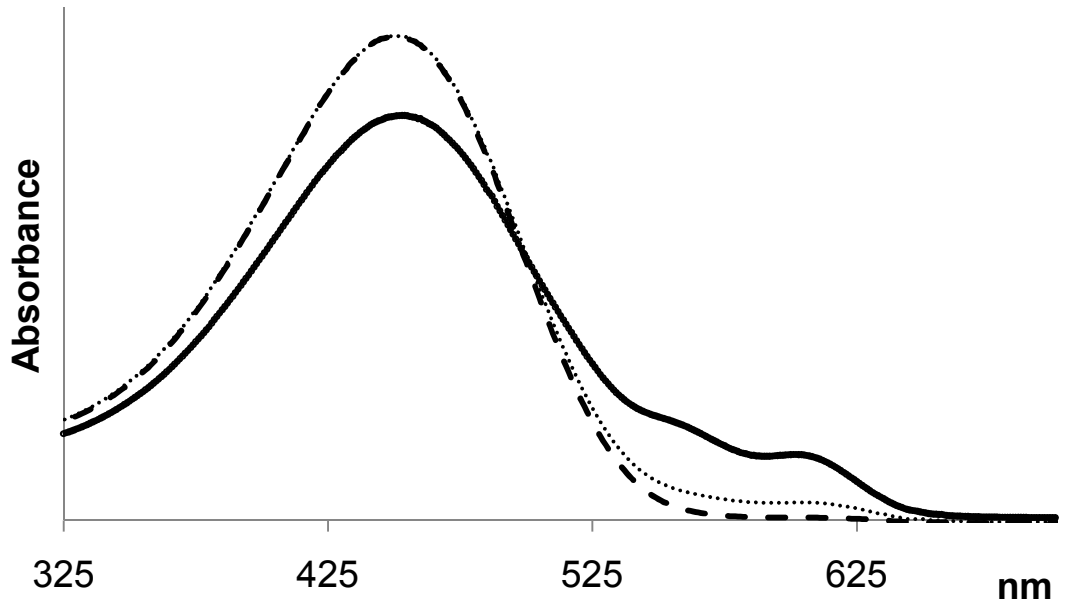


**Figure 6.4**. UV-vis absorption spectra of the diluted P3HT solutions at different volume percent of poor solvent MeOH, 0 % (- - - -), 10 % (▪▪▪▪▪) and 15 % (——).

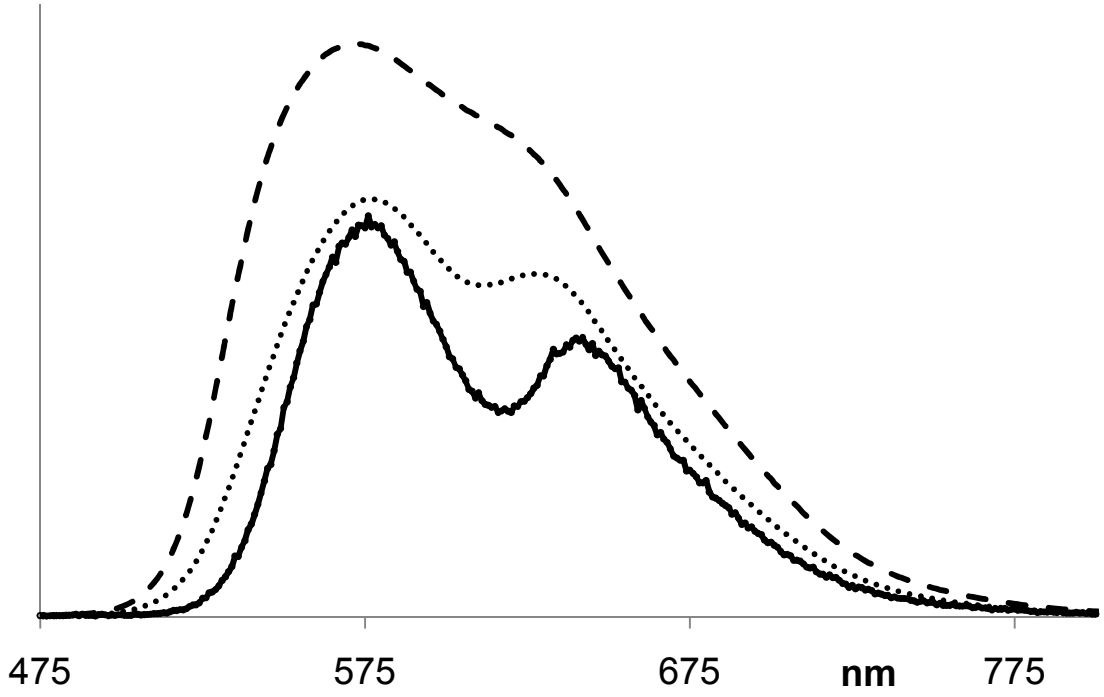


**Figure 6.5**. Fluorescence spectra of diluted pristine P3HT (- - - -), 10 % MeOH aggregated P3HT (▪▪▪▪▪) and 5 min sonicated P3HT (——) solutions.

ultrasonicated solutions (2 mins, 70°C). This reversibility of the color and the UV-vis spectra indicates formation of aggregates instead of a chemical change.

Further evidence for ultrasound-induced aggregation of polymer chains is apparent from dynamic light scattering (DLS). Solutions of P3HT showed a significant increase in the hydrodynamic radius from ca. 7 nm for pristine solutions to ca. 25 nm for solutions that had been ultrasonicated for one minute. However, due to strong absorbance of the laser (He-Ne, 632nm), reliable hydrodynamic radii could not be obtained for solutions ultrasonicated for longer times.

### 6.3.2. Solid state studies on sonicated P3HT

The ultrasound-induced changes in the properties of $CHCl_3$ solutions of P3HT give rise to changes in the properties of thin films prepared by spin coating the solutions (3mg/mL, 1500 rpm). The solid state spectra of thin films (ca. 20 nm) indicate a bathochromic shift of the absorption maximum ($\lambda_{max}$) from 548 nm (films prepared from pristine solution) to 559 nm for films prepared from ultasonicated solutions, Figure 6.6. The spectra of films prepared from the ultrasonicated P3HT solutions show a more pronounced shoulder at ~605 nm. These effects are similar to changes noted previously upon thermal annealing of P3HT films[15] whereby a red-shift of the $\lambda_{max}$ corresponds to a higher degree of the planarization of the conjugated backbone[21] and a pronounced shoulder is ascribed to improved interchain packing.[15] Atomic force microscopy (AFM) shows significant differences in the topography and phase images between pristine films and films prepared from ultrasonicated solution. AFM images of films prepared from pristine solutions appear smooth and are relatively featureless, Figure 6.7A,[5] whereas

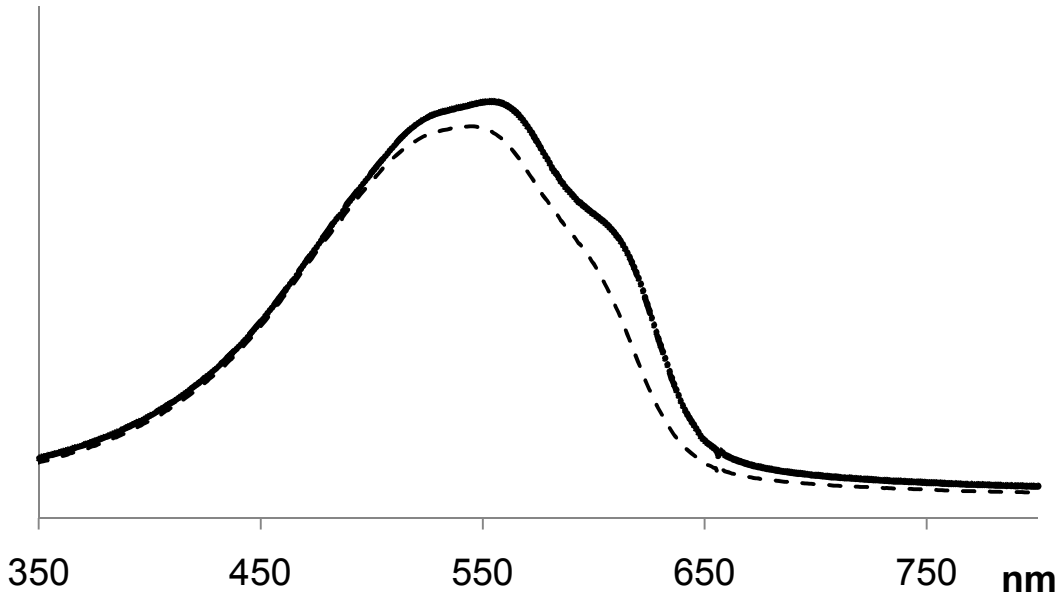


**Figure 6.6**. UV-vis absorption spectra of the P3HT films spin cast from chloroform solution at different sonication times, t=0 (- - - -) and t = 5 min (▬▬).

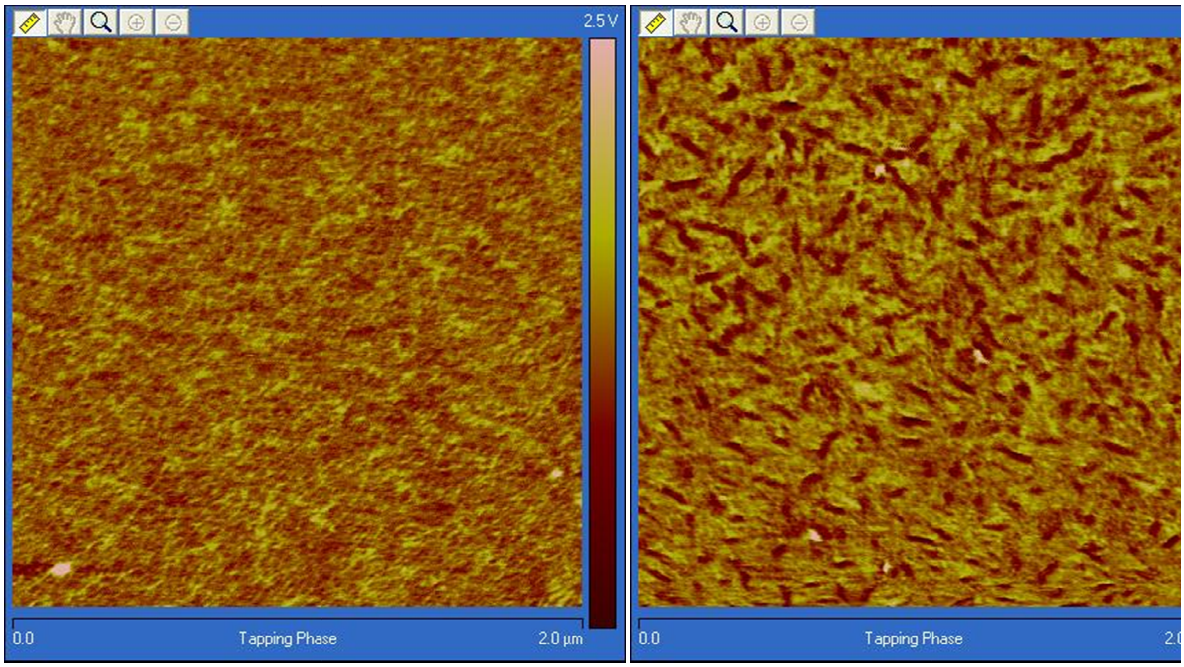


**Figure 6.6**. Tapping mode AFM images of P3HT films prepared from A. before sonication B. after 5 min sonication.

films formed from ultrasonicated P3HT solutions have a morphology indicative of nanoribbon-like structure, Figure 6.7B. Similar morphologies observed in solvent-aggregated films suggests that ultrasonication induces aggregation and brings about these morphological changes.[21]

### 6.3.3. Electrical Measurements on sonicated P3HT

Typical plots of source-drain current ($I_D$) versus gate voltage ($V_G$) obtained for FETs prepared from pristine and sonicated solutions are shown in Figure 6.2 (bottom contact FETs were prepared by spin coating ~20 nm P3HT films onto gold source and drain electrodes on a silicon dioxide gate dielectric.) FETs prepared from ultrasonicated solutions showed substantially higher currents compared to those prepared from pristine solutions, resulting in a increase in the linear region ($V_D$ = -3 V) field-effect mobility from $1.4 \times 10^{-4}$ $cm^2$ $V^{-1}s^{-1}$ to $1.1 \times 10^{-2}$ $cm^2$ $V^{-1}s^{-1}$. A similar increase in mobility was noted for solutions that had been subjected to ultrasonication for only one minute, even though the spectra of the solution and films were not substantially changed upon such short irradiation times. The enhancement of the field effect mobility[15] and electrical conductivity[16] has been previously reported for films prepared from solutions of P3HT which had been aggregated by the addition of a poor solvent and have been attributed to favorable π-π interactions between polymer chains resulting in well ordered films with increased charge carrier mobility.[5]

### 6.3.4. Chemical Analysis of sonicated P3HT

While ultrasonication commonly causes degradation of polymers,[19] $^{1}$H NMR spectra and gel-permeation chromatograms of P3HT and a model trimer (3,3''-dioctyl-2,2':5',2''-terthiophene) remain unchanged upon brief exposure to the low-power ultrasonication, indicating no decrease in molecular weight or other change in chemical structure.

## 6.4. CONCLUSIONS

Accordingly, we suggest that the two order of magnitude enhancement in the field effect mobility of films prepared from ultrasonicated solutions of P3HT is due to aggregation in solution which translates to an increase in the molecular order in the solid state. Thus, spectroscopic (UV-Vis and PL), DLS, AFM and measurements of mobility allow us to correlate the ultrasound-induced color change to aggregation of polymer chains, which translates into an increase in the field-effect mobility of films prepared from the irradiated solutions. This operationally-simple process constitutes a novel method to significantly improve the field effect mobility of PAT-based FETs, thereby potentially eliminating the need for dielectric surface modifications or further processing of the device. Extension of this investigation to probe the effect of solvent, regioregularity, and temperature on the aggregation and the field effect mobility of the polymer FET will provide further insight into the new phenomena reported here.

## 6.5. REFERENCES


(1) Bao, Z.; Dodabalapur, A.; Lovinger, A. J. *Appl. Phys. Lett.* **1996**, *69*, 4108.

(2) Sirringhaus, H.; Brown, P. J.; Friend, R. H.; Nielsen, M. M.; Bechgaard, K.; Langeveld-Voss, B. M. W.; Spiering, A. J. H.; Janssen, R. A. J.; Meijer, E. W.; Herwig, P. *Nature* **1999**, *401*, 685.

(3) Tsumura, A.; Koezuka, H.; Ando, T. *Appl. Phys. Lett.* **1986**, *49*, 1210.

(4) Suslick, K. S.; Price, G. J. *Annual Review of Materials Science* **1999**, *29*, 295.

(5) Genevieve, S.; Junying, L.; Rui, Z.; Tomasz, K.; Richard, D. M.; Zhenan, B., David, J. G., Eds.; SPIE: 2007; Vol. 6658, p 665810.

(6) Kymakis, E.; Kornilios, N.; Koudoumas, E. *Journal of Physics D* **2008**, *41*, 165110.

(7) Du Pasquier, A.; Mastrogiovanni, D. D. T.; Klein, L. A.; Wang, T.; Garfunkel, E. *Appl. Phys. Lett.* **2007**, *91*, 183501.

(8) Liu, C. Y.; Holman, Z. C.; Kortshagen, U. R. *Nano Lett.* **2009**, *9*, 449.

(9) Berson, S.; De Bettignies, R.; Bailly, S.; Guillerez, S. *Adv. Funct. Mater.* **2007**, *17*, 1377.

(10) Yeong Don, P.; Hwa Sung, L.; Yeon Joo, C.; Donghoon, K.; Jeong Ho, C.; Sichoon, L.; Kilwon, C. *Adv. Funct. Mater.* **2009**, *19*, 1200.

(11) Yamamoto, T.; Komarudin, D.; Arai, M.; Lee, B. L.; Suganuma, H.; Asakawa, N.; Inoue, Y.; Kubota, K.; Sasaki, S.; Fukuda, T. *J. Am. Chem. Soc* **1998**, *120*, 2047.

(12) McCullough, R. D.; Lowe, R. D.; Jayaraman, M.; Anderson, D. L. *J. Org. Chem.* **1993**, *58*, 904.

(13) Moulé, A. J.; Meerholz, K. *Adv. Mater* **2008**, *20*, 240.

(14) Park, Y. D.; Cho, J. H.; Jang, Y.; Lee, H. S.; Ihm, K.; Kang, T. H.; Cho, K. *Electrochem. Solid-State Lett.* **2006**, *9*, G317.

(15) Lu, G.; Yang, X. *J. Mater. Chem.* **2008**, *18*, 1984.

(16) Arnrutha, S. R.; Jayakannan, M. *J. Phys. Chem. B* **2008**, *112*, 1119.

(17) Nguyen, T. Q.; Doan, V.; Schwartz, B. J. *J. Chem. Phys.* **1999**, *110*, 4068.

(18) Nguyen, T. Q.; Yee, R. Y.; Schwartz, B. J. *J. Photochem. Photobiol., A* **2001**, *144*, 21.

(19) Wu, M.; Yang, G.; Wang, M.; Wang, W.; Liu, T. *Chem. Res. Chin. Univ.* **2008**, *24*, 653.

# CHAPTER 7

# SONAGASHIRA CROSS-COUPLING POLYMERIZATIONS IN SUPERCRITICAL CARBON DIOXIDE

## 7.1. INTRODUCTION

The use of conjugated organic polymers as semiconductors in electronic applications holds great promise. A major incentive for the development of semiconducting conjugated polymers (e.g. poly(3-alkylthiophene), polyacetylene, polyaniline) is their potential in power efficient, flexible, robust and inexpensive electronic and optoelectronic devices.[1] Poly(arylene ethynylene)s, and in particular poly(1,4-phenylene ethynylene)s (PPEs), have potential in the development of new sensors,[2] field effect transistors,[3] light emitting diodes,[4] solar cells[5] and sheet polarizers.[6] The conventional method to prepare PPEs is the Pd/Cu-catalyzed Sonagashira coupling of dihaloarenes (typically iodides and bromides) with diethynylarenes in the presence of an amine base.[7] This represents an AA + BB type polycondensation reaction (Figure 7.1A). Extensive studies to optimize the polymerization conditions include evaluation of the source of Cu and Pd, and the identity of the amine base.[7] As an extension of this work we have recently developed the polymerization of 2,5-dialkoxy-1-ethynyl-4-iodobenzenes (i.e., polymerization of a single AB type difunctional monomer, Figure 7.1B).[8] However, all of these methods use an amine (e.g., piperidine, morpholine, diisopropylamine and triethylamine[7]) as the solvent or with a cosolvent (e.g., toluene or

THF). These amines and cosolvents are toxic and flammable; making it desirable to consider the development of more environmentally benign methods.

Supercritical carbon dioxide ($scCO_2$) has gained considerable interest as an economically feasible "green" medium for chemical reactions and processing, with the potential to replace the use of conventional organic solvents.[9,10] $scCO_2$ is nonflammable, non-toxic and can be easily separated from reaction products by depressurization. Its critical point of 31.1 $^oC$ at 7.3 MPa is easily to achieve in the laboratory and in industrial settings. While a variety of polymerizations to afford conjugated polymers have been conducted in $scCO_2$, most of these consists of the oxidative polymerization of arenes and heteroarenes (e.g., thiophene, aniline) in the presence of a chemical oxidant (e.g., Fe(III)).[11] These include the preparation of poly(3-undecylthiophene)/polystyrene composites,[12] control of the morphology of polyaniline microtubes,[13] and the polymerization of fluoroalkyl-substituted thiophenes.[14] In all of these cases, the polymer was not soluble in $scCO_2$ and precipitated during the polymerization reaction. The first demonstration of the solubility of a conjugated polymer in sc-$CO_2$ was of a polythiophene bearing $scCO_2$-philic perfluorooctyl side chains.[15] However, the synthesis of conjugated polymers by the oxidative polymerization of arenes and heteroareneshas largely been supplanted by arene-arene cross coupling reaction of aryl halides with organometallic reagents.

A number of classes of homogenous and heterogenous catalytic organometallic cross-coupling reactions between small molecules have been performed in $scCO_2$.[16-18] Holmes[17] and Tumas[18] independently reported Pd-catalyzed carbon-carbon couplings by Heck, Suzuki and Sonagashira reactions in $scCO_2$ using fluorinated phosphine ligands to

impart solubility of the transition metal catalyst in the reaction medium. Bhanage and coworkers later described a Heck reaction in an $scCO_2$ /watersystem using a water soluble catalyst.[19] More recently, Early *et. al.* successfully performed Suzuki and Heck couplings in $scCO_2$ using $Pd(OAc)_2$ and $P(t\text{-}Bu)_3$.[20] The success of these transition metal catalyzed coupling reactions for the synthesis of small molecules motivated our efforts to explore the preparation of PPEs in $scCO_2$, and thereby expand the utility of $scCO_2$ to the preparation of macromolecules by organometallic cross coupling polymerizations. Preparation of high molecular weight polymers by step-growth polycondensations has a stringent requirement that the coupling take place with very high efficiency. Herein we report the use of $scCO_2$ as a solvent to prepare a poly(1,4-phenylene ethynylene) in an operationally simple procedure which avoids these use of large quantities of amines.

## 7.2. EXPERIMENTAL

### 7.2.1. Synthesis of poly(1,4-dinonyloxyphenylene ethynylene)s.

The diiodo monomer **VII-1** and dialkyne monomer **VII-2** were synthesized by previously described methods.[8] A mixture of **VII-1** (727.0 mg, 1.18 mmol) and **VII-2** (500 mg, 1.22 mmol), $Pd(PPh_3)_4$ (41.4 mg, 0.06 mmol) and CuI (13.6 mg, 0.07 mmol) was degassed and placed in a 250 mL stainless steel autoclave (Parr Instrument Co., IL, USA, Model 4576; Figure 7.2) under a stream of nitrogen. The autoclave was equipped with a jacket for circulating water for heating or cooling. Freshly distilled diisopropylamine (Table 1) was added to the mixture and the reactor was pressurized with $CO_2$ to 1500 psi and heated to 60 $^oC$ for 24 h. $CO_2$ was removed by depressurization of the system and the resulting residue was dissolved in $CHCl_3$ (25 mL). The solution

was poured into methanol to precipitate the polymer. The solid was collected by filtration and subjected to sequential extractions in a Soxhlet extractor with MeOH, acetone and hexanes, followed by $CHCl_3$. The solvent was removed from the $CHCl_3$ fraction and the residue (710 mg, 70% yield) was characterized by NMR and GPC.

## 7.3. RESULTS AND DISCUSSIONS

Polymerization of diiodide **VII-1** and dialkyne **VII-2** was achieved by Pd/Cu-catalyzed Sonogashira coupling in $scCO_2$, Figure 7.3. The stoichiometry of the cross couping of an aryl iodide and an alkyne requires one mole equivalent of a base (with respect to the alkyne). However, conventional polymerizations of diiodides and diethynylenes to afford PPEs make use of a large excess of amine (70 to 100 mole excess relative to the amount of monomer(s)), whereby they serve as the solvent, or as a co-solvent with a relatively non-polar aprotic solvent such as THF, toluene or chloroform. Attempts to synthesize PPE in $scCO_2$ using one and three mole equivalent of diisopropylamine led to no polymerization. This may be caused by consumption of the amine in an equilibrium reaction with $CO_2$, rendering it unavailable as a base to promote the reaction.

Increasing the amount of amine to just 7 mole equivalents resulted in successful polymerization. For example, polymerization of monomers **VII-1** and **VII-2** gave the 2,5-bisnonyloxy substituted PPE. The $^1H$ NMR of the polymer that was extracted into chloroform is shown in Figure 7.5. The peak at ca. 7.0 ppm represents the hydrogen atoms of the 2,5-dialkoxy-1,4-phenylene unit, while the rest of the peaks represent the. alkoxy side chains. The molecular weight of the PPE calculated by comparison of the

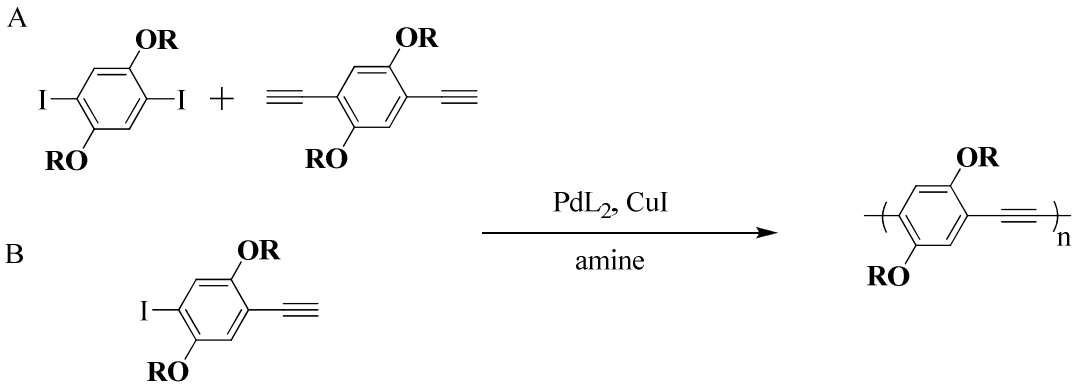


**Figure 7.1.** Preparation of poly(2,5-disubstituted-1,4-phenylene ethynylynes) by A) AA + BB type condensation B) AB type of condensation.

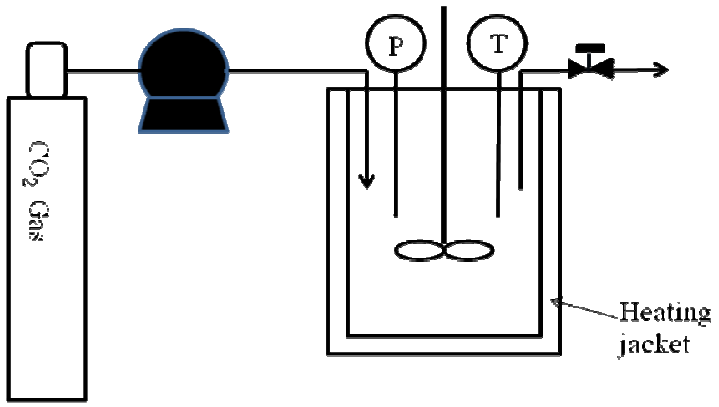


**Figure 7.2.** Schematic diagram of the experimental set up.

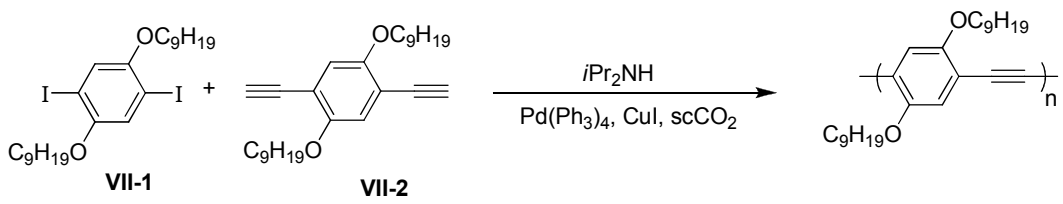


**Figure 7.3.** Preparation of bisnonyloxy-PPE.

integral for the peak in the $^1$H NMR spectrum at δ7.34 (arising from the end groups) and at δ7.0 (from hydrogen atoms of the internal repeat units) was 6.2 kD, while the molecular weight estimated by GPC (THF, polystyrene calibration standards) was 13.6 kD. For rigid polymers, the molecular weight measured by GPC, which uses coil-type polystyrene as a standard, is generally 1.5 to 2 times higher than the molecular weight measured by NMR. In order to study the effect of reaction time on molecular weight we ran the polymerization for 48 h at 60 ºC and obtained PPEs with slightly higher molecular weight of 7.6 kD (by end group analysis) and 8.6 kD (by GPC) (Table 1). With a degree of polymerization of 19, the PPEs prepared by this method are sufficiently conjugated to have attained a minimum HOMO-LUMO gap (e.g., a maximum $\lambda_{max}$). While the molecular weight might be limited by precipitatation of the polymer from the reaction medium, the fact that the coupling takes place with high efficiency is undisputable: a DP of 19 corresponds to a coupling efficiency of over 94%. This efficiency is achieved even though the polymerization is performed at a very low concentration of monomers in $scCO_2$ (ca. 1 mM) relative to a typical concentration of 100 to 500 mM in conventional polymerizations.

**Table 1.** Results of the PPE polymerization with different concentration of amines and at different reaction times.

| Sample | Amine (mole equivalent) | Time (hours) | Result |
|---|---|---|---|
| 1 | 1 mol | 24 | no polymerization |
| 2 | 3 mol | 24 | no polymerization |
| 3 | 7 mol | 24 | $M_n$=6.2 kD |
| 4 | 7 mol | 48 | $M_n$=7.6 kD |

## 7.4. CONCLUSIONS

We have demonstrated the first synthesis of poly(1,4-substituted phenylene ethynylene) by Sonagashira cross-coupling of diiodide and diethynyl monomers in $scCO_2$ as the reaction medium. The polymerization required significantly lower amounts of added amine than in conventional polymerization. The polymers were prepared in good yields and with moderate molecular weights. This operationally simple procedure, using an environmentally benign solvent and only a small amount of amine, provides significant potential benefits in terms of cost and minimization of ecological impact.

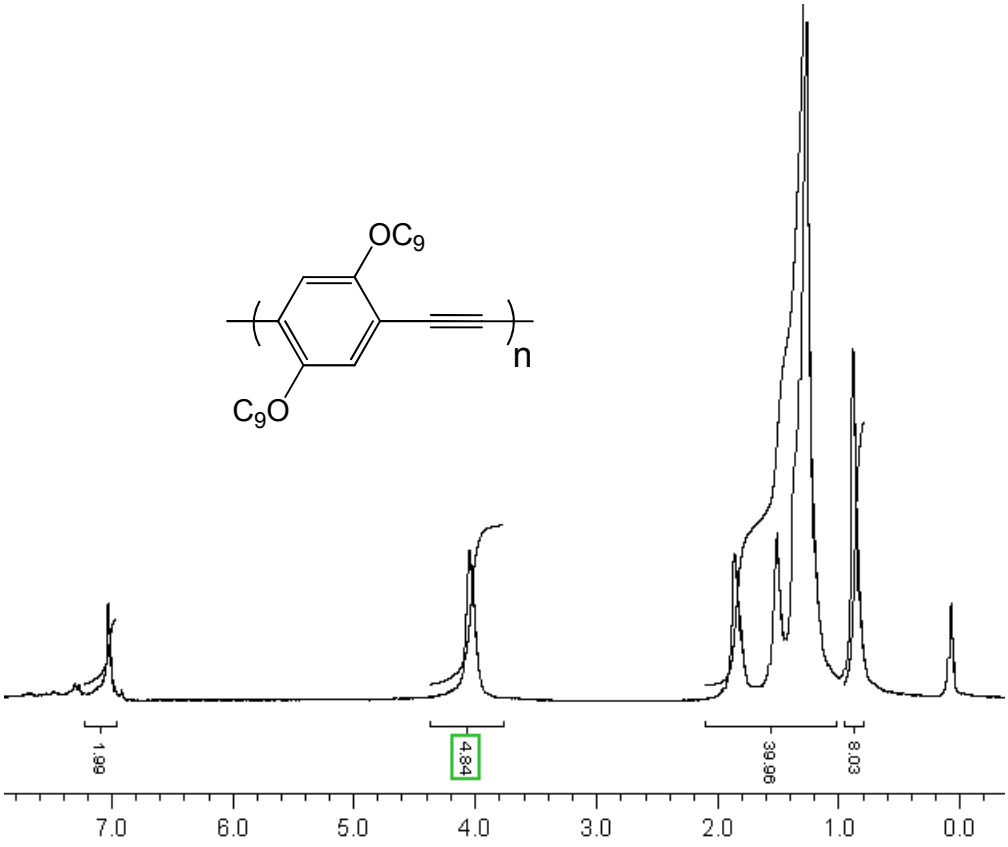


**Figure 7.5.** $^{1}$H NMR of bisnonyloxy PPE

## 7.5. REFERENCES


(1) Skotheim, T. A. *Handbook of Conducting Polymers* New York, 1986.

(2) McQuade, D. T.; Pullen, A. E.; Swager, T. M. *Chem. Rev.* **2000**, *100*, 2537.

(3) Xiao, X. Y.; Nagahara, L. A.; Rawlett, A. M.; Tao, N. J. *J. Am. Chem. Soc.* **2005**, *127*, 9235.

(4) Pang, Y.; Li, J.; Hu, B.; Karasz, F. E. *Macromolecules* **1998**, *31*, 6730.

(5) Mwaura, J. K.; Pinto, M. R.; Witker, D.; Ananthakrishnan, N.; Schanze, K. S.; Reynolds, J. R. *Langmuir* **2005**, *21*, 10119.

(6) Weder, C.; Sarwa, C.; Bastiaansen, C.; Smith, P. *Adv. Mater.* **1997**, *9*, 1035.

(7) Bunz, U. H. F. *Chem. Rev.* **2000**, *100*, 1605.

(8) Nambiar, R. R.; Brizius, G. L.; Collard, D. M. *Adv. Mater.* **2007**, *19*, 1234.

(9) Jessop, P. G.; Ikariya, T.; Noyori, R. *Chem. Rev.* **1999**, *99*, 475.

(10) Oakes, R. S.; Clifford, A. A.; Rayner, C. M. *Journal of the Chemical Society-Perkin Transactions 1* **2001**, 917.

(11) Kerton, F. M.; Lawless, G. A.; Armes, S. P. *J. Mater. Chem.* **1997**, *7*, 1965.

(12) Abbett, K. F.; Teja, A. S.; Kowalik, J.; Tolbert, L. *Macromolecules* **2003**, *36*, 3015.

(13) Du, J. M.; Zhang, J. L.; Han, B. X.; Liu, Z. M.; Wan, M. X. *Synth. Met.* **2005**, *155*, 523.

(14) Ganapathy, H. S.; Hwang, H. S.; Lim, K. T. *Ind. Eng. Chem. Res.* **2006**, *45*, 3406.

(15) Li, L.; Counts, K. E.; Kurosawa, S.; Teja, A. S.; Collard, D. M. *Adv. Mater.* **2004**, *16*, 180.

(16) Hitzler, M. G.; Poliakoff, M. *Chem. Commun.* **1997**, 1667.

(17) Carroll, M. A.; Holmes, A. B. *Chem. Commun.* **1998**, 1395.

(18) Morita, D. K.; Pesiri, D. R.; David, S. A.; Glaze, W. H.; Tumas, W. *Chem. Commun.* **1998**, 1397.

(19) Bhanage B. M., I. Y., Shirai M., Arai M. In *Tetrahedron Lett.* 1999; Vol. 40, p 6247.

(20) Early, T. R.; Gordon, R. S.; Carroll, M. A.; Holmes, A. B.; Shute, R. E.; McConvey, I. F. *Chem. Commun.* **2001**, 1966.

# APPENDIX A

## SPECTROSCOPIC CHARACTERIZATION OF SYNTHETIC PRODUCTS

$^{1}$H NMR spectra were recorded at room temperature using a Varian Mercury spectrometer (300 MHz), and the $^{13}$C NMR spectra were obtained at 100 MHz using a Bruker AMX spectrometer. IR spectra were recorded on a Bruker Vector 22 spectrometer.

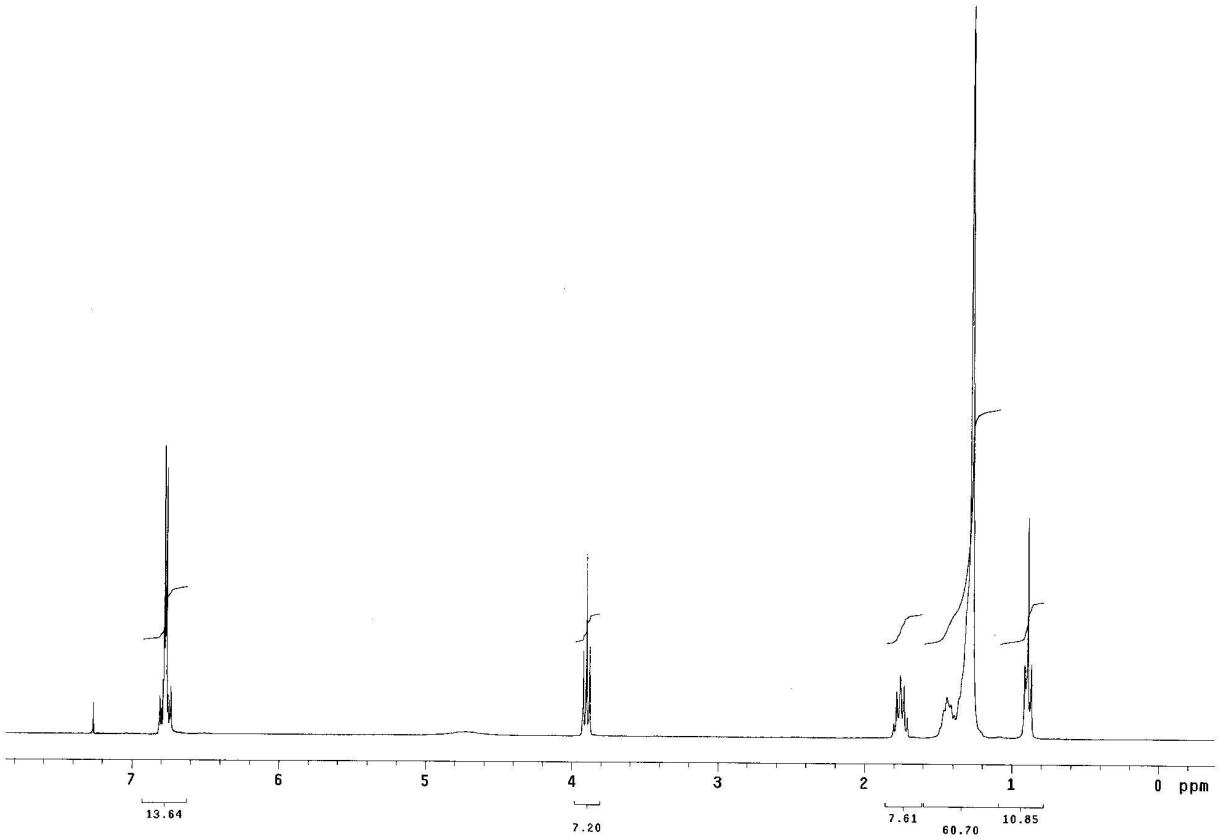


**Figure A.1.** $^{1}$H NMR of 4-Dodecyloxyphenol, **II-1b**.

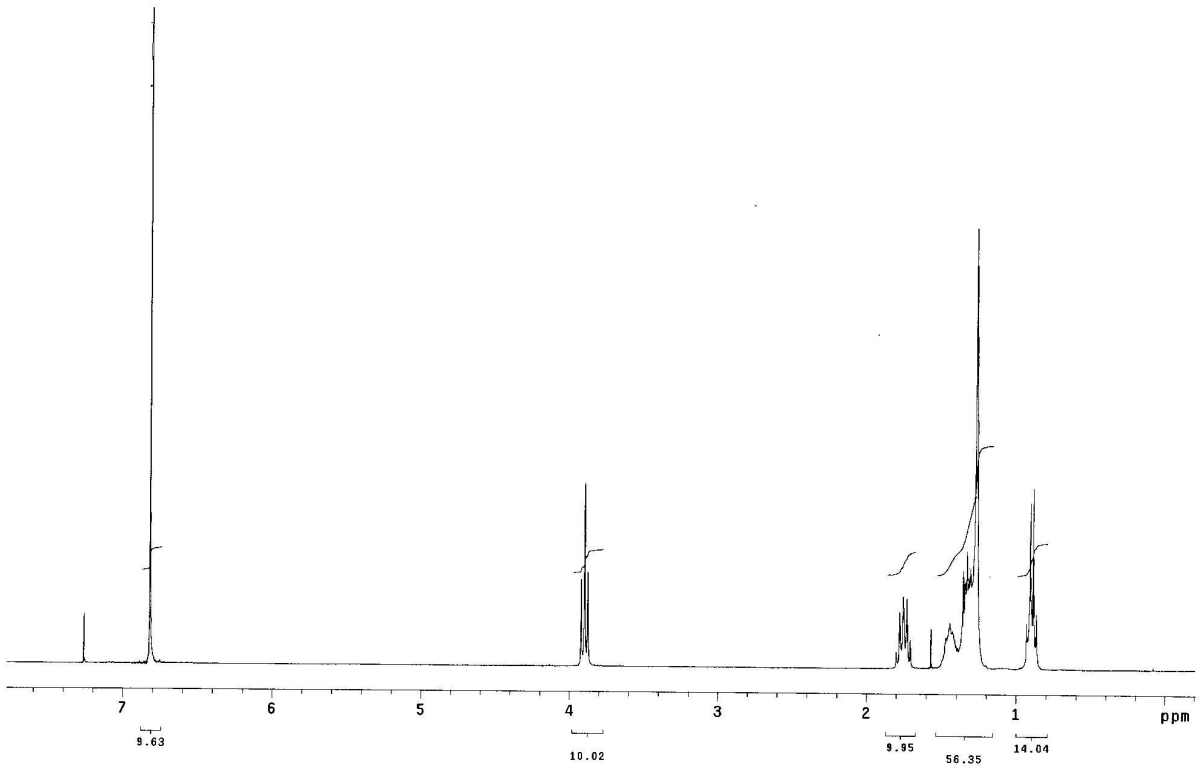


**Figure A.2.** $^{1}$H NMR of 1-Dodecyloxy-4-hexyloxybenzene, **II-2b.**

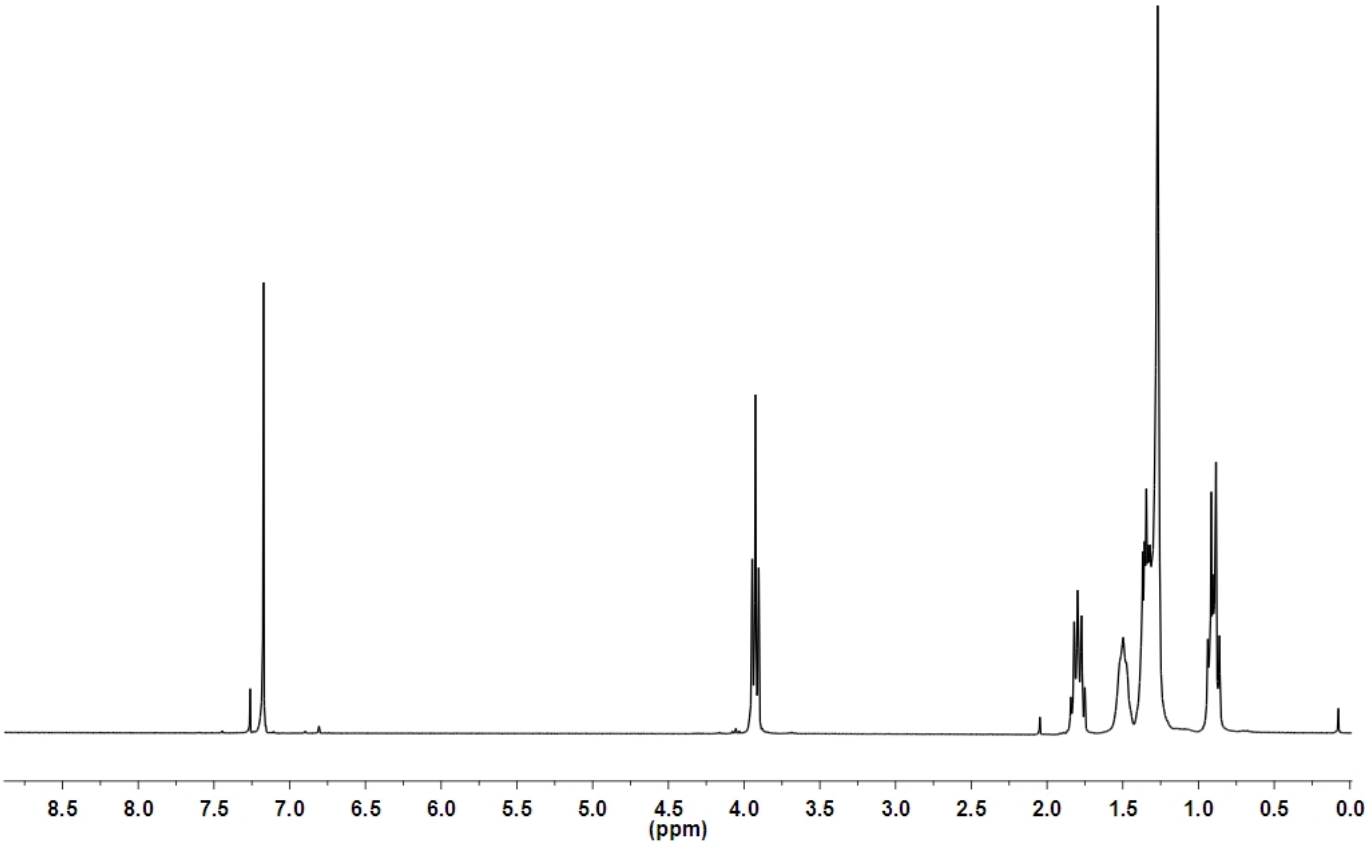


**Figure A.3.** $^{1}$H NMR of 1-Dodecyloxy-4-hexyloxy-2,5-diiodobenzene, **II-3b**

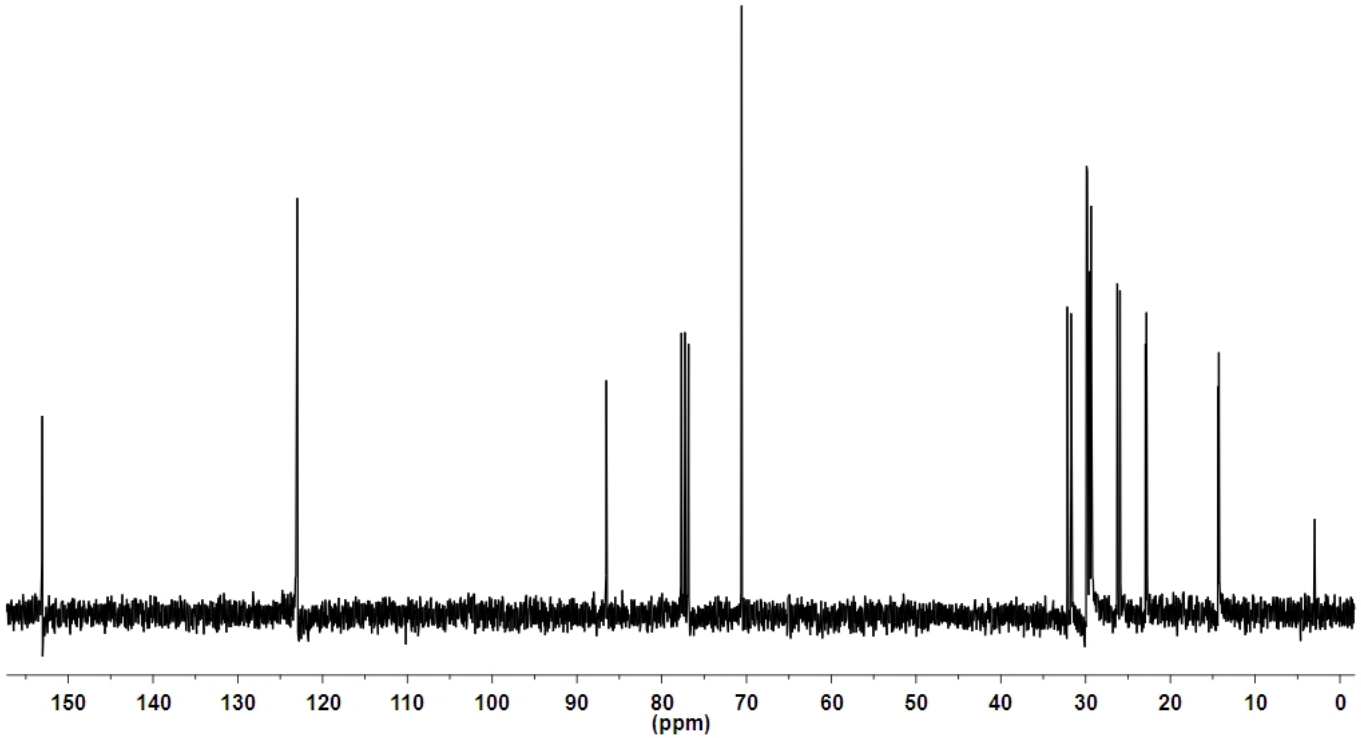


**Figure A.4.** $^{13}$C NMR of 1-Dodecyloxy-4-hexyloxy-2,5-diiodobenzene, **II-3b.**

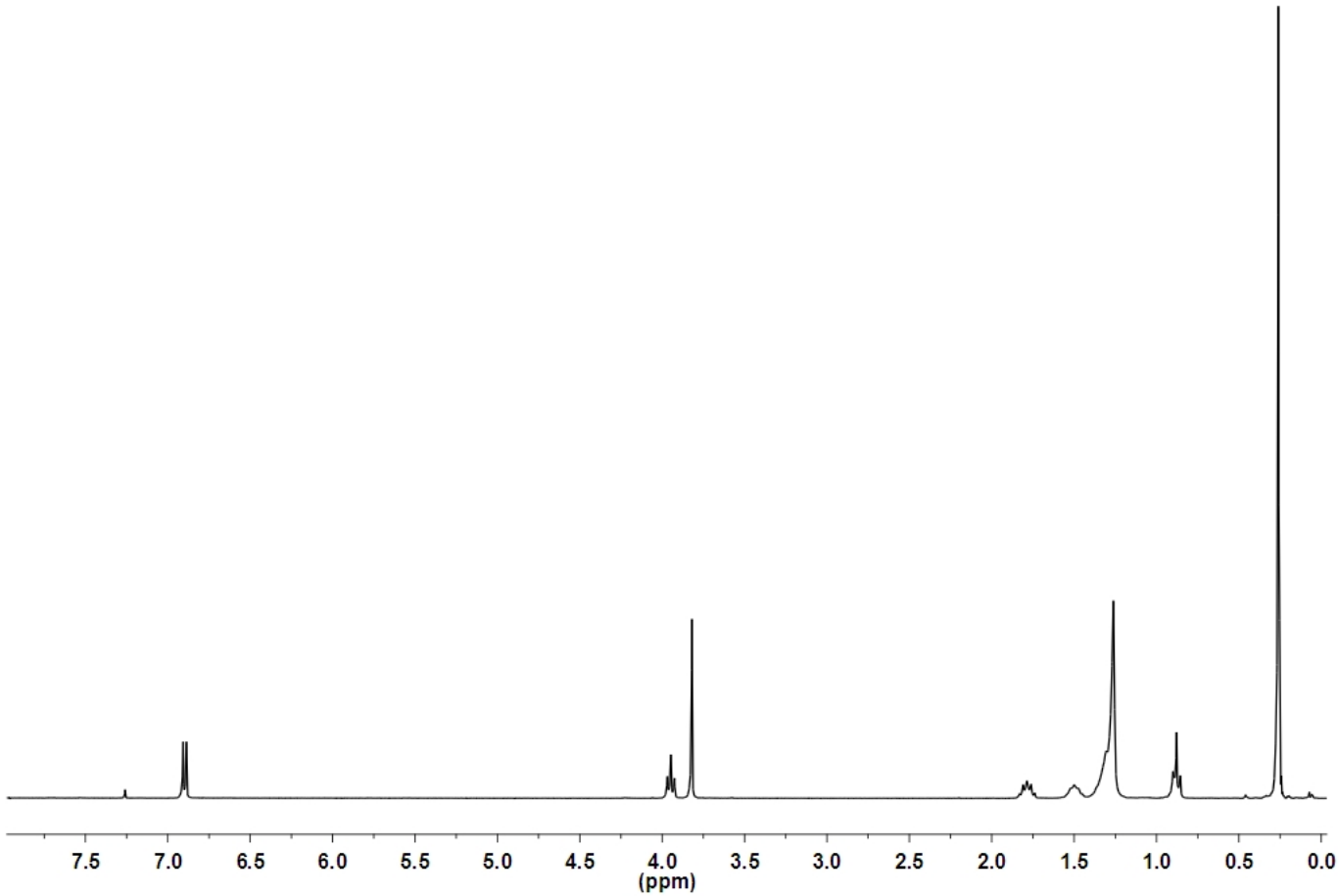


**Figure A.5.** $^{1}$H NMR of [(2-Dodecyloxy-5-methoxy-1,4-phenylene)di-2,1- ethynediyl]bis[trimethylsilane], **II-4a**

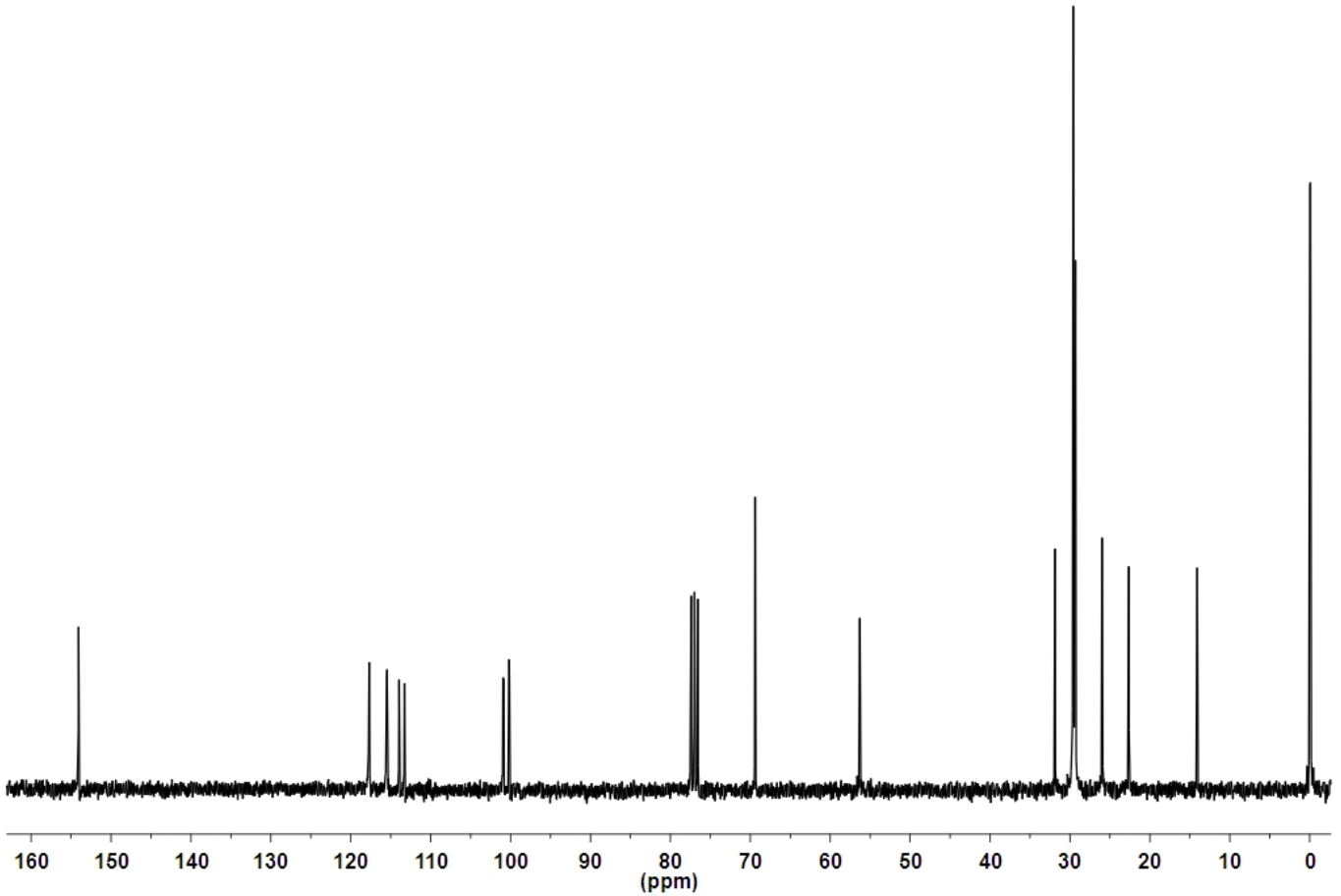


**Figure A.6.** $^{13}$C NMR of [(2-Dodecyloxy-5-methoxy-1,4-phenylene)di-2,1- ethynediyl]bis[trimethylsilane], **II-4a**

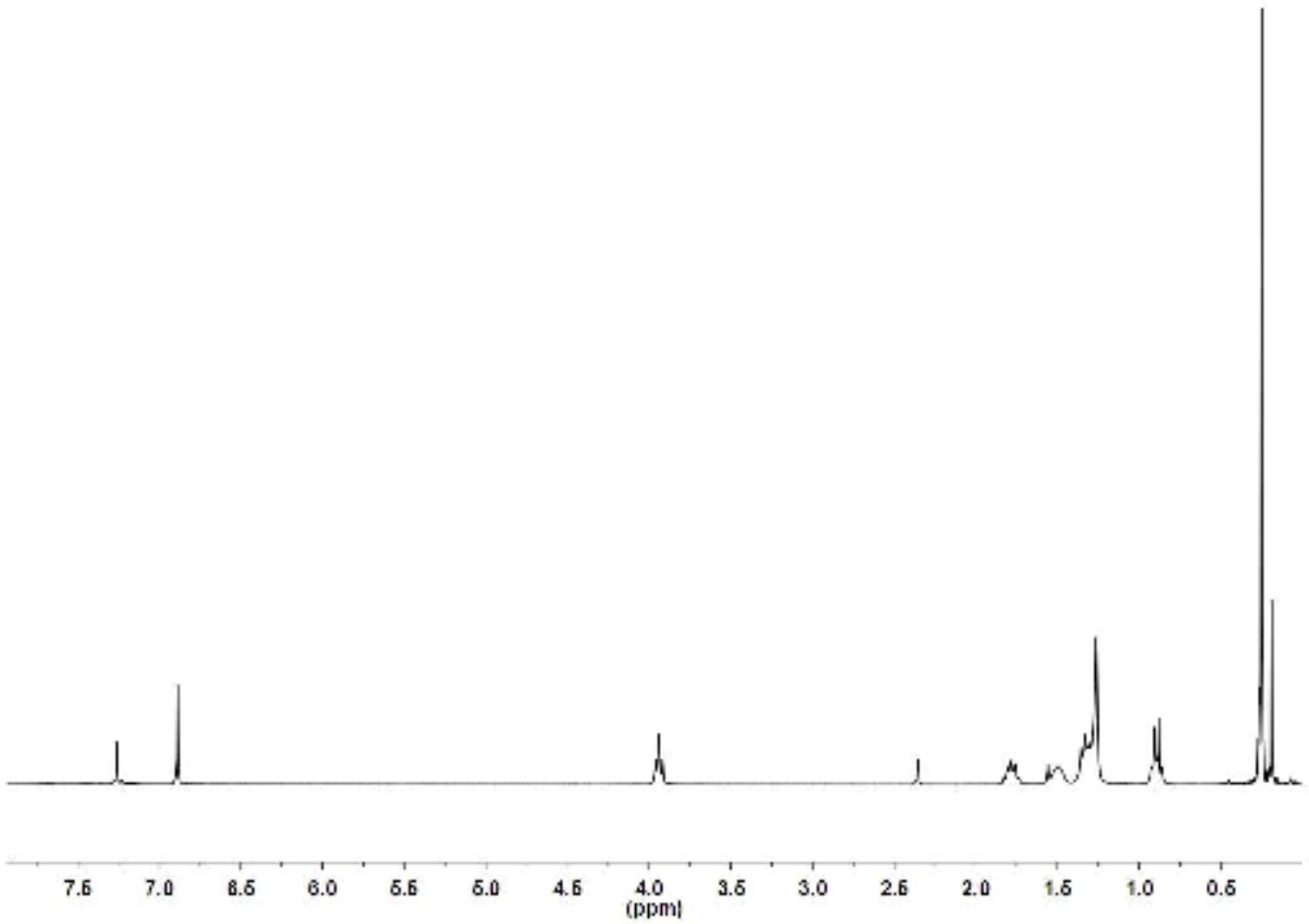


**Figure A.7.** $^{1}$H NMR of [(2-Dodecyloxy-5-hexyloxy-1,4-phenylene)di-2,1-ethynediyl]bis[trimethylsilane], **II-4b**

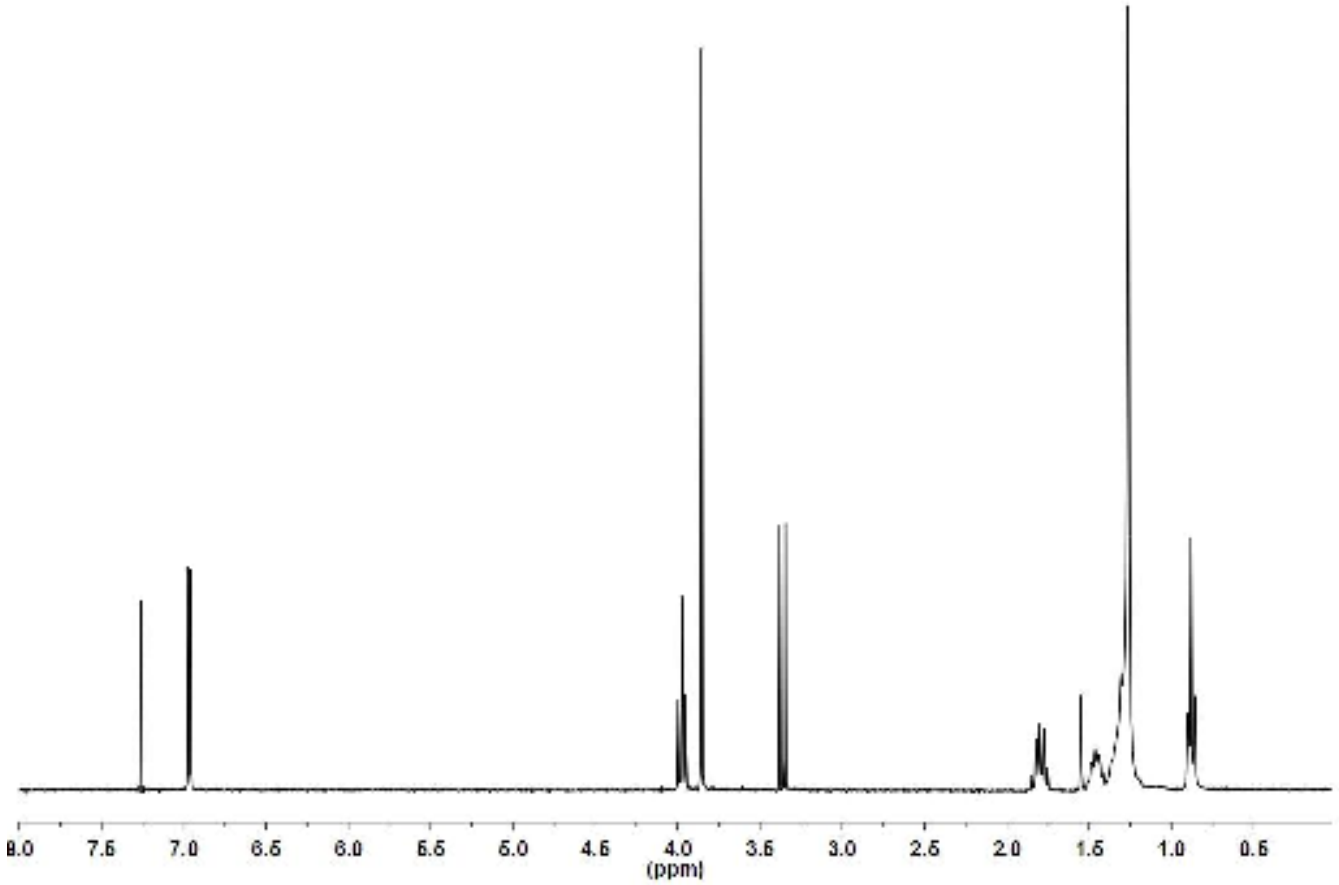


**Figure A.8.** $^{1}$H NMR of 4-Dodecyloxy-2,5-diethynylanisole, **II-5a.**

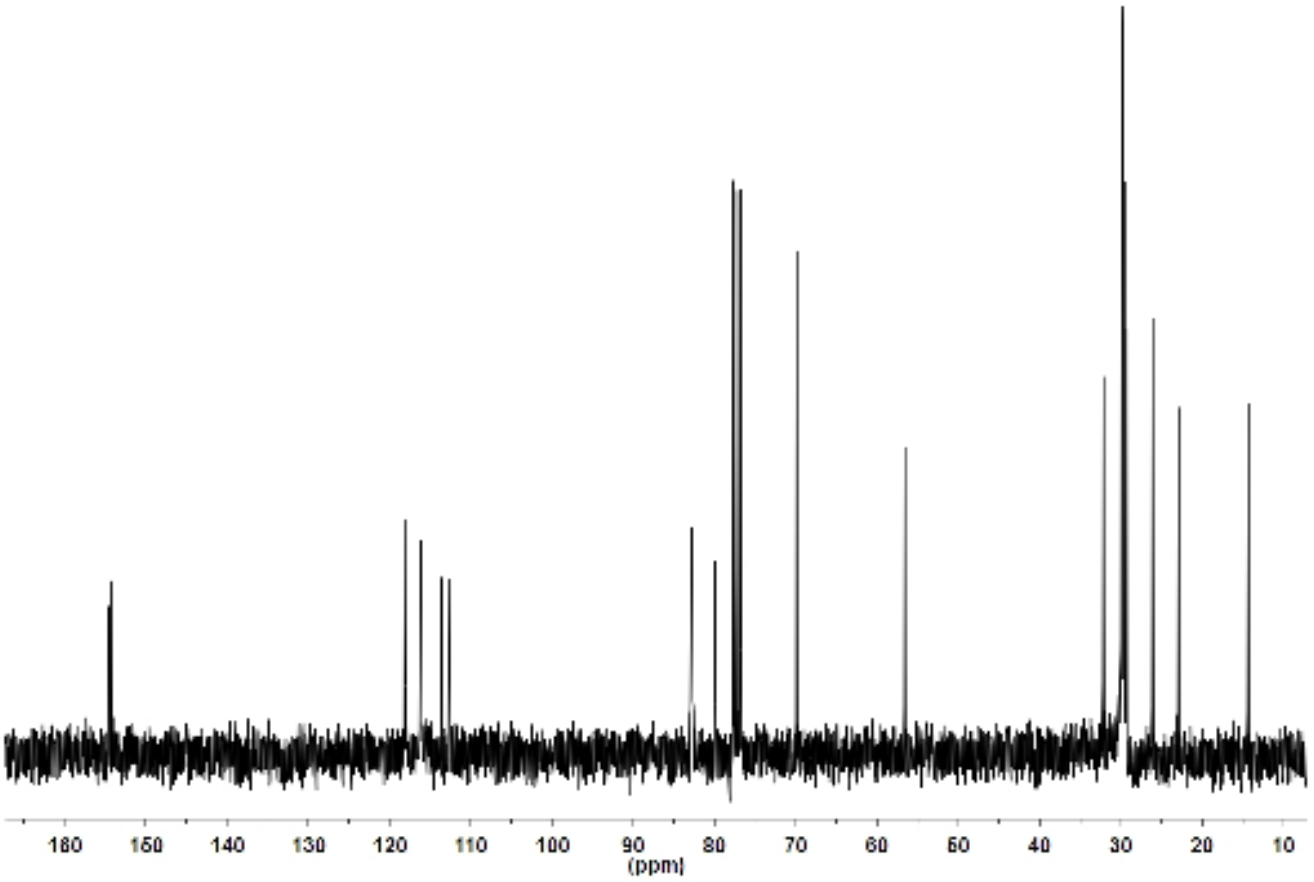


**Figure A.9.** $^{13}C$ NMR of 4-Dodecyloxy-2,5-diethynylanisole, **II-5a.**

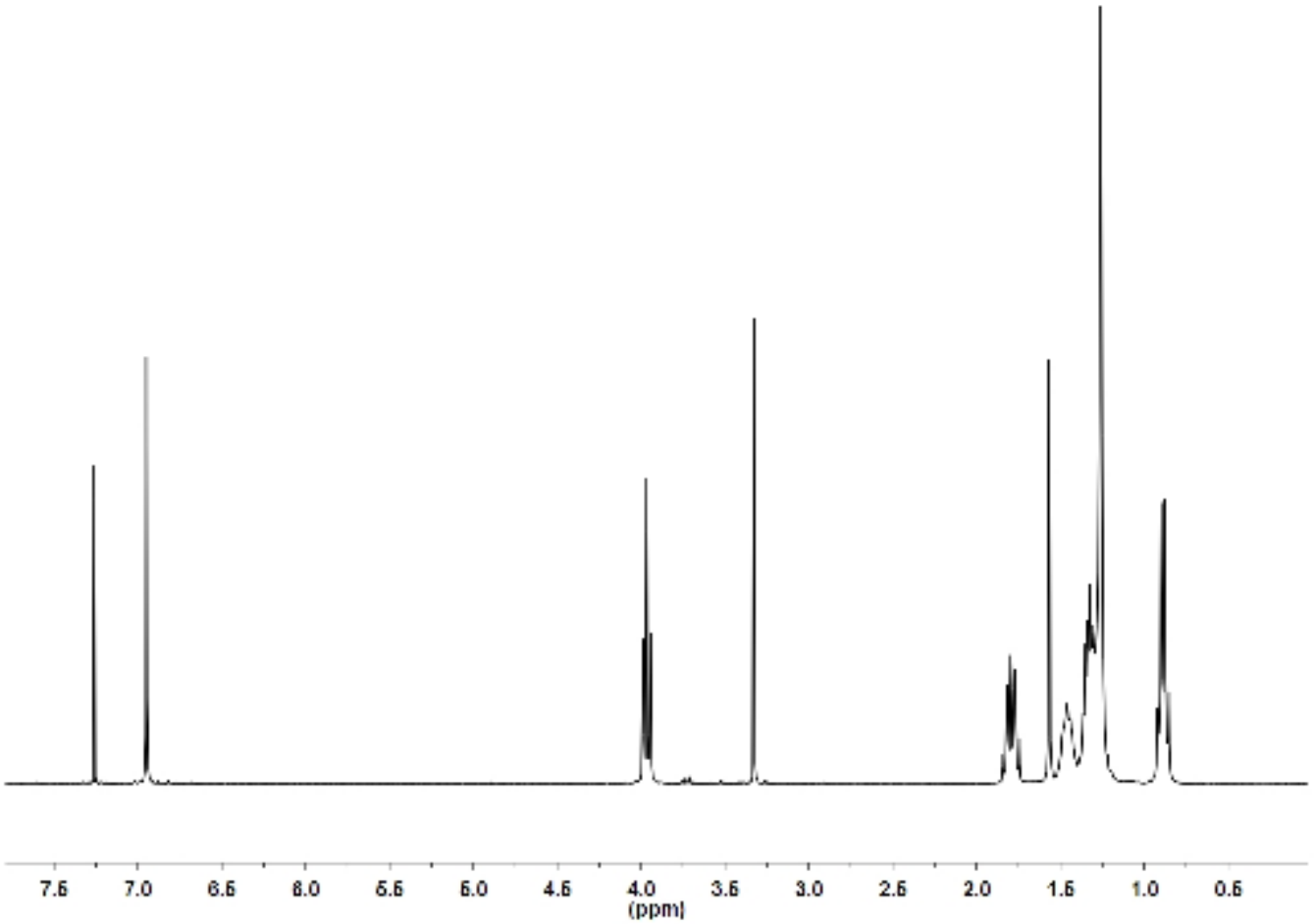


**Figure A.10.** $^{1}$H NMR of 1-Dodecyloxy-2,5-diethynyl-4-hexyloxybenzene, **II-5b.**

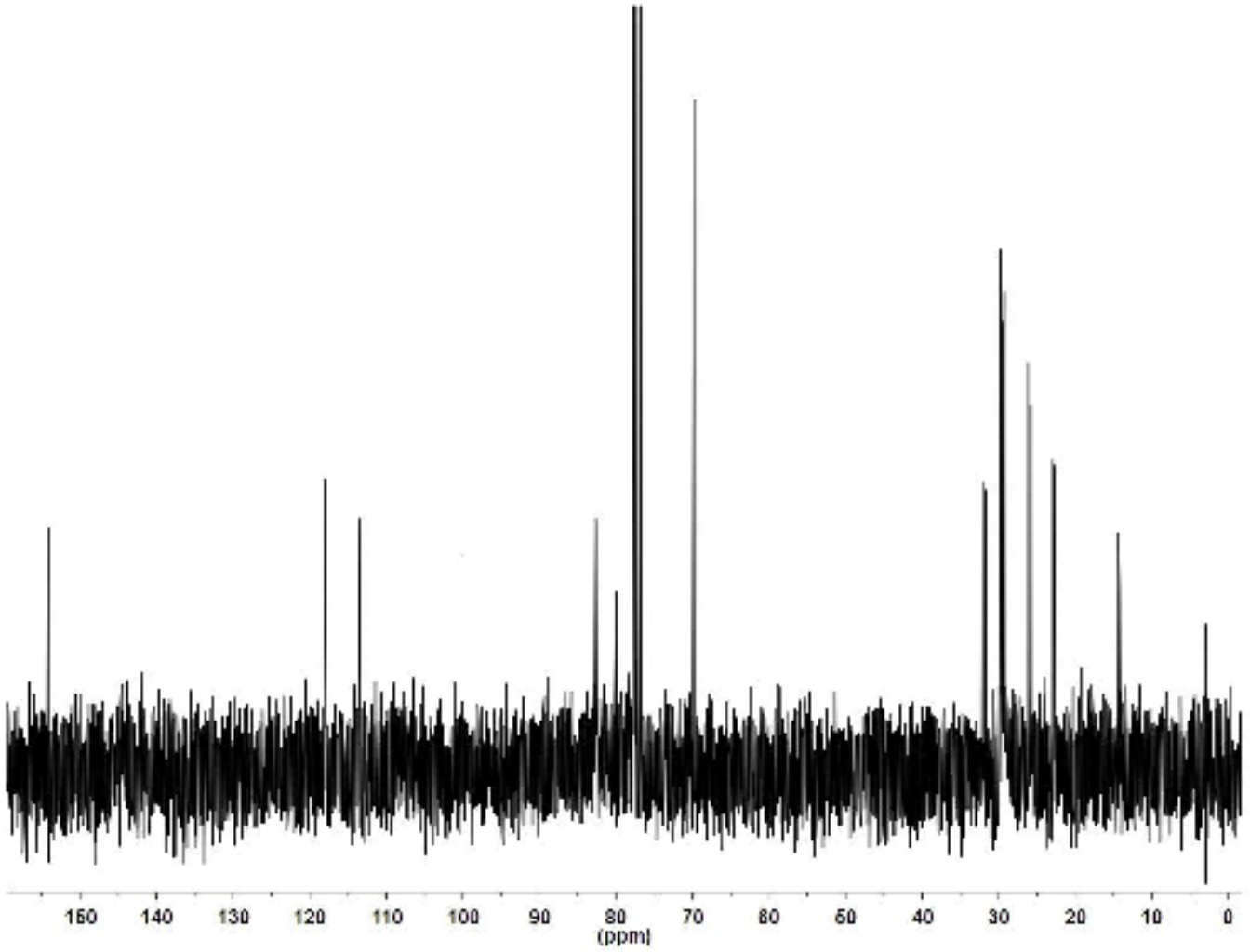


**Figure A.11.** $^{13}C$ NMR of 1-Dodecyloxy-2,5-diethynyl-4-hexyloxybenzene, **II-5b.**

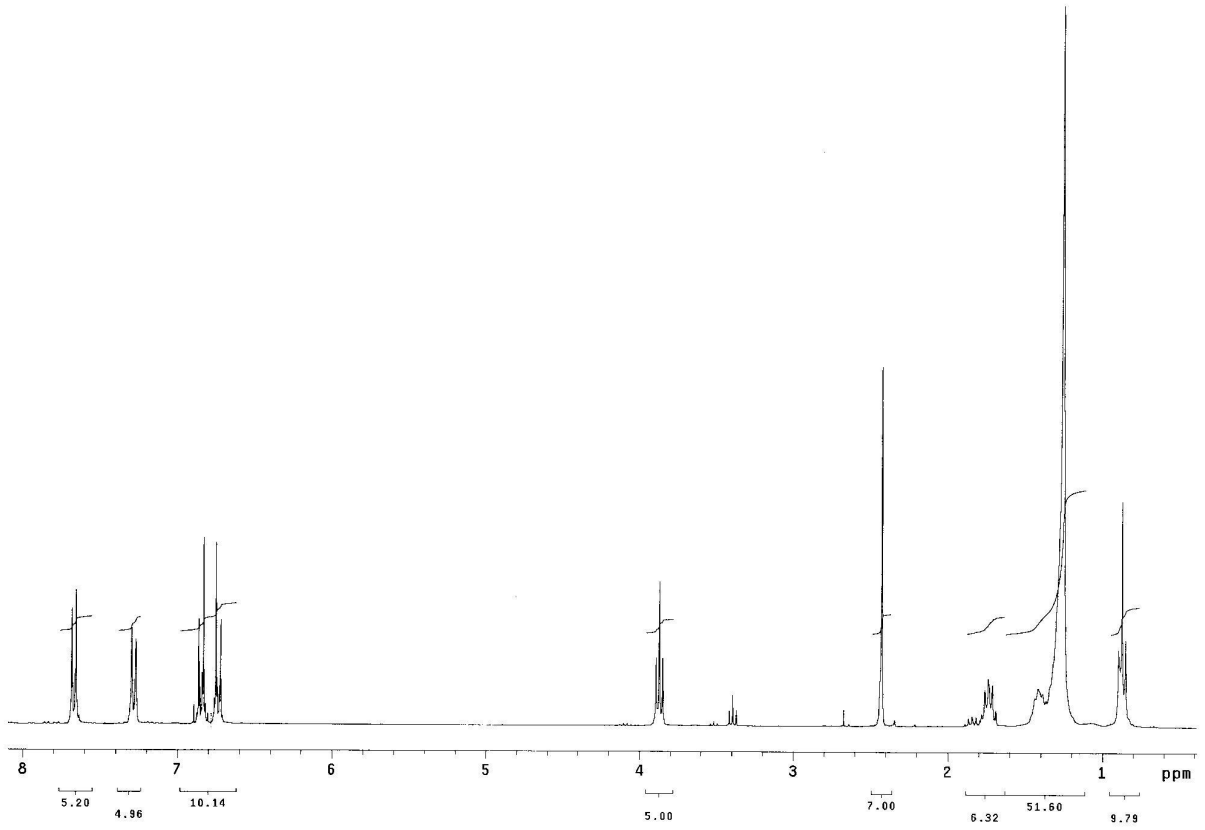


**Figure A.12.** $^{1}$H NMR of 4-Dodecyloxyphenyl *p*-toluenesulfonate**, II-6b.**

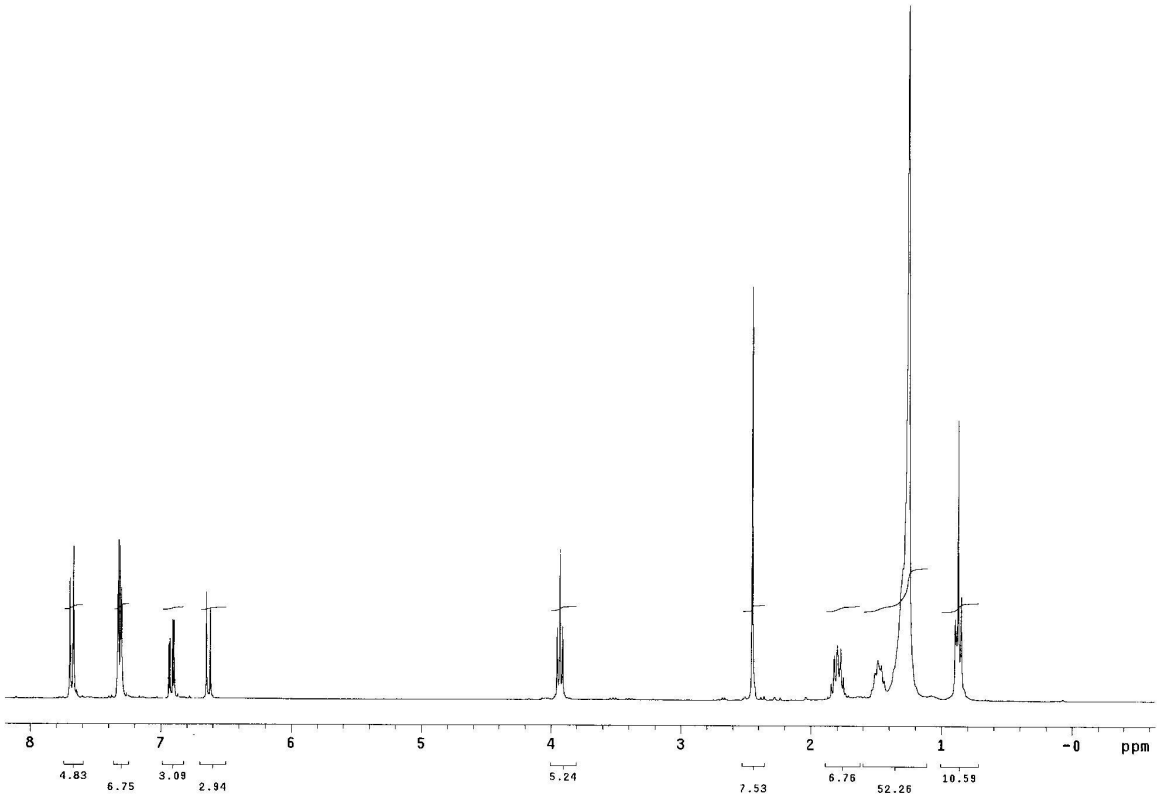


**Figure A.13.** $^{1}$H NMR of 4-Dodecyloxy-3-iodophenyl *p*-toluenesulfonate, **II-7b.**

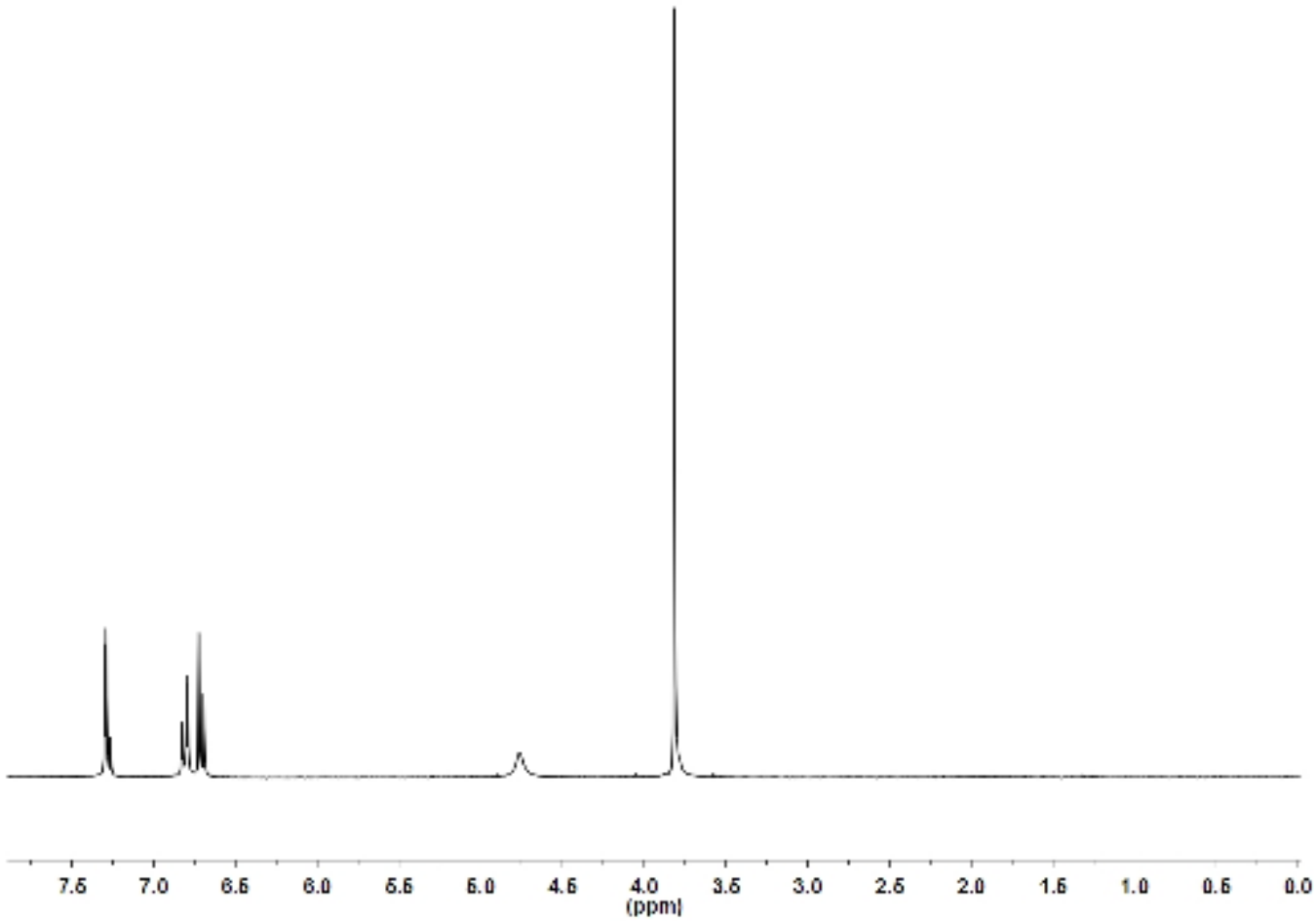


**Figure A.14.** $^{1}$H NMR of 3-Iodo-4-methoxyphenol, **II-8a.**

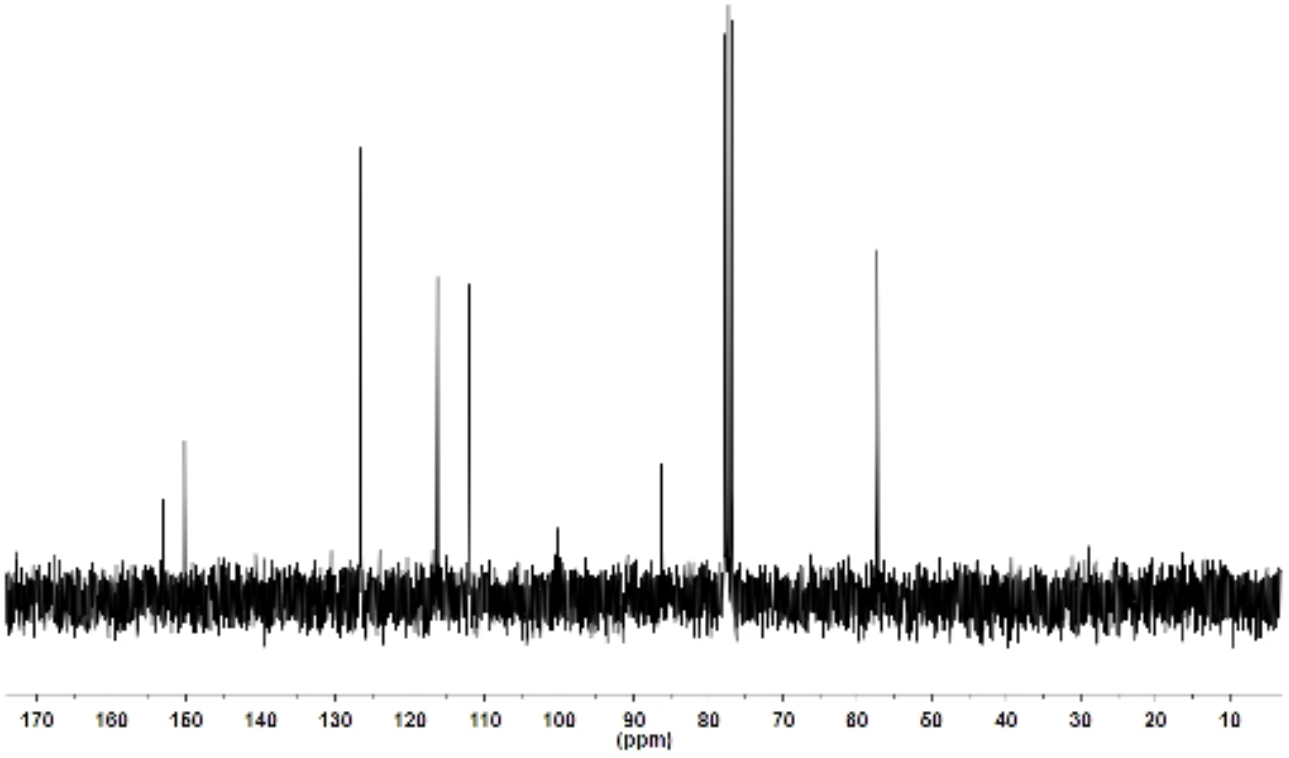


**Figure A.15.** $^{13}C$ NMR of 3-Iodo-4-methoxyphenol, **II-8a.**

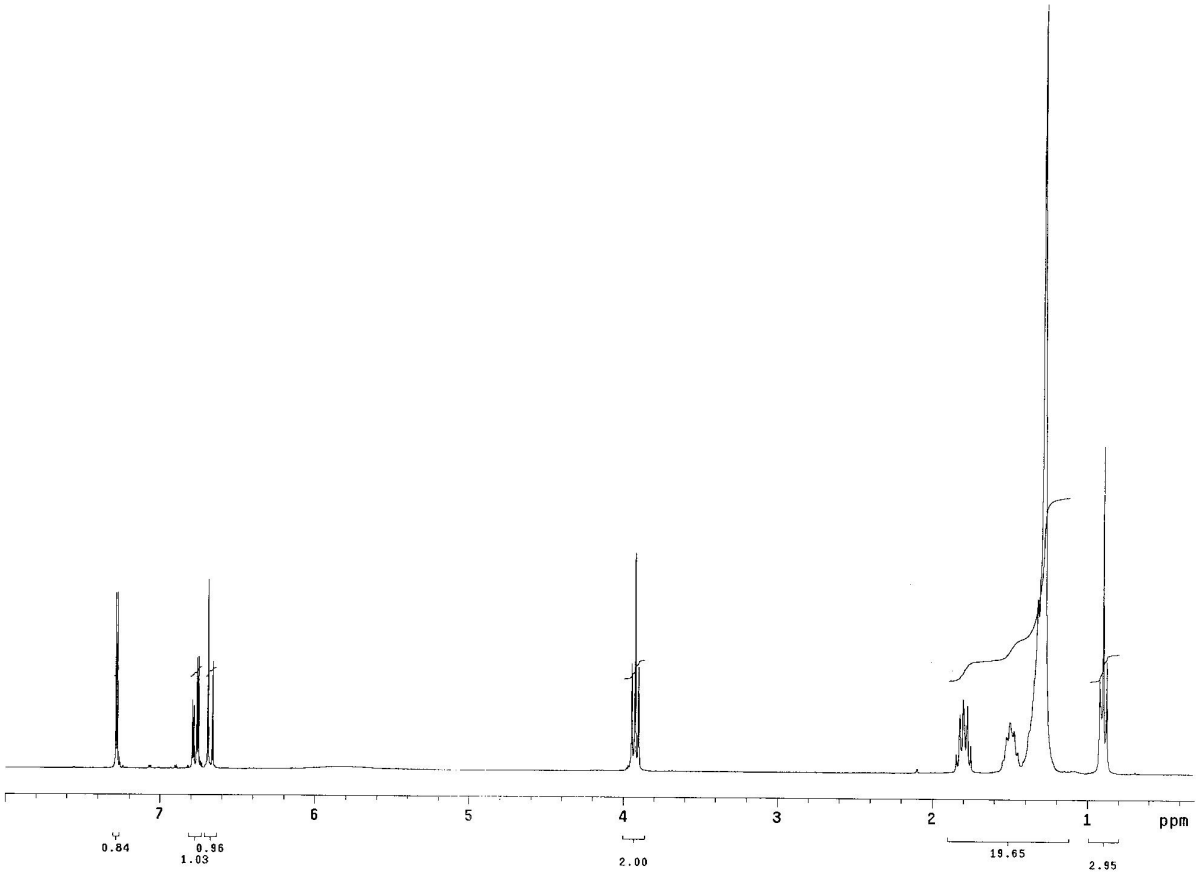


**Figure A.16.** $^{1}$H NMR of 4-Dodecyloxy-3-iodophenol, **II-8b.**

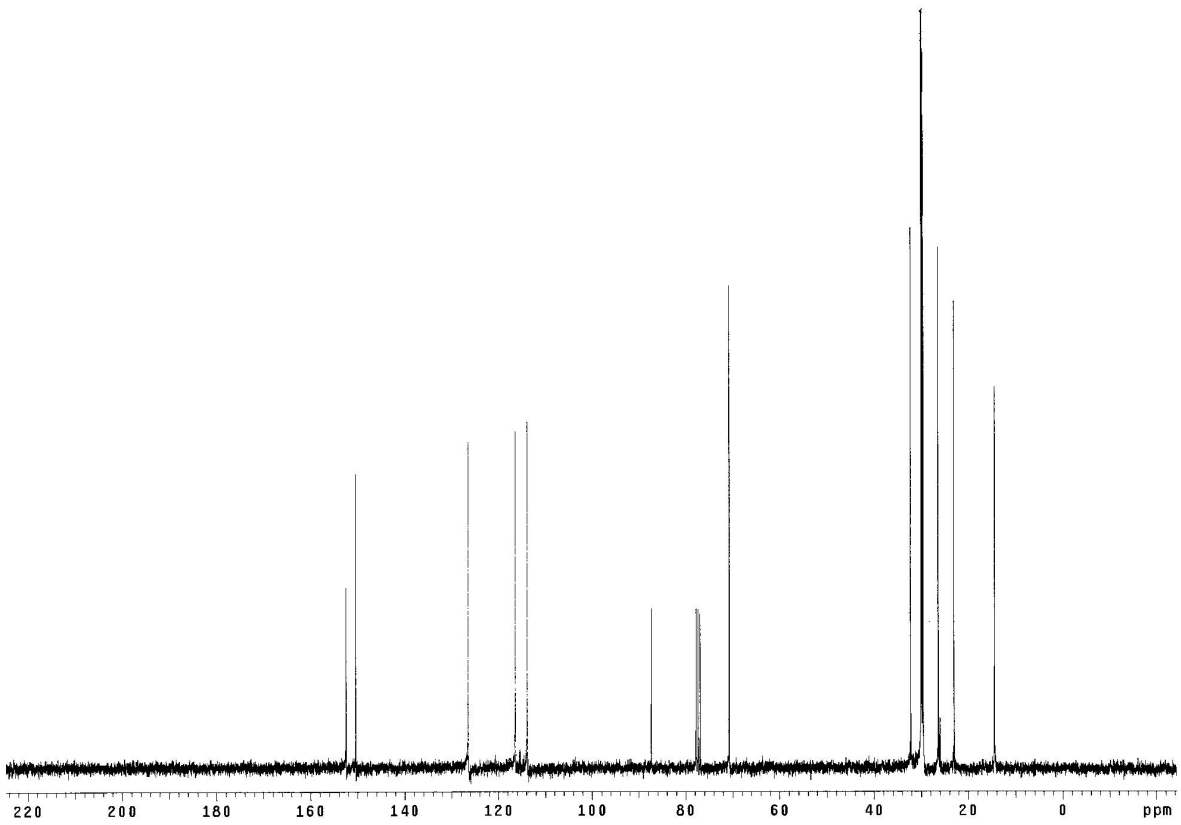


**Figure A.17.** $^{13}$C NMR of 4-Dodecyloxy-3-iodophenol, **II-8b.**

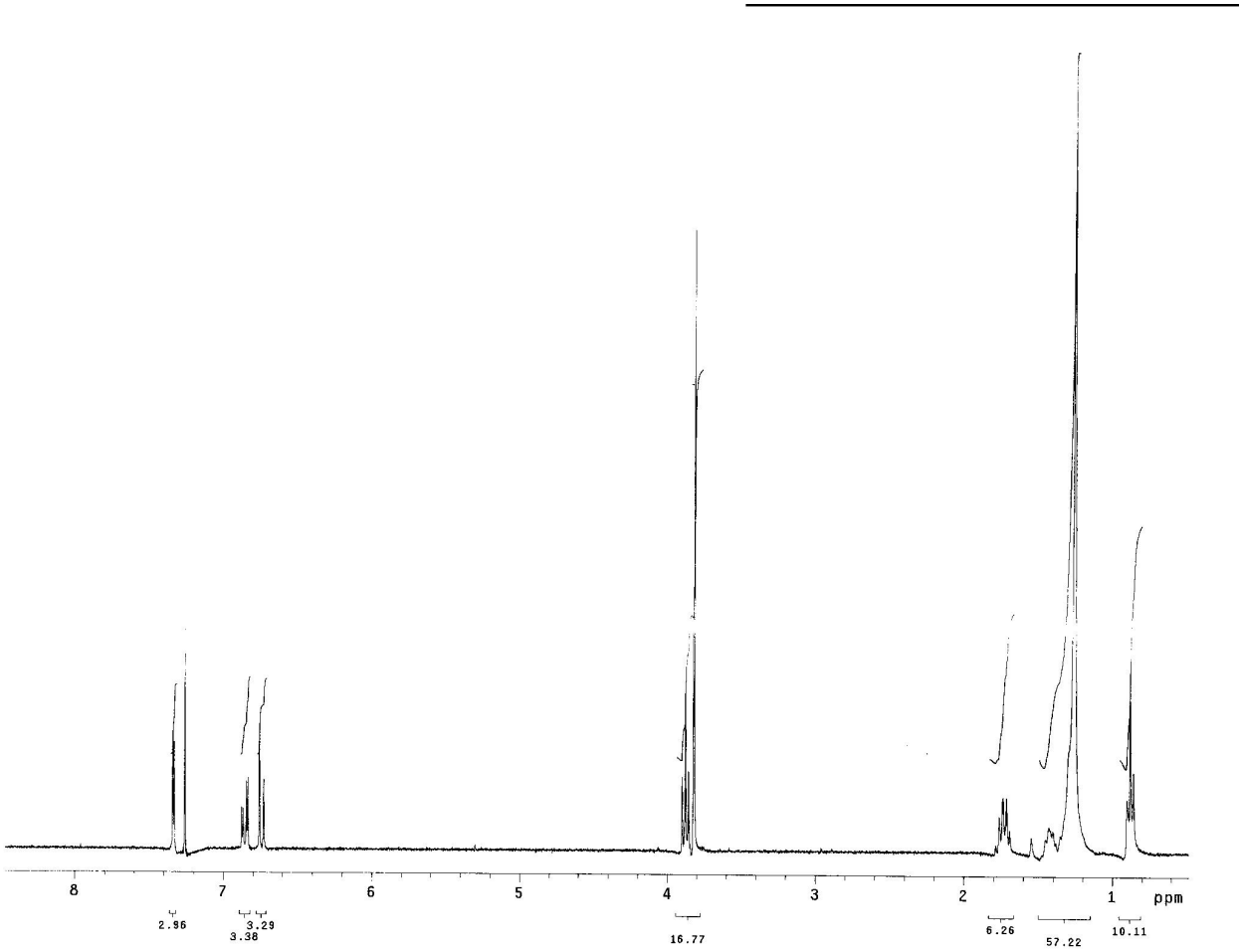


**Figure A.18.** $^{1}$H NMR of 4-Dodecyloxy-2-iodoanisole, **II-9a.**

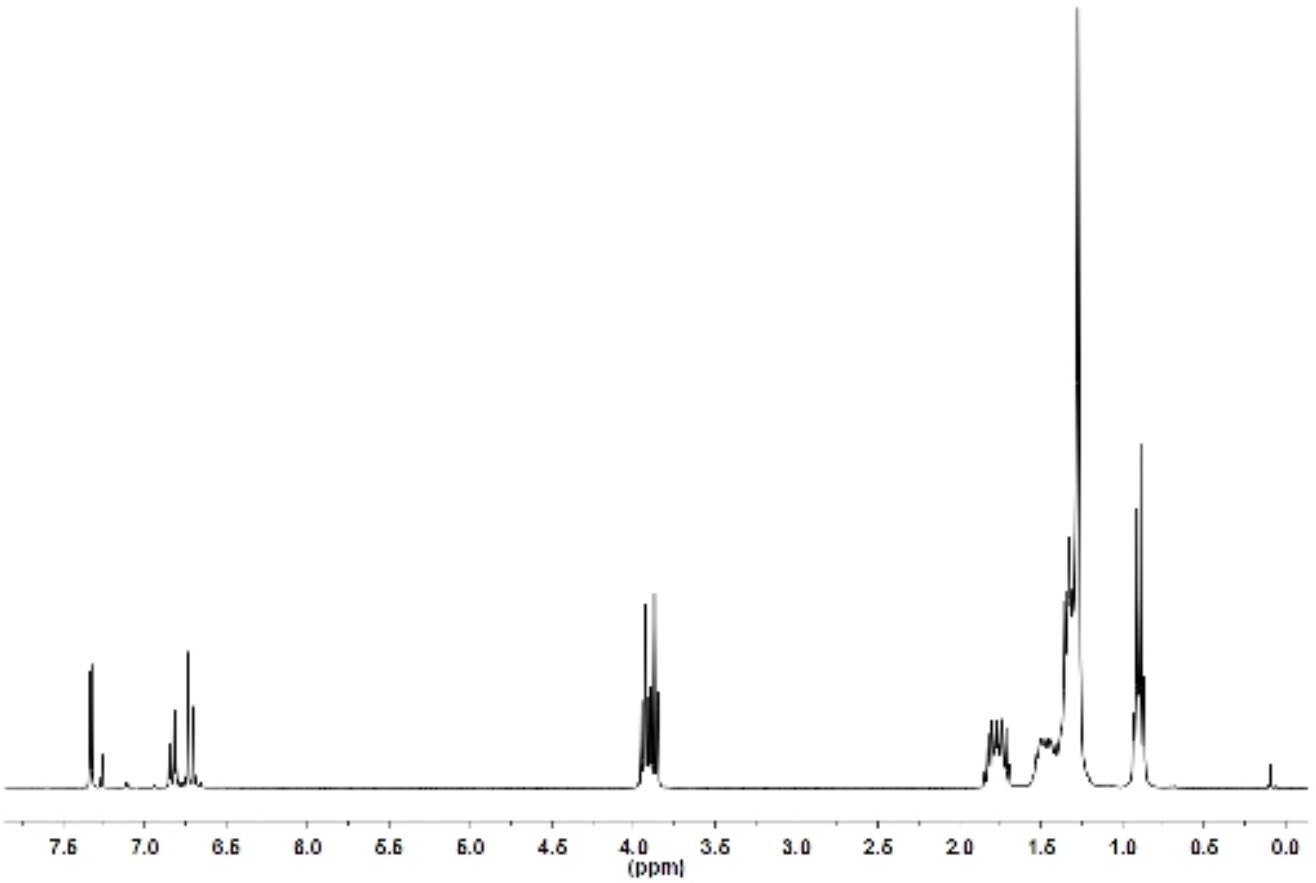


**Figure A.19.** $^{1}$H NMR of 1-Dodecyloxy-4-hexyloxy-2-iodobenzene, **II-9b.**

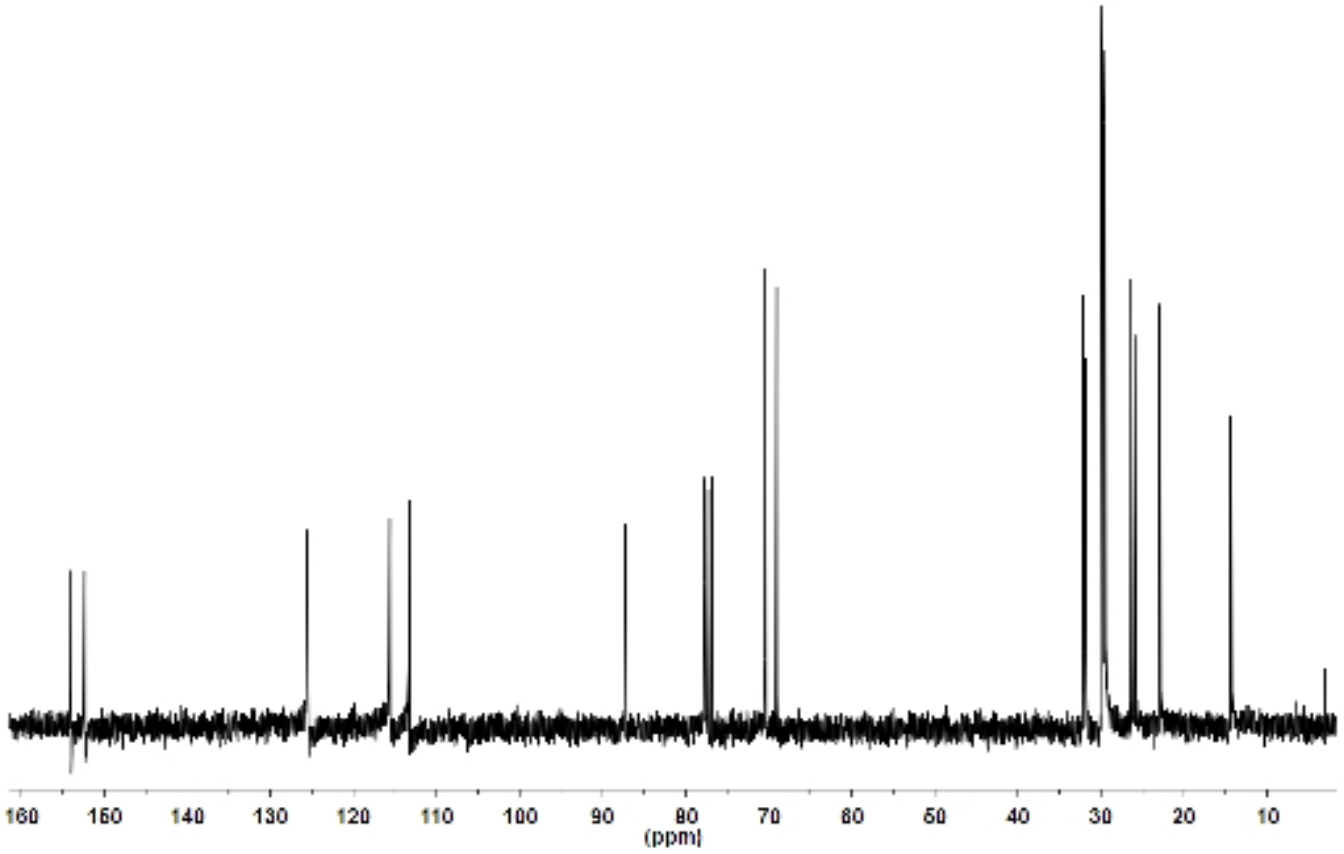


**Figure A.20.** $^{13}C$ NMR of 1-Dodecyloxy-4-hexyloxy-2-iodobenzene, **II-9b.**

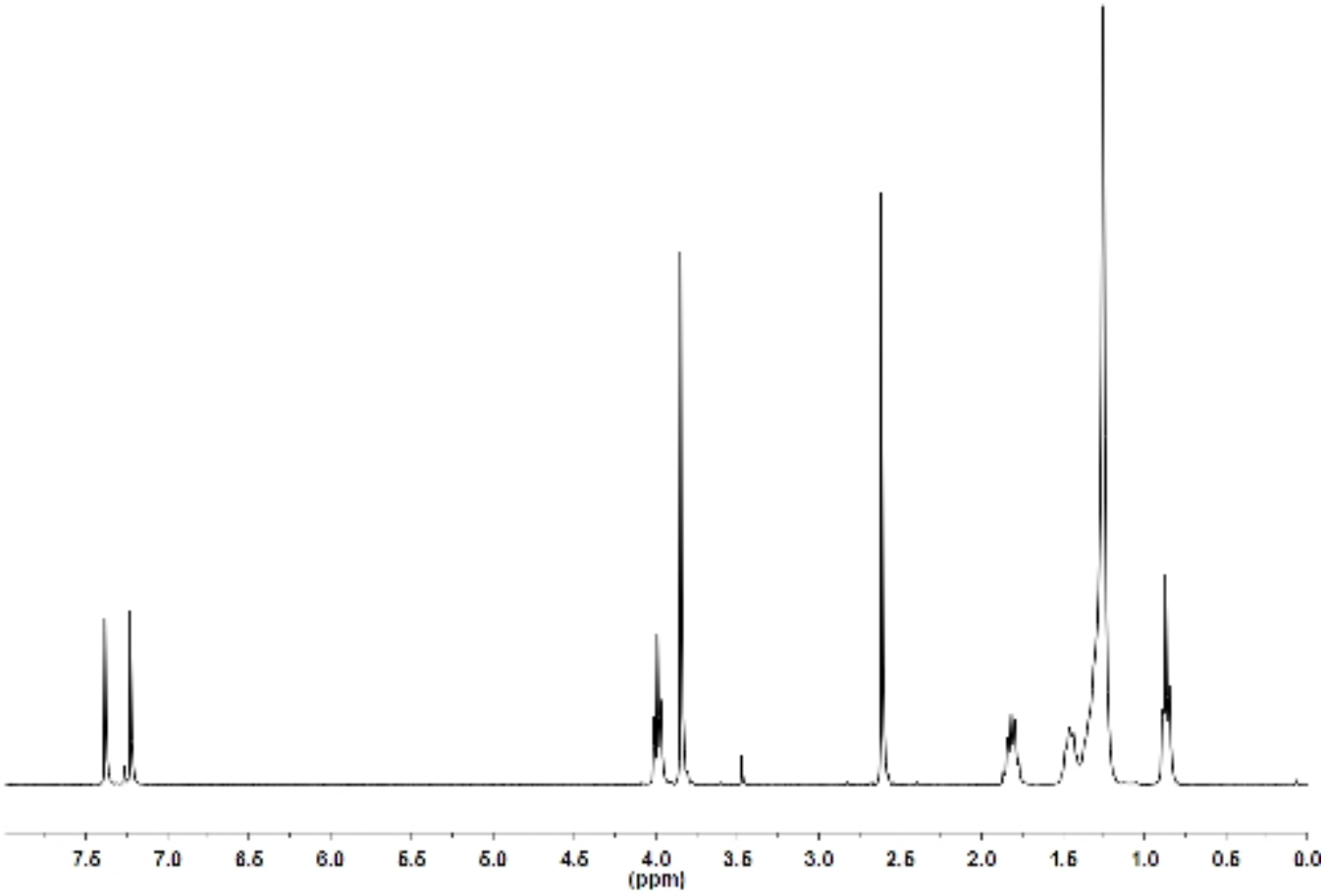


**Figure A.21.** $^{1}$H NMR of 2-Dodecyloxy-4-iodo-5-methoxyacetophenone, **II-10.**

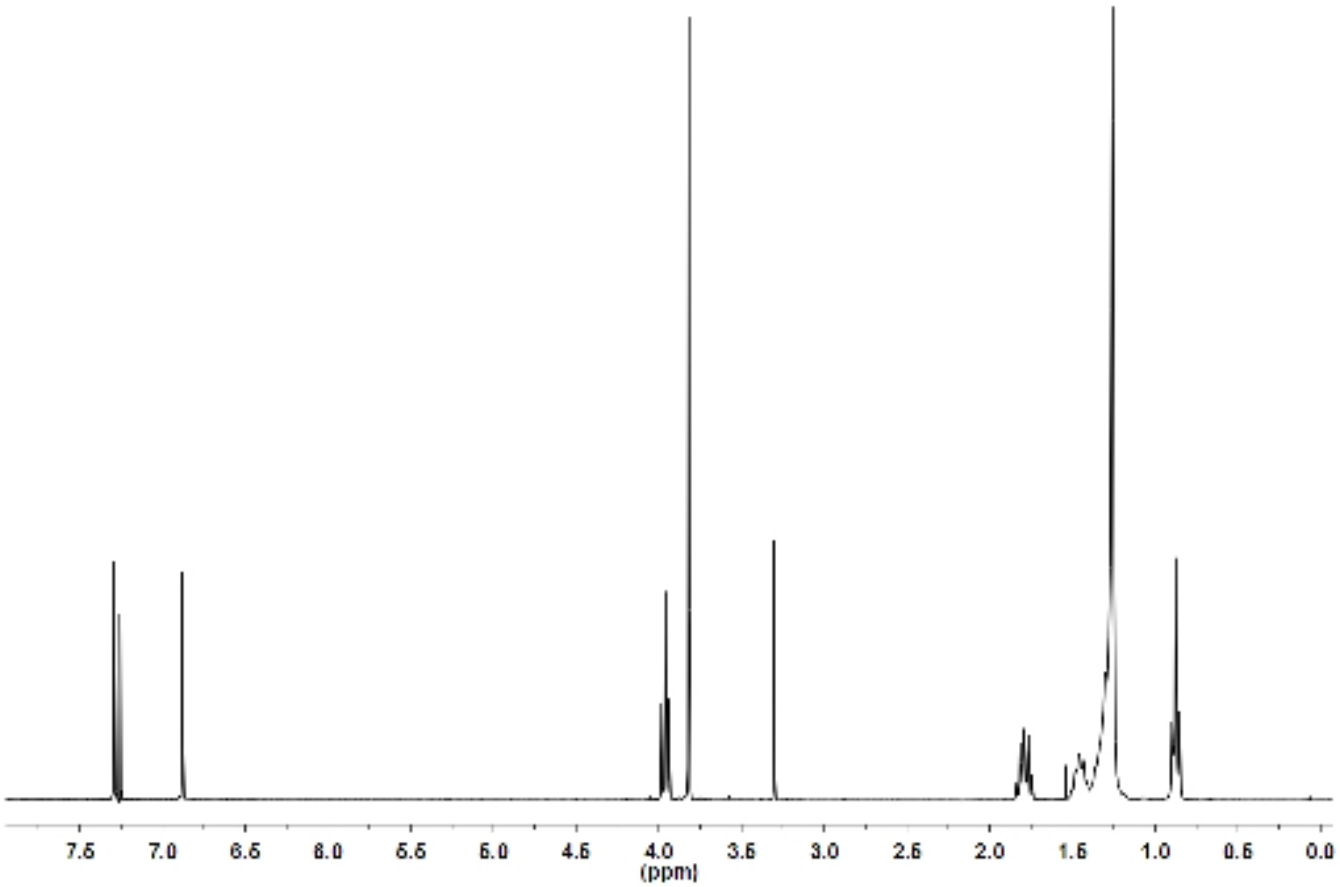


**Figure A.22.** $^{1}$H NMR of 4-Dodecyloxy-5-ethynyl-2-iodoanisole, **II-13a.**

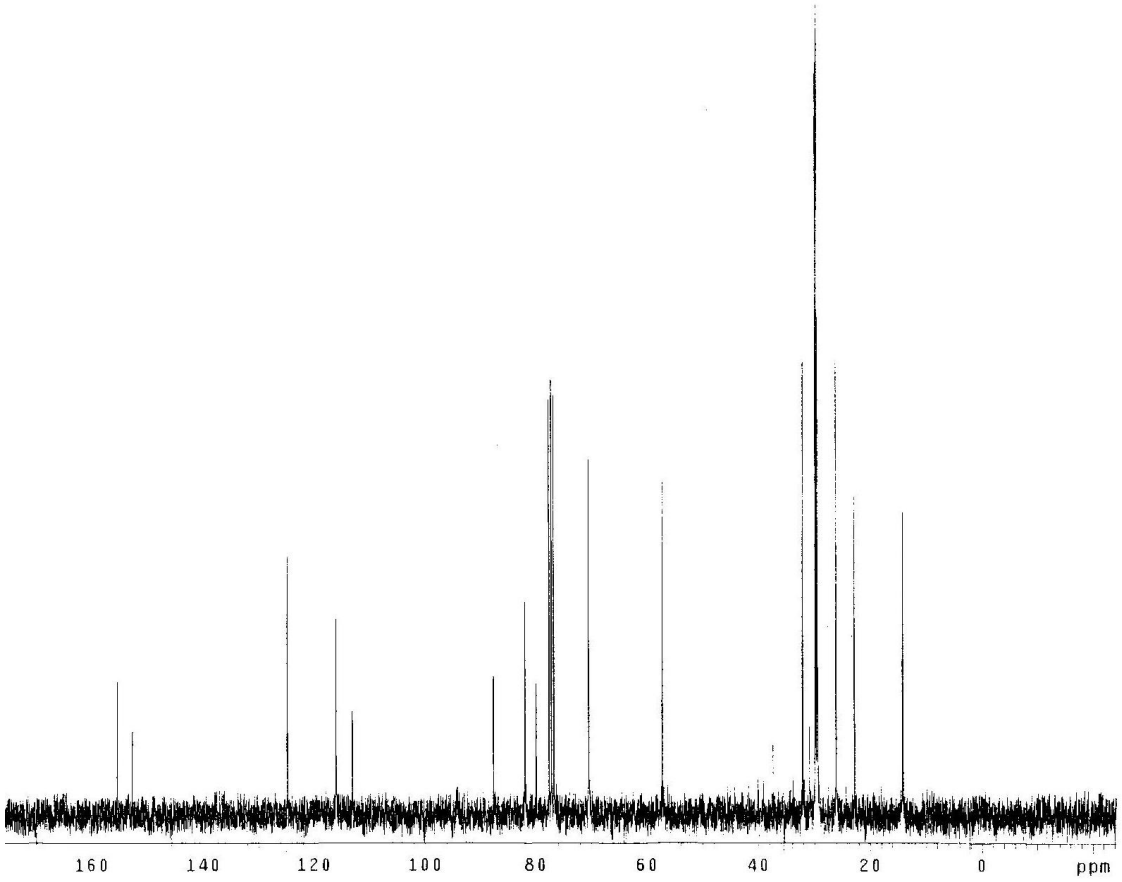


**Figure A.23.** $^{13}C$ of NMR 4-Dodecyloxy-5-ethynyl-2-iodoanisole, **II-13a.**

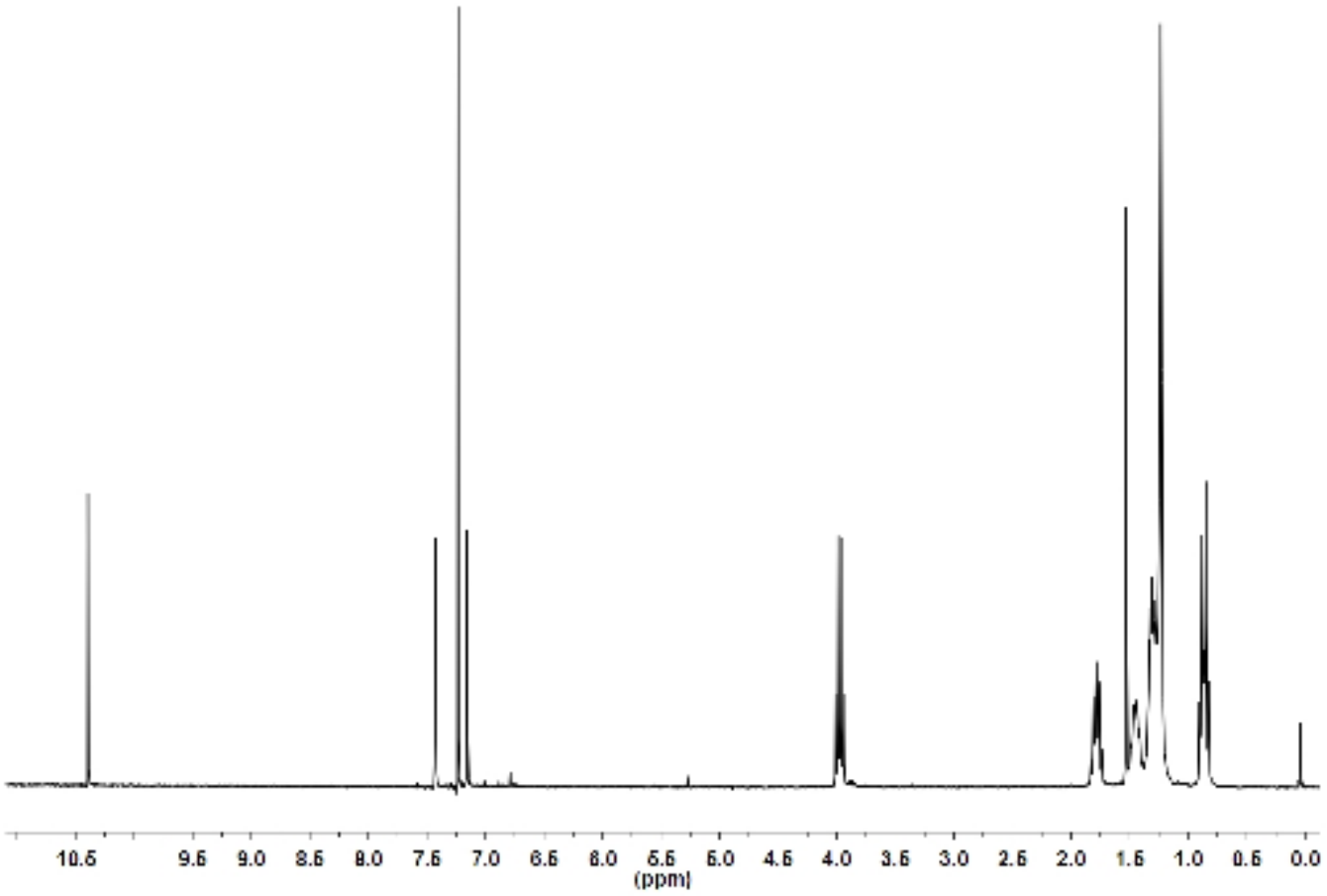


**Figure A.24.** $^{1}$H NMR of 5-Dodecyloxy-2-hexyloxy-4-iodobenzaldehyde, **II-14.**

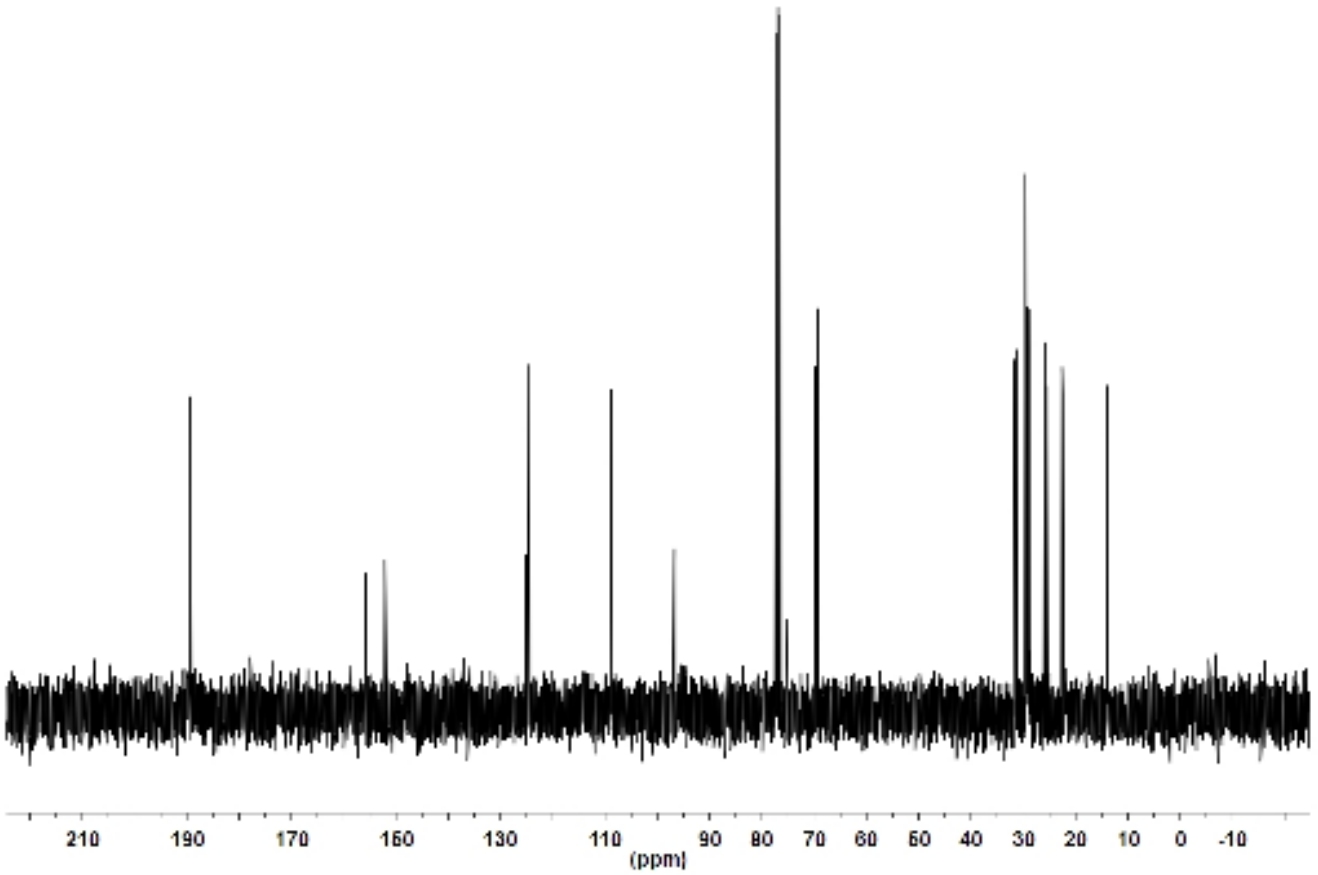


**Figure A.25.** $^{13}$C NMR of 5-Dodecyloxy-2-hexyloxy-4-iodobenzaldehyde, **II-14.**

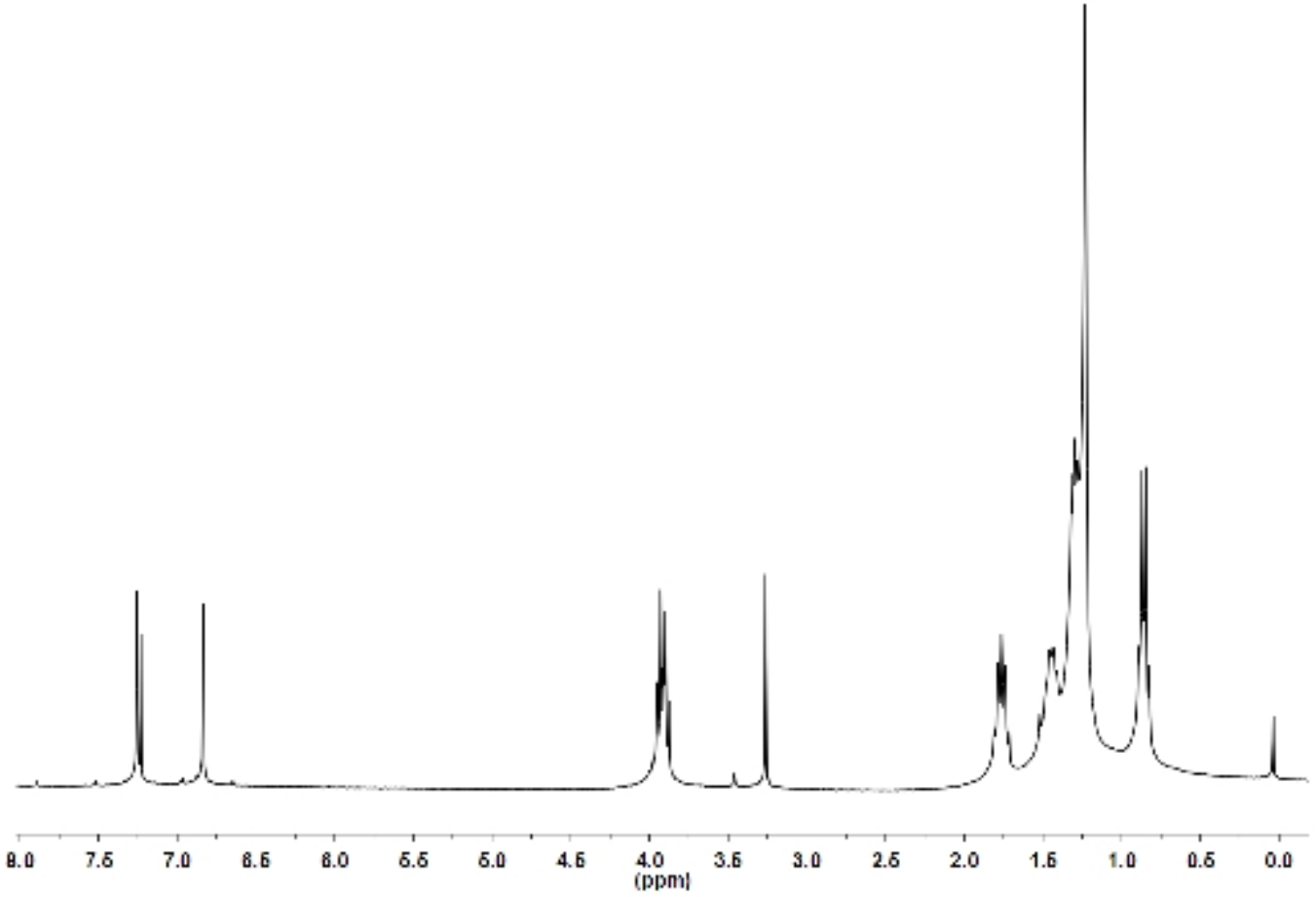


**Figure A.26.** $^{1}$H NMR of 1-Dodecyloxy-5-ethynyl-4-hexyloxy-2-iodobenzene, **II-13b.**

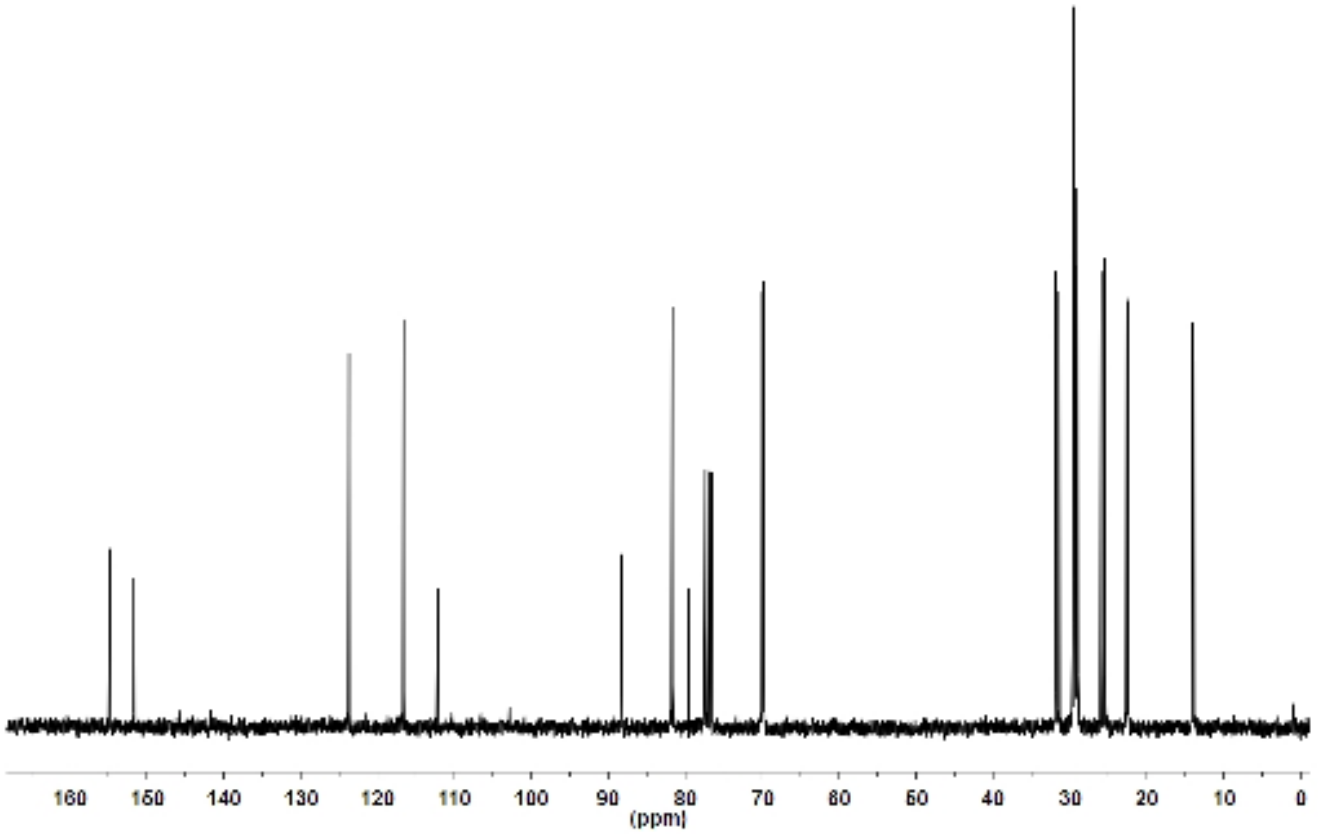


**Figure A.27.** $^{13}$C NMR of 1-Dodecyloxy-5-ethynyl-4-hexyloxy-2-iodobenzene, **II-13b.**

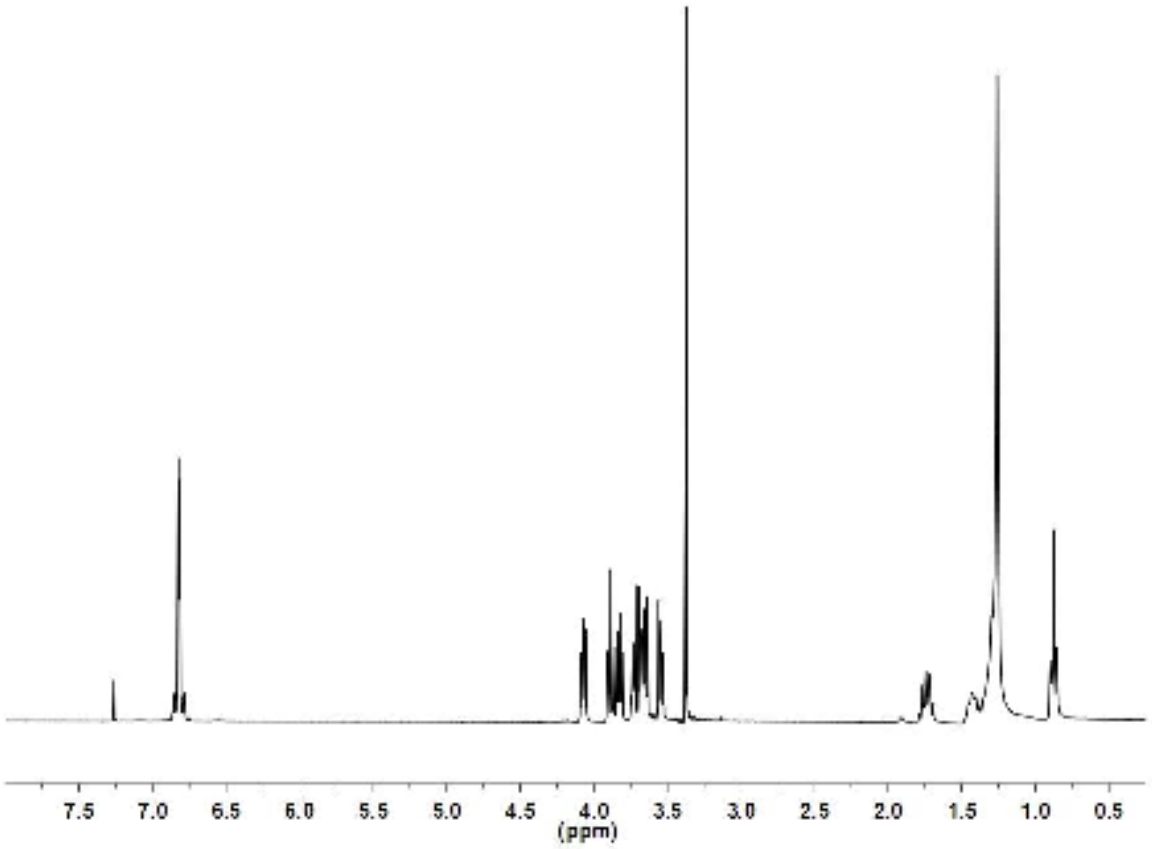


**Figure A.28.** $^{1}$H NMR of 1-Dodecyloxy-4-(2-(2-(2-methoxyethoxy)ethoxy)ethoxy)benzene, **III-1.**

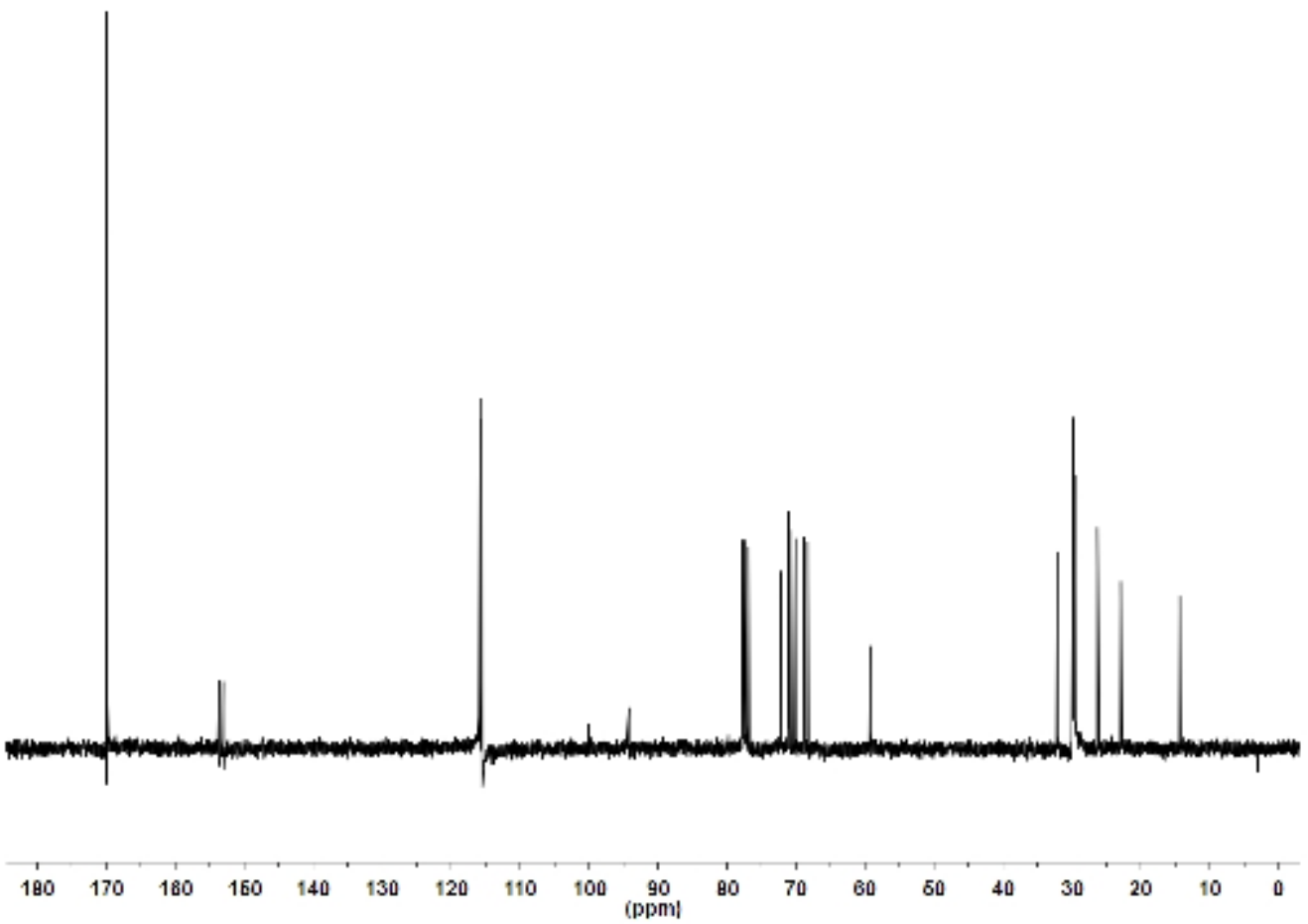


**Figure A.29.** $^{13}$C NMR of 1-Dodecyloxy-4-(2-(2-(2-methoxyethoxy)ethoxy)ethoxy)benzene, **III-1.**

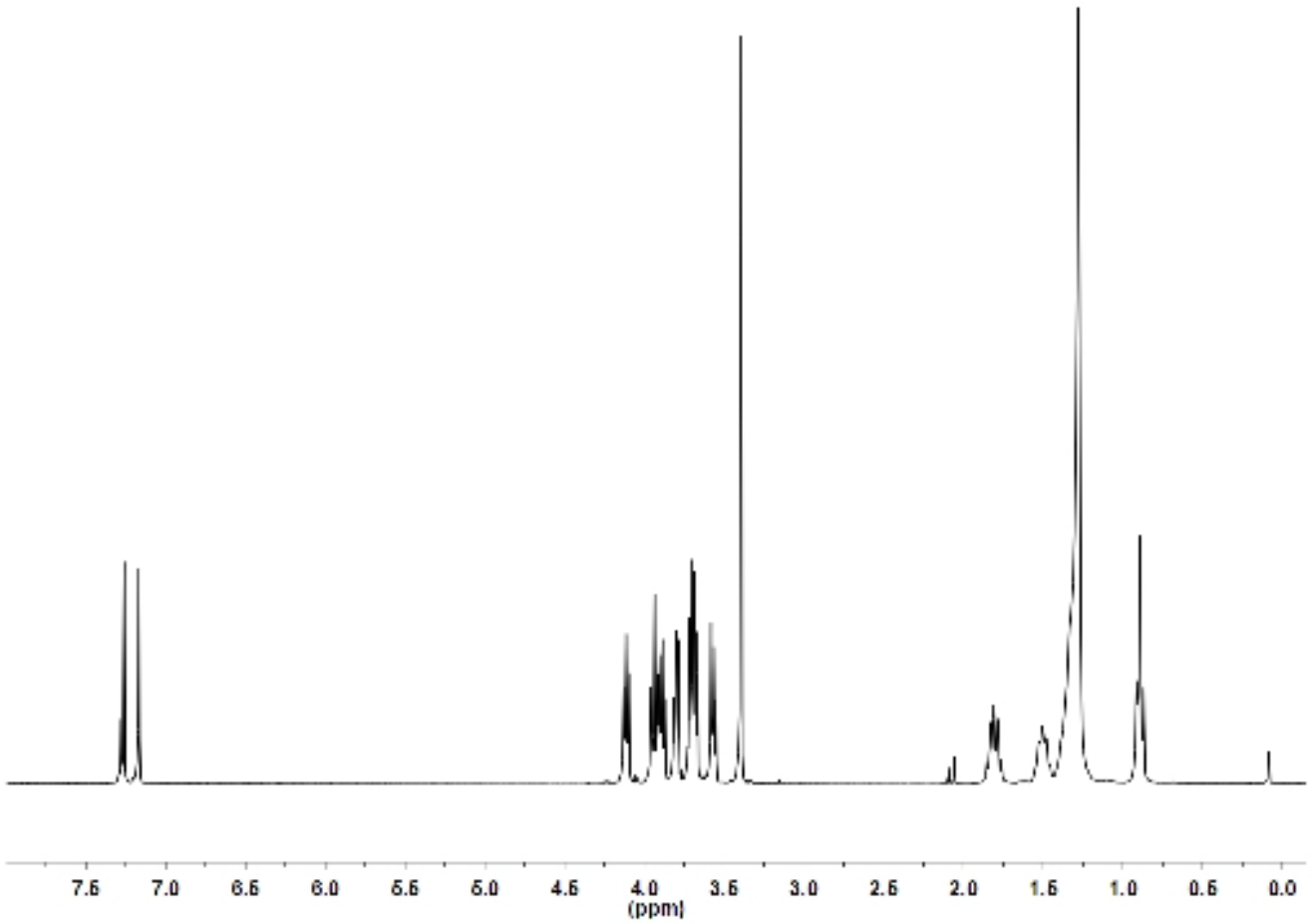


**Figure A.30.** $^{1}$H NMR of 1-Dodecyloxy-2,5-diiodo-4-(2-(2-(2-methoxyethoxy)ethoxy)ethoxy)benzene, **III-2.**

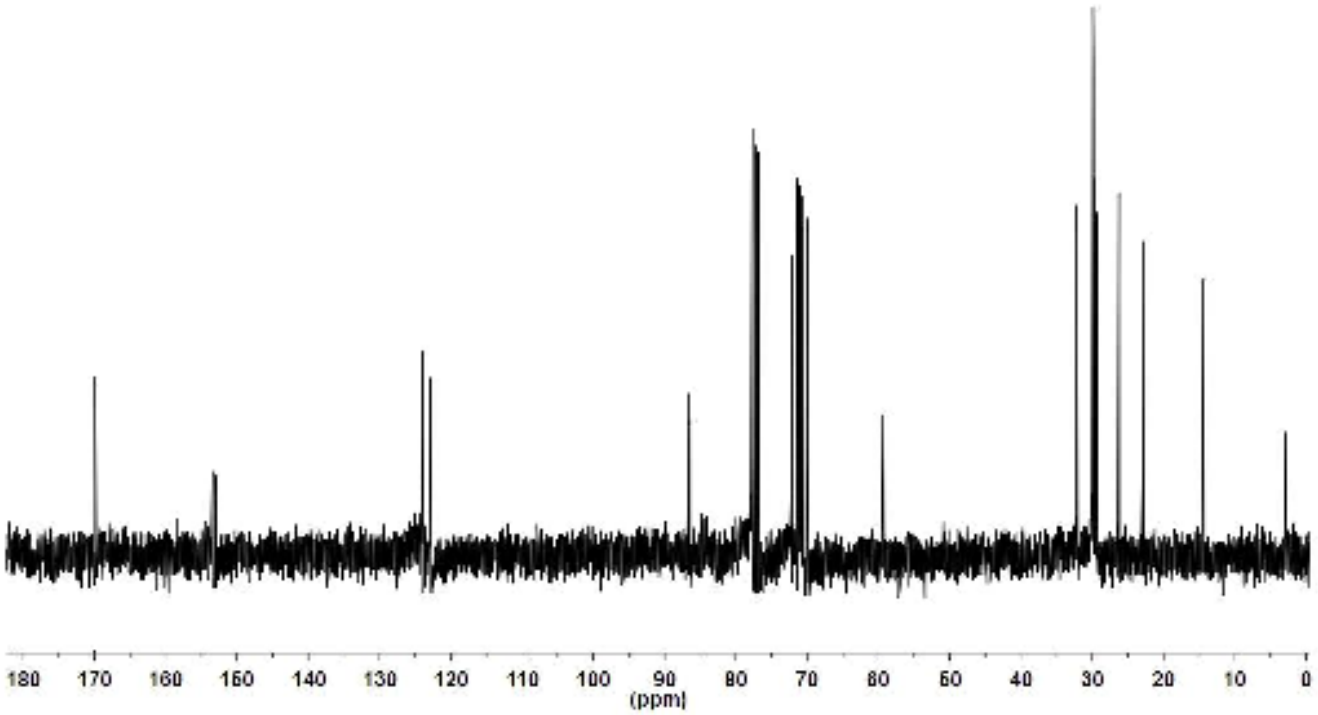


**Figure A.31.** $^{13}$C NMR of 1-Dodecyloxy-2,5-diiodo-4-(2-(2-(2-methoxyethoxy)ethoxy)ethoxy)benzene, **III-2.**

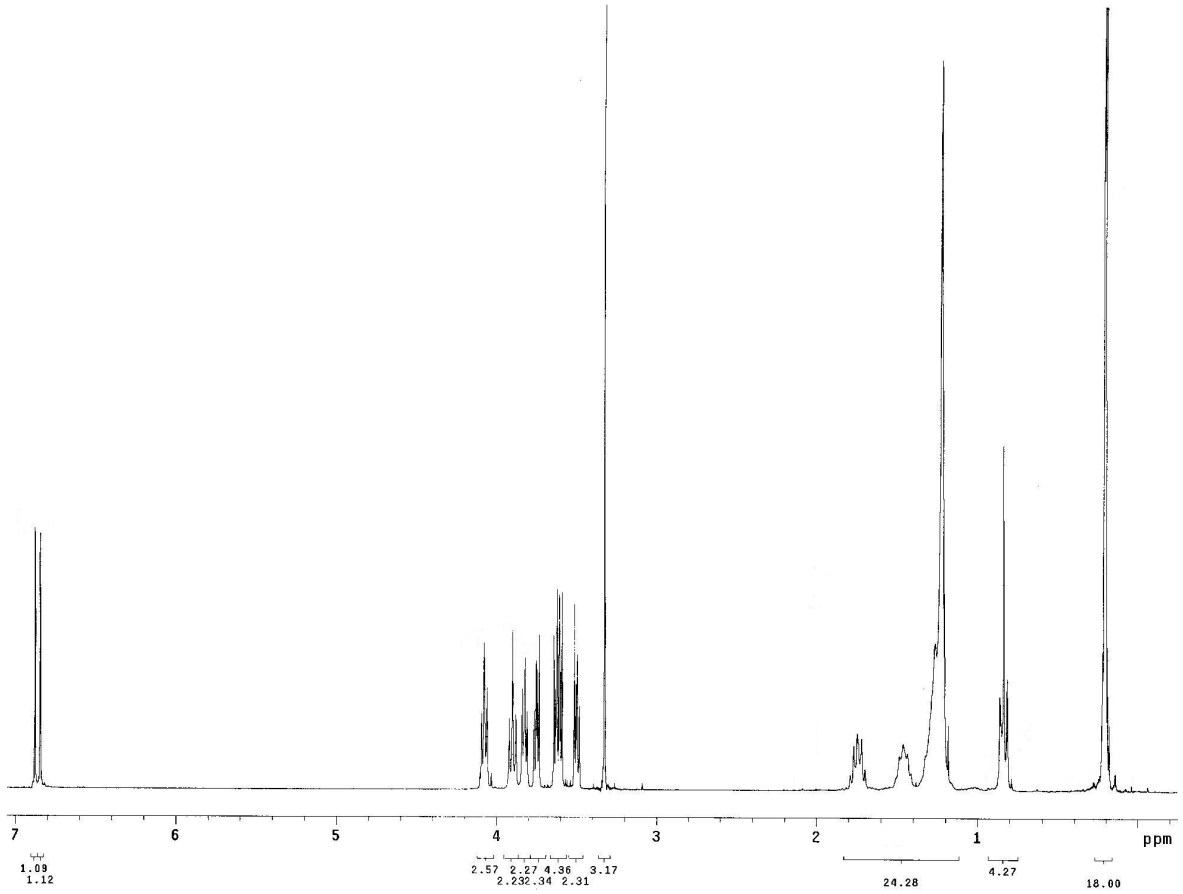


**Figure A.32.** $^{1}$H NMR of (2-(Dodecyloxy)-5-(2-(2-(2-methoxyethoxy)ethoxy) ethoxy)- 1,4-phenylene)bis(ethyne-2,1-diyl)bis(trimethylsilane), **III-3.**

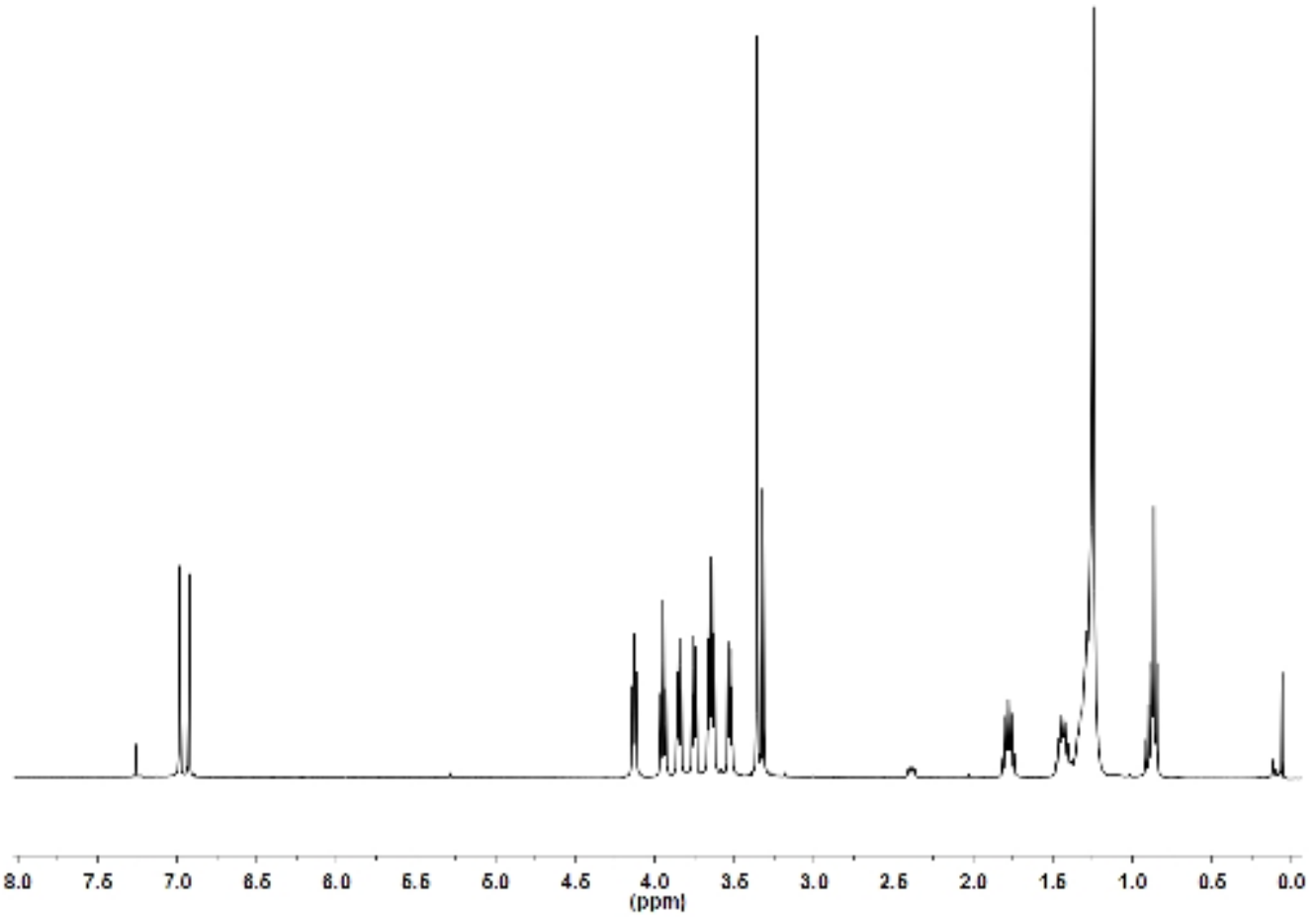


**Figure A.33.** $^{1}$H NMR of 1-(Dodecyloxy)-2,5-diethynyl-4-(2-(2-(2-methoxyethoxy)ethoxy)ethoxy)benzene, **III-4.**

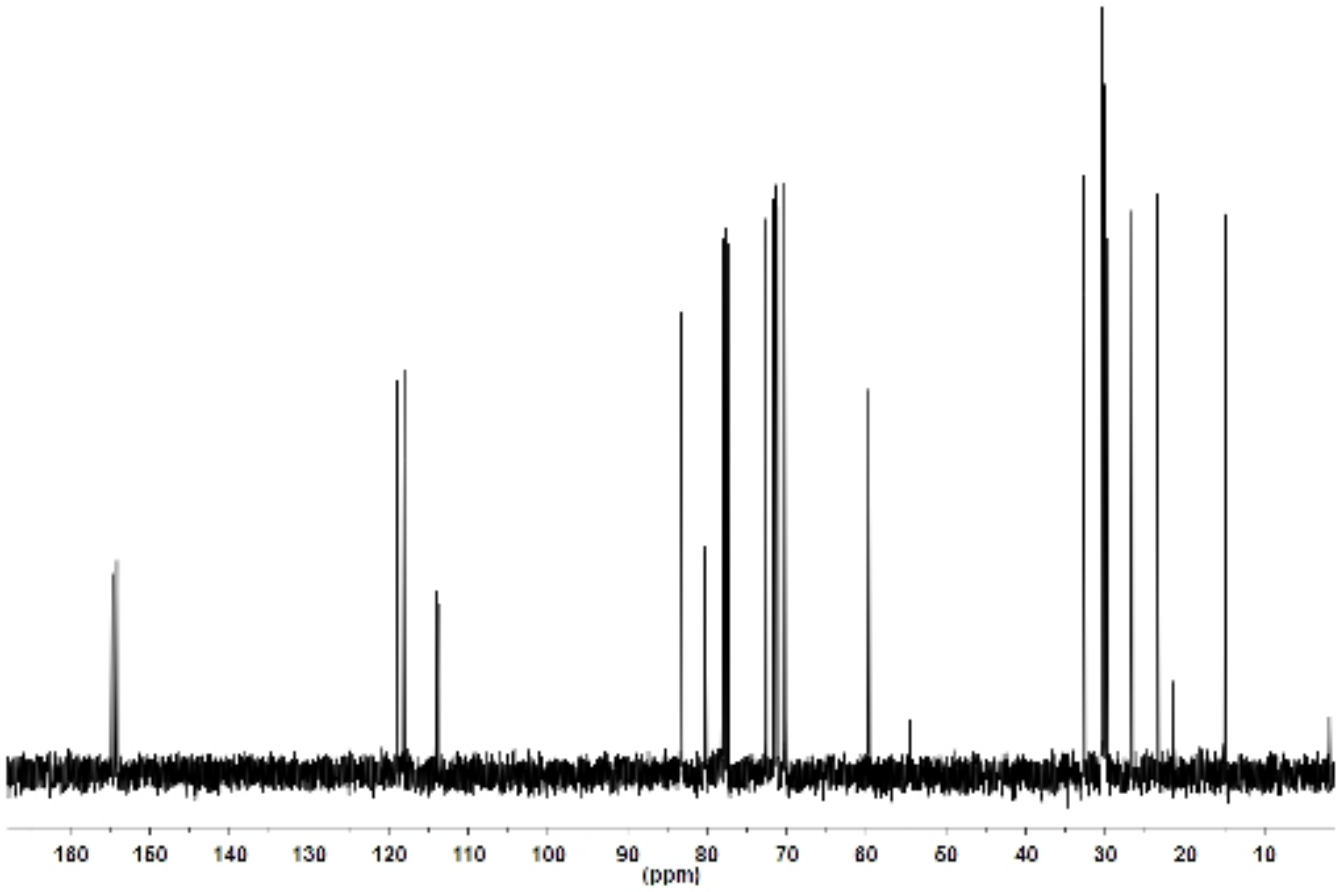


**Figure A.34.** $^{13}$C NMR of 1-(Dodecyloxy)-2,5-diethynyl-4-(2-(2-(2-methoxyethoxy)ethoxy)ethoxy)benzene, **III-4.**

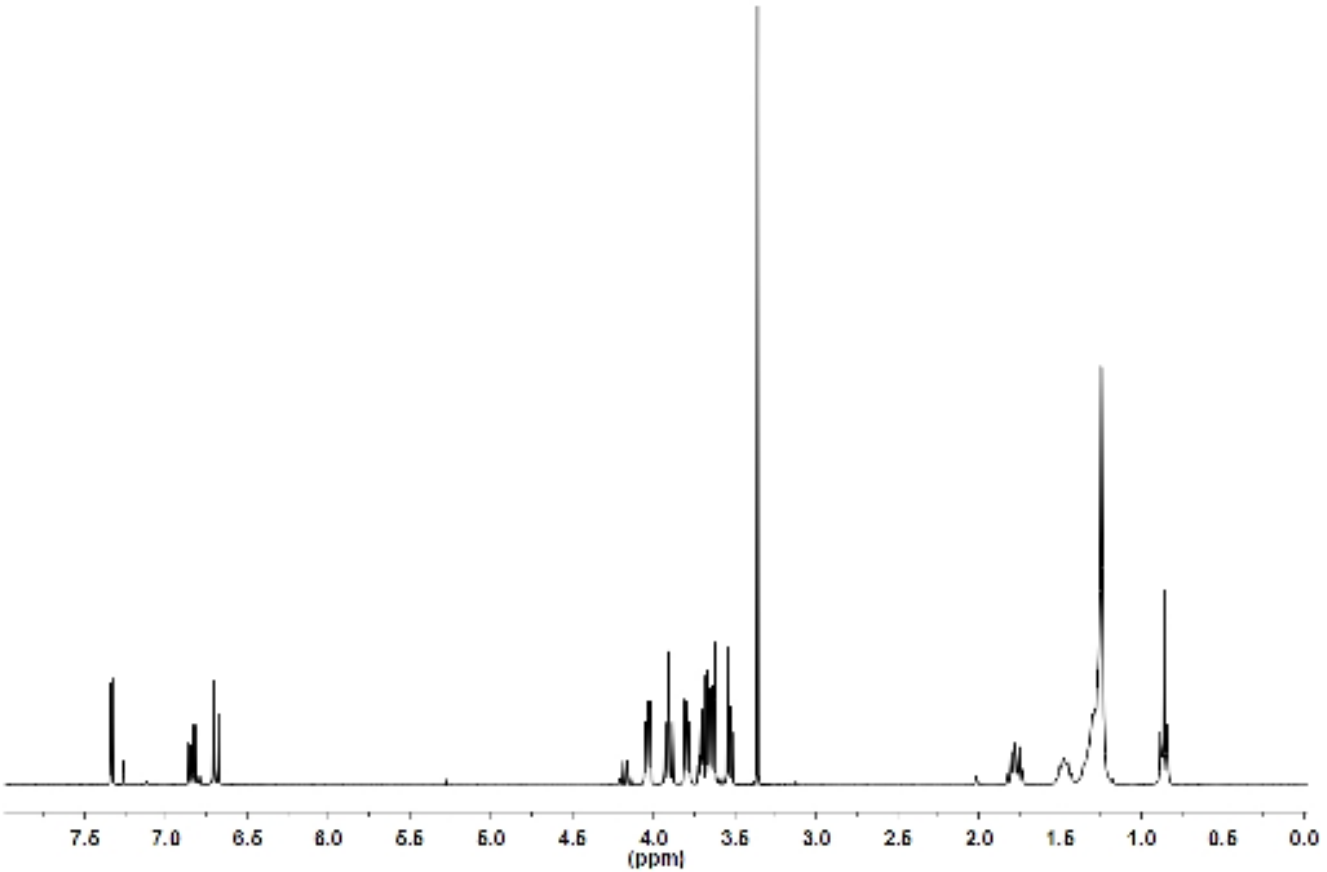


**Figure A.35.** $^{1}$H NMR of 1-(Dodecyloxy)-2-iodo-4-(2-(2-(2-methoxyethoxy)ethoxy)ethoxy)benzene, **III-5.**

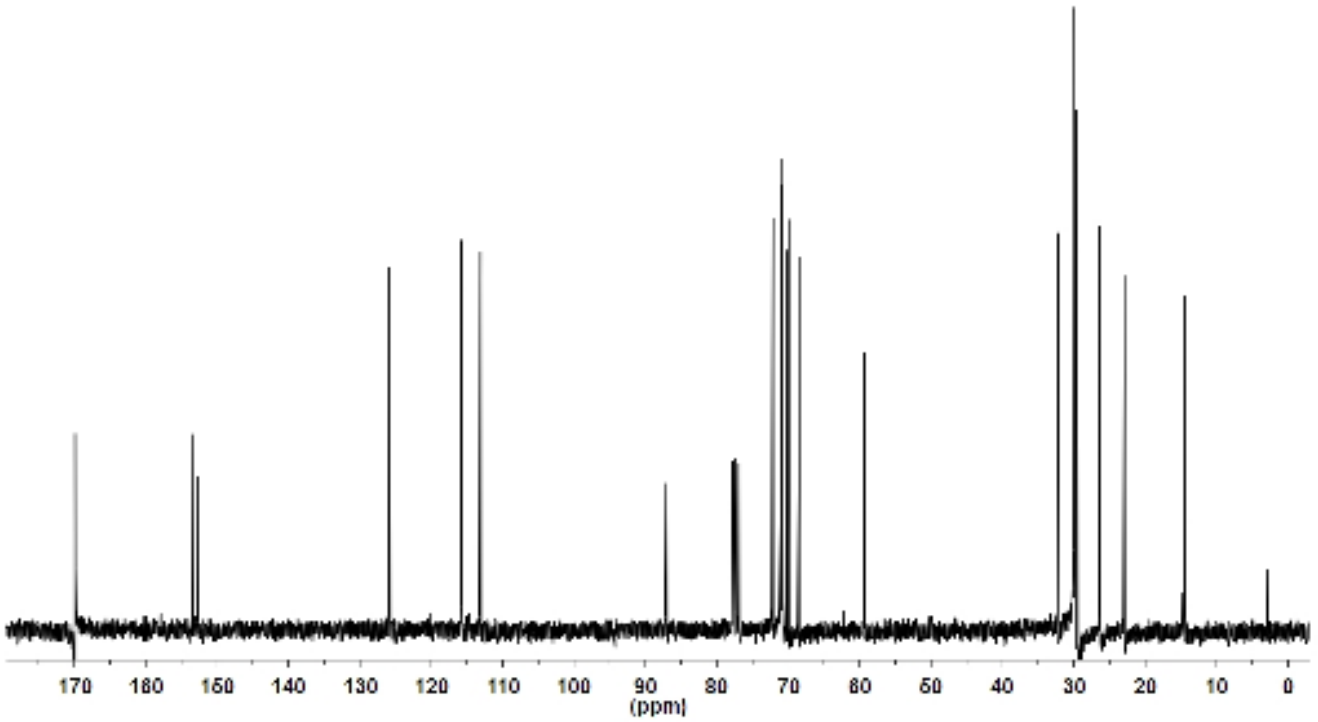


**Figure A.36.** $^{13}$C NMR of 1-(Dodecyloxy)-2-iodo-4-(2-(2-(2-methoxyethoxy)ethoxy)ethoxy)benzene, **III-5.**

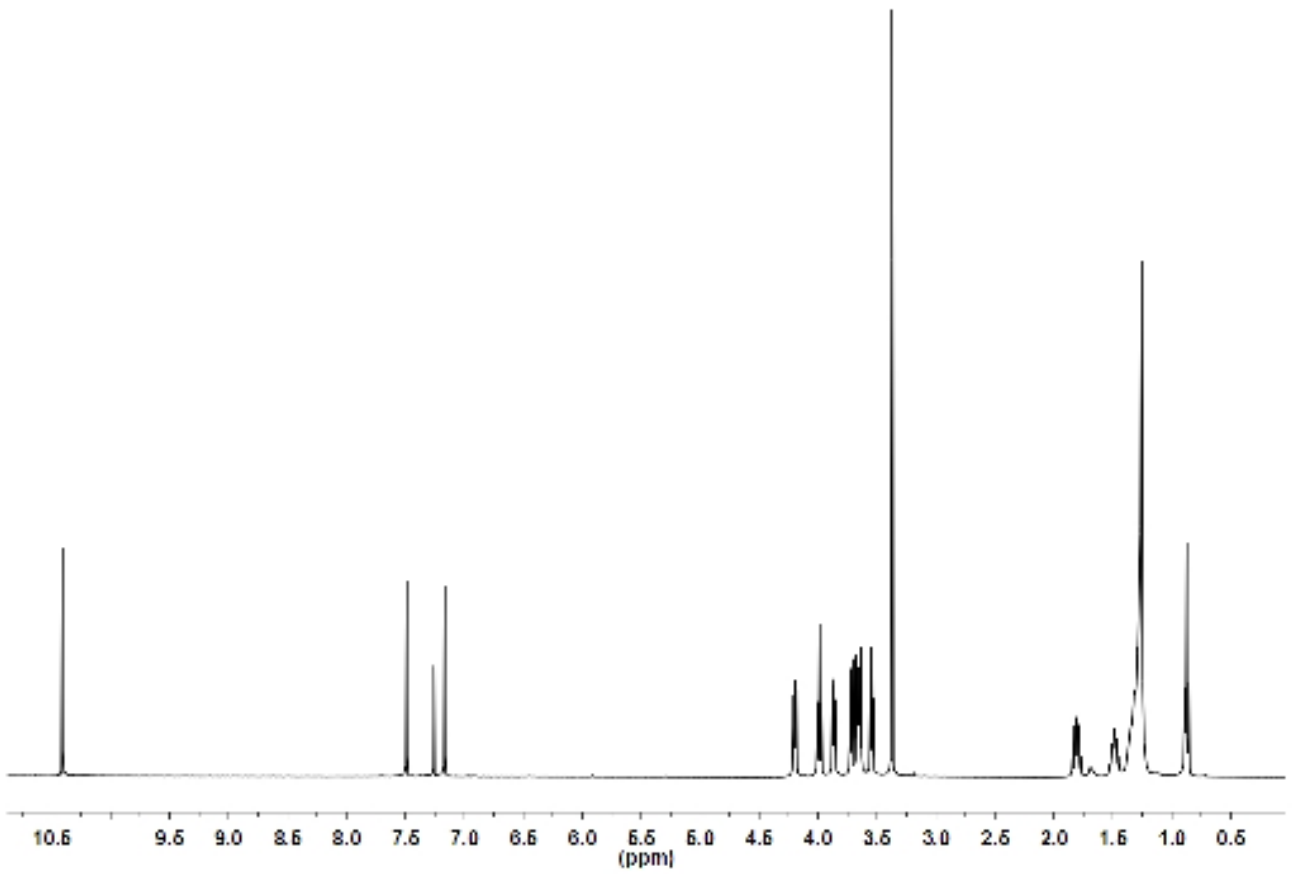


**Figure A.37.** $^{1}$H NMR of 5-(Dodecyloxy)-4-iodo-2-(2-(2-(2-methoxyethoxy)ethoxy)ethoxy)benzaldehyde, **III-6.**

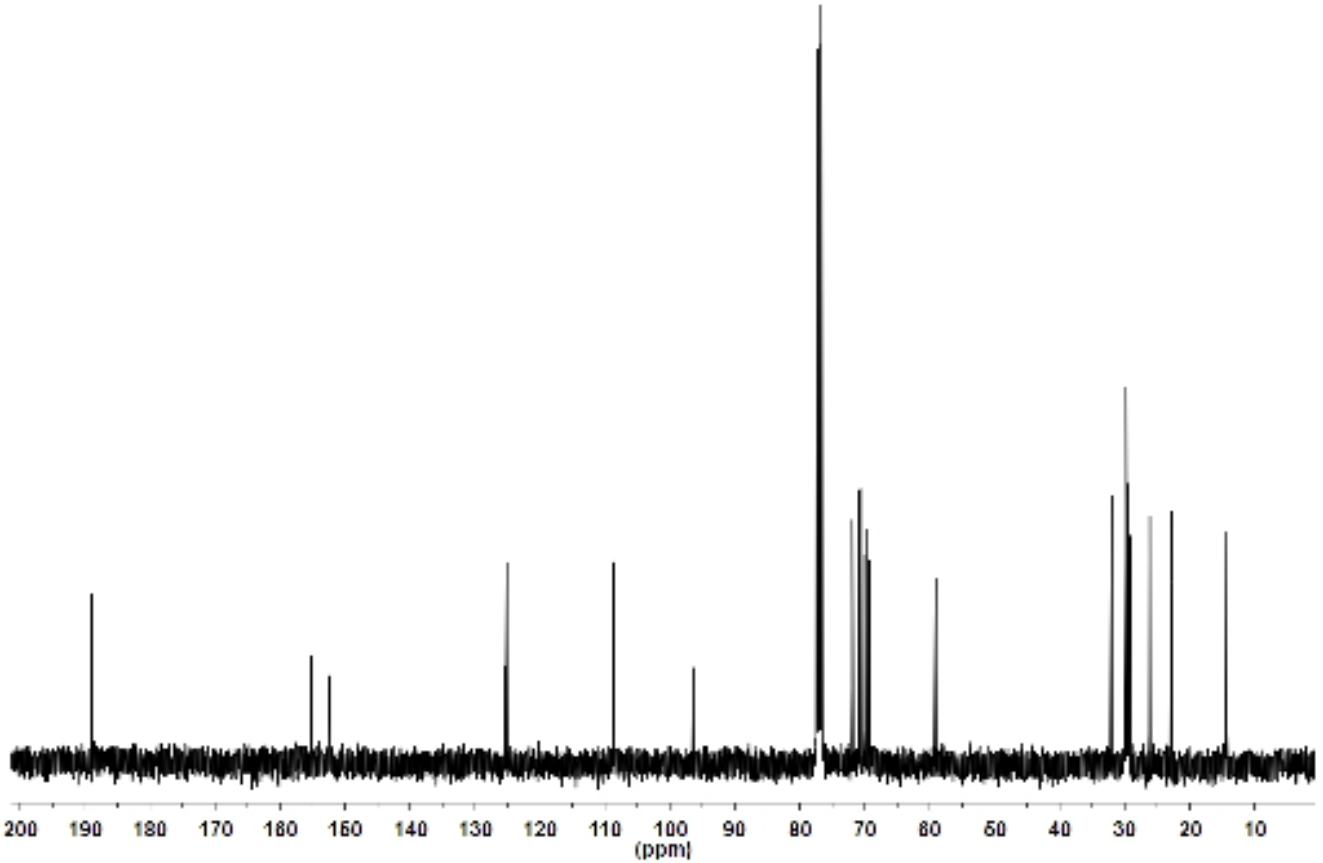


**Figure A.38.** $^{13}$C NMR of 5-(Dodecyloxy)-4-iodo-2-(2-(2-(2-methoxyethoxy)ethoxy)ethoxy)benzaldehyde, **III-6.**

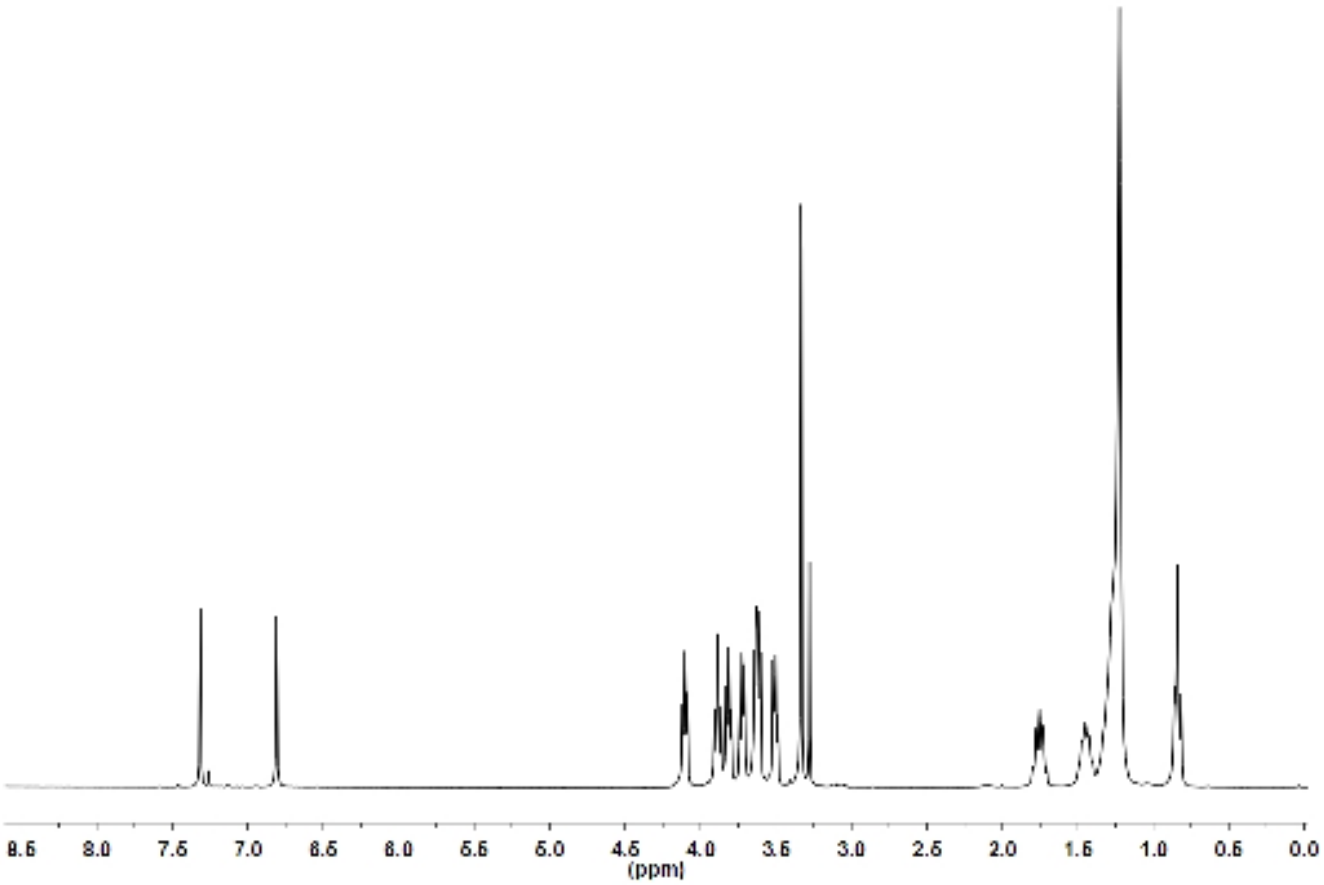


**Figure A.39.** $^{1}$H NMR of 1-(Dodecyloxy)-5-ethynyl-2-iodo-4-(2-(2-(2-methoxyethoxy)ethoxy)ethoxy)benzene, **III-7.**

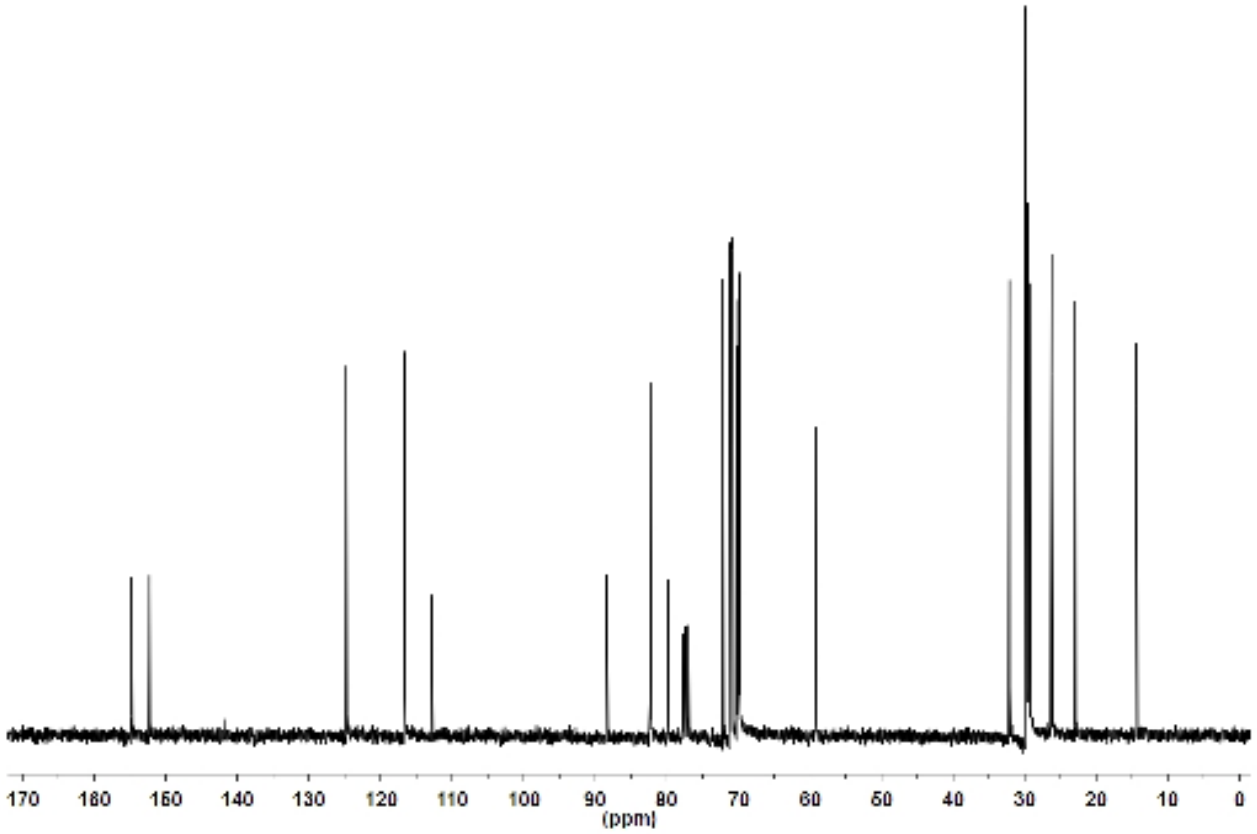


**Figure A.40.** $^{1}$H NMR of 1-(Dodecyloxy)-5-ethynyl-2-iodo-4-(2-(2-(2-methoxyethoxy)ethoxy)ethoxy)benzene, **III-7.**

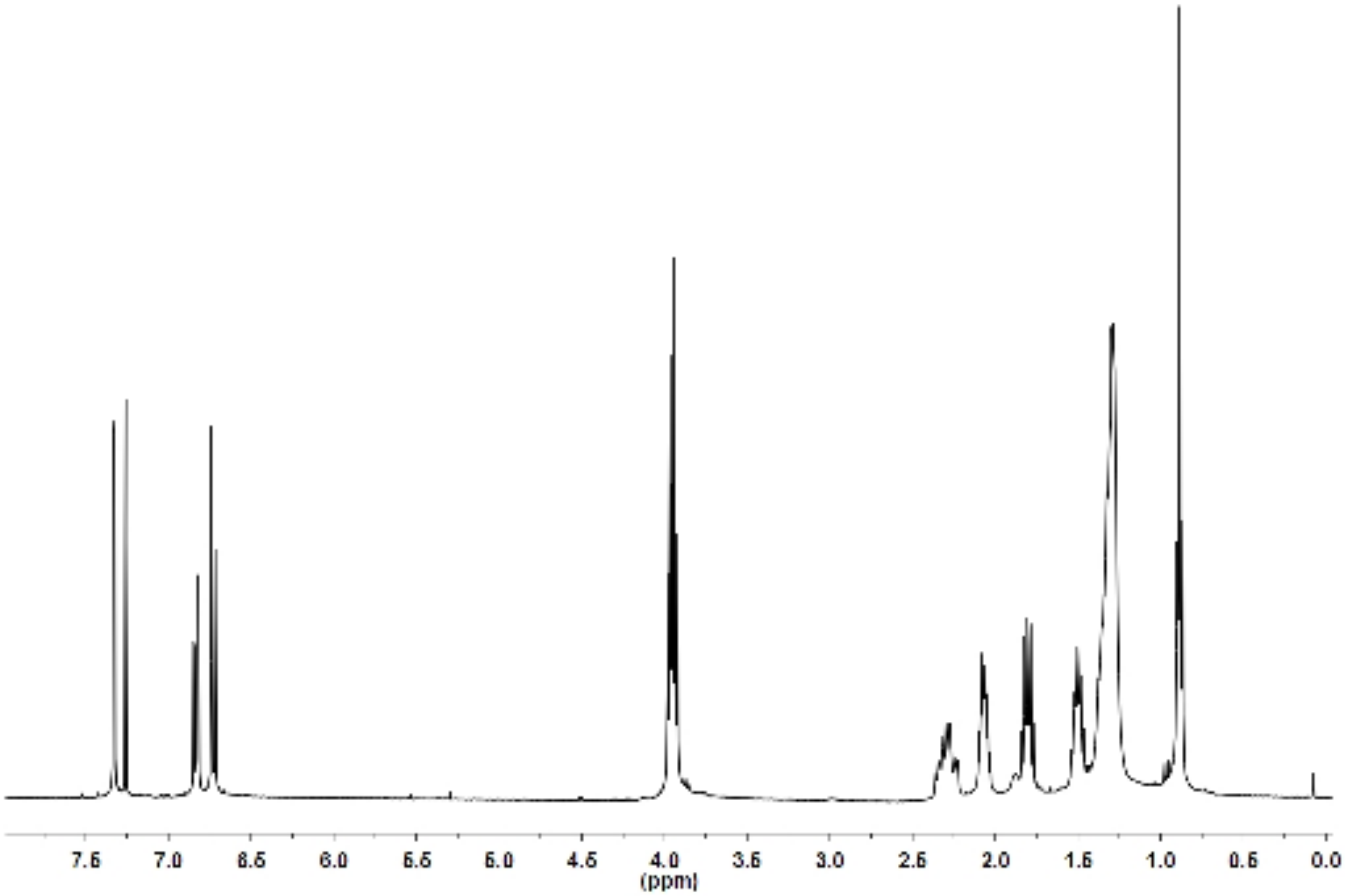


**Figure A.41.** $^{1}$H NMR of 2-Iodo-1-(nonyloxy)-4-(4,4,5,5,6,6,7,7,8,8,9,9,9-tridecafluorononyloxy)benzene, **IV-1.**

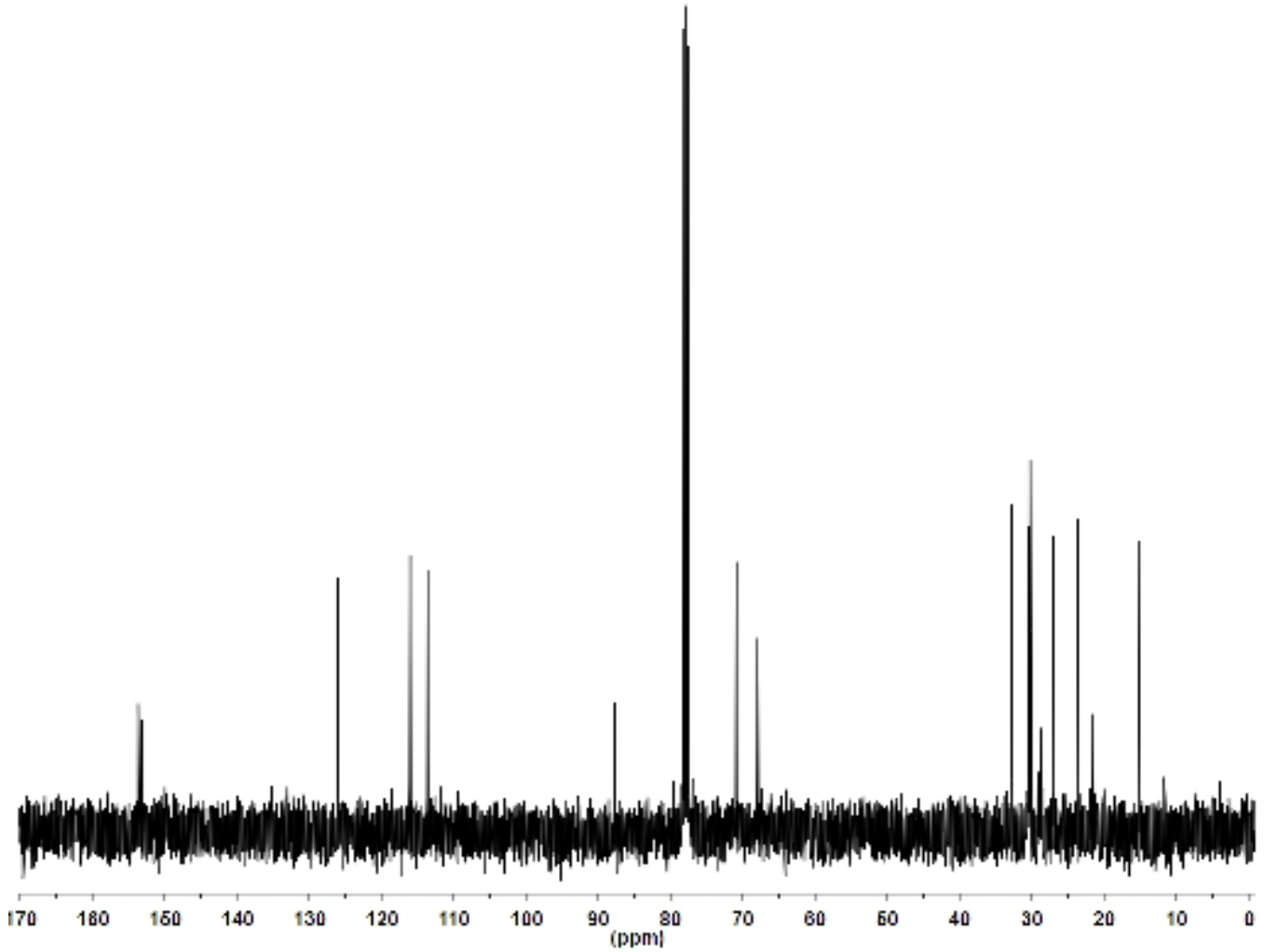


**Figure A.42.** $^{13}$C NMR of 2-Iodo-1-(nonyloxy)-4-(4,4,5,5,6,6,7,7,8,8,9,9,9-tridecafluorononyloxy)benzene, **IV-1.**

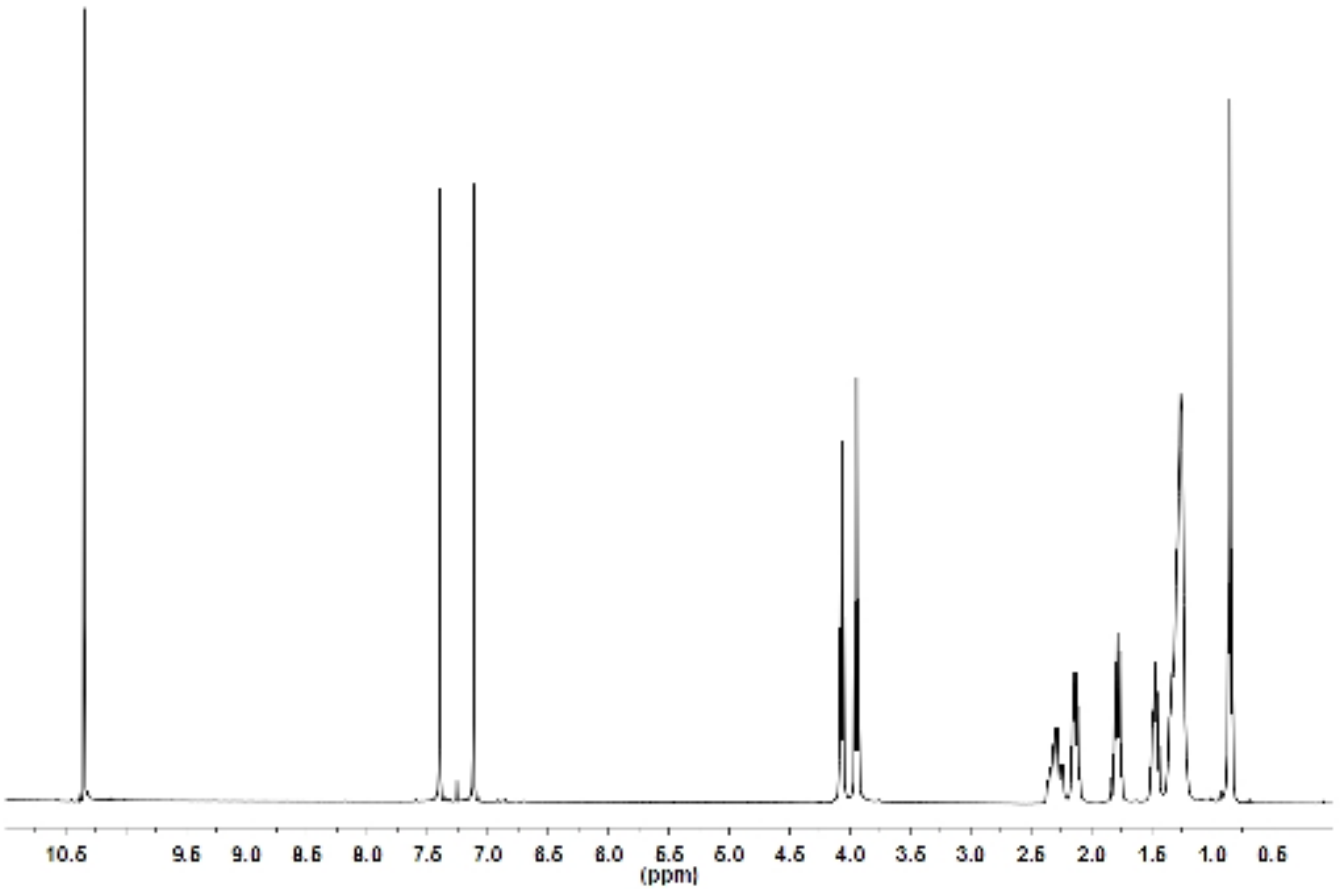


**Figure A.43.** $^{1}$H NMR of 2-(4,4,5,5,6,6,7,7,8,8,9,9,9-Tridecafluorononyloxy)-4-iodo-5-(nonyloxy)benzaldehyde, **IV-2.**

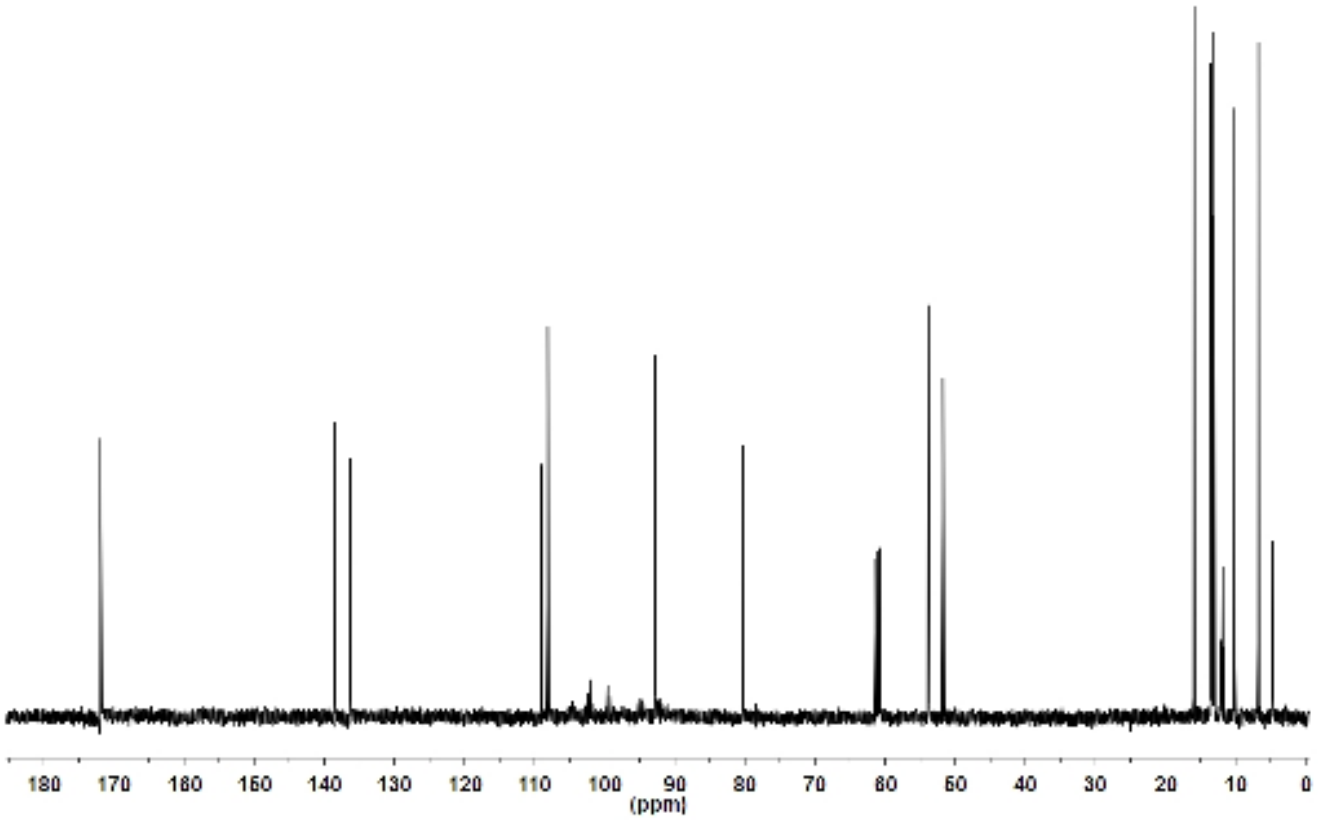


**Figure A.44.** $^{13}$C NMR of 2-(4,4,5,5,6,6,7,7,8,8,9,9,9-Tridecafluorononyloxy)-4-iodo-5-(nonyloxy)benzaldehyde, **IV-2.**

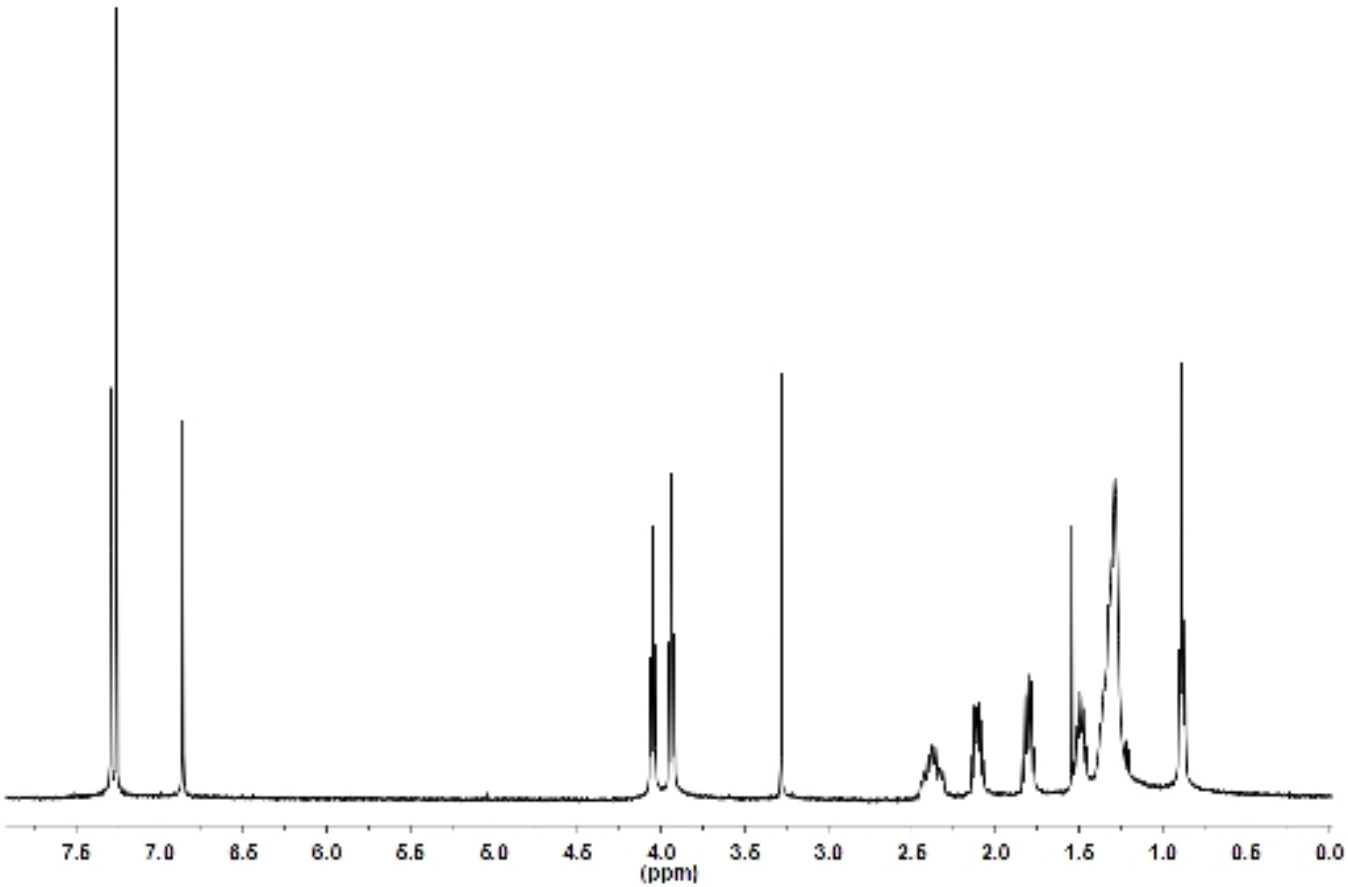


**Figure A.45.** $^{1}$H NMR of 1-Ethynyl-2-(4,4,5,5,6,6,7,7,8,8,9,9,9-tridecafluorononyloxy)-4-iodo-5-(nonyloxy)benzene, **IV-3.**

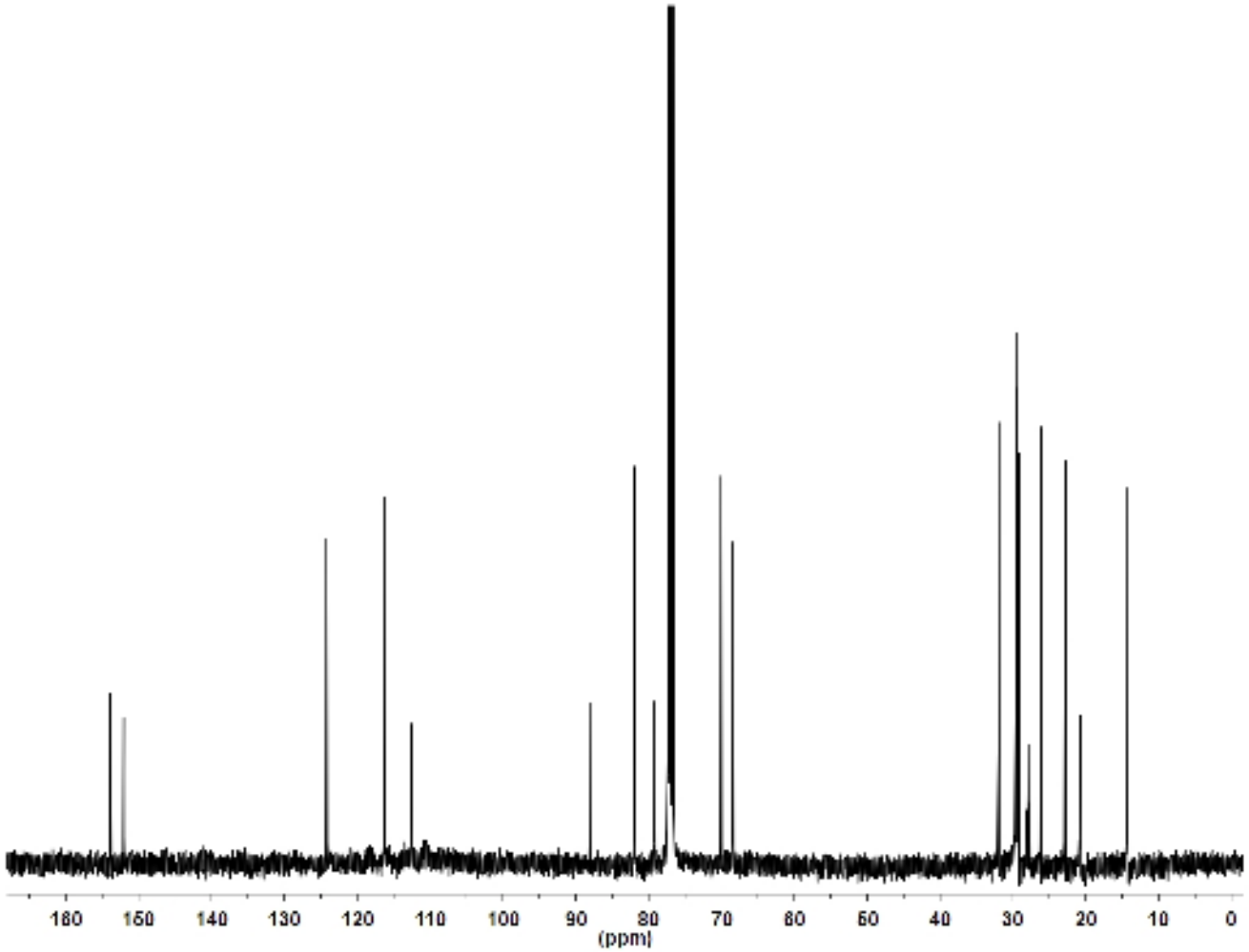


**Figure A.46.** $^{13}C$ NMR of 1-Ethynyl-2-(4,4,5,5,6,6,7,7,8,8,9,9,9-tridecafluorononyloxy)-4-iodo-5-(nonyloxy)benzene, **IV-3.**

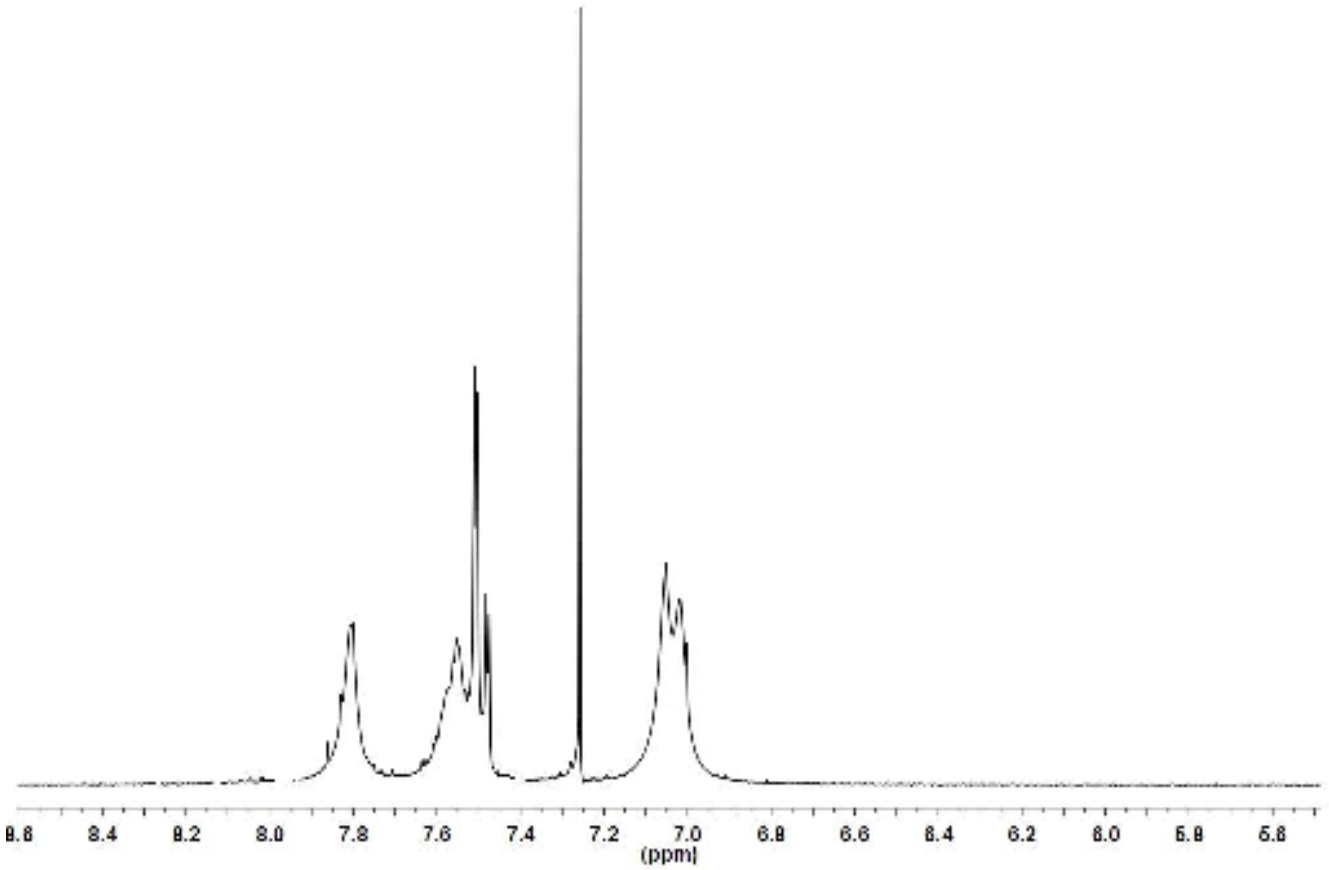


**Figure A.47.** $^{1}$H NMR of 4-Bromo-1,2-bis(dibromomethyl)benzene, **V-1.**

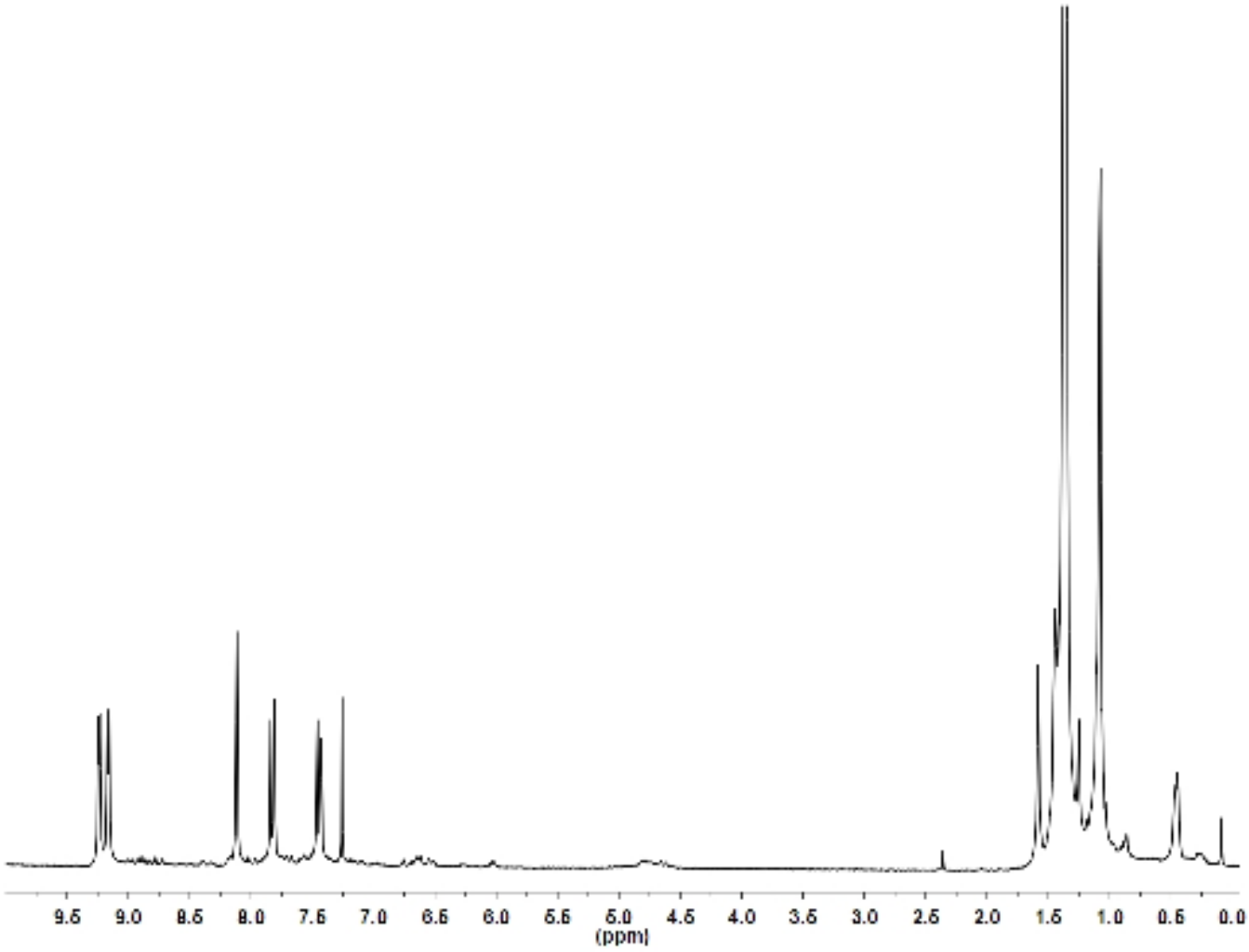


**Figure A.48.** $^{1}$H NMR of 6,13-Bis(triisopropylsilylethynyl)-2,9-dibromopentacene, **V-4.**

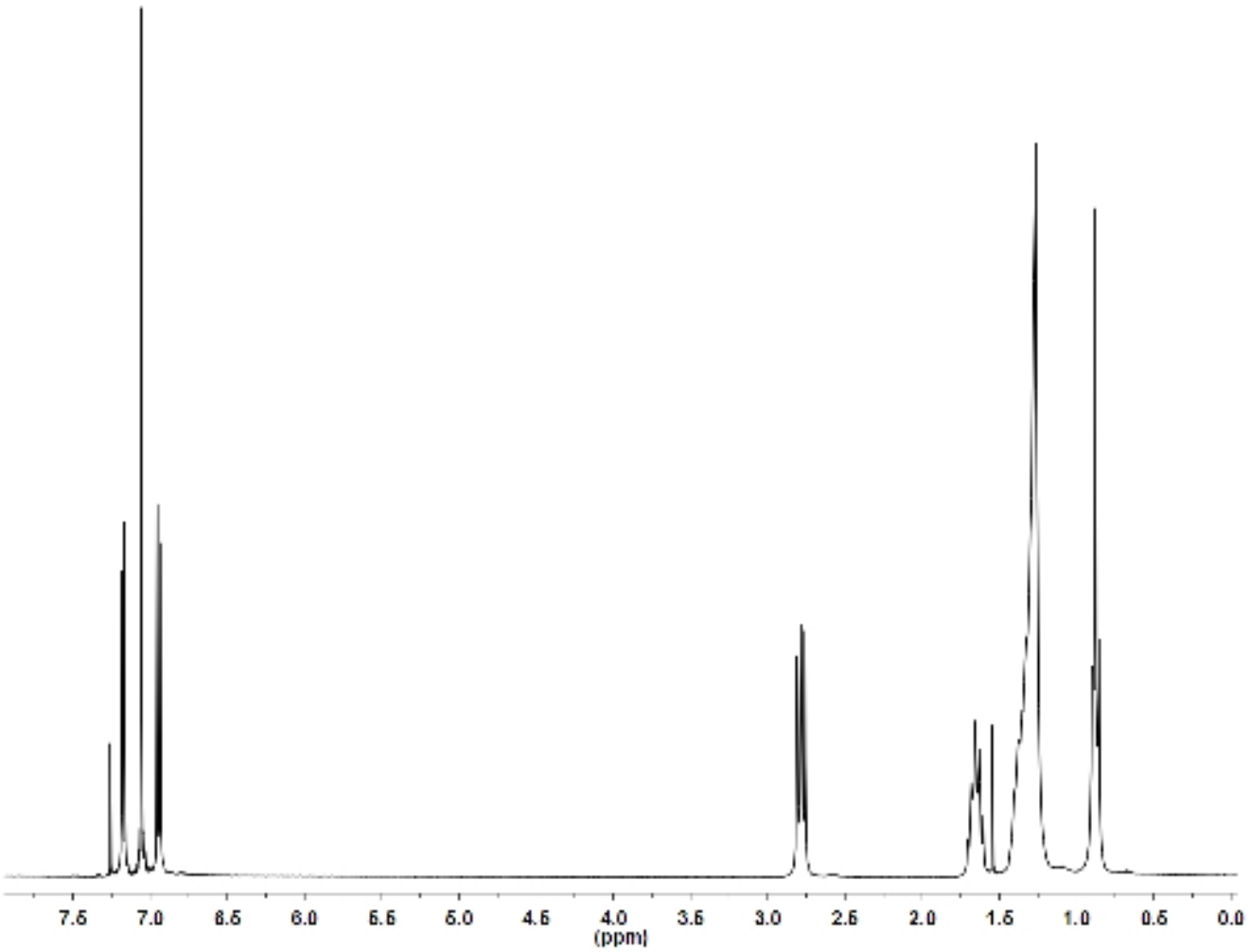


**Figure A.49.** $^{1}$H NMR of 3,3’’-Dioctyl-2,2’:5’,2’’-terthiophene, **V-7.**

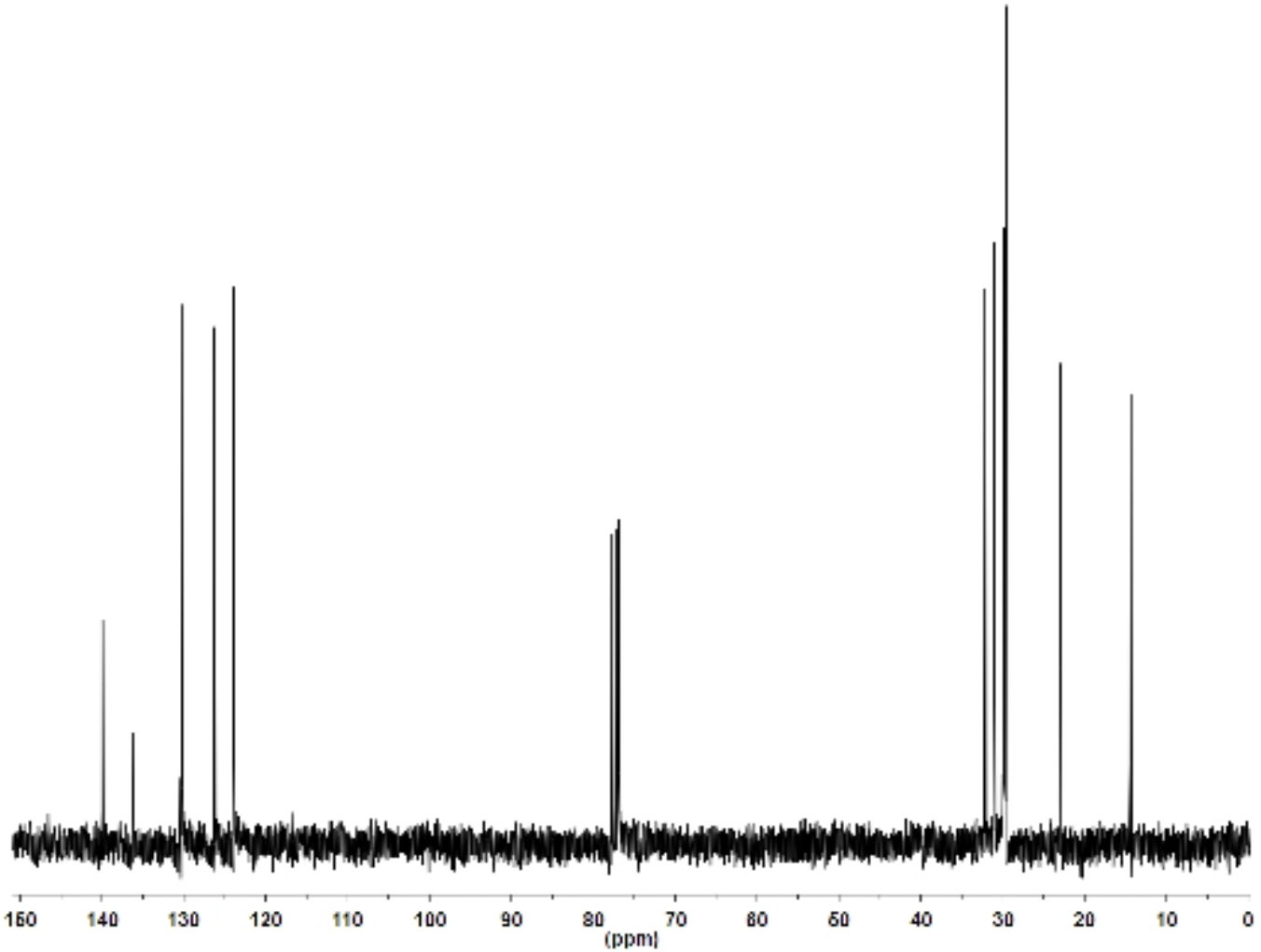


**Figure A.50.** $^{13}$C NMR of 3,3’’-Dioctyl-2,2’:5’,2’’-terthiophene, **V-7.**

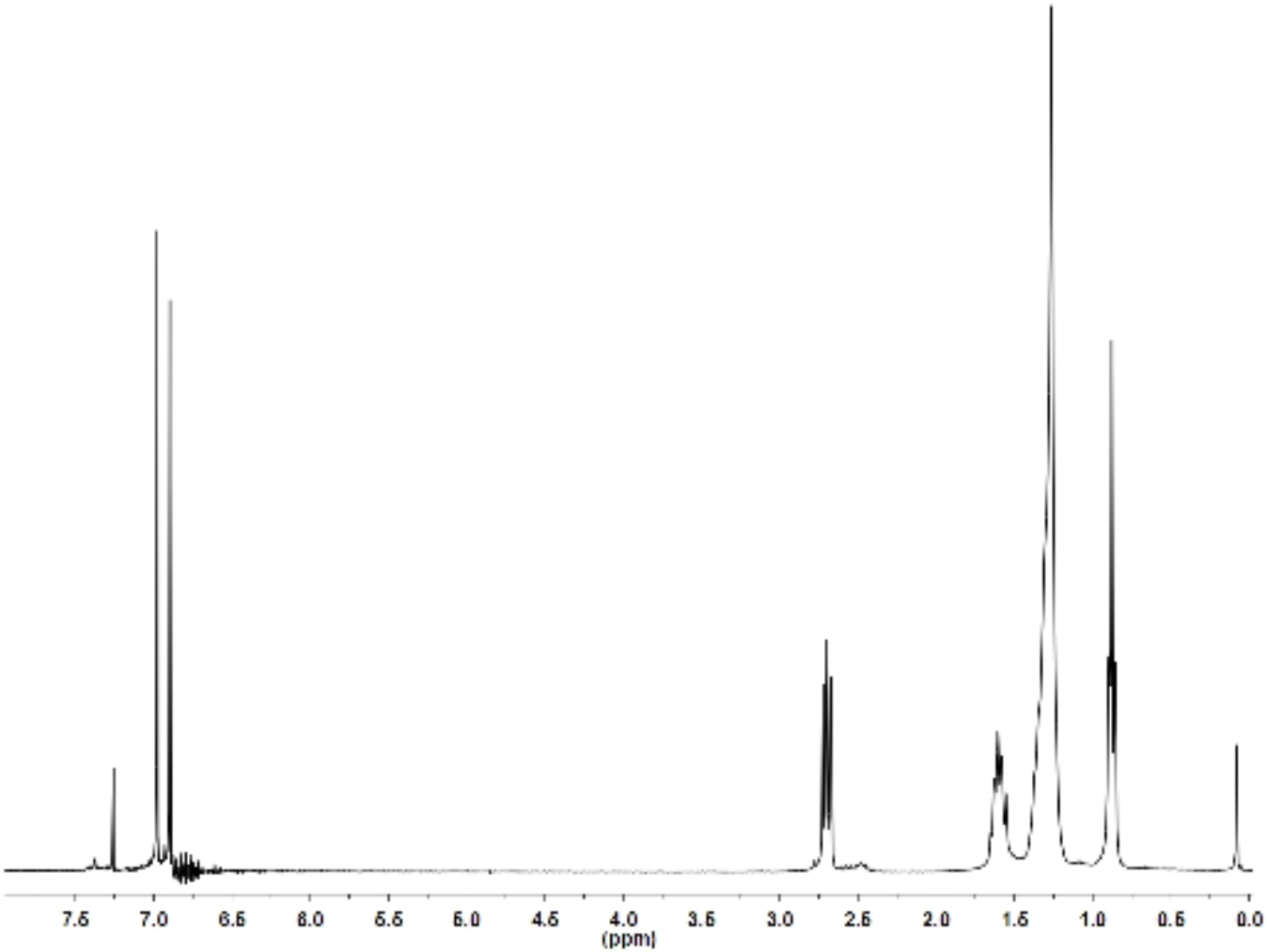


**Figure A.51.** $^{1}$H NMR of 3,3’’-Dioctyl-5,5”-dibromo-2,2’:5’,2’’-terthiophene, **V-8.**

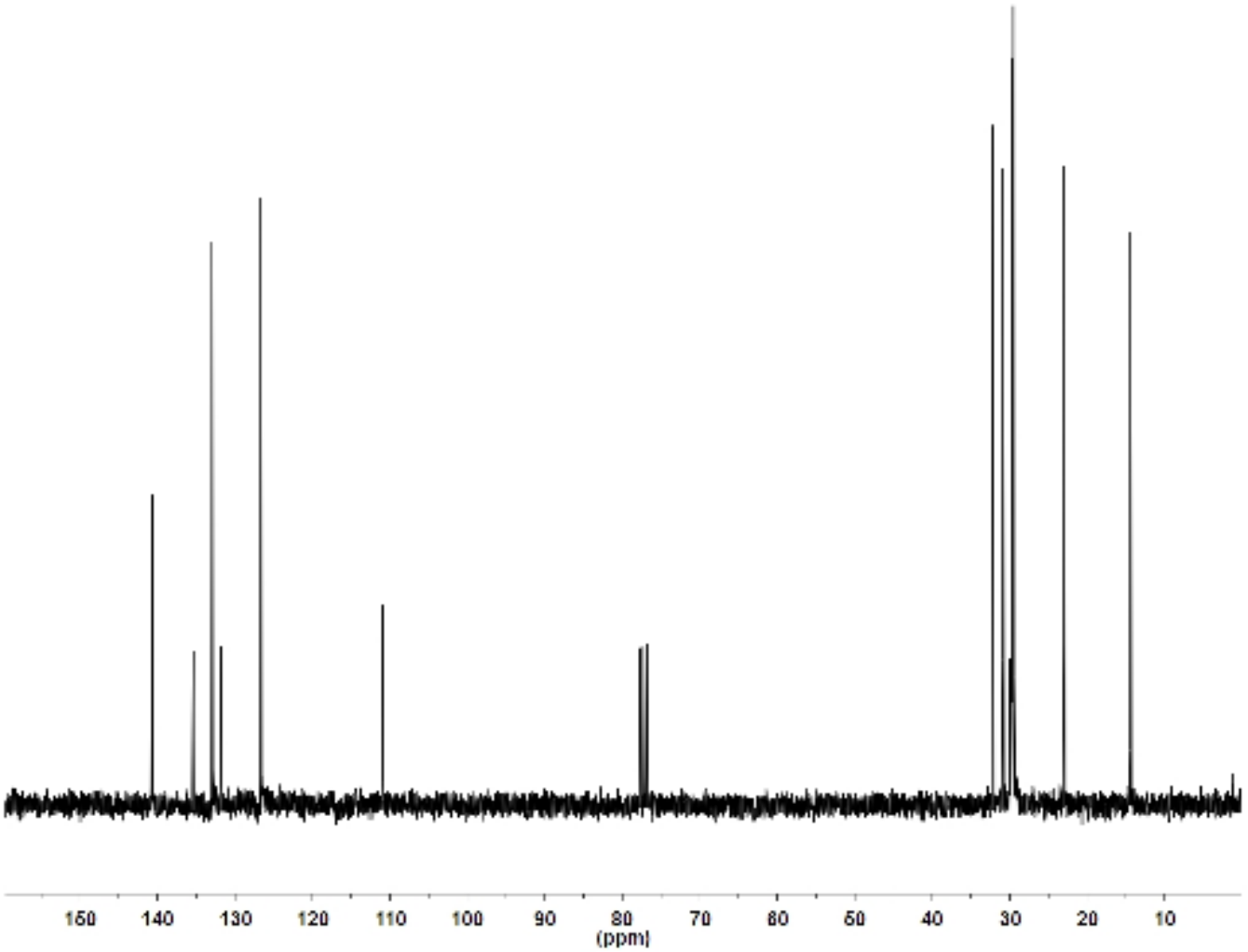


**Figure A.52.** $^{13}$C NMR of 3,3’’-Dioctyl-5,5”-dibromo-2,2’:5’,2’’-terthiophene, **V-8.**

# VITA

## RAKESH R. NAMBIAR

Rakesh Nambiar was born in Kannur, India. He attended undergraduate school in Mumbai, India, and received a M.S. in Chemistry from University of Missouri-Rolla. In 2006, he began pursuing his doctorate degree in chemistry at Georgia Institute of Technology and started his work towards the synthesis of conjugated polymers/materials. He defended his thesis in December of 2009.